2007

Three dimensional behavior of retaining wall systems

Kevin Abraham
Louisiana State University and Agricultural and Mechanical College

THREE DIMENSIONAL BEHAVIOR OF RETAINING WALL SYSTEMS

A Dissertation

Submitted to the Graduate Faculty of the
Louisiana State University and
Agricultural and Mechanical College
in partial fulfillment of the
requirements for the degree of
Doctor of Philosophy

in

The Department of Civil and Environmental
Engineering

by
Kevin Abraham
B.S., Southern University, 1984
M.S., Mississippi State University, 1995
May 2007

ACKNOWLEDGMENTS

I express my sincere appreciation to Dr. Richard Avent and Dr. Robert Ebeling for serving as Chairman and Co-chairman, respectively, of my dissertation research. I thank you both for your continued guidance and for your technical support throughout this effort. A special gratitude goes to Dr. Robert Ebeling for his unending support efforts, even during a time of personal physical challenges. Dr. Bob you are truly an asset to the profession. I would also like to acknowledge the other members of my doctoral committee, Dr. Khalid Alshibli, Dr. George Voyiadjis, Dr. Marc Levitan, and Dr. Ralph Portier, thank you for your input and insight. I also acknowledge Louisiana State University.

Special thanks go to Dr. Deborah Dent, Acting Director, Information Technology Laboratory, for her continued support and encouragement. I also would like to thank former Information Technology Laboratory Directors' Dr. N. Rahakrishnan and Dr. Jeffery Holland for their support. I acknowledge Dr. Cary Butler, Acting Chief, Engineering and Informatic Systems Division, Information Technology Laboratory; and Mr. Chris Merrill, Chief, Computational Science and Engineering Branch, Information Technology Laboratory for their support.

A special thanks to my wife Mrs. Benita Abraham, Mrs. Cheri Loden, Ms. Vickie Parrish, Ms. Shawntrice Jordan, Mrs. Doris Bolden, and Mr. Edward Huell for their assistance in preparing this manuscript, and to Mrs. Helen Ingram for her assistance during the literature review.

I give all the glory, honor, and praise to God the Father, God the Son (Jesus), and God the Holy Spirit, the Triune God, for with you all things are possible. I would like to thank my church covering and family at Word of Faith Christian Center in Vicksburg, Mississippi.

Thank you, Bishop Kevin Wright and Pastor Leslie Wright, Pastor Reginald Walker and Minister Sherry Walker, for your spiritual guidance, support, and prayers.

I extend a special thanks to my mother, Ms. Lola M. Abraham. Thank you so much for being the “best” Mom in the world and encouraging me to be the best I can be. I want to thank all of my family members for your support and encouragement.

A very special thanks goes to my loving wife, Mrs. Benita Abraham, and my children, Kevin and Keanna (my Tootie-Fruity) to whom I dedicate my research. Benita, I thank you dearly for your unwavering support, understanding, and assistance and allowing me to pursue my dreams. I am so grateful that you kept the family intact during my many days and nights of absence. You are truly a gift from God. Keanna, I thank you for being my inspiration. Finally, I extend gratitude to all my friends for their continued support.

TABLE OF CONTENTS

LIST OF TABLES

LIST OF FIGURES

ABSTRACT

The objective of this study was to perform an engineering assessment of key three-dimensional (3-D) soil-structure interaction (SSI) features of selected earth retaining walls utilizing the nonlinear finite element method (FEM). These 3-D features are not explicitly incorporated in conventional two-dimensional (2-D) procedures that are commonly used to design these retaining walls. The research objective was accomplished utilizing the nonlinear FEM.

The retaining walls selected for this research were described in detail. Design methodologies and computed responses for the walls based on conventional 2-D design procedures were summarized. Key engineering features of these structures such as construction sequence and system loading were identified. Three-dimensional responses relating to these wall systems that are not explicitly included in current 2-D methodologies were described.

An engineering assessment of key 3-D SSI responses of the retaining wall systems utilizing 3-D FEM analyses was performed. Results from the 3-D nonlinear (FEM) analyses were used to determine the state of stress in the soil adjacent to the structure, which indicates the amount of shear strength in the soil that has been mobilized. Three-dimensional nonlinear FEM analyses were used to compute deformations of the structure and the surrounding soil resulting from SSI behavior. Deformations resulting from the interaction between the structure and the soil are not explicitly included in simplified 2-D design procedures. Results of the comprehensive 3-D analyses were compared with full-scale field test results for the walls as a means to validate the FEM models. The 3-D responses of the wall systems were summarized to quantify their impact on the overall behavior of the retaining walls.

Finally, an assessment of simplified 2-D procedures was performed for the selected retaining walls, based on insight gained and critical factors identified by the comprehensive 3-D analyses. It is envisioned that the behavior of these specific retaining walls can be further understood and the critical features can be identified by the comprehensive 3-D analyses. It is also envisioned that the 3-D nonlinear FEM approach can provide useful information to help validate or possibly enhance simplified 2-D limit equilibrium and simplified computer-aided procedures used to analyze these walls.

CHAPTER 1

INTRODUCTION

The U.S. Army Corps of Engineers is responsible for designing and maintaining a substantial number of flood-control and navigation structures. One type of structure that is commonly designed and maintained by the Corps is the retaining wall. Retaining walls are used primarily to retain soil backfill and water loads. These walls include flexible cantilever and anchored walls and tieback walls. Some of these retaining walls are over 30 ft in height and are therefore subject to large earth and/or water loading. Some of the older retaining walls are currently being examined to determine if rehabilitation is feasible to enable the walls to meet stability requirements or if new structural systems are required.

The large earth pressure and water loads applied to the tall walls (greater than 15 ft of exposed or free height) resulted in construction of massive and costly wall systems. As a part of evaluating new or replacement wall systems, the Corps is also examining newer, innovative wall systems that are more cost effective than traditional retaining wall systems. Cost considerations are forcing Corps Districts to investigate alternate retaining wall systems.

For example, the U.S. Army Engineer District, Jacksonville, considered a new composite sheet-pile wall system for use on one of their recent projects as shown in Figure 1.1. A continuous cantilever wall is formed by a series of 4-ft-diameter pipe piles spaced at regular intervals, with flexible sheet piles spanning between the piles. Typically, a flexible cantilever wall has an exposed height of less than 15 ft, EM-1110-2-2504 (1994). The Jacksonville composite wall has a 30-ft free height. Flexible walls with free heights greater than 15 ft usually have additional structural support provided by an anchorage system. This composite

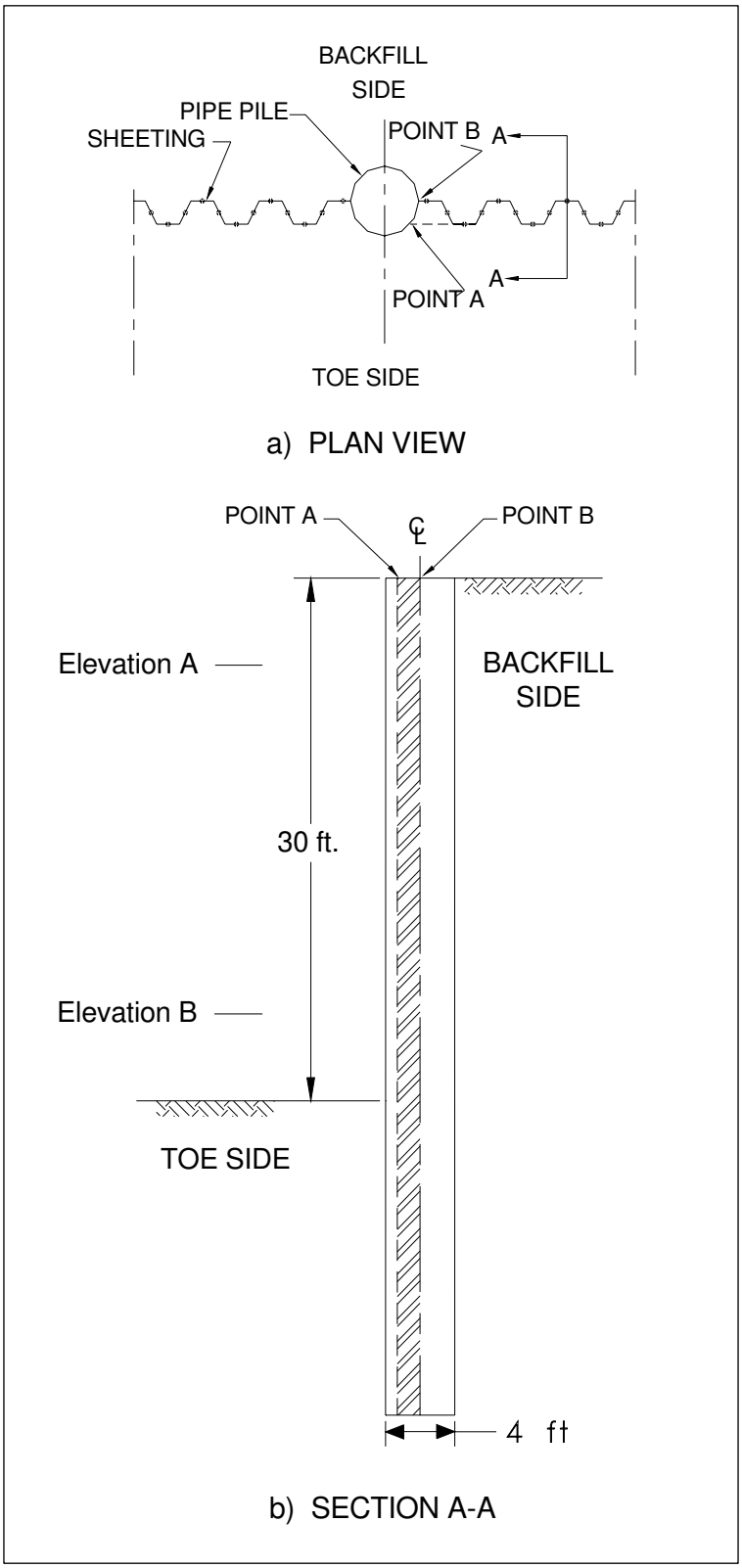

Figure 1.1. Plan and section view of composite sheet-pile wall

wall system was considered for use in an investigation to determine the feasibility of using a flexible cantilever wall with an exposed height greater than 15 ft. A combination of the stiffness of the pipe pile and sheet pile would provide the only resistance to the increased soil and water loads that result from the increase in exposed height of wall. This wall system has some key structural features. The pipe piles provide the flexural restraint of the system. The sheet piles serve as lagging, which is a structural support used to help prevent the soil that is transverse to the wall from raveling.

Deformations of the pipe pile and the sheet pile will not be the same due to differences in stiffness as shown in Figure 1.2a. At elevation A (Figure 1.1), the wall displacements are likely to be sufficient to fully mobilize the shear resistance of the retained soil, resulting in active earth pressures acting on the pipe piles and sheet-pile lagging as shown in Figure 1.2b. The pipe piles have a larger longitudinal bending stiffness EI (where E is the modulus of elasticity and I is the moment of inertia) than the more flexible sheet-pile lagging system, especially when the transverse features such as the interlock deformation are taken into account. Therefore, the deformations of the pipe pile are less than the deformations of the sheet piles. The differing stiffnesses of the wall components may lead also to a three-dimensional (3-D) stress flow phenomenon of the retained soil around the pipe pile as shown in Figure 1.2c. This 3-D phenomenon of soil pressure transfer from a “yielding” mass of soil onto the adjoining “stationary” soil mass in the out-of-plane direction is commonly referred to as arching. Terzaghi (1959) observed that arching also takes place if one part of a yielding support moves out more than the adjoining parts.

Current 2-D conventional design procedures for flexible cantilever walls do not take into account this 3-D stress flow phenomenon. This phenomenon may have a significant effect on

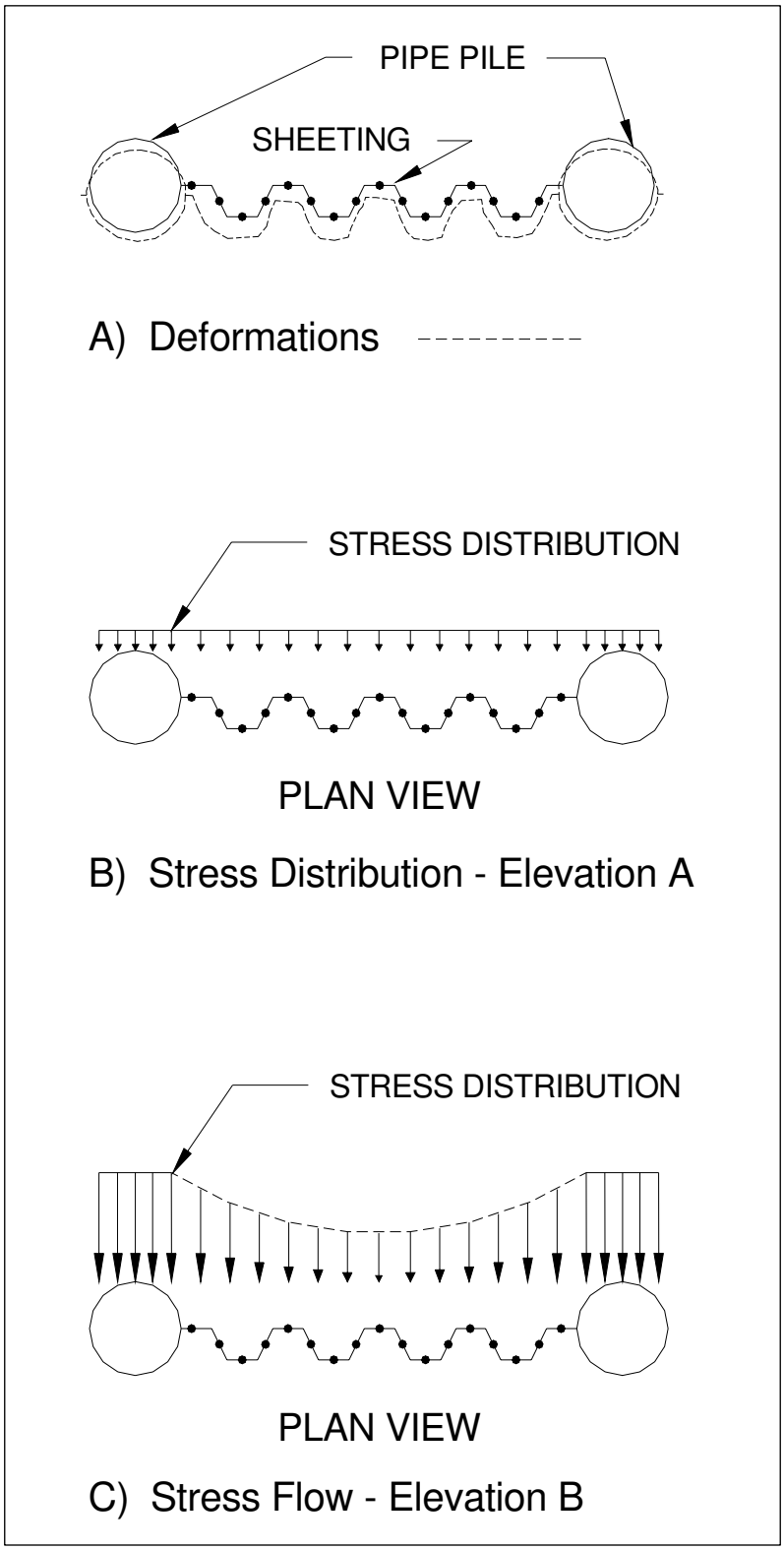

Figure 1.2. Stress flow and deformation of composite sheet-pile wall

the distribution of earth pressures and consequently bending moments and shear forces acting on a structure. No current design procedure is available for this innovative composite-wall system.

The procedures commonly used by Corps Districts for evaluating the safety of retaining walls are the conventional 2-D force and moment equilibrium methods. These methods are usually the same general methods used to design these walls. Many of these design procedures are believed to be conservative and impose limitations that prevent the designer from obtaining the most efficient design. The conservatism is usually attributed to conventional 2-D design procedures that are based on classical limit equilibrium analysis without regard to deformation-related responses and due to 2-D approximations of what is often a 3-D problem. The limitations of conventional design procedures include not being able to take into account the variability of material properties and not being able to capture all the aspects of SSI that exist in earth retaining walls.

Today, it is common within the Corps to use computer-aided engineering procedures to assess the structural integrity and stability of these earth-retaining walls. Analytical tools such as the nonlinear FEM are being implemented in computer-based design procedures to model the wall behavior as a function of the stiffness of the wall, foundation soil, and the structure-to-soil interface. These tools provide a means to evaluate the conventional equilibrium-based design methods that are used to analyze and design earth-retaining structures. These advanced nonlinear FEM procedures are a means to understanding the SSI behavior of retaining wall systems. These analytical tools can be used to identify and investigate the appropriateness of simplified assumptions used in conventional 2-D analysis of what is actually a 3-D structure.

1.1 OBJECTIVES

This research project had two objectives. The first objective was to perform an engineering assessment of key 3-D SSI aspects of two tieback retaining wall systems with multiple rows of prestressed anchors that are not considered in conventional 2-D analysis and design procedures. The assessment was done by performing comprehensive SSI analyses using 3-D nonlinear FEM procedures. These selected retaining wall systems have potential for use on Corps of Engineers projects. The second objective was to perform an assessment of simplified 2-D limit equilibrium and simplified 2-D computer-aided procedures for these wall systems utilizing the results from the comprehensive 3-D FEM analyses.

1.2 METHODOLOGY

A series of comprehensive SSI nonlinear FEM analyses was performed to assess key 3-D SSI aspects of the retaining walls that are not considered in conventional 2-D design procedures. For the retaining wall systems, 3-D nonlinear FEM analyses will be employed in the assessment. Based on an evaluation, a 3-D version of an SSI finite element computer program was selected and used in these analyses. The assessment of SSI aspects of the retaining wall systems will take into consideration design parameters such as spacing of structural members, exposed (free) height of the walls, and depth of embedment of the walls.

The performance of the wall systems was assessed based on investigating issues such as the state of stress in the soil adjacent to the structure, computed soil pressures, and deformations of the structure and surrounding soil.

The final phase of this research was to provide an assessment of simplified 2-D limit equilibrium procedures for the selected retaining walls, based on insight gained and critical factors identified by the comprehensive 3-D FEM analyses.

1.3 SCOPE OF WORK

A review of related research on retaining wall systems was performed and a summary of the findings was documented. A wall system from each of the following two types of earth-retaining walls will be investigated in this research effort.

1. Flexible tieback wall.
2. Slurry trench, tremie concrete wall (stiff).

Figures 1.3 and 1.4 showed section and plan views for wall types designated above as 1 and 2, respectively.

Current design and analysis methodologies for the selected wall systems based on current 2-D procedures were summarized. Key engineering features of these structures such as construction sequence and system loading were also identified. The 3-D responses that are not included in current 2-D design methodologies for these selected wall systems were also described. The idealized 3-D responses for above-mentioned wall types 1 and 2 are shown in Figures 1.5 and 1.6, respectively.

A series of comprehensive SSI nonlinear FEM analyses was performed to assess key 3-D SSI aspects of the retaining walls. For the retaining wall systems, 3-D nonlinear FEM analyses will be employed in the assessment. Based on an evaluation, a 3-D version of an SSI finite element computer program will be selected and used in these analyses. The selected program will be evaluated based on factors including the following:

3. Available constitutive (stress-strain) models incorporated.
4. Ability to model the construction sequence.
5. Ability to allow for the relative movement between the soil and the structure using interface elements.

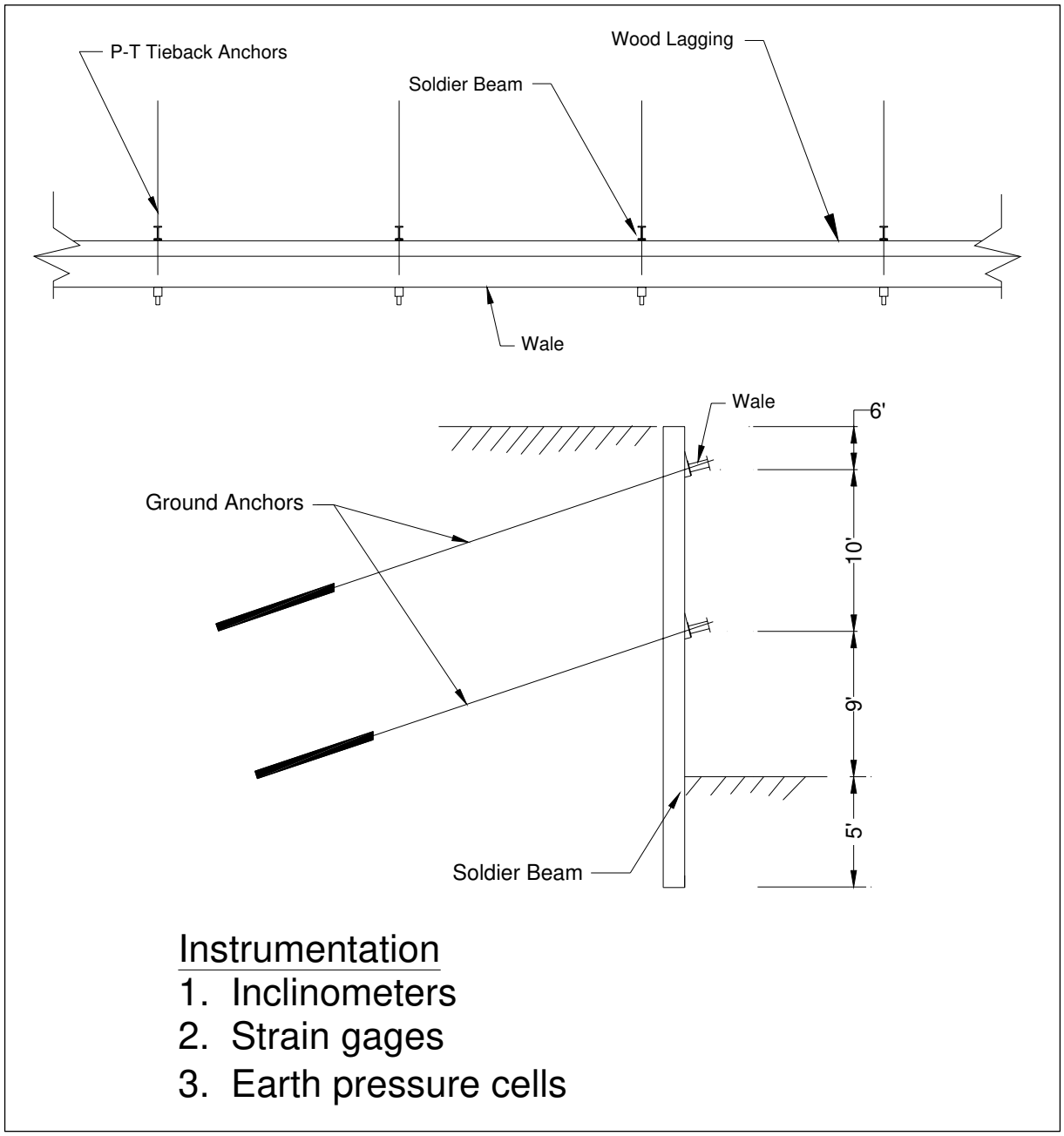

Figure 1.3. Plan and section view of flexible soldier beam and lagging with post-tensioned tieback anchors

6. Accuracy in computing the normal pressures and shear stresses acting on retaining structures.

The assessment of SSI aspects of the retaining wall systems took into consideration the following design issues where applicable:

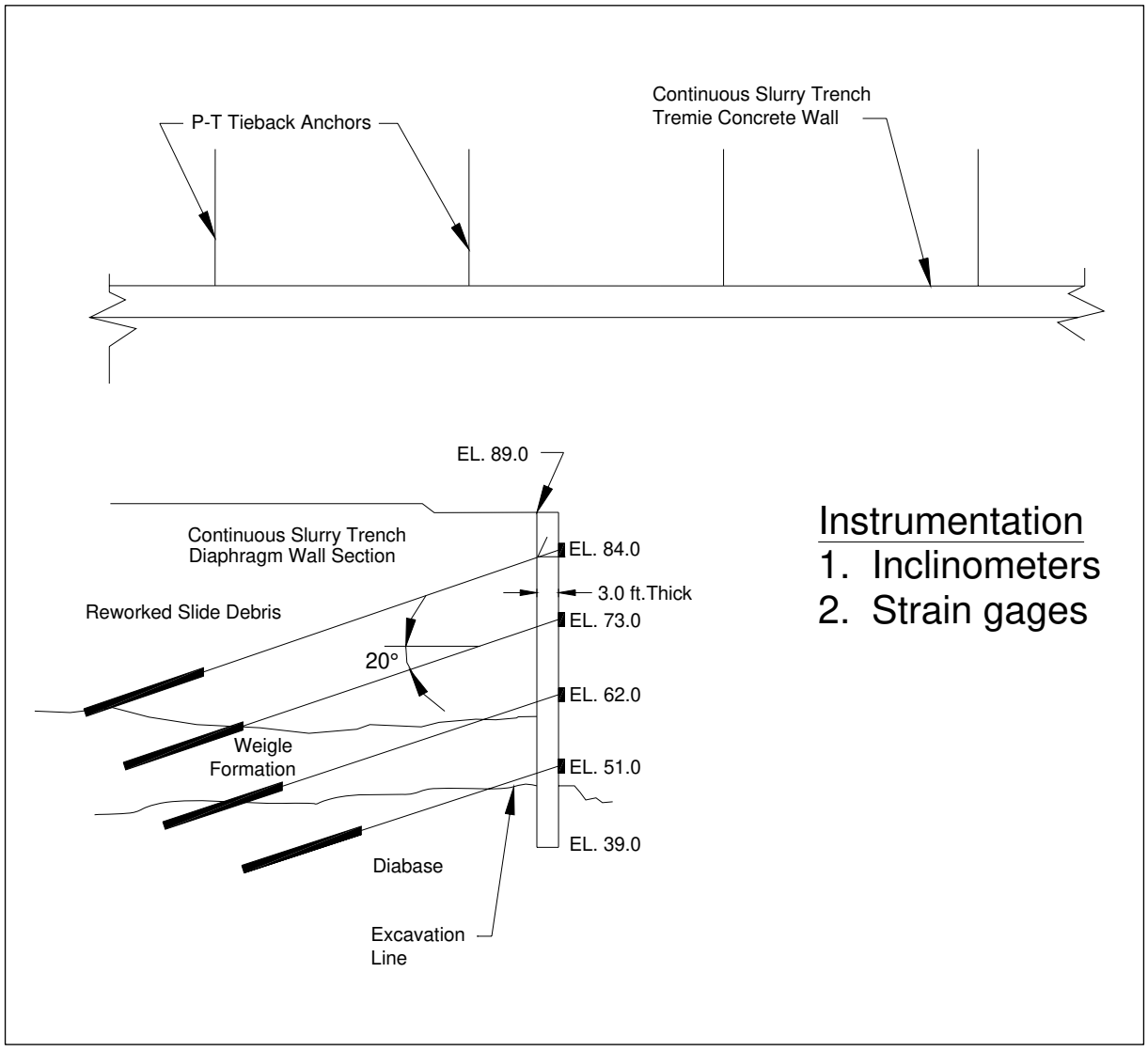

Figure 1.4. Plan and section view of slurry trenched tremie concrete wall with post-tensioned tieback anchors

1. Sizing of the structural members.
2. Spacing of structural members.
3. Exposed (free) height of the walls.
4. Depth of embedment of the walls.
5. Soil types.
6. Range in parameters for the constitutive model of typical soils.

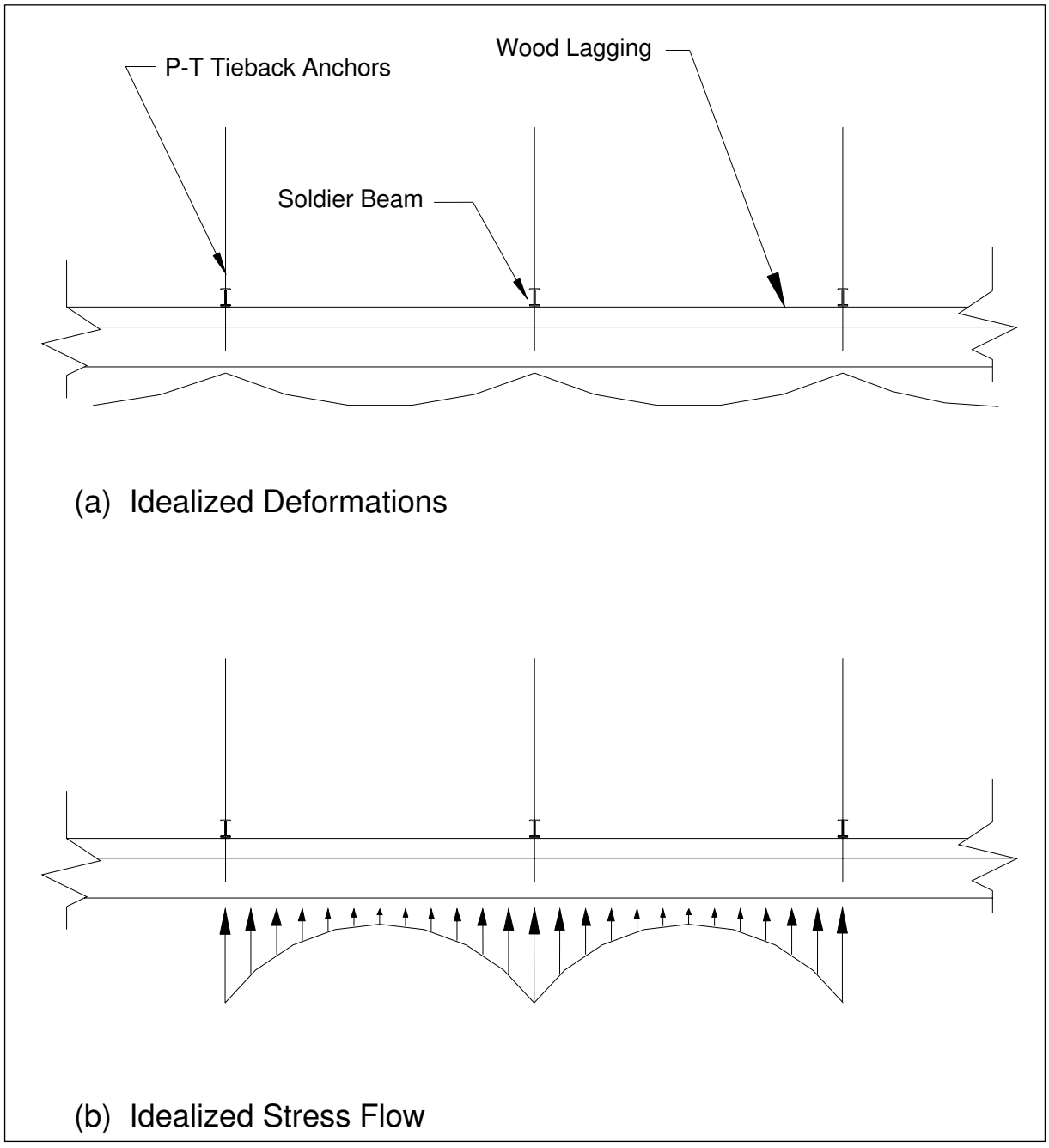

Figure 1.5. 3-D effects on flexible tieback wall

The performance of the wall systems was assessed by utilizing the SSI analyses to investigate the following:

1. Compared the stresses in the structural members computed from 3-D nonlinear (FEM) analyses to allowable stresses for the corresponding structural members.

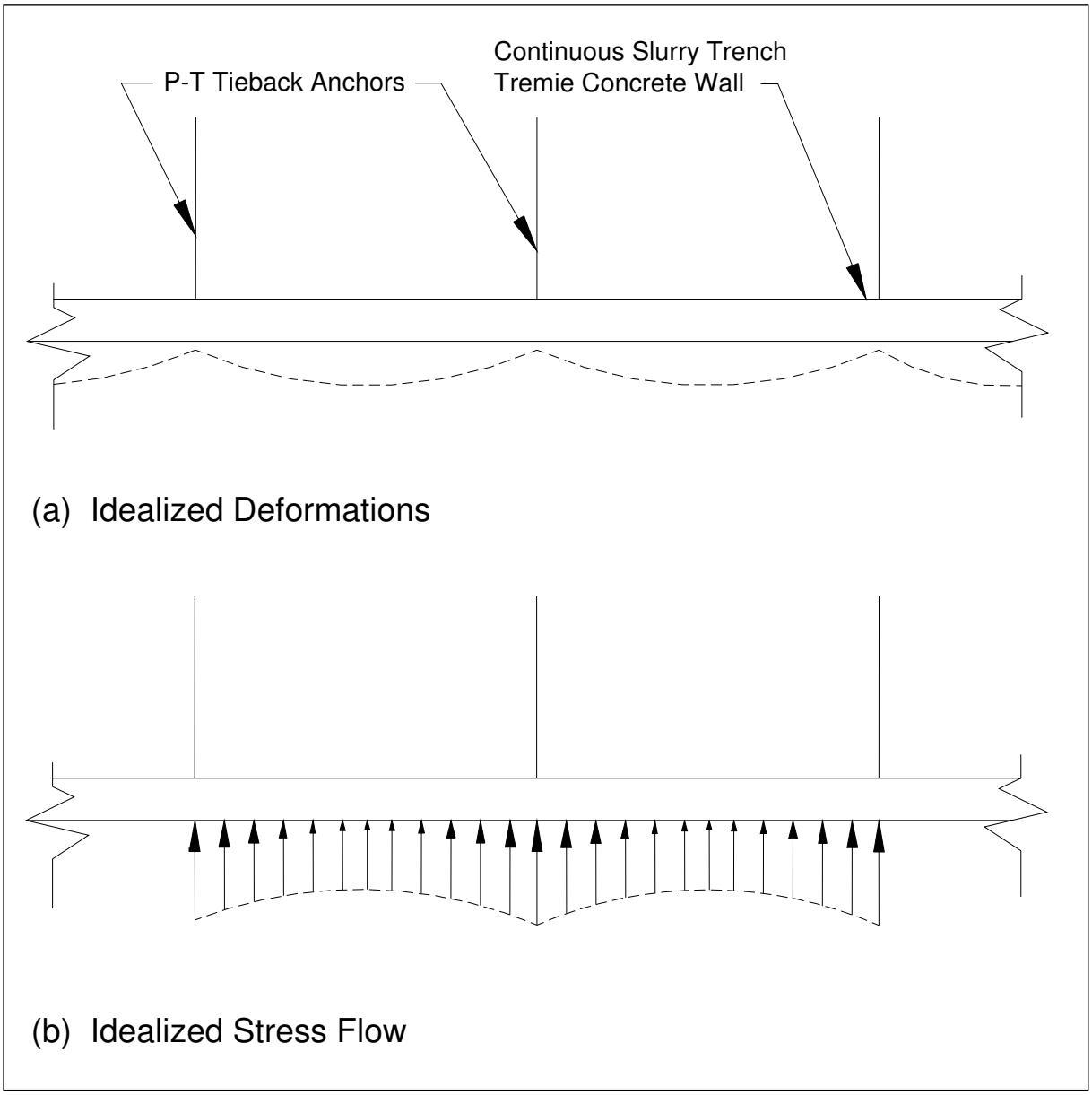

Figure 1.6. 3-D effects on continuous slurry trench, tremie concrete wall

2. Used the results from 3-D nonlinear (FEM) analyses to determine the state of stress in the soil regions adjacent to the structure. One means of assessing the state of stress in soil from FEM analyses is to relate computed stresses to earth pressure coefficients. Stresses in soil, horizontal (σ_h), vertical (σ_v), and shear τ_{xy} indicate the soil reaction to various loading. The ratio of horizontal stress to vertical stress,

(σ_h/σ_v) is defined as the horizontal earth pressure coefficient. Three general soil stress states are considered in soil-structure systems: at rest, active, and passive. These soil stress states can be described in terms of earth pressure coefficients K_o, K_a, and K_p, respectively. The computed stresses from the FEM analyses were compared to these stress states. Additionally, the ratio of mobilized shear stress to maximum available shear stress can be used to assess the soil response to given loadings. This ratio indicates the amount of shear strength in the soil that has been mobilized. When the available shear strength exceeds the maximum available shear strength, the soil is at a stress state in which its shear resistance has been mobilized; i.e., the soil is in a state of shear failure.

3. Used the computed soil pressures and deformations of the structure and surrounding soil from nonlinear (FEM) analyses to assess the overall stability and safety against failure mechanisms such as sliding and overturning for the retaining wall system.

The final phase of this research endeavor was to perform an assessment of simplified 2-D limit equilibrium procedures and simplified 2-D computer-aided procedures, based on insight gained and critical factors identified by the comprehensive 3-D FEM analyses of the selected retaining wall systems and for typical soil types.

Finally, it was proposed to provide an assessment of simplified 2-D limit equilibrium procedures for the selected retaining walls, based on insight gained and critical factors identified by the comprehensive 3-D analyses. Current 2-D limit equilibrium design procedures used by the Corps of Engineers for the two focused walls in this study are as follows: (1) flexible tieback walls are outlined in Strom and Ebeling (2001) and Ebeling, Azene, and Strom (2002), and (2) stiff tieback walls are outlined in Strom and Ebeling (2001),

Strom and Ebeling (2002a,b), and the computer program CMUTIANC (Dawkins, Strom and Ebeling 2003) was used.

It is envisioned that the behavior of these specific retaining walls can be further understood and the critical factors can be identified by the comprehensive 3-D FEM analyses. It is also envisioned that the 3-D nonlinear FEM approach can provide vital information relating to the wall response to given loadings that could help validate or possibly enhance 2-D simplified limit equilibrium and simplified computer-aided procedures used to analyze these walls.

CHAPTER 2

LITERATURE REVIEW

A review of related research in the area of SSI analysis of selected retaining wall systems was performed. The focus of this review was on three wall systems, flexible sheet-pile walls, diaphragm retaining walls, and tieback walls. A summary of the major findings of the research was documented. These findings included: (1) responses of wall systems to loading, (2) sequence of construction, (3) instrumentation results, (4) design methodologies utilized for these selected wall systems, and (5) analytical tools such as the FEM and computer-based tools that were utilized in the studies.

2.1 FLEXIBLE SHEET-PILE WALLS

Published data on field and model studies of instrumented anchored sheet-pile walls were reviewed. A limited number of case studies on instrumented anchored sheet-pile walls in situ have been reported in the literature. From a review of the published cases, it was concluded that the greater portion of data available in the literature are for model tests of anchored sheet-pile walls. The reason for this is that comprehensive full-scale tests are very costly, and consequently the number of full-scale investigations reported is much smaller than the number of model tests. However, full-scale testing is the preferred means for obtaining a quantitative assessment of the sheet-pile wall performance. In this investigation, the number of case studies was further limited to anchored steel sheet-pile walls with granular backfills, because this is the type of structural system that is commonly used by the Corps of Engineers. A summary of model tests and field tests for anchored sheet piles follows.

2.1.1 Model Tests

Tschebotarioff (1948) conducted extensive large-scale (1:10) model tests at Princeton University in New Jersey. Sand was used as backfill for these tests. In one series of tests strain gauges were used to measure bending moments. Bending moments obtained from the strain measurements were less than those from conventional methods. It was noted that the point of contraflexure occurred at or near the dredge line. Tschebotarioff (1948) developed a design procedure, which was a modification of the Equivalent Beam Method, based on information gained in the model tests. The design procedure was based on the assumption that a hinge is formed at the dredge line.

Tschebotarioff (1948) also investigated the effect(s) of the method of construction on earth pressures. He compared test results of models in which dredging was the last construction step with models in which backfilling was the last construction step. When dredging was the last operation, evidence of vertical arching was indicated with larger pressures occurring at the anchor and the dredge line. For the test cases where backfilling was the last operation, no evidence of arching was found. It was concluded that during backfilling, no condition existed to provide an abutment for the arch at or above the anchor level.

Rowe (1957) performed approximately 900 small-scale model tests on anchored sheet-pile walls. He conducted two types of tests denoted as pressure tests and flexibility tests. The pressure tests were conducted to obtain the pressure distribution existing on a sheet-pile wall undergoing movement. The flexibility tests were carried out to study the influence of pile flexibility on design factors.

Some important results of Rowe's pressure tests were as follows:

1. When backfilling was complete, the distribution of earth pressure followed Coulomb's theory of active earth pressures with no wall friction.
2. During dredging, with no anchor yield, the pressure at the tie rod level increased. This increase continued until passive failure, provided no yield at the anchor was allowed.
3. Outward yield of the tie rods caused a breakdown of the arching. The yield necessary to completely relieve the arching at the tie rod level varied with the amount of surcharge and the tie rod depth. A maximum tie rod yield $H/1000$ (where H is the wall height) was sufficient to relieve the arching in all test cases.

From the flexibility tests, Rowe established a relationship between the degree of sheet-pile flexibility given by $\rho = (\alpha H + D)^4 / EI$ and reduction in bending moment where αH is the distance from the dredge line to the top of the backfill, D is the depth of penetration, and EI is flexural stiffness of the pile. The test results led to Rowe's design procedure, which was presented in the form of charts. These charts relate the moment reduction allowed as a percentage of free earth support moment versus the flexibility of the pile. Rowe concluded the following from these tests:

1. The major part of moment reduction was due to flexure below the dredge line. The more flexible the wall is, the greater the moment reduction.
2. There was moment reduction without arching.
3. The moment reduction was also dependent upon location of dredge line and the density of the sand.
4. Moment reduction was independent of anchor location and surcharge loads.
5. Flexure below the dredge level reduced the tie rod force.

Lasebnik (1961) performed comprehensive large-scale model tests on sheet-pile walls. Unlike other researchers, Lasebnik used individual sheet piles interlocked to form a wall for the model. He used a model flexibility factor similar to that established by Rowe (1957). In the case of dense soil in the foundation, Lasebnik found that the height of wall above the dredge line αH must be employed to determine the wall flexibility. Some of his principal conclusions are as follows:

1. Sheet-pile flexibility has a large effect on bending moment and anchor force. Reduction in bending moment is especially pronounced in the range of $\rho = 0.2 - 0.6$. Anchor force for a rigid wall with nonyielding anchorage could be 30 to 40 percent larger than that determined by Coulomb's soil pressure theory.
2. The total active pressure against a flexible wall is 25 to 30 percent smaller than that against a rigid wall.
3. The shape of the passive pressure diagram agreed with Tschebotarioff's (1948) and Rowe's (1957) test results.
4. Roughness of the sheet pile has no significant effect on decreasing the active pressure, and consequently decreasing the bending moment.
5. Bending moments and anchor forces depend, to a great extent, on the yield of the anchor system. This is especially true for bulkheads driven in dense soil. Yield of the anchor decreased the anchor force and bending moment at the sheet-pile midspan and increased the bending moment at the point of the sheet-pile fixity in the soil.

2.1.2 Field Tests

Hakman and Buser (1962) conducted tests on anchored sheet-pile walls at the Port of Toledo, Ohio. The tests consisted of measurements on a steel sheet-pile wall using strain

gauges, slope indicator equipment, and conventional surveying equipment to evaluate bending moments in the sheet piling and stresses in the anchor tie rods. Hydraulically placed sand was used as backfill material. All bending moments computed from the slope indicator data were less than those obtained using Tschebatarioff's (1948) Equivalent Beam Method. Hakman and Buser also reported that large differential water levels occurred even though weep holes were provided to drain the porous backfill material.

An extensive study was undertaken from 1960 to 1964 on the sheet-pile bulkheads at Burlington Beach Wharf in Hamilton Harbor and Ship Channel Extension in Toronto Harbor, Canada (Matich, Henderson, and Oates 1964). The bending moments and deflected shapes were deduced from slope indicators. Tie rod deformations were measured using strain gauges. The bulkheads were monitored during construction to measure deflections and movements induced by driving the piles and by dredging. The readings showed that large lateral deflections up to 20 in. resulted from the driving operation; thus computed moment values far exceeded theoretical moments.

Baggett and Buttling (1977) conducted a test program on a 240-m-long anchored steel sheet-pile river wall near Middlesborough, United Kingdom. The wall design was based on the Free Earth Support Method and was compared to three European design methods. Wall movements and tie rod loads were monitored during and after construction to compare measured loads in the tie rods and wall bending moments with calculated values. Measurements of the deflected shape of the sheet piles were made by inclinometers fixed along the length of the wall. Bending moments were deduced from the deflected shapes. It was concluded that the inclinometer worked well and produced reasonable data on the

deflected shapes of the wall. The maximum bending moments deduced were approximately equal to the design value. The measured tie rod loads were comparable to design values.

2.2 DIAPHRAGM RETAINING WALLS

Gourvenec and Powrie (2000) carried out a series of 3-D finite element analyses to investigate the effect of the removal of sections of an earth berm supporting an embedded retaining wall. For the selected wall-berm geometry and soil conditions considered in the analyses, relationships between the wall movement, the length of berm section removed, the spacing between successive unsupported sections, and the time elapsed following excavation were investigated.

The finite element analyses (FEA) were carried out using the computer program CRISP (Britto and Gunn 1987). Each analysis modeled a 7.5-m-deep cutting retained by a 15-m-deep, 1-m-thick diaphragm wall. The analysis started with the wall already in place. The 3-D finite element mesh used in the analyses was composed of 720 linear strain brick elements. Separate analyses were carried out for each excavation geometry rather than modeling excavation progressively in a single analysis so that the wall displacements calculated over a given time period could be compared directly.

The results of the (FEA) showed that the removal of a section of an earth berm resulted in localized displacements near the unsupported section of the wall. The maximum wall movement occurred at the center of the unsupported section. Additionally, the magnitude of wall movements and the extent of the wall affected by the removal of a section of berm increased with the length of the berm section removed and with time following excavation.

For a wall along which bays of length B are excavated simultaneously at regular intervals separated by sections of intact berm of length B', the degree of discontinuity β is defined as

the ratio of the excavated length to the total length, i.e., $\beta = B/(B + B')$. The finite element results indicated the following:

1. For a given wall-berm geometry, ground conditions, and time period, there is a critical degree of berm discontinuity ($\beta = B/(B + B')$) that is independent of the length of unsupported section B, such that if the degree of discontinuity β of a berm-supported wall is less than its critical value β_{crit}, displacements increase in proportion to the length of unsupported sections.
2. The analyses also showed that if β exceeds its critical value, then displacements are a function of not only the length of unsupported section but also of the degree of discontinuity β. As β increases above its critical value, displacements increase more rapidly with continued increases in β.

2.3 TIEBACK WALLS

Caliendo, Anderson, and Gordon (1990) conducted a field study on the performance of a soldier pile tieback retention system for a four-story below ground parking structure in downtown Salt Lake City, Utah. One area of significance was the soft clay profile in which most of the tiebacks were anchored.

The field measurements consisted of obtaining slope inclinometer measurements on several soldier piles and strain gauge measurements at various points along the lengths of a number of bar tendons. Each of the 300 plus tiebacks was tested in the field before the tiebacks were locked off at design load. Three types of tests were performed: performance, creep, and proof.

A 2-D FEA on a typical section was performed using the program SOILSTRUCT. The program was first developed by Professors G. W. Clough and J. M. Duncan (Clough and

Duncan 1969) and has been modified by a number of researchers including Hasen (1980) and Ebeling, Peters, and Clough (1990). The finite element results were compared with the field measurements.

Some major findings from this test program include the following:

1. The maximum deflection for the three major soldier piles that were monitored by the slope indicators was approximately 1 in. (25.40 mm) into the excavation. This movement occurred approximately two-thirds of the length down the wall after the final level of excavation.
2. A finite difference approach for establishing bending moments from measured deflections did not yield reasonable results despite "smoothing" of the field curves.
3. Strain gauge and tieback test results showed the load distribution curves decreased as construction progressed, and integration of the strain data for the tieback tendons when compared to the total movements measured during proof testing indicated that the back of the anchor did not move.
4. The finite element analysis (FEA) results provided good correlation with the measured field results:
    a. The FEA displacements were nearly identical to the slope indicator readings after results were adjusted to be relative to the bottom of the wall.
    b. The FEA displacement results followed the construction steps, with displacements moving into and away from the excavation as the excavation and tieback preloading occurred, respectively.

c. The maximum bending moment from the FEA was in good agreement with the design moment based on a simply supported beam loaded with a conventional trapezoidal distribution.

Mosher and Knowles (1990) conducted an analytical study of a 50-ft-high temporary tieback reinforced concrete diaphragm wall at Bonneville Lock and Dam on the Columbia River. The wall was installed by the slurry trench method of construction. This temporary wall was used to retain soil from the excavation for the construction of a new lock at the site and to retain the foundation soil of the Union Pacific Railroad that was adjacent to the wall. The design of the wall had come under scrutiny due to the close proximity to the railroad line. This temporary wall was designed to limit settlement of the soil behind the wall upon which the adjacent railroad tracks were founded. This study focused on three objectives: (a) to provide a means for additional confirmation of procedures used in the design of the wall, (b) to predict potential wall performance during excavation and tieback installation, and (c) to assist in the interpretation of instrumentation results.

To ensure that the wall would perform as designed, it was reevaluated using FEA. The FEA provided analytical measures of wall and soil behavior. The FEA results were used as a means to evaluate the wall design and instrumentation data. The computer program SOILSTRUCT was used to perform the 2-D analytical analysis.

The initial FEA in general showed qualitatively that the wall responded satisfactorily to the various loadings it experienced. The FEA confirmed the adequacy of the wall design. The soil stiffnesses used in the initial analyses were conservative values so that the deflections predicted by the analysis should be greater than those actually experienced by the wall. The final phase of the study was to perform parametric studies to obtain values of soil stiffness

parameters that would better represent the measured behavior of the wall. The parametric studies indicated that the relative value of the hyperbolic soil stiffness modulus is an influential parameter in the results of the FEA. Increases of the modulus values for primary and unload-reload provided results that closely approached the observed behavior. There was close agreement between the observed wall deflections and bending moments and the analytical results. These results showed the accuracy of the nonlinear soil model, the finite element technique for SSI analysis of problems of this type.

Liao and Hsieh (2002) presented results of three tieback excavations performed in the alluvial soil in Taipei, Taiwan. The excavation depths varied from 12.5 to 20 m. Diaphragm walls and multilevel tieback anchors were used to support each cut and tieback excavation. The lateral movements of the diaphragm walls were monitored by inclinometers. The monitored data showed that most of the diaphragm wall movement occurred during the excavation/anchor installation stage. However, the total wall movement toward the excavation could not be pushed back by subsequently applied tieback loads. The maximum wall movements were observed to occur near the bottom of the final excavation stage and ranged from 33 mm to 80 mm.

The change in anchor loads at different tieback levels during excavation was measured with electrical load cells mounted under the anchor head. The measured anchor loads were a combination of lateral earth pressure and groundwater pressure. The tieback loads measured were used only to back-calculate the apparent lateral pressure diagrams for future tieback load designs. To establish the anchor diagram for the tieback excavation, the apparent-pressure procedure suggested originally by Terzaghi and Peck (1967) for generating the strut load diagrams for braced excavation was adapted to this prestressed-anchor tieback system.

Other conclusions of this test program included the following:

1. In general, the lateral pressure diagrams back-calculated by the method of Terzaghi and Peck showed a trend of increasing approximately linearly with depth.
2. The measured lateral pressure diagrams for the tieback anchors approximated the summation diagrams of groundwater pressure and lateral pressure calculated using the method pioneered by Terzaghi and Peck for braced excavations. However, the summation diagrams tend to underestimate the magnitude of the tieback load near the ground surface and near the base of the excavation.

CHAPTER 3

EVALUATION OF THREE-DIMENSIONAL GEOTECHNICAL ENGINEERING ANALYSIS TOOLS

3.1 BACKGROUND

An evaluation of two current three-dimensional (3-D) Finite Element Method (FEM) analysis software used for Soil-Structure Interaction (SSI) analysis of retaining walls was performed. The purpose of this evaluation was to select an appropriate computer program to be used in the engineering assessment of the case study walls.

The programs were evaluated based on factors including the following:

1. Available geotechnical related constitutive (stress-strain) models incorporated.
2. Ability to model the key construction sequencing steps related to retaining walls.
3. Ability to allow for the relative movement between the soil and the structure using interface elements.
4. Accuracy in computing the normal pressures and shear stresses acting on retaining structures.

The two 3-D FEM programs evaluated were SAGE-CRISP 3-D Bundle (Wood and Rahim 2002) and Plaxis 3-D Tunnel (Brinkgreve, Broere, and Waterman 2001). A brief summary of major facilities available in each program is presented.

3.1.1 SAGE-CRISP 3-D Bundle

SAGE-CRISP 3-D Bundle can perform the following types of analyses: undrained, drained, or consolidation analysis of 3-D or 2-D plane strain or axisymmetric (with axisymmetric loading) solid bodies. SAGE-CRISP 3-D Bundle has the following geotechnical constitutive models incorporated:

1. Homogeneous anisotropic linear elastic, non-homogeneous isotropic linear elastic (properties varying with depth).
2. Elastic-perfectly plastic with Tresca, Von Mises, Mohr-Coulomb (associative and non-associative flow), or Drucker-Prager yield criteria.
3. Elastic-plastic Mohr-Coulomb hardening model, with hardening parameters based on cohesion and/or friction angle.
4. Critical state based models -Cam clay, modified Cam clay, Schofield's (incorporating a Mohr-Coulomb failure surface), and the Three Surface Kinematic Hardening model.
5. Duncan and Chang Hyperbolic model.

Element types include linear strain triangle, cubic strain triangle, linear strain quadrilateral and the linear strain hexagonal (brick) element, beam, and bar (tie) elements. Interface elements are only available in 2-D analysis (not 3-D). SAGE-CRISP 3-D Bundle allows for the following boundary conditions: prescribed incremental displacements or excess pore pressures on element sides, nodal loads or pressure (normal and shear) loading on element sides. The program calculates loads simulating excavation or construction when elements are removed or added.

3.1.2 PLAXIS 3-D Tunnel

PLAXIS 3-D Tunnel is a special purpose 3-D finite element program used to perform deformation and stability analyses for various types of tunnels and retaining structures founded in soil and rock. PLAXIS 3-D Tunnel can model drained and undrained soil behavior. For undrained layers excess pore pressures are calculated and elastoplastic

consolidation analysis may be carried out. Steady pore pressures may be generated by input of phreatic lines or by groundwater flow analysis.

PLAXIS 3-D Tunnel has the following geotechnical constitutive models incorporated:

1. Linear elastic.
2. Mohr-Coulomb.
3. Soft-Soil model (Cam-Clay type).
4. Soft-Soil Creep model (Cam-Clay type with time-dependent behavior).
5. Hardening Soil model (Hyperbolic with double hardening).
6. Jointed Rock.

Element types consist of 6-node and 15-node volume elements and interface elements. The program has a fully automatic mesh generation routine that allows for rapid finite mesh generation. Special elements to model walls, plates, anchors, and geotextiles are incorporated within PLAXIS 3-D Tunnel. PLAXIS 3-D Tunnel allows for the following boundary conditions: prescribed displacements, pore water pressures, nodal loads or pressure (normal and shear) loadings. The program has a fully automatic load stepping procedure. A key feature of PLAXIS 3-D Tunnel is the staged construction analysis type that enables simulation of the construction process (including wall placement, excavation, and installation of anchors). A factor of safety calculation by means of phi-c-reduction is included in the program. Table 3.1 shows a comparison between Plaxis 3-D Tunnel and SAGE-CRISP 3-D Bundle for some key features identified for assessment of the case study wall systems. Plaxis 3-D Tunnel was chosen for use in the engineering assessment of the case study retaining walls. A summary of program operation, elements and selected constitutive models follows.

Table 3.1. Comparison of Features SAGE-CRISP 3-D Bundle and Plaxis 3-D Tunnel

Program / Features	SAGE-CRISP 3-D Bundle	Plaxis 3-D Tunnel
a. Higher order geotechnical related constitutive models incorporated	Yes	Yes
b. Construction sequence modeling including excavation	Yes	Yes
c. Interface elements incorporated	No	Yes
d. Automatic mesh generation	No*	Yes
* SAGE-CRISP 3-D Bundle using a separate program for mesh generation.		

3.1.2.1 Program Operation

A key feature also of Plaxis 3-D Tunnel is its user friendliness. The input pre-processor and output post-processor are completely functional within the program. Input of a problem geometry is done using cad type drawing tools. Material properties and boundary conditions are assigned using dialogue boxes and click or drag and drop operations.

After the geometry, material properties, and boundary conditions are input, the next phase is to generate the finite element mesh. Selecting the mesh generation tool in Plaxis will fill each of the delineated polygon regions of the model first with triangular finite elements. The generation of a 3-D finite element model begins with the creation of a vertical cross-section model. The vertical cross-section model is a representation of the main vertical cross-section of the problem of interest, including all objects that are present in any vertical cross-section of the full 3-D model. For example, if a wall is present only in a part of the 3-D model, it must be included in the initial cross-section model. Moreover, the cross-section model should not only include the initial condition, but also conditions that arise in the

various calculation phases. From the cross-section model, a 2-D mesh must be generated first followed by, an extension into the third dimension (the z-direction). This is done by specifying a single z-coordinate for each vertical plane that is required to define the 3-D model. In the 3-D model, vertical planes at specified z-coordinates are referred to as z-planes, whereas volumes between two z-planes are denoted as slices (Figure 3.1). Plaxis 3-D Tunnel will generate a fully 3-D finite element mesh based on the 2-D meshes in each of the specified z-planes. In the 3-D model, each z-plane is similar and includes all objects that are created in the cross-section model. Although the analysis is fully 3-D, the model is essentially 2-D, since there is no variation in z-direction. However, in subsequent load steps it is possible to activate or deactivate objects that are not active in a certain z-plane or a slice individually and thus create a true 3-D situation. After the mesh generation is complete, the next step in the problem is to define initial conditions. Plaxis has implemented a module that allows for the specification of initial pore pressure and flow conditions, staged construction steps, and initial linear elastic stress calculations.

The main processing portion of the program is referred to as Plaxis Calculations. This module allows the user to define the sequence of construction for a given problem. If the problem is a simple loading, then the user would simply enter the load multiplier and the program would automatically step the load up to calculate the deformations. For fill/ excavation problems, the loading events can be edited graphically by again clicking on and/or off clusters of elements.

The output of a 3-D Tunnel analysis can be viewed with one of two output post-processors. The first is called Plaxis Output. This program reads the output stresses and deformations from the analysis and plots the results over the original mesh for a single

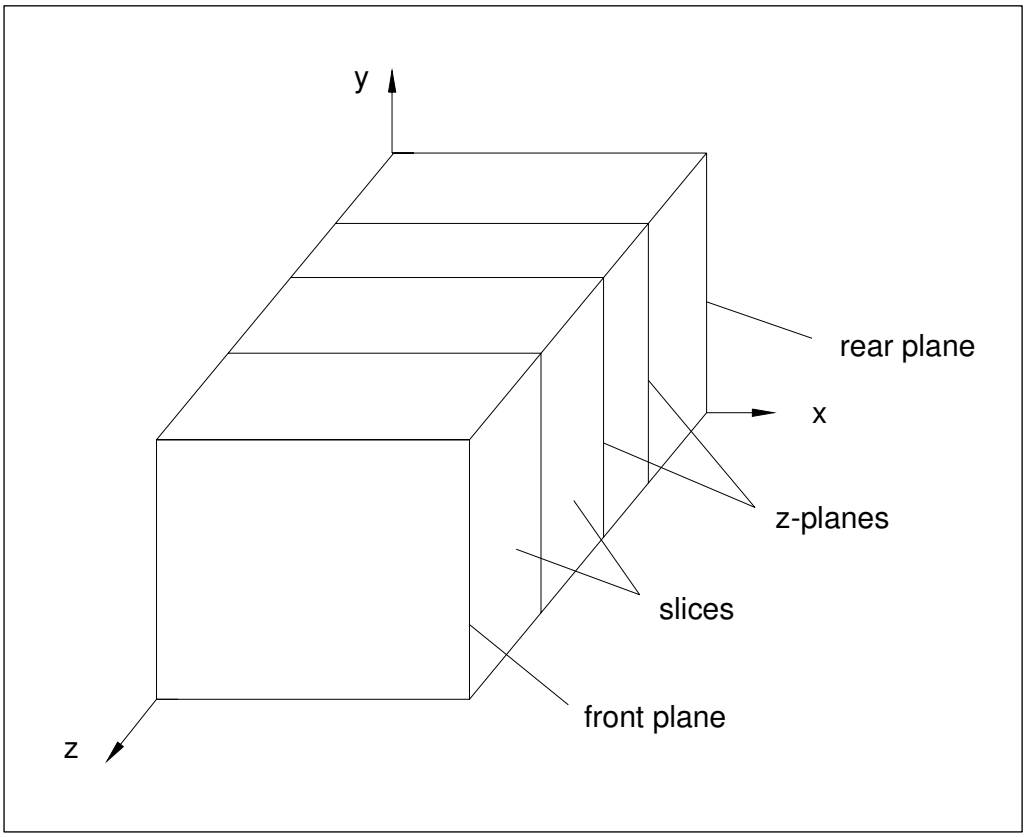

Figure 3.1. Definition of z-planes and slices in Plaxis 3-D Tunnel

loading step. The data can be plotted as contours, shadings, or vectors. The second post-processor is called Plaxis Curves. This program allows for the plotting of monitored variables throughout the entire analysis. For example, one might select the toe point of a levee, or the top of a retaining wall for monitoring. The movement of the selected point can be plotted against the loading multiplier imposed on the model.

3.1.2.2 Elements

The elements parameter has been preset to the 15-node wedge element for a 3-D analysis and it cannot be changed. This type of volume element for soil behavior gives a second order interpolation for displacements and the integration involves six stress points. The 15-node wedge element is composed of a 6-node triangle in x-y-direction and a 8-node quadrilateral in z-direction as shown in Figure 3.2.

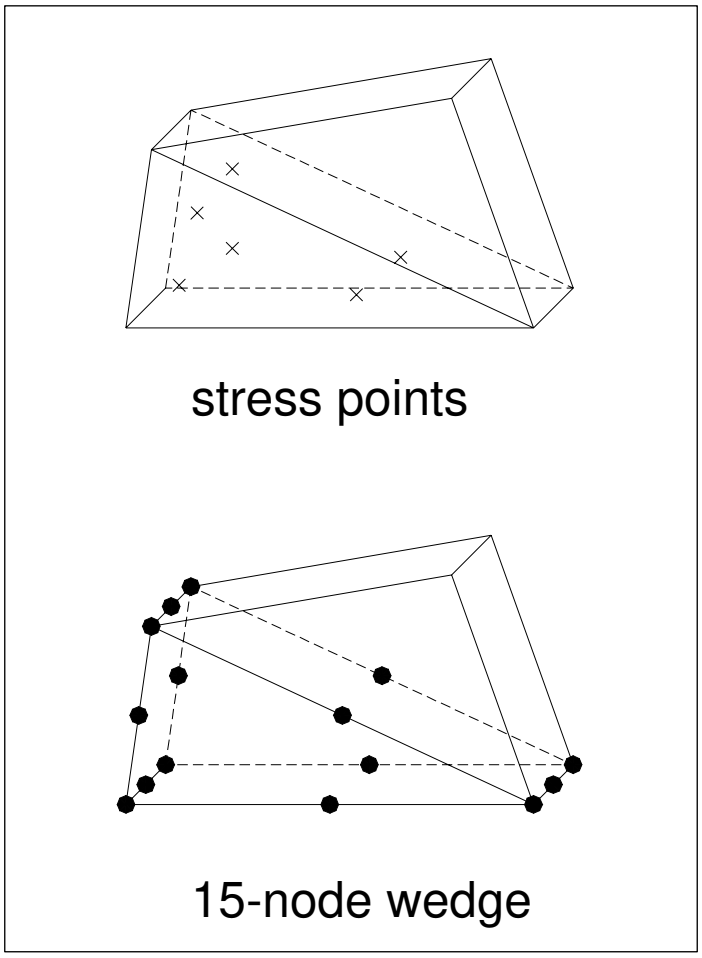

Figure 3.2. Plaxis 3-D tunnel wedge finite element

In addition to the soil elements, 8-node plate elements, are used to simulate the behavior of walls, plates and shells. Plates are structural objects used to model slender structures with a significant flexural rigidity (or bending stiffness) and a normal stiffness in the three-dimensional model. Plates in the 3-D finite element model are composed of 2-D 8-node plate elements with six degrees of freedom per node: three translational degrees of freedom (u_x, u_y, u_z,) and three rotational degrees of freedom (θ_x, θ_y,θ_z) (Figure 3.3). The 8-node plate elements are compatible with the 8-noded quadrilateral face (in z-direction) of a soil element. The plate elements are based on Mindlin's beam theory (Bathe 1982). This theory allows for beam deflections due to shearing as well as bending. The Mindlin beam theory has been extended

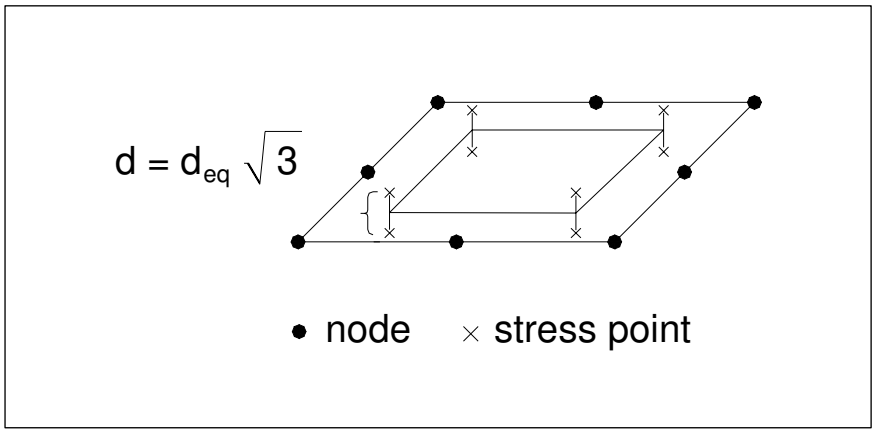

Figure 3.3. Plate element (node and stress point positions)

for plates. In addition to deformation perpendicular to the plate, the plate element can change length in each longitudinal direction when a corresponding axial force is applied. Plate elements can become plastic if a prescribed maximum bending moment or maximum axial force is reached.

The 8-node geogrid elements are used to simulate the behavior of geogrids and wovens. Geogrids are slender quasi- two-dimensional structures with a normal stiffness but with no bending stiffness. Geogrids can only sustain tensile forces and no compression. These objects are generally used to model soil reinforcements. The only material property of a geogrid is an elastic normal (axial) stiffness EA. Geogrids are composed of two-dimensional 8-node geogrid elements with three degrees of freedom in each node (u_x, u_y, u_z,). The 8-node geogrid elements are compatible with the 8-noded quadrilateral face (in the z-direction) of a soil element (Figure 3.4).

Additionally, the 16-node interface elements are used to simulate the soil-structure interaction that occurs at the interface between materials of different properties. Figure 3.5 shows how interface elements are connected to soil elements. Interface elements consist of eight pairs of nodes, compatible with the 8-noded quadrilateral face (in the z-direction) of a

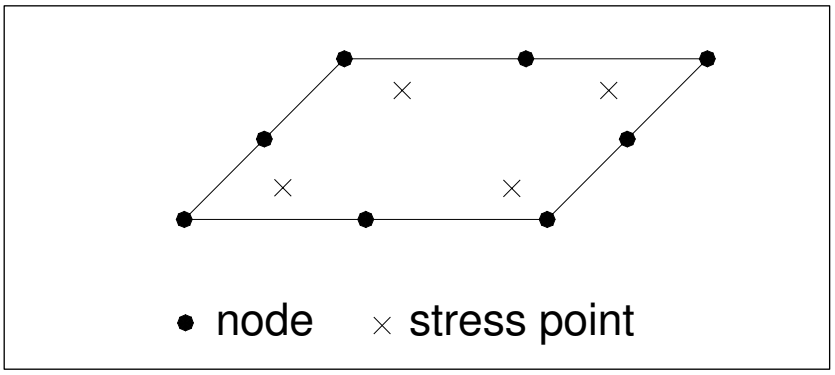

Figure 3.4. Geogrid element (node and stress point positions)

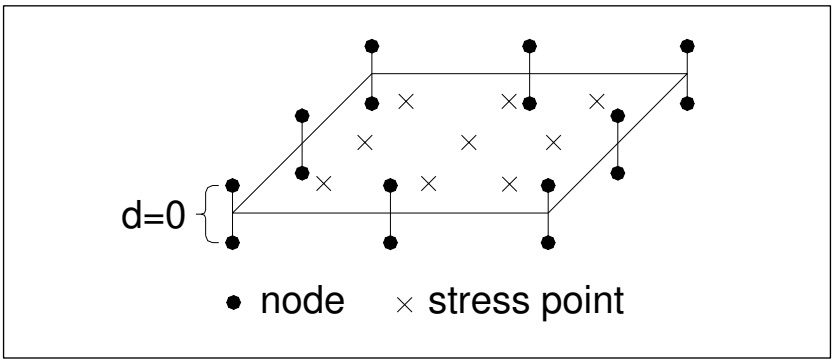

Figure 3.5. Interface element (node and stress point positions)

soil element. In the figure, the interface elements are shown to have a finite thickness, but in the finite element formulation the coordinates of each node pair are identical, which means that the element has a zero thickness. Each interface has assigned to it a 'virtual thickness' which is an imaginary dimension used to define the material properties of the interface.

Finally, the geometry creation mode allows for the input of fixed-end anchors and node-to-node anchors. Node-to-node anchors are springs that are used to model ties between two points. A node-to-node anchor is a two-node elastic spring element with a constant spring stiffness (normal stiffness). This element can be subjected to tensile forces (for anchors) as well as compressive forces (for struts). Node-to-node anchors can be pre-stressed during a plastic calculation. Node-to-node anchors in combination with geogrid elements were used the model ground anchors for the case study walls.

3.1.2.3 Constitutive Models

The relationship between stress and strain is an important aspect of finite programs since the programs compute stresses or deformation in a soil continuum subjected to external loading. The simplest relationship between stress and strain is the linear relationship known as Hooke's Law.

$$\sigma = E\varepsilon \qquad \text{Equation 3.1}$$

where σ is stress, E is Modulus of Elasticity, and ε is strain.

This relationship is for ideal conditions and may be applicable for some materials, however most soils do not behave in accordance with this model. Soil is heterogeneous, exhibits non-linear stress strain behavior and has a strength limit, and is sensitive to water moving through its pores. Therefore the simple Hooke's Law stress-strain representation of soil is not always sufficient. Researchers have attempted to emulate the behavior of soil by means of constitutive models. Comprehensive mathematical formulations have been developed instead of the simple "E" in Hooke's Law. In these formulations, the soil stiffness may change as the sample is strained in shear or hydrostatically instead of having a constant stiffness. Constitutive models provide mean to track these changes and also impose limits such as failures or yield surfaces. It is should be noted that most geotechnical finite element programs contain a basic linear-elastic model. This model is often used in preliminary analyses or when very little soil information is available.

As previously mentioned Plaxis 3-D Tunnel has various constitutive model incorporated. Plaxis contains two constitutive models that are commonly used for either cohesive or cohesionless soils. The first constitutive model is the Mohr-Coulomb (MC) model. In this model the yield condition an extension of Coulomb's friction law from basic soil mechanic

expanded to three dimensions. Figure 3.6 shows the MC failure surface in principal stress space.

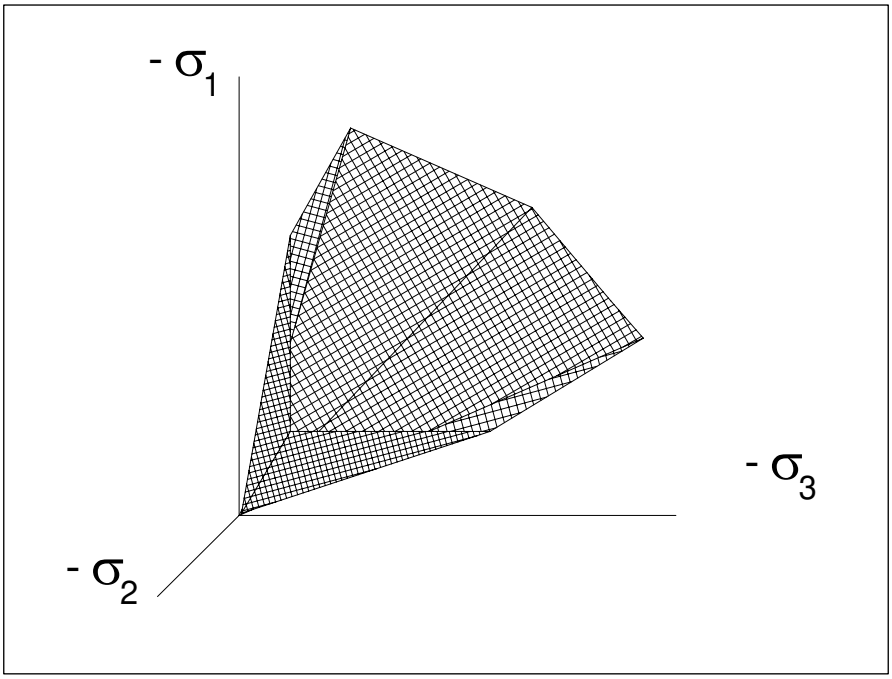

Figure 3.6. Mohr-Coulomb yield surface in principal stress space

The failure surface, in this case, is directional, meaning that it depends on the type of loading (i.e., triaxial compression, triaxial extension, etc.). The equations for the failure surface are the following:

$$f_1 = \frac{1}{2}\left|\sigma'_2 - \sigma'_3\right| + \frac{1}{2}\left|\sigma'_2 + \sigma'_3\right| sin\,\varphi - c\,cos\,\varphi \le 0$$

$$f_2 = \frac{1}{2}\left|\sigma'_3 - \sigma'_1\right| + \frac{1}{2}\left|\sigma'_3 + \sigma'_1\right| sin\,\varphi - c\,cos\,\varphi \le 0$$

$$f_3 = \frac{1}{2}\left|\sigma'_1 - \sigma'_2\right| + \frac{1}{2}\left|\sigma'_1 + \sigma'_2\right| sin\,\varphi - c\,cos\,\varphi \le 0$$

The basic parameters necessary to define the MC model are the following:

1. Failure Surface
    a. φ Friction Angle
    b. c cohesion

c. ψ Dilation Angle

2. Stiffness

   a. E Young's Modulus

   b. ν Poisson's Ratio

The MC model represents a 'first-order' approximation of soil and rock behavior (Brinkgreve and Broere 2001).

The second constitutive model incorporated in Plaxis 3-D tunnel that is commonly used either for cohesive and cohesionless soils is the Hardening Soil (HS) model. The HS model is an advanced model for simulation of soil behavior. The soil stiffness is described more accurately by using different input stiffnesses: the triaxial loading stiffness, E_{50}, the triaxial unloading stiffness, E_{ur} and the oedometer loading stiffness, E_{oed}. The basic parameters for the hardening soil model are as follows:

1. Failure parameters as in the MC model

   a. φ Friction Angle

   b. c cohesion

   c. ψ Dilation Angle

2. Hyperbolic Stiffness Parameters

   a. E_{50}^{ref} Secant stiffness in standard triaxial test at Pref

   b. E_{oed}^{ref} Tangent Stiffness for primary oedometer loading at Pref

   c. m Power for stress level dependency of stiffness

   d. E_{ur}^{ref} Unloading/reloading stiffness

   e. ν_{ur} Poisson's Ratio for unloading-reloading

   f. P^{ref} Reference Stress for stiffness

g. R_f Failure ratio

In contrast to the MC model, the HS model also accounts for the stress-dependency of the stiffness moduli, i.e., all the stiffnesses increase with confining pressure. Additionally, a triaxial test on sand will likely not appear as the elastic perfectly plastic curve in Figure 3.7. When subjected to primary deviatoric loading, soil shows a decreasing stiffness and simultaneously irreversible plastic strain develop . The observed relationship between the axial strain and the deviator stress can approximated by a hyperbola as shown in Figure 3.8.

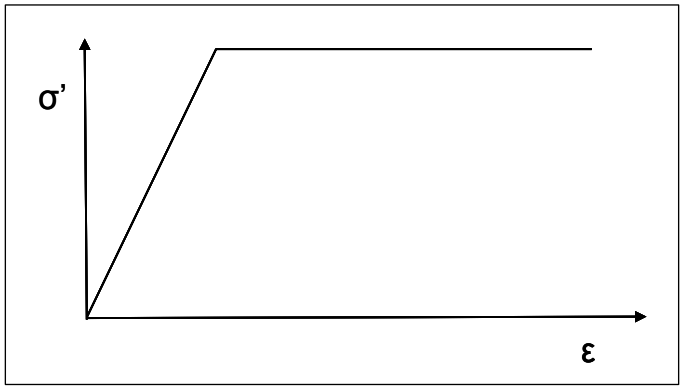

Figure 3.7. Elastic perfectly plastic stress-strain curve

As with the Mohr-Coulomb model, when the state of stress reaches the failure surface, perfectly plastic strains occur. In contrast to the elastic perfectly-plastic MC model, the yield surface of hardening plasticity HS model is not fixed in the principal stress space, but can expand as a result of plastic strains. The HS model includes a hardening cap that models both shear hardening resulting from irreversible strains due to primary deviatoric loading and compression hardening due to oedometer and isotropic loading . When a cohesionless material is loaded in isotropic compression, the material will likely not continually strain elastically as the Mohr-Coulomb model would imply. In fact, plastic volumetric strains will occur. In order to describe these strains, a hardening cap was formulated. Figures 3.9 and 3.10 show the hardening soil model with its cap in both p-q and principal stress space respectively.

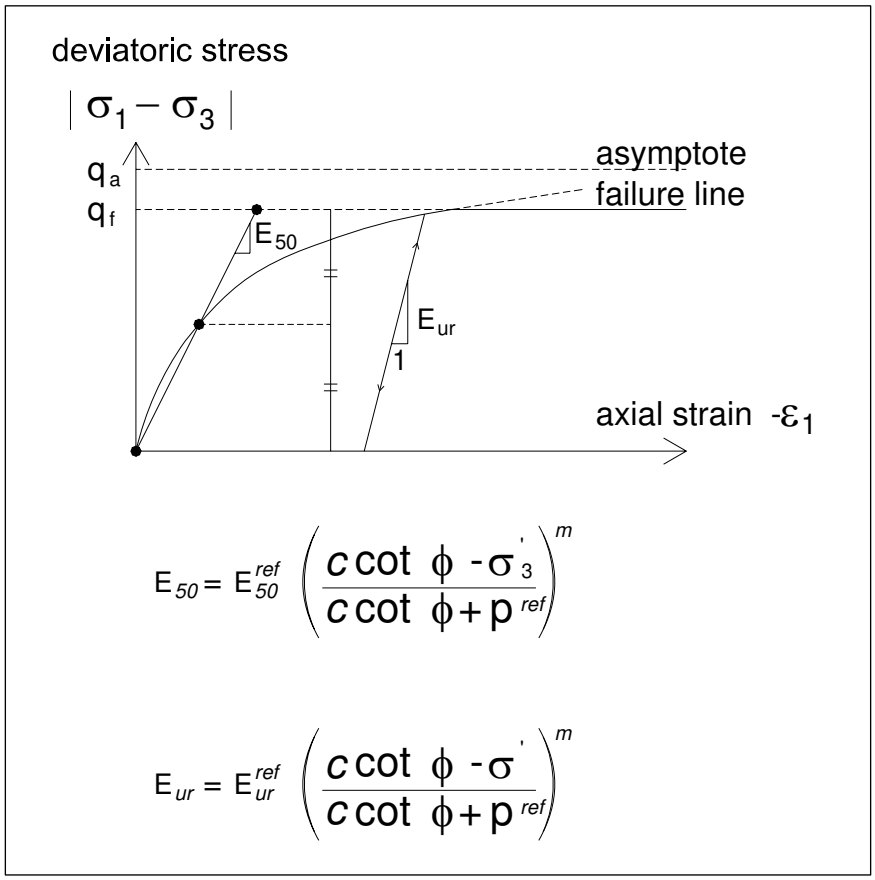

Figure 3.8. Hyperbolic stress-strain relation in primary loading for a standard drained triaxial test

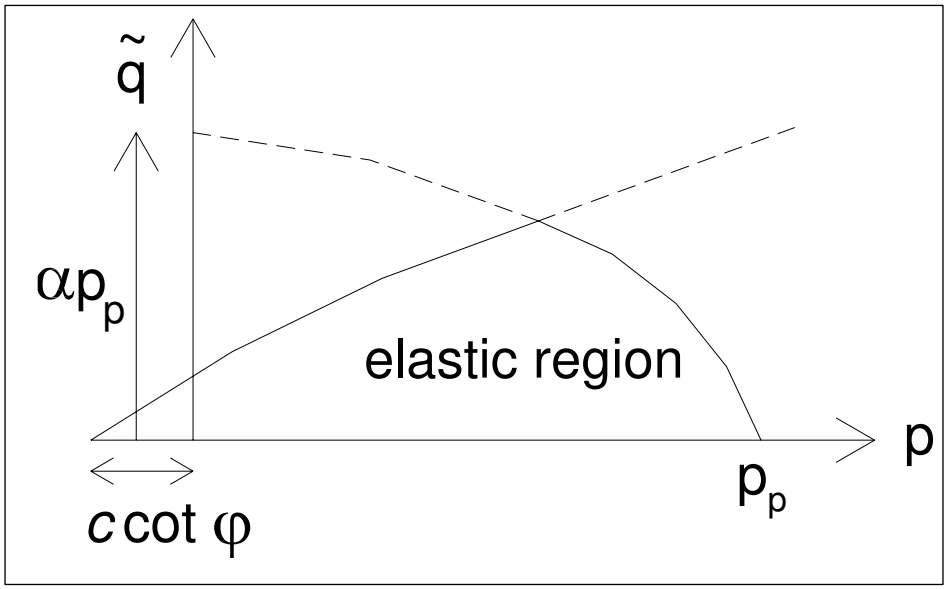

Figure 3.9. Yield surface of Hardening soil model in p-q space

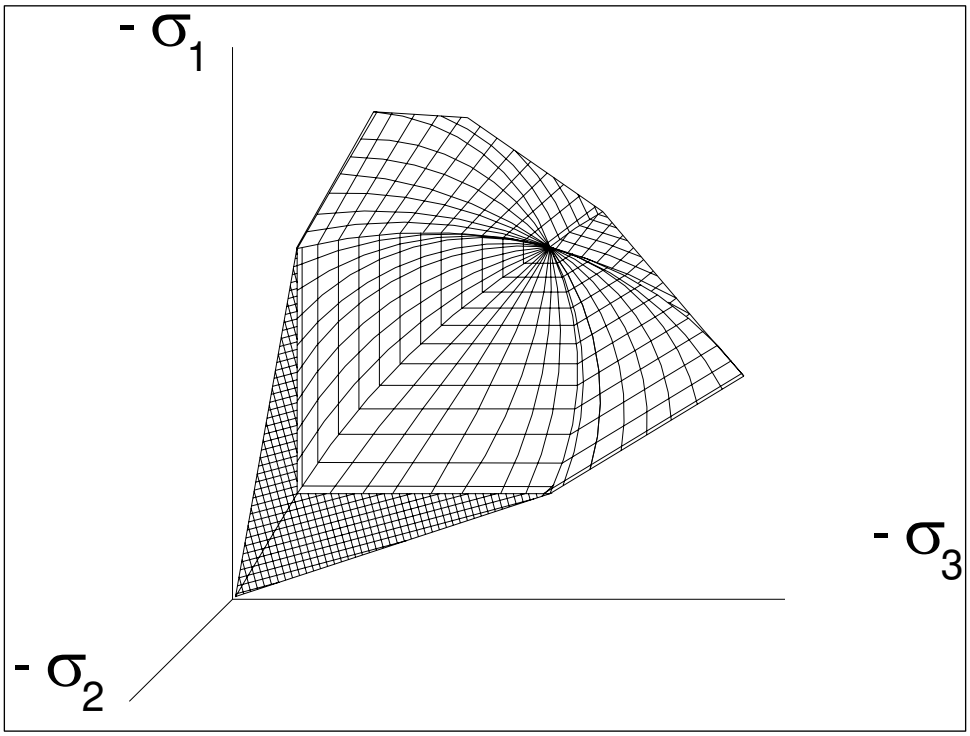

Figure 3.10. Representation of total yield surface of the Hardening soil model in principal stress space

CHAPTER 4

SUMMARY OF CURRENT DESIGN METHODS FOR THE EARTH RETAINING WALL SYSTEMS ANALYZED

4.1 BACKGROUND

This phase of research focused on identifying and summarizing current procedures used in the design and analysis of the selected earth-retaining structures. Additionally, Three Dimensional (3-D) effects relating to these structures were described. These effects were investigated in the Soil-Structure Interaction (SSI) engineering assessments of these structures using 3-D Finite Element Method (FEM) of analysis to determine the impact of the 3-D effects on the overall behavior of the structural systems.

4.2 TIEBACK WALL SYSTEMS

The type of retaining wall system investigated in this research was the tieback wall. Tieback walls are often used for temporary support of excavation systems. The temporary support is used to confine the area of excavation in order to protect railroads, structures, highways, and other fabricated features that are located in areas adjacent to the excavation. Tieback walls can also be used as permanent structures. Examples of permanent tieback walls include: approach walls and guide walls on navigation projects, and retaining walls on railroad and highway projects.

There are various types of tieback wall systems used in practice. They include:

1. Vertical sheet-pile system with wales and post-tensioned tieback anchors.
2. Soldier beam system with wood or reinforced concrete lagging and post-tensioned tieback anchors. Note: for a wood-lagging system, a permanent concrete facing is required.

3. Secant cylinder pile system with post-tensioned tie back anchors.
4. Discrete concrete slurry wall system (soldier beams with concrete lagging) with post-tensioned tieback anchors.
5. Continuous reinforced concrete slurry wall system with post-tensioned tieback anchors.

Table 4.1 shows general stiffness categorization for these wall systems. As shown in Table 4.1, the vertical sheet pile system with wales and post-tensioned tieback anchors and the soldier beam system with wood or reinforced concrete lagging and post-tensioned tieback anchors are generally designated as "flexible" tieback wall systems. The secant cylinder, discrete concrete slurry wall, and continuous reinforced concrete slurry wall systems tend to be less flexible and are designated as "stiff" tieback wall systems. Additionally, these walls systems can be quantified in terms of the structural rigidity (EI) per foot run of the wall section and in terms of the relative flexural stiffness (EI/L^4). The term E is the modulus of elasticity, I is the moment of inertia of the wall section and L is the span length, i.e., the vertical spacing of supports. These stiffness quantifications were based on guidance presented in FHWA-RO-75. Table 4.2 shows stiffness quantifications for specific retaining wall systems. A "flexible" soldier beam system with wood lagging and post-tensioned tieback anchors and a "stiff" continuous reinforced concrete slurry wall system with post-tensioned tieback anchors were selected for investigation in this research endeavor. These two wall systems are commonly used in Corps of Engineers designs. It is believed that investigating the behavior of both a flexible and stiff designated tieback wall will provide a broad understanding of the performance of tieback wall systems.

Table 4.1. Stiffness Categorization of Focus Walls
(after Strom and Ebeling 2002a)

Focus Tieback Wall System Description	Wall Stiffness Category	
	Flexible	Stiff
Vertical sheet-pile system	√	
Soldier beam system	√	
Secant cylinder pile		√
Continuous reinforced concrete slurry wall system		√
Discrete concrete slurry wall system		√

Table 4.2. General Stiffness Quantification for Focus Wall Systems
(after Strom and Ebeling 2002a)

Wall Stiffness	Wall System	EI $\left(\frac{\text{kip} \bullet \text{ft}^2/\text{ft}}{\text{run} \times 10^4}\right)$	EI/L^4 (ksf/ft)
Flexible	Vertical sheet-pile system	0.3 to 5.0	3.7[(1)]
	Soldier beam system	0.1 to 4.0	1.5[(2)]
Stiff	Secant cylinder pile	0.8 to 250.0	239.8[(3)]
	Continuous reinforced concrete slurry wall	30.0 to 150.0	123.1[(4)]
	Discrete concrete slurry wall system	35.0 to 160.0	92.3[(5)]

(1) Relative stiffness based on PZ 27 sheetpiling.
Per Olmstead Prototype Wall.
(2) Relative stiffness based on HP 12×53 soldier beams spaced at 8.0 ft on center (OC).
Per FHWA-RD-97-130 design example.
(3) Relative stiffness based on 5.0-ft-diam caisson piles spaced at 7.0 ft OC.
Per Monongahela River Locks and Dams 2 Project.
(4) Relative stiffness based on 3.0-ft-thick continuous slurry trench wall.
Per Bonneville Navigation Lock Temporary Tieback Wall.
(5) Relative stiffness based on W36×393 soldier beams spaced at 6.0 ft OC with concrete lagging.
Per Bonneville Navigation Lock Upstream Wall.

4.3 TIEBACK WALL PERFORMANCE OBJECTIVES

4.3.1 Safety with Economy Design

Common factors of safety used in practice for the design of anchored wall systems range between 1.1 and 1.5 applied to the shear strength of the soil and used in the calculation of the earth-pressure coefficient that characterizes the magnitude of the total force applied to the wall (FHWA-RD-98-065). Factor of safety values adopted vary with the importance of the wall, the consequences of failure, the performance objective (i.e., "safety with economy" or "stringent displacement control") and economics.

Factors of safety in the range from 1.1 to 1.2 are generally considered unacceptable for the design of permanent walls. Walls constructed with factors of safety between 1.1 and 1.2 may be stable, but may also experience undesirable displacements near the wall (FHWA-RD-98-065). Therefore, factors of safety in this range should be used with caution and only for temporary walls where large displacements are considered to be acceptable. Tieback wall designs based on strength only, without special consideration of wall displacement, are termed safety with economy designs. For flexible wall systems, the tieback anchors and wall system can be designed for soil-pressure conditions approaching active state conditions. As such, the apparent earth-pressure used in the design can be based on a factor of safety of 1.3 applied to the shear strength of the soil per the design recommendation of FHWA-RD-97-130. For stiff wall systems, active earth pressures in the retained soil can often be assumed and used in a construction sequencing analysis to size anchors and determine wall properties. The earth pressure distribution for this type of analysis would be in accordance with classical earth pressure theory, i.e., a triangular distribution with the absence of a water table.

The general practice for safety with economy design is to keep anchor prestress loads to a minimum consistent with active, or near-active, soil-pressure conditions (depending upon the value assigned to the factor of safety). This means the anchor size would be smaller, the anchor spacing larger, and the anchor prestress lower than those found in designs requiring stringent displacement control.

4.3.2 Stringent Displacement Control Design

Another performance objective for a tieback wall can be to restrict wall and soil movements during excavation to a tolerable level so that structures adjacent to the excavation will not experience distress. An example of this type of performance was as for the Bonneville temporary tieback wall (Mosher and Knowles 1990). According to FHWA-RD-81-150, the tolerable ground surface settlement may be less than 0.5 in. if a settlement-sensitive structure is founded on the same soil used for supporting the anchors. Tieback wall designs that are required to meet specified displacement control performance objective are termed stringent displacement control designs. Selection of the appropriate design pressure diagram for determining anchor prestress loading depends on the level of wall and soil movement that can be tolerated. Walls built with factors of safety between 1.3 and 1.5 applied to the shear strength of the soil may result in smaller displacements if stiff wall components are used (FHWA-RD-98-065).

A stringent displacement design to minimize outward movement of the wall would proceed using soil pressures at a magnitude approaching at-rest rest conditions (i.e., a factor of safety of 1.5. applied to the shear strength of the soil). It should be recognized that even though the use of a factor of safety equal to 1.5 is consistent with an at-rest (i.e., zero soil-displacement condition) with earth-pressure coefficients (as shown in Figures 3 through 6 of

Engineer Manual 1110-2-2502 (Headquarters, Department of the Army 1989)), there are several types of lateral wall movement could still occur. These include cantilever movements associated with installation of the first anchor; elastic elongation of the tendon anchor associated with a load increase; anchor yielding, creep, and load redistribution in the anchor bond zone; and mass movements behind the ground anchors (FHWA-SA-99-015). It also should be recognized that a stiff rather than flexible wall system may be required to reduce bending displacements in the wall to levels consistent with the performance objectives established for the stringent displacement control design. A stringent displacement control design for a flexible wall system, however, would result in anchor spacing that are closer and anchor prestress level that are higher than those for a comparable safety with economy design. If displacement control is a critical performance objective for a project being designed, the use of stiff rather than flexible wall system should be considered (Strom and Ebeling 2002).

4.4 PROGRESSIVE DESIGN OF TIEBACK WALL SYSTEMS

Progressive type analyses (starting with the simplest design tool and progressing to more comprehensive design tools when necessary) are highly recommended with most designs (Strom and Ebeling 2002). Some of the more comprehensive analysis tools used for stiff wall system analysis (construction-sequencing analysis based on classical earth pressure distributions and beam on inelastic foundation analysis) are not generally considered feasible for flexible walls systems. This is because apparent pressure diagrams are “envelopes” based on measurements during construction that include the effects of wall flexibility, soil arching, preloading of supports facial stiffness, and construction sequencing. However, with stiff wall systems these effects will not affect the earth-pressure distribution to the same extent as they affect flexible wall systems. Therefore, in practice construction sequencing analyses and beam

on inelastic foundation analyses are considered viable tools for the investigation of the behavior of stiff wall systems. Progressive type analyses were utilized in this research effort.

4.5 TIEBACK ANALYSIS AND DESIGN PROCEDURES

There are four general methods used in the analysis and design of tieback wall systems that are described in Strom and Ebeling (2001). These methods were designated as:

1. Beam on rigid supports (RIGID) method.
2. Beam on elastic supports (WINKLER) method.
3. Linear-elastic finite element (LEFEM) method.
4. Nonlinear finite element-soil structure interaction (NLFEM) method.

A brief summary of key features of these methods is presented.

4.5.1 RIGID Analysis Method

The terminology of RIGID analysis is in accordance with that used by Kerr and Tamaro (1990). The tieback wall is assumed to be a continuous elastic member (with a constant value of EI) supported on fixed ground anchors. In the RIGID method, the soil loads are predetermined and considered to be following loads that are independent of wall displacements. Thus, in this method the redistribution of earth pressures due to wall movements is not considered. The soil loading can have a trapezoidal distribution (from apparent earth pressure envelopes) or typical triangular distribution from conventional equilibrium procedures. The foundation soil on the front side of the wall is assumed to act as a fictitious support at the point of zero net pressure that prevents translation of the wall. The RIGID analysis method is illustrated in Figure 4.1.

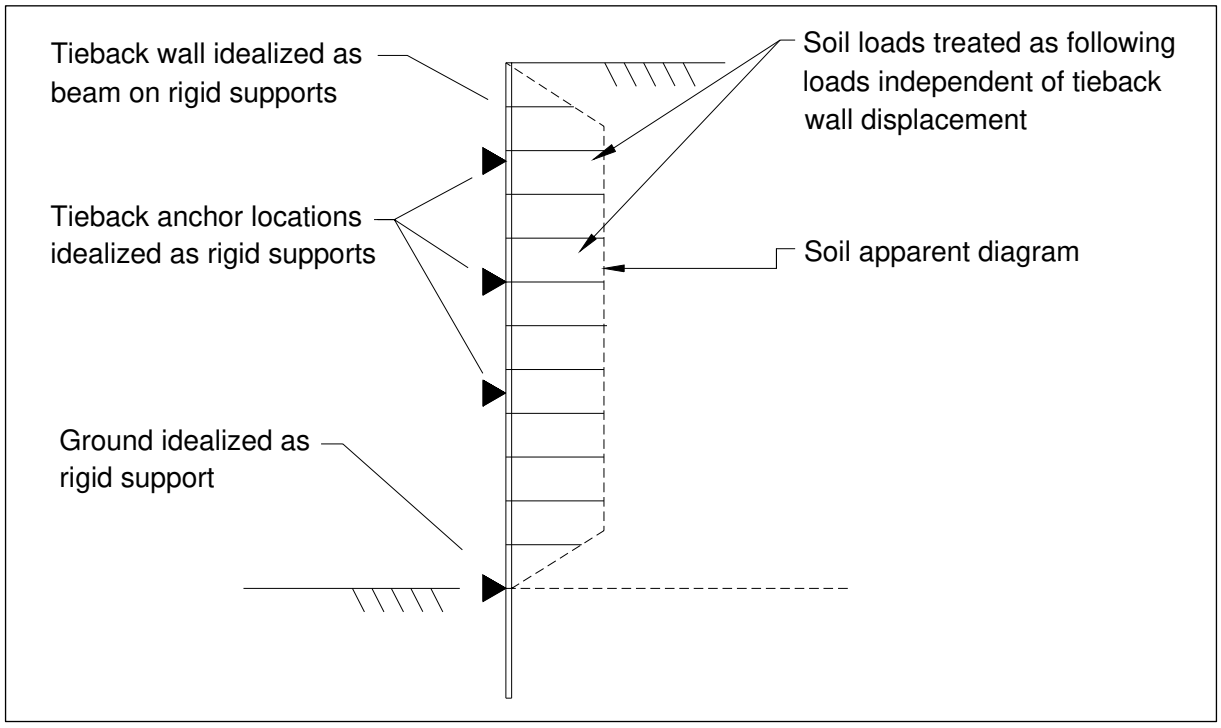

Figure 4.1. Equivalent beam on rigid supports method (RIGID)

4.5.2 WINKLER Method

The WINKLER method is a beam on elastic foundation method of analysis. This method is based on a one-dimensional (1-D) finite element representation of the wall/soil system. The tieback wall is considered to be continuous flexural member with stiffness EI and is modeled as linearly elastic beam-column elements. The wall is supported by set of infinitely closely spaced distributed nonlinear springs with stiffness (K) to represent the soil, and discrete nonlinear preloaded concentrated springs to model the anchors. The soil springs are preloaded to at-rest pressure conditions to represent the condition that exists prior to excavation. As the excavation occurs (i.e., removal of soil springs in the excavation region), the wall moves toward the excavation. This movement is the result of the at-rest preload in the soil on the backside (unexcavated) side of the wall. The soil springs on the excavation side must carry more load than at-rest loads in order to help keep the wall system in equilibrium.

Additionally, at the ground anchor locations, the tiebacks represented by a preload anchor springs also contribute to the overall system equilibrium. The fundamental assumption in the WINKLER spring analysis method is that each spring used to represent the soil acts independently (i.e., the behavior of one spring has no effect on the behavior of adjacent springs). The WINKLER analysis method as represented in Figure 4.2 can be used in a staged excavation analysis or as a final analysis where the completed structure is "wished" into place without consideration of system displacements that occurred during each stage of construction.

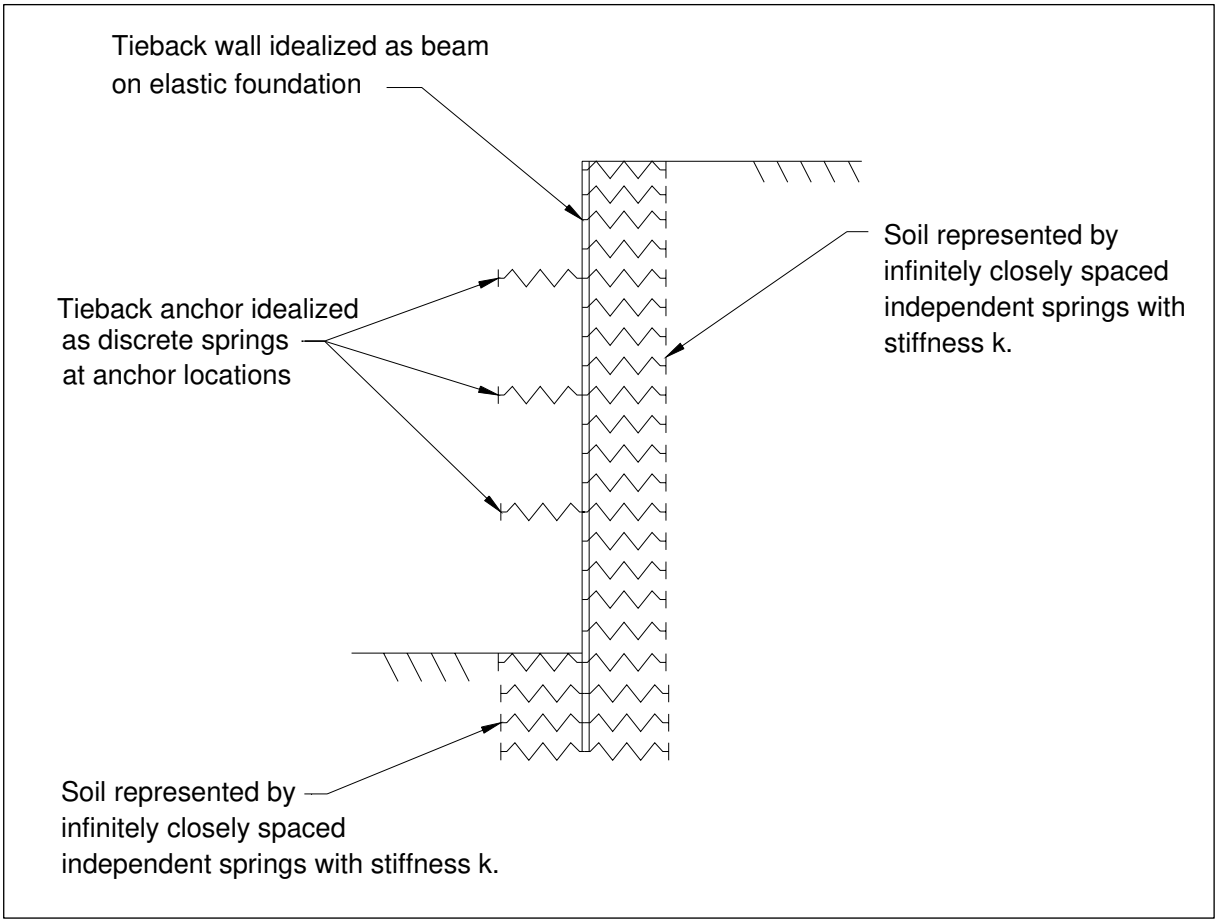

Figure 4.2. Beam on elastic foundation method (WINKLER)

4.5.3 Linear Elastic Finite Element Method (LEFEM) and Nonlinear Finite Element Method (NLFEM)

4.5.3.1 Background

The finite element method (FEM) of analysis is an analytical procedure that has been used to approximate the complex interaction that occurs between soil and structures. FEM procedures explicitly include many parameters within an analysis that are essential in obtaining accurate responses at the soil to structure interface. This type of analysis is called a Soil-Structure Interaction (SSI) analysis. In a FEM SSI analysis the soil and structural elements are modeled as finite elements possessing certain stress-strain characteristics. SSI procedures can be used to simulate the actual construction process. The construction process during the course of an analysis is modeled in a series of increments. This process allows the stress-strain model to simulate the stress-strain response during each sequence of loading. This is important because the stress-strain response of soil and soil-to structure interface is nonlinear and stress path dependent. SSI studies have shown that in order to compute accurate values of stresses and displacements within a soil foundation, soil backfill, and a structure, the sequence of construction operation at the site must be simulated in the analysis. (Mosher and Knowles 1990 with respect to tieback diaphragm wall); (Ebeling, Mosher, Abraham and Peters 1993, Ebeling and Mosher 1996, Ebeling, Peters, and Mosher 1997 with respect to a lock wall at Red River Lock and Dam No. 1); (Ebeling and Wahl 1997, North Wall at McAlpine Locks), and (Abraham 1995 with respect to anchored sheet-pile walls) are good examples of state-of-the-art procedures for SSI analyses.

A finite element mesh is developed to model the complete construction process. Elements are either added or removed from the mesh during the course of the analysis. However, elements not existing at a given stage of analysis are represented by low stiffness elements

often referred to as “air elements.” When the stage of construction reaches a given region of the mesh that is comprised of air elements, the properties of these elements are changed to those properties corresponding to soil or structural elements.

Another important feature of a FEM SSI analysis is its ability to allow for the relative movement between the soil and structure by the use of interface elements. This feature is of great importance for accurately computing the normal pressures and shear stresses acting on retaining structures. Unlike conventional equilibrium procedures, these SSI procedures do not require the use of pre-determined earth pressure distribution being applied to the structure, but allows for the development of the stresses through the soil-structure interaction that occurs during the construction process.

4.5.3.2 Linear Elastic Finite Element Method (LEFEM)

A linear material is described as material behavior in which the magnitude of the response of a material is directly proportional to the magnitude of the loads applied to the material. This behavior can be visualized by a stress-strain curve shown in Figure 4.3. Elastic materials undergo only recoverable deformations, i.e., they return to their initial state when the load is removed. These materials have a unique stress-strain relationship given by the generalized Hooke’s law that may be written as

$$\sigma = E\,\varepsilon \qquad \text{Equation 4.1}$$

where σ is stress , ε is strain, and E is the modulus of elasticity.

SSI analysis problems have been modeled as linear elastic problems, based on the following assumptions Liu (1998):

1. Material behavior is elastic.
2. Small deformation (loading pattern is not changed due to the deformed shape).

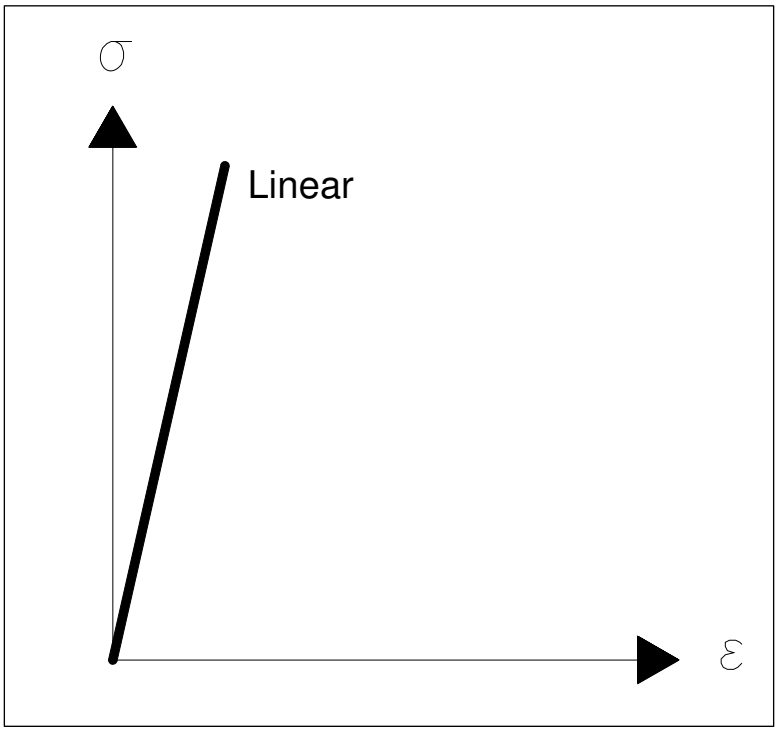

Figure 4.3. Illustration of linear stress-strain relationship

LEFEM has been used in a stage excavation analysis and in a loss of anchorage analysis to evaluate bending moment demands and anchor loads in diaphragm walls. An example of the use of the linear elastic finite element is described in the American Society of Civil Engineers (ASCE) publication authored by members of the Structural Engineering Institute's (SEI) Technical Committee on Performance of Structures During Construction (ASCE/SEI 2000). This example consists of using linear finite elements to model the diaphragm wall and linear WINKLER springs to model the soil on the excavation side of the wall. Initial stresses equal to at-rest soil pressures were assigned to the WINKLER soil springs. On the unexcavated (active) side, the soil pressures on the wall are applied through distributed loads. These active pressures were assumed to be unchanged throughout the entire sequence of excavation. A finite element mesh was used to model the diaphragm wall to capture plate-bending effects for stage excavation analysis, and to capture anchor load redistribution effects

for loss of anchorage analyses. Figure 4.4 illustrates the LEFEM in combination with linear WINKLER springs with respect to a staged excavation analysis.

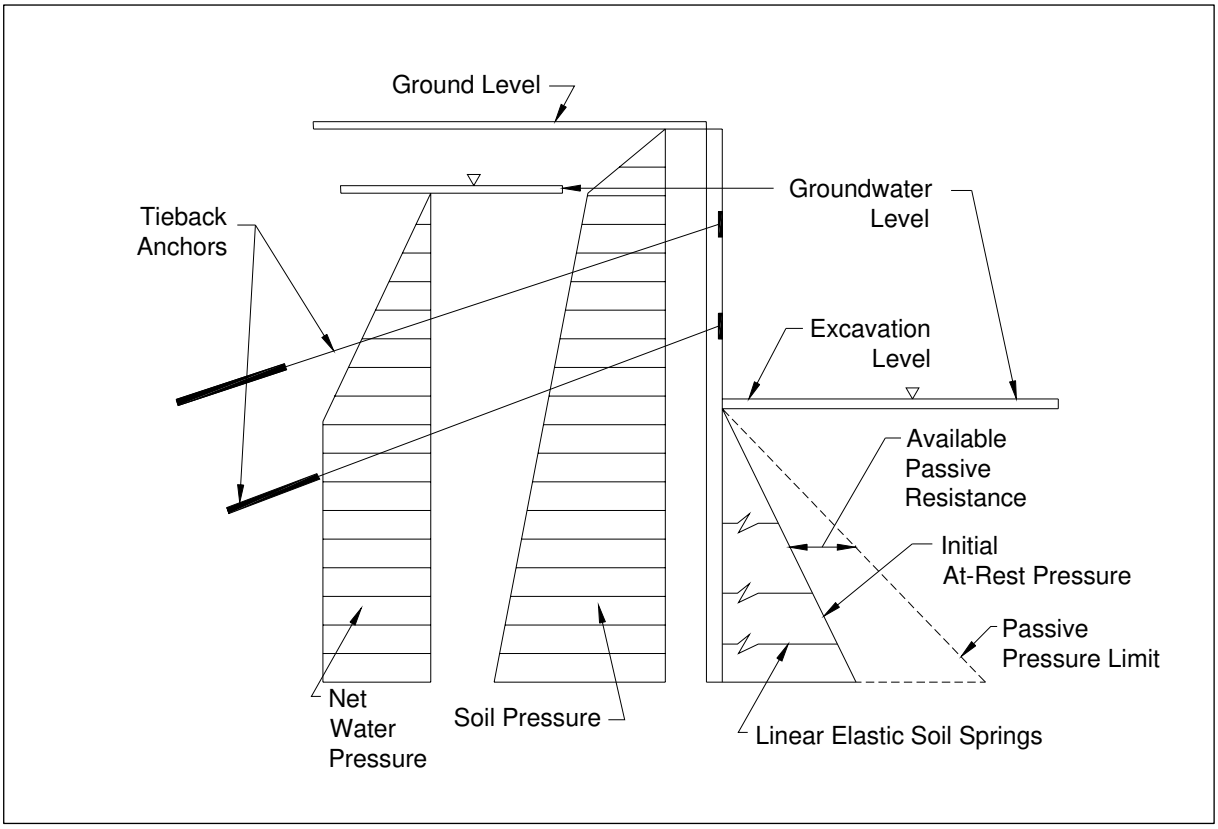

Figure 4.4. Linear elastic finite element model (LEFEM) of diaphragm wall in combination with linear Winkler soil springs

A linear analysis can provide important information about the behavior of a structure, and can be a good approximation of the behavior a structure in many cases. Linear analysis is also the bases for most nonlinear analysis.

4.5.3.3 Nonlinear Finite Element Method (NLFEM)

A nonlinear material is described as material behavior in which the magnitude of the response of a material is not directly proportional to the magnitude of the loads applied to the material. A nonlinear material behavior can be visualized on a stress vs. strain plot as shown in Figure 4.5.

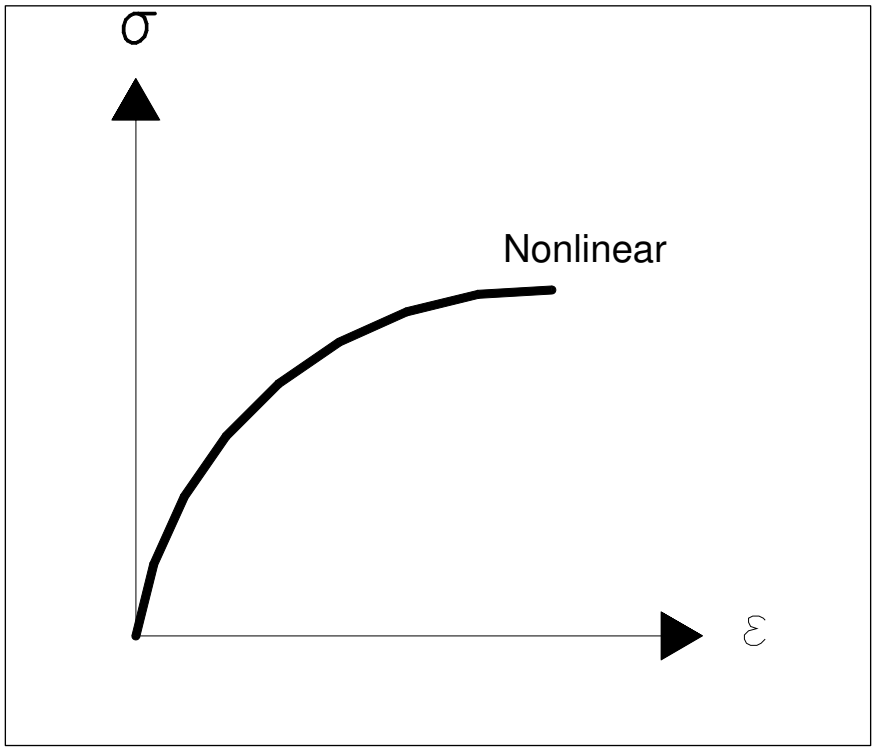

Figure 4.5. Illustration of nonlinear stress-strain relationship

The Nonlinear Finite Element Method (NLFEM) has been used in sequence of construction analyses to capture soil-structure interaction effects. The actual stress-strain response of soil and soil-to-structure interfaces in these analyses is nonlinear and stress path dependent. In these analyses, soil nonlinearities can be evaluated and soil pressures can be allowed vary as a result of the structural and related soil deformations.

An example of use of the NLFEM with respect to a stage construction of a tieback diaphragm wall is the Bonneville temporary tieback wall (Strom and Ebeling 2001) and Mosher and Knowles (1990). Figure 4.6 illustrates how the NLFEM is used for this tieback wall system. The soil is represented with finite elements that have nonlinear stress-strain material properties. The tieback anchors are modeled as bar elements with pre-stress loads applied. The results of each stage of construction were studied, from the in situ condition and wall construction through the excavation and tieback installation procedure. It was

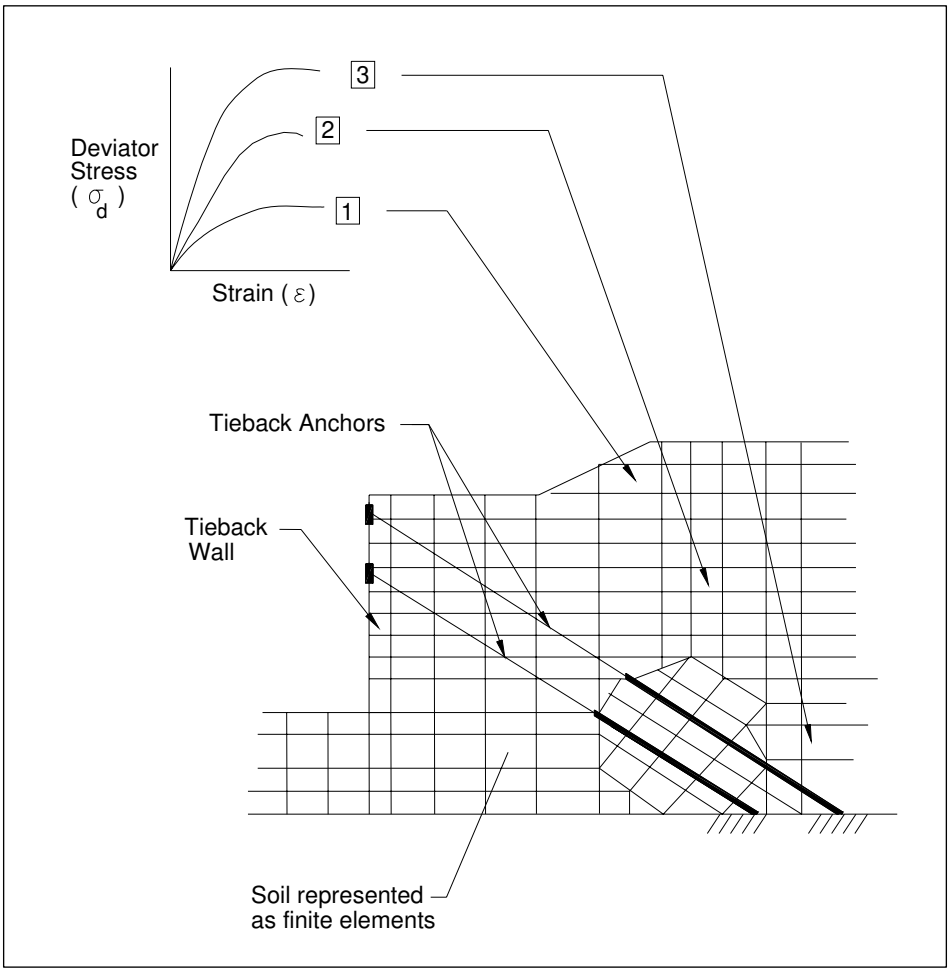

Figure 4.6. Example of nonlinear finite element model (NLFEM)

demonstrated through the comprehensive NLFEM analysis of Bonneville lock temporary tieback wall that the behavior assumed using simplified procedures was inconsistent with observed behavior.

4.6 DESIGN METHODS FOR FLEXIBLE TIEBACK WALL SYSTEMS

4.6.1 Background

A typical vertical sheet-pile system with wales and post tensioned tieback anchors is shown in Figure 4.7. The vertical sheet-pile system is usually constructed by driving a line of interlocking Z-type steel piling using traditional-pile driving equipment to form a continuous wall. The function of the wall is to resist earth pressure and water loads. Wales are horizontal

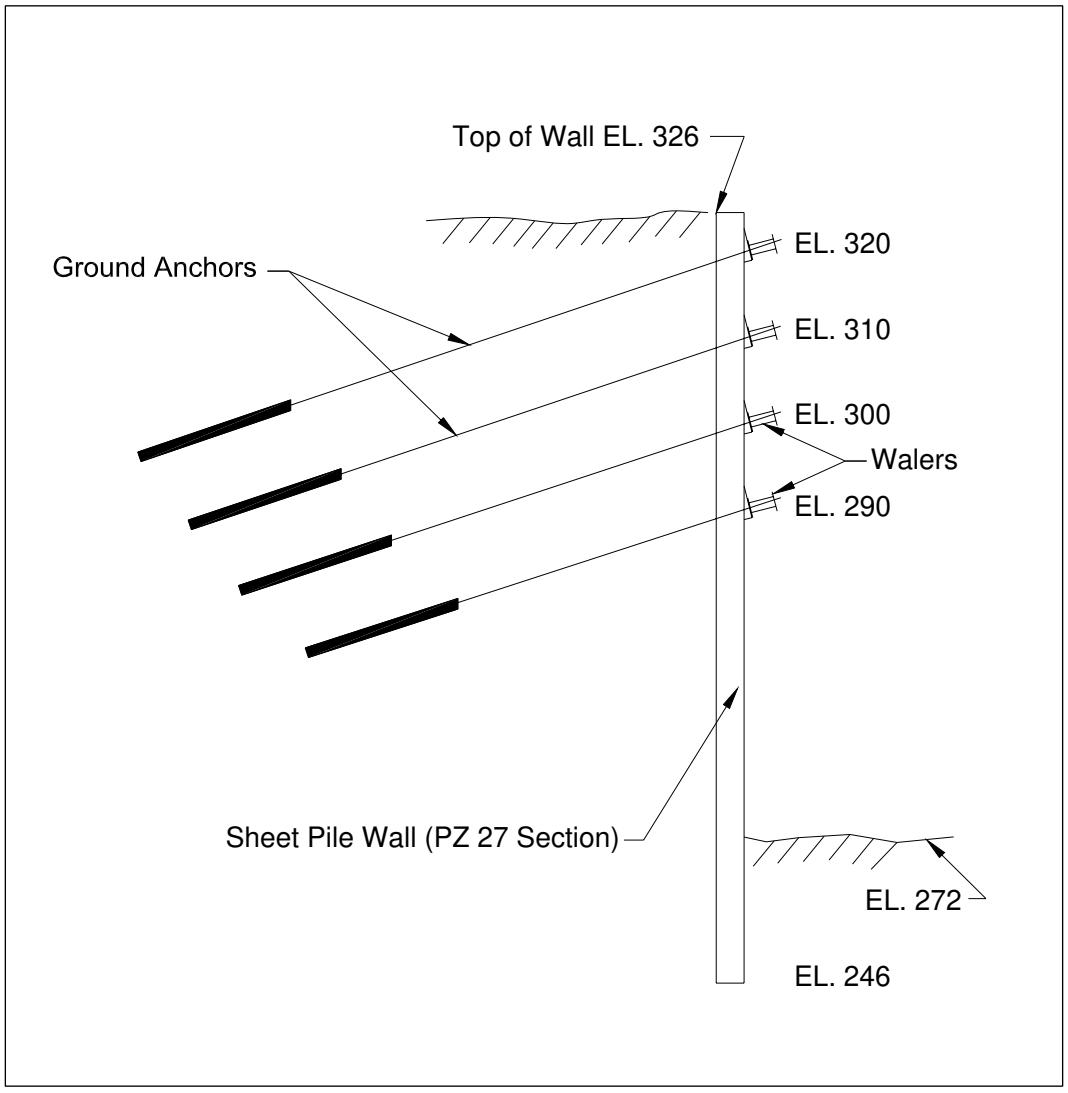

Figure 4.7. Vertical sheet-pile system with post-tensioned tieback anchors (per Olmstead Prototype wall and after Strom and Ebeling 2001)

stiffeners that span between the tieback anchors. These stiffeners transfer loads from the sheet pile to the tieback anchors. Wales normally consist of standard steel channel sections.

Prestressed grouted tieback anchors or (often termed ground anchors) are structural elements used to transfer an applied tensile load to the ground. The basic components of a ground anchor include the anchorage, the unbonded length, and the bond length. These and other components of a tieback anchor are shown in Figure 4.8. The anchorage consists of the anchor head, bearing plate, and trumpet that transmits the prestress force from the prestressing

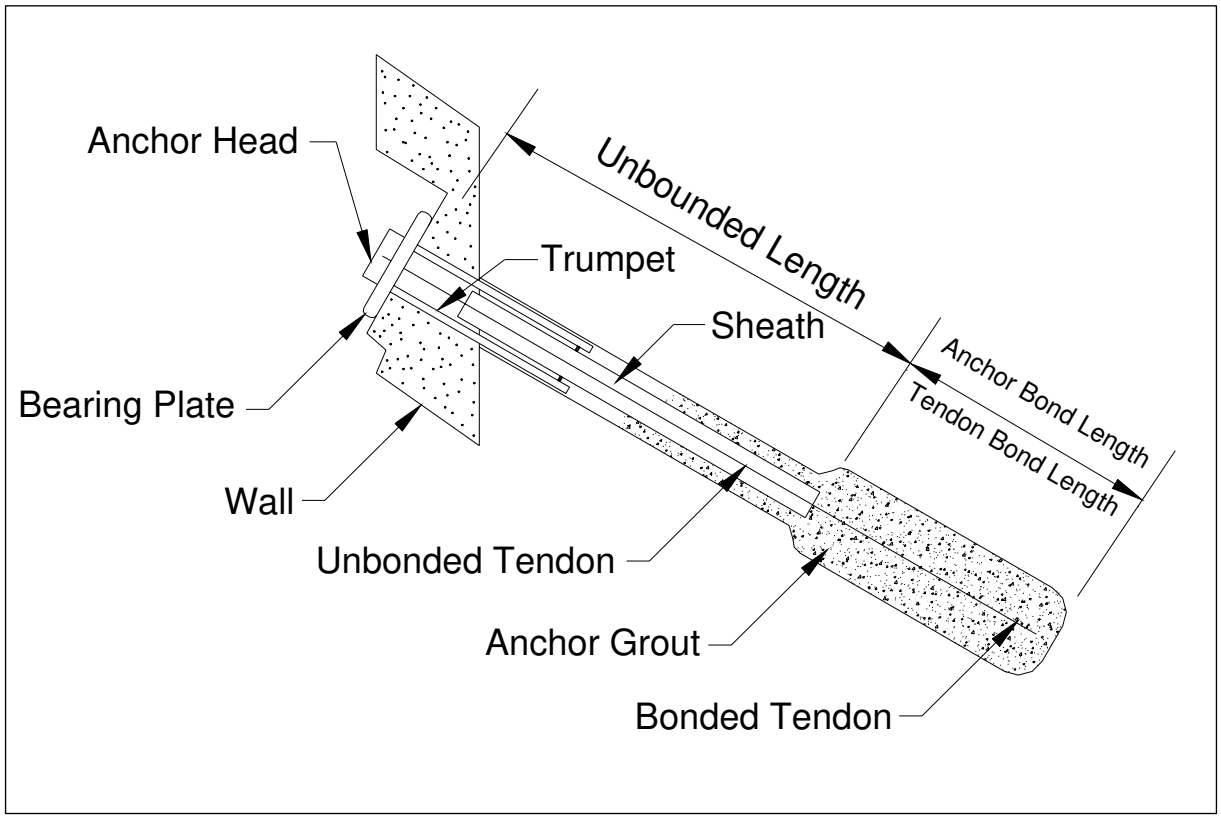

Figure 4.8. Components of a ground anchor (after Figure 8.1 Strom and Ebeling 2001 and Figure 1 of Sabatini, Pass and Bachus 1999)

steel (bar or strand) to the tieback wall. The unbonded length is that portion of the prestressing steel that is free to elongate elastically and transfer the resisting force from the bond length to the tieback wall. A bondbreaker is a smooth plastic sleeve that is placed over the tendon in the unbonded length to prevent the prestressing steel from bonding to the surrounding grout. The bondbreaker also enables the pre-stressing steel in the unbonded length to elongate without obstruction during testing and stressing, and leaves the prestressing steel unbonded after lock-off. The tendon bond length is the length of the prestressing steel that is bonded to the grout and transmits applied tensile force to the ground. The anchor bond length should be located behind the critical failure surface as shown in Figure 4.9. A portion of the complete tieback anchor assembly is referred to as the tendon. The tendon includes the prestressing steel

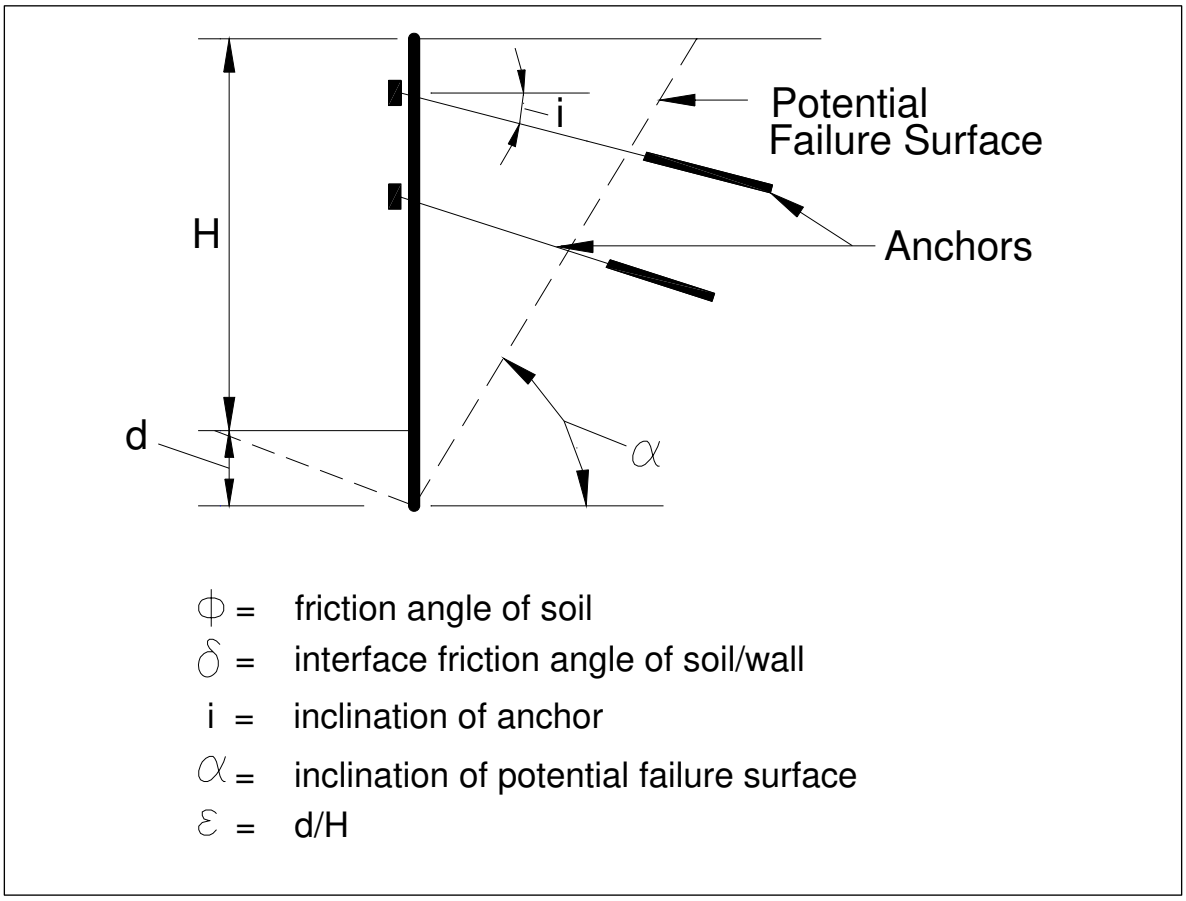

Figure 4.9. Potential failure surface for ground anchor wall system

element (strands or bars), corrosion protection, sheaths, but specifically excludes the grout. The sheath is a smooth or corrugated pipe or tube that protects the prestressing steel in the unbonded length from corrosion. The grout is a portland cement-based mixture that provides load transfer from the tendon to the grout and provides corrosion protection for the tendon. There are three main ground anchor types that are currently used in the United States:

1. Straight-shaft gravity-grouted ground anchors (Type A).
2. Straight-shaft pressure-grouted ground anchors (Type B).
3. Post-grouted ground anchors (Type C).

Although not common today in U.S. practice, another type of anchor is the under-reamed anchor (Type D). These ground anchor types are illustrated in Figure 4.10.

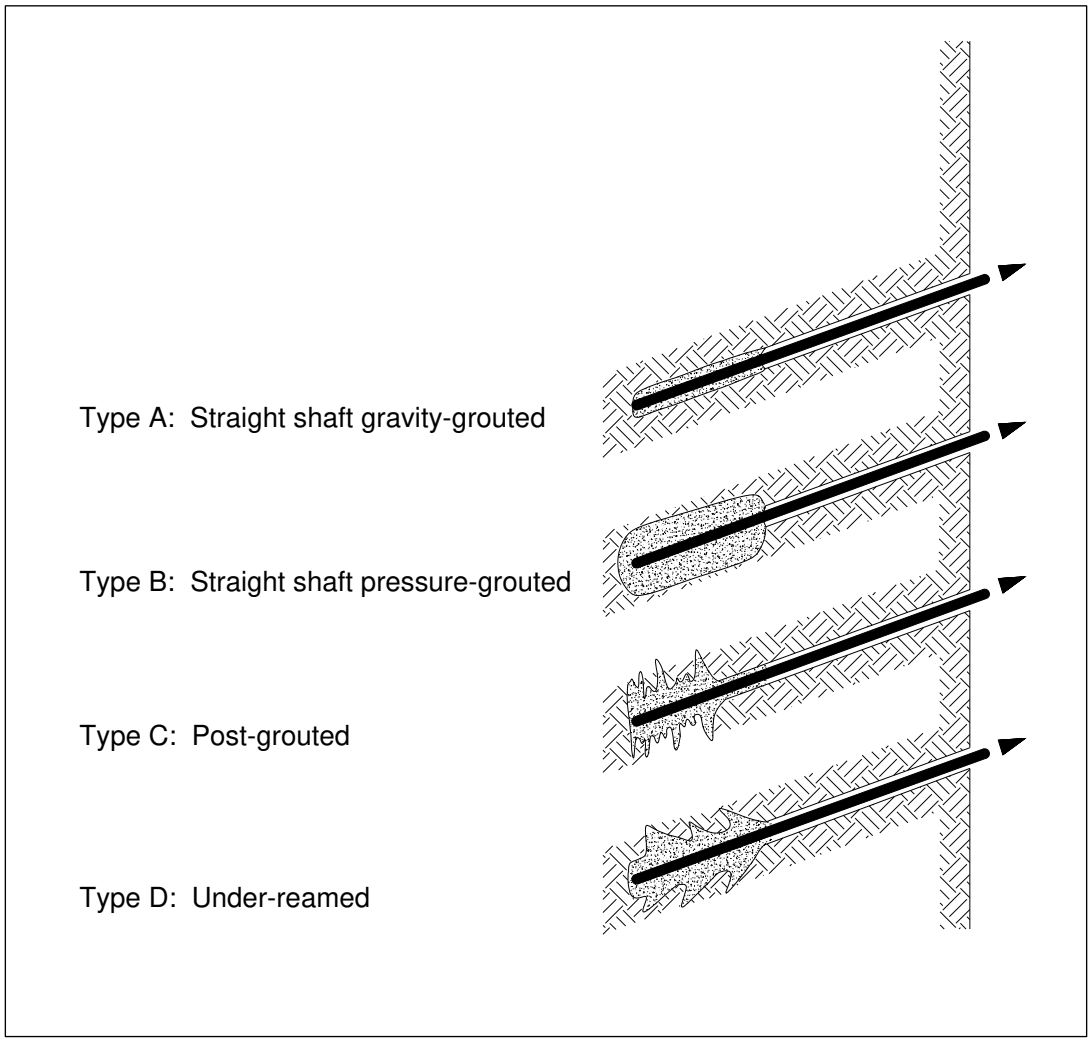

Figure 4.10. Main types of a ground anchors (after Figure 8.2 Strom and Ebeling 2001 and Figure 4 of Sabatini, Pass and Bachus 1999)

4.6.2 Overview of Design Methods for Flexible Tieback Walls

In general practice, the use of soil pressure envelopes (often referred to as apparent pressure diagrams) as loading on a beam on rigid support analysis provides an efficient means for initial layout and sometimes a final design of tieback wall systems. Apparent pressure diagrams were first developed by Terzaghi and Peck (1967) and Peck (1969). Figure 4.11 shows apparent pressure diagrams proposed by Peck (1969). These diagrams represent an envelope of pressures on braced excavation wall systems. The pressure diagrams were

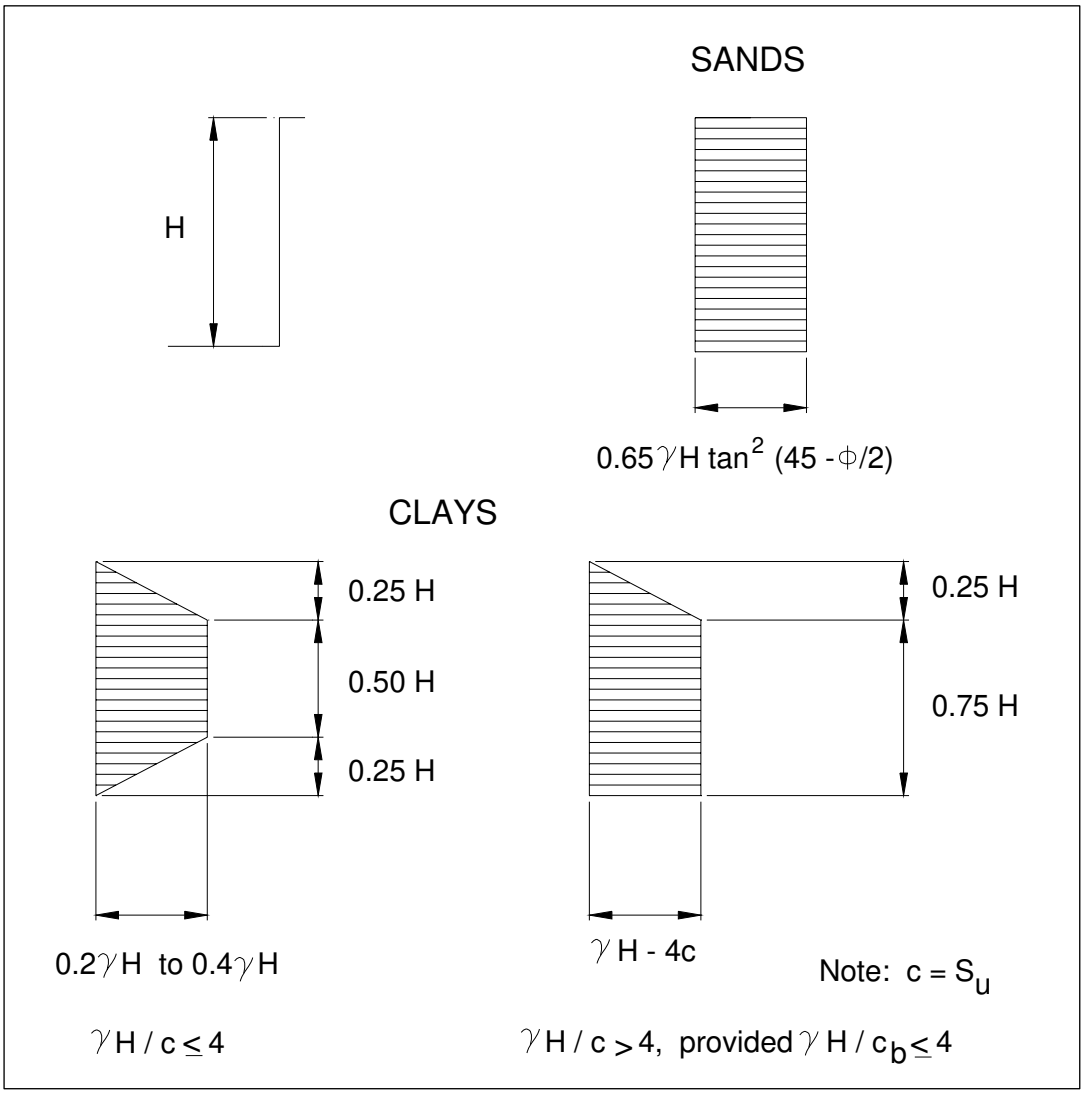

Figure 4.11. Apparent earth pressure diagrams by Terzaghi and Peck

obtained by back-calculations from field measurement of strut loads. However, these soil pressure envelopes or apparent earth pressure diagrams were not intended to represent the actual earth pressure distribution acting on the tieback wall system, but instead they constituted hypothetical pressures. These hypothetical pressures were a basis from which there could be calculated strut loads that might be approached but would not be exceeded in the actual cut.

Design procedures used by the Federal Highway Administration (FHWA) publication (Weatherby 1998; Sabatini, Pass, and Bachus 1999) utilize apparent earth pressure diagrams that are modifications of the apparent earth pressure diagrams developed by Terzaghi and Peck. Figures 4.12 and 4.13 show recommended apparent earth pressure diagrams and formulas for walls supported by a single row of anchors and multiple rows of anchors respectively. The FHWA procedures include a modified equation by Henkel (1971) used to calculate the maximum earth pressure ordinate for the Terzaghi and Peck (1967) soft to medium clay apparent pressure diagram. This modification was due to an assumed failure mechanism in which deep-seated movements occurred which were not considered by Peck and Terzaghi. Henkel found that Peck's method under-predicted the back-calculated values of active earth pressure coefficients when considering deep seated movements for excavations. The FHWA design procedures proposed by Weatherby (1998) also includes a variation in the Terzaghi and Peck's apparent earth pressure distribution for sand and stiff to hard fissured clay. Weatherby noted that the earth pressure distribution for anchored wall with flexible elements is influenced by the prestressing and lock-off procedure used for each anchor. He noted that earth pressures concentrate at anchor locations. The apparent earth pressure diagrams for anchored walls in sand and stiff to hard fissured clay require that the location of the uppermost and lowermost anchor be known. Thus, the distribution of earth pressure is influenced by the excavation depth (as in the case of Terzaghi and Peck apparent earth pressure diagrams), and also influenced by the location of the anchors.

Additionally, FHWA procedures (Weatherby 1998; Sabatini, Pass, and Bachus 1999) allow the apparent earth pressure diagrams to be constructed based on a "total load" approach. The total load on the wall is determined from a limit equilibrium analysis and factors of safety

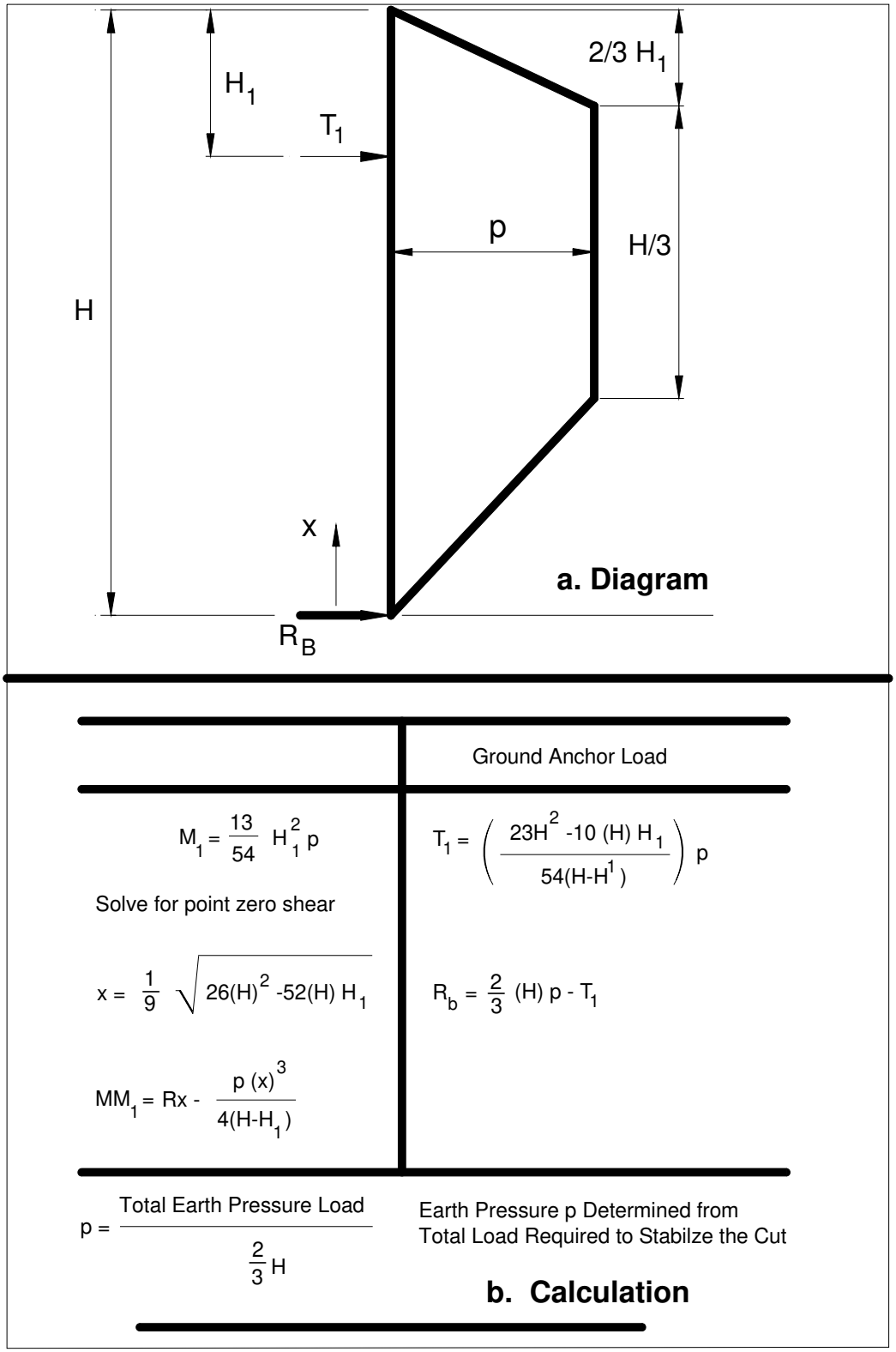

Figure 4.12. Recommended apparent pressure diagram by FHWA for a single row of anchors (after Strom and Ebeling 2001)

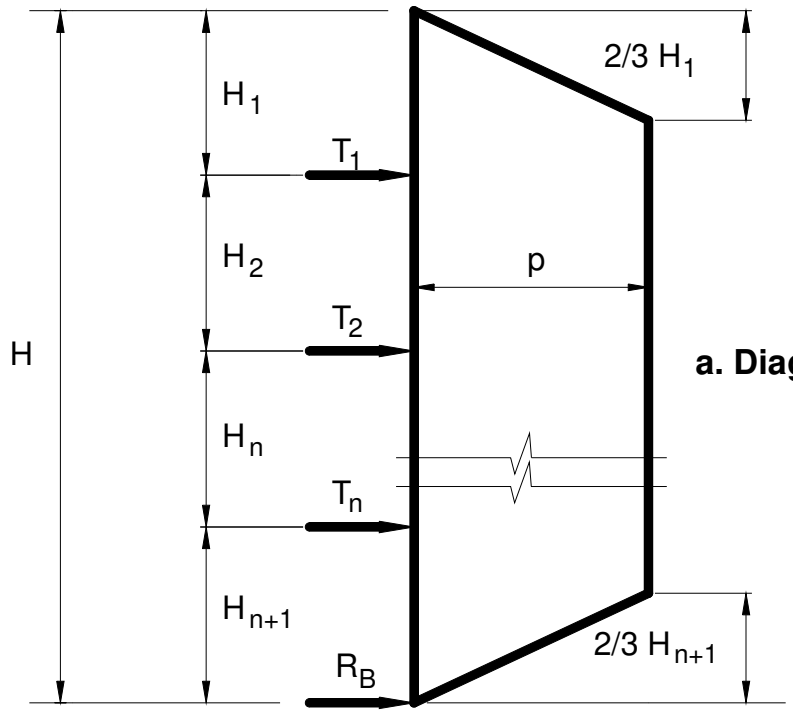

a. Diagram

Soldier Beam Moments

M_2 = larger of MM_1 or MM_2

M_n = larger of MM_{n+1} or MM_n

$$M_1 = \frac{13}{54} H_1^2 p$$

$$MM_1 = \frac{1}{10} H_2^2 p$$

$$MM_2 = \frac{1}{10} H_3^2 p$$

$$MM_{n-1} = \frac{1}{10} H_n^2 p$$

$$MM_n = \frac{1}{10} H_{n+1}^2 p$$

Ground Anchor Load and Subgrade Reaction

$$T_1 = \left(\frac{2}{3} H_1 + \frac{1}{2} H_2\right) p$$

$$T_2 = \left(\frac{H_2}{3} + \frac{H_3}{2}\right) p$$

$$T_n = \left(\frac{H_n}{2} + \frac{23 H_{n+1}}{48}\right) p$$

$$R_B = \left(\frac{3}{16} H_{n+1}\right) p$$

b. Calculation

$$p = \frac{\text{Total Earth Pressure Load}}{H - \frac{1}{3} H_1 - \frac{1}{3} H_{n+1}}$$

Earth pressure p determined from total load required to stabilze the cut

Figure 4.13. Recommended apparent pressure diagram by FHWA for multiple rows of anchors (after Strom and Ebeling 2001)

are applied to active limit state conditions to obtain a total design load. This total design load is converted to an apparent pressure diagram, which is used as the basis for determining anchor loads and wall bending moments (Figures 4.12 and 4.13). Long, Weatherby, and Cording (1998) showed that the total load from Terzaghi and Peck's (1967) diagram for sand and soft-to-medium clay are equal to the total loads using limiting equilibrium analysis with a factor of safety approximately equal to 1.3 applied to the soil shear strength.

The use of limiting equilibrium analysis for determining ground anchor forces requires that a consistent definition for a factor of safety be used (Long, Weather, and Cording 1998). In practice, there are two approaches used for incorporating factors of safety. In the first approach the total active load (determined by Coulomb, Rankine, or limiting equilibrium) is increased by a factor of safety to obtain the total design load. This approach load is defined as the FS_{Load} method since the factor of safety is applied to the active pressure load. In the second approach, the factor of safety is applied to the soil strength parameters (effective cohesion, c' and the effective angle of internal friction, φ'). This method is defined as the $FS_{Strength}$. In the $FS_{Strength}$ method described in the Corps of Engineers Manual (EM) 1110-2-2502 (Headquarters, of Army (HQDA) 1989), the factor of safety is applied as a strength mobilization factor to the soil strength. The basic equation for factor of safety applied to the shear strength is given as:

$$FS = tan(\varphi') / tan(\varphi' mob) \qquad \text{Equation 4.2}$$

where $\varphi' mob$ is the mobilized angle of internal friction.

Solving for $(\varphi' mob)$ yields:

$$(\varphi' mob) = tan^{-1}\{tan\varphi' / FS\} \qquad \text{Equation 4.3}$$

As mentioned above, the total load represented by the apparent pressure diagram is based on active earth pressure relationship based on limiting equilibrium analysis with a factor of safety of 1.3 applied to the shear strength of the soil. Thus, the $FS_{Strength}$ method for incorporating the factor of safety is the preferred method of the Corps of Engineers for limiting equilibrium analysis. These above modifications to the original Terzaghi and Peck apparent earth pressure diagrams are incorporated into a procedure termed the RIGID analysis procedure for wall with homogenous soil profiles. The RIGID analysis procedure using the apparent earth pressure approach results in "hand calculations" of ground anchor loads and bending moments (Figures 4.12 and 4.13). These diagrams are intended to represent a loading envelope used to design the structural components of flexible tieback wall system reflecting the entire construction and in service history. These diagrams do not represent loads that might exist on the wall at any one time.

4.6.3 Three-Dimensional (3D) Effects on Flexible Tieback Wall Systems

A fundamental 3-D effect on a flexible tieback wall system with multiple rows of prestressed anchors is the presence of discrete or finite constraints along the out of plane direction. Figure 1.3 showed a cross section and plan view of a typical anchored sheet-pile wall system. The plan view shows discrete or finite constraints along the out of plane direction. The actual response of the wall to loading is influence by each of these constraints. A 2-D approximation of the effects of finite constraints is by taking the response of a single constraint and distributing its response between constraints based on the spacing of constraints. This distributed response is assumed to be representative of the actual response of any cross section the wall system taken in the out of plane direction. However, the overall response of the wall system to discrete or finite constraints can be best modeled by

performing a 3-D analysis. Also, a 3-D analysis can be used to evaluate the overall accuracy of the 2-D approximation of the response of a tieback wall system.

Another 3-D effect on this flexible tieback wall system is the phenomenon of soil pressure transfer called arching. An idealized 3-D response for this flexible wall system was shown in Figure 1.5. The simplifying assumptions made in conventional design calculations concerning the linear increase in active and passive pressures in a material do not take into account the interaction between the soil and the structure. Studies have shown that this can have a significant effect on the distribution of earth pressures and the resulting bending moments and shear forces acting on a structure. Dr. Karl Terzaghi defined arching as follows: "If one part of the support of a mass of soil yields, while the remainder stays in place, the soil adjoining the yielding part moves out of its original position between adjacent stationary masses of soil. The relative movement within the soil is opposed by a shearing resistance within the zone of contact between the yielding and the stationary masses. Since the shearing resistance tends to keep the yielding mass in its original position it reduces the pressure on the yielding part of the support and increases the pressure on the adjoining stationary part. This transfer of pressure from a yielding mass of soil onto adjoining stationary parts is commonly called the arching effect and the soil is said to arch over the yielding part of the support. Arching also takes place if one part of a yielding support moves out more than the adjoining parts." (Terzaghi 1959). Therefore, arching involves two parts: a reduction of the earth pressure on a yielding portion of a structure and an increase of the earth pressure on the adjoining portions. The essential features of arching can be demonstrated by the concept of ''trap door" test as shown in Figure 4.14(a). If a section of the wall deflects outward more than the neighboring wall sections (Figure 4.14(b)), the soil adjacent to it will tend to follow.

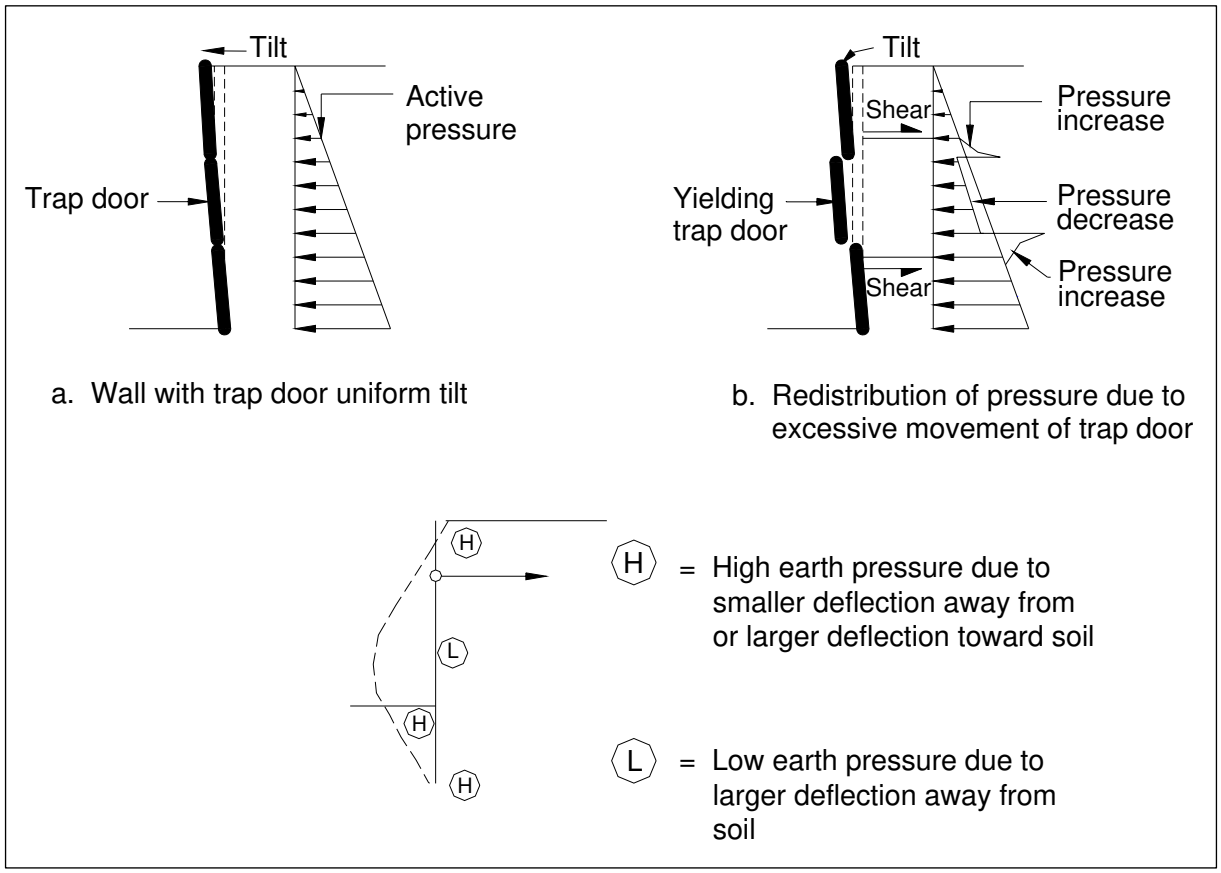

Figure 4.14. Effect of irregular deformation “arching”

Thus the soil pressure on the yielding “trap door” section will decrease. Horizontal shear will develop along the boundaries of this section of soil that resists the yielding of the trap door section of wall. This will cause the soil pressures to increase on the adjoining parts of the wall. These two effects are illustrated in Figure 4.15(a). For a flexible sheet pile wall, these same effects are responsible for the observed pressure redistribution that occurs when the wall deflects. As shown in Figure 4.15(b), the earth pressures both behind and in front of the wall below the dredge level are changed from the classical free earth support distribution as a result of the wall deflections. Behind the wall, the pressures near the top and bottom are increased due to small inward deflections in these areas, while the pressure between the dredge and anchor levels tends to be reduced due to the relatively large outward deflection

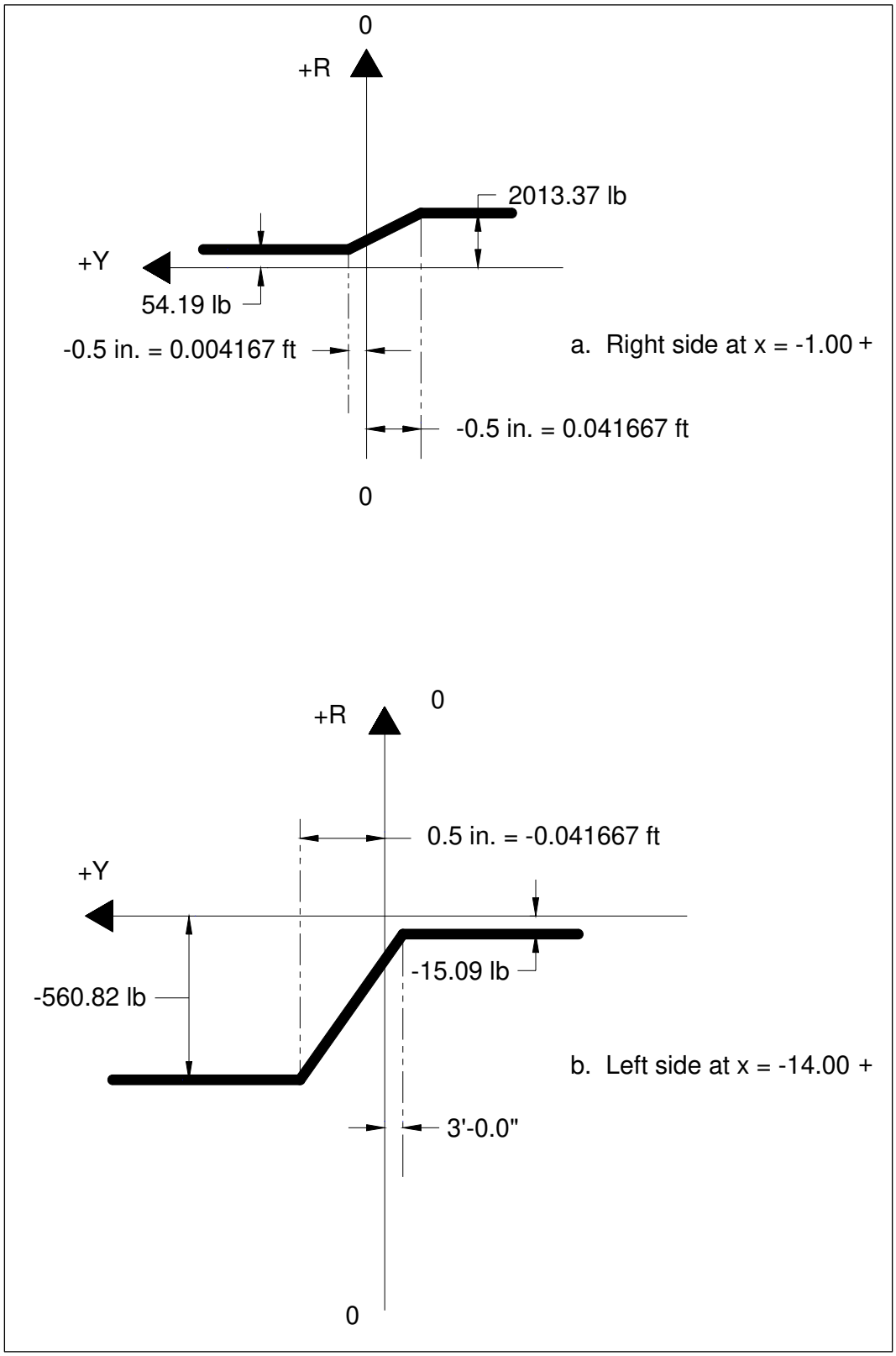

Figure 4.15. Representation of tieback anchor load-deformation response by Winker method (after Figure 2.13 of Strom and Ebeling 2002)

there. Professor Rowe found in his 1948 model tests that these changes in earth pressure were responsible for observed reductions in bending moments on the wall. He observed increased earth pressures behind the wall near the bottom and increased pressure in the front of the wall just below dredge level. These combined pressures produced a clockwise moment that reduces the maximum moment in the wall. Rowe called this "flexure below the dredge level."

Another similar 3-D effect on a flexible tieback wall system is earth pressure redistribution due to the wall flexibility, stressing of ground anchors, construction-sequencing effects, and lagging flexibility. These all cause the earth pressures behind flexible walls to redistribute to, and concentrate at, anchor support locations (FHWA-RD-98-066). This redistribution effect in flexible wall systems cannot be captured by equivalent beam on rigid support methods or by beam on inelastic foundation analysis methods where the active and passive limit states are defined in terms of Rankine or Coulomb coefficients. Additionally, full-scale wall tests on flexible wall systems (FHWA-RD-98-066) indicated the active earth pressure used to define the minimum load associated with the soil springs behind the wall had to be reduced by 50 percent to match measured behavior. It is noted that apparent earth-pressure diagrams used in equivalent beam on rigid support analyses were developed from measured loads, and thus include the effects of soil arching, stressing of ground anchors, construction-sequencing effects, and lagging flexibility, they provide a better indication of the strength performance of flexible tieback wall systems. However, the apparent-pressure diagrams do not represent the actual earth pressure distribution acting on the tieback wall system at any time. Thus, a complete 3-D SSI analysis would provide the best estimate of the actual earth pressure distribution occurring on the wall and provide best approximation of the actual response of the tieback wall.

4.7 DESIGN METHODS FOR STIFF TIEBACK WALL SYSTEMS

4.7.1 Background

As previously described, the measure of wall stiffness for wall systems can be defined as the variation on the inverse of Rowe's flexibility number for walls and is expressed by EI/L^4 where EI is the stiffness of the wall, and L is the distance between supports. Table 4.1 also showed categories for both flexible and stiff wall systems with respect to focus wall systems presented in the Strom and Ebeling (2001) report. Additionally, Table 4.1 showed general stiffness quantifications in terms of flexural stiffness (EI) per foot run of wall and in terms of the relative flexural stiffness (EI/L^4). The stiffness quantifications were based on an approach described in FHWA-RO-75. A continuous reinforced concrete slurry wall system, categorized as a "stiff wall" was selected for investigation in this research endeavor. This type of wall system is commonly used in Corps of Engineers design projects.

4.7.2 Overview of Design Methods for Stiff Tieback Walls

Other researchers have concluded that a key factor in the evaluation of stiff tieback wall systems is to perform construction-sequence analyses, since for such systems the temporary construction stages are often more demanding than the final permanent condition (Kerr and Tamaro 1990). Although numerous types of construction-sequencing analyses have been used in the design of tieback wall systems, there are three construction sequencing procedures considered to be the most promising for the evaluation and design of Corps of Engineer tieback wall systems (Strom and Ebeling 2002). These three procedures are:

1. Equivalent beam on rigid supports by classical methods (identified as the RIGID 2 method).

2. Beam on inelastic foundation methods using elastoplastic soil-pressure deformation curves (R-y curves) that account for plastic (nonrecoverable) movements (identified as the WINKLER 1 method).
3. Beam on inelastic foundation methods using elastoplastic soil-pressure deformation curves (R-y curves) for the resisting side only with classical soil pressures applied on the driving side (identified as WINKLER 2 method).

Descriptions of the (RIGID 1 Method) and above-mentioned construction-sequencing methods for stiff tieback wall systems are summarized in the following paragraphs.

4.7.2.1 RIGID 1 Method

In this method, a vertical section of the tieback is modeled as a multiple-span beam supported on rigid supports located at the tiebacks in the upper region of the wall. The lowermost rigid support is assumed to occur at finish grade. The wall is loaded on the driving side with an apparent earth pressure loading. In general practice, the use of soil-pressure envelopes as loading for a beam on rigid support analysis provides an expedient method for the initial layout and sometimes the final design of tieback wall systems. However, these soil-pressure envelopes, or apparent pressures diagrams were not intended to represent the real distribution of earth pressure, but instead constituted hypothetical pressures. These hypothetical pressures were a basis from which there could be calculated strut loads that might be approached but would not be exceeded during the entire construction process. As previously discussed, apparent pressure diagrams, were based on measurements made during construction that included effects of soil arching, wall flexibility, preloading of supports, construction sequencing, etc. However, with stiff wall systems, these effects will not affect the earth pressure distribution to the same extent as for flexible wall systems. Therefore, in

practice, construction sequencing analyses and beam on inelastic foundation analyses are considered valid tools for the investigation of stiff wall systems (Strom and Ebeling 2002). However, the RIGID 1 method can be used as a preliminary design tool to estimate upper anchor loads and bending moments in the upper region of the wall. Refer to Figure 4.1 for an illustration of the Rigid 1 method.

4.7.2.2 RIGID 2 Method

The RIGID 2 method, as with the RIGID 1 method, models a vertical section of the tieback wall as a multiple span beam supported on rigid supports that are located at tieback points. The lowest support location is assumed to be below the bottom of the excavation at the point of zero net pressure (Ratay 1996). In the method, two earth pressure diagrams are used in each of the incremental excavation, anchor placement, and pre-stressing analyses. Active earth pressure (or at-rest pressure when wall displacements are critical) is applied to the driving side of the wall and extends from the top of ground to the actual bottom of the wall. Passive earth pressure (based on a factor of safety of 1.0 applied to the shear strength of soil) is applied to the resisting side of the wall and extends from the bottom of the excavation to the actual bottom of the wall. The RIGID 2 method is useful for determining if the wall and anchor capacities determined by the RIGID 1 analysis are adequate for stiff wall systems and is used for redesigns of both flexible and stiff tieback wall systems to ensure that strength is adequate for all stages of construction. However, a RIGID 2 analysis does not provide useful information regarding to displacement demands on the tieback systems.

4.7.2.3 WINKLER 1 Method

The WINKLER 1 method incorporates idealized elasto-plastic springs to represent the soil load-deformation response and anchor springs to represent the tieback anchor

load-deformation response. Figure 4.15 illustrates the key features of an elasto-plastic springs representing the soil-deformation response. One popular procedure of modeling the elasto-plastic curves (R-y) representing the soil springs is based on the reference deflection method (FHWA-RD-98-066) is incorporated in the WINKLER 1 method and is incorporated in the CASE computer program CMULTIANC (Dawkins, Strom and Ebeling 2003). In the WINKLER 1 method, the elasto-plastic curves can be shifted with respect to the undeflected position of the tieback wall to capture plastic (non-recoverable) movements that may occur in the soil during construction stages. (e.g., excavating, anchor placement and prestressing of anchors). The R-y curve shifting can be used to consider nonrecoverable active yielding that occurs in the retained soil during first-stage excavation (i.e., cantilever-stage excavation). Following the first-stage excavation, the R-y curve shifting can help capture the increase in earth pressure that occurs behind the wall as anchor prestress load is applied and during the second stage excavation. This curve shifting procedure is described in example problems in (Strom and Ebeling 2002). Figure 4.16 shows graphical results of R-y shifting of the first stage excavation for a stiff tieback wall system with a single tieback anchor. This problem was taken from FHWA-RD-81-150 and is identified as the "Soletanche Wall Example." The WINKLER 1 method is useful for determining if the anchor and wall capacities determined by a RIGID 1 or RIGID 2 analysis are adequate. The WINKLER 1 method also can be used to redesign stiff tieback wall system to ensure that strength is adequate for all stages of construction. This method provides information on "relative" displacement demands when it becomes necessary to meet displacement-based performance objectives. Refer to Figure 4.2 for an illustration of the WINKLER 1 method.

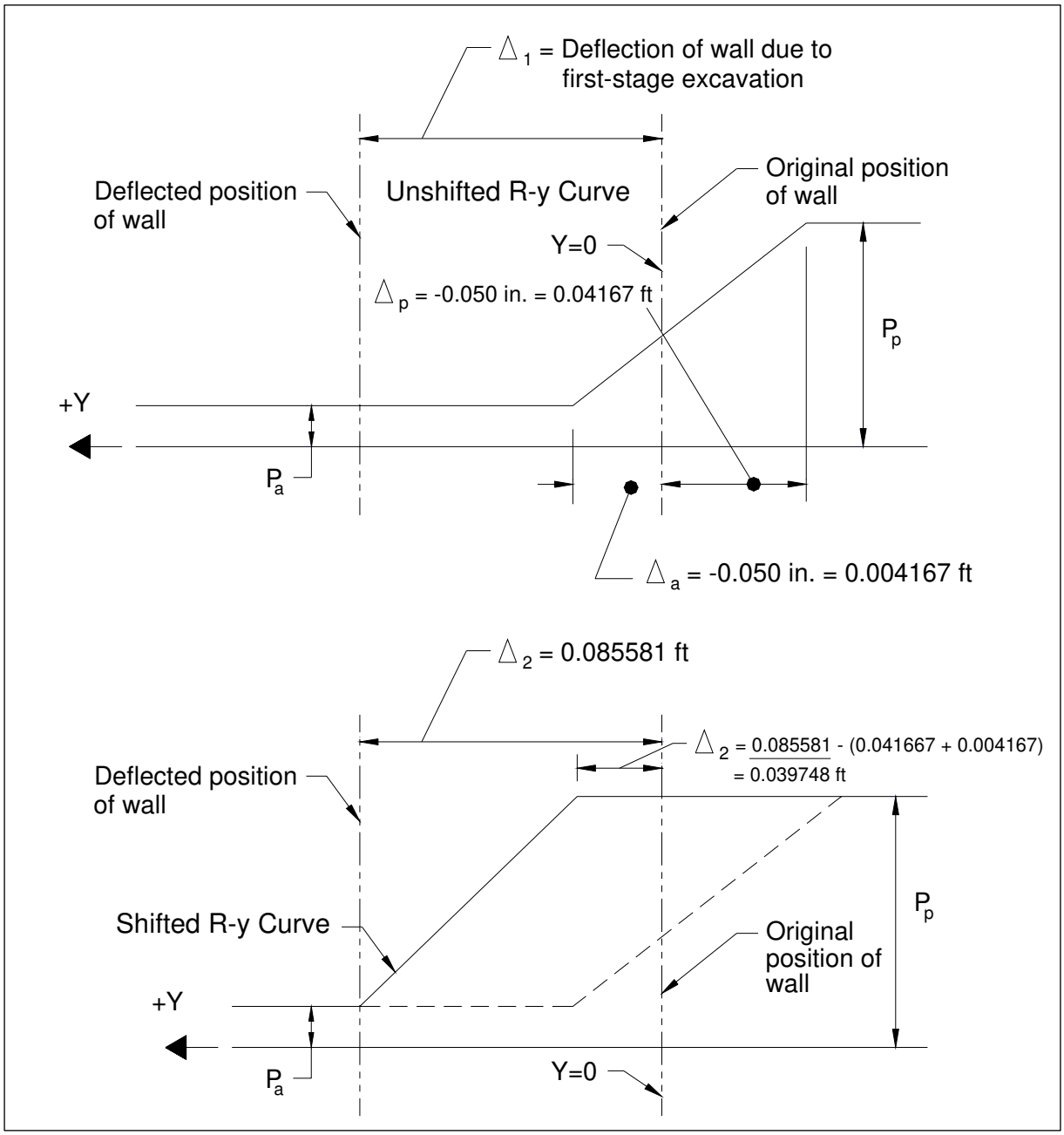

Figure 4.16. Example of R-Y curve shifting for first stage excavation of stiff tieback wall (after Figure 2.16 of Strom and Ebeling 2002)

4.7.2.4 WINKLER 2 Method

The WINKLER 2 method idealizes a simple beam on inelastic foundation and uses the soil loading on the driving side of the wall in an incremental analysis consisting of excavation, anchor placement, and anchor prestressing. The elasto-plastic curves representing

the soil springs are based the reference deflection method, which is also utilized in the WINKLER 1 method. Anchor springs are used to represent the ground anchor load-deformation response. In this method, the R-y curve shifting is not included and thus the WINKLER 2 method is unable to capture the non-recoverable plastic movements that may occur during various stages of construction. The WINKLER 2 method is not considered to be as reliable as the WINKLER 1 method. However, the WINKLER 2 method has been shown to be useful for determining if the wall and anchor capacities determined by a RIGID 1 or RIGID 2 analysis are adequate. The WINKLER 2 method also permits the redesign of stiff tieback wall systems to ensure that strength is adequate for all stages of construction.

4.7.3 Three-Dimensional (3D) Effects on a Stiff Tieback Wall System

As with the flexible tieback wall, a fundamental geometrical effect of the presence of discrete or finite constraints along the out of plane direction is also applicable for stiff tieback walls. Figure 1.4 showed a cross section and plan view of a typical continuous slurry trenched tremie concrete wall (i.e., stiff) wall system. The plan view shows discrete or finite constraints along the out of plane direction. The actual response of the wall to loading is influence by each of these constraints. Generally, 2-D analysis approximate the effects of finite constraints by taking the response of a single constraint and distributing its response between constraints based on the spacing of constraints. This distributed response is assumed to be representative of the actual response of any cross section along the wall system taken in the out of plane direction. However, the overall response of the wall system with discrete or finite constraints can be best modeled by performing a 3-D analysis. Also, a 3-D analysis can be used to evaluate the overall accuracy of the 2-D approximation of the response of a slurry trenched tremie concrete wall (i.e., stiff wall system).

Another 3-D effect on tieback wall systems is earth pressure redistribution due to the soil arching, stressing of ground anchors, construction-sequencing effects, and wall flexibility. An idealized 3-D response for this stiff wall system was shown in Figure 1.6. As shown, the earth pressures have a more uniform distribution than the distribution for a flexible wall system. This indicates that the earth pressure redistribution (soil arching) would be less for a stiff wall system than for a flexible wall system.

CHAPTER 5

ENGINEERING ASSESSMENT OF CASE STUDY RETAINING WALL NO. 1

5.1 BACKGROUND

5.1.1 Project Site Description

The Bonneville Lock and Dam is located on the Columbia River, approximately 42 miles east of Portland, OR. Because the Oregon-Washington state boundary follows the Columbia River channel, the lock and dam site was divided between the two states. The new lock was constructed on the Oregon side of the river and landward (southwest) of the old lock. The new lock has a greater lockage volume (30-million-ton capacity) than the old lock (13-million-ton capacity) and it helps reduce shipping bottlenecks at this location on the river.

The temporary tieback wall retains the sides of the excavation for construction of the lock channel and an upstream miter gate section. This wall was completed in February 1998 and adjoins a permanent guard wall that protects the upstream channel. Both walls were installed by the slurry trench method of construction. At the beginning of this project, the main northwest rail line of the Union Pacific Railroad (UPRR) was relocated parallel to and 50 ft landward from the temporary tieback wall. This relocation required the excavation of a large volume of the slope and highway fill materials. A plan view of the project site is shown in Figure 5.1.

5.1.2 Project Site Geology

Extensive exploration, sampling, and testing were performed to characterize this site. The site geology is a result of ancient landslides, alluvial and volcanic deposits from floods. The temporary wall is located near the toe of the Tooth Rock Landslide. A large amount of the

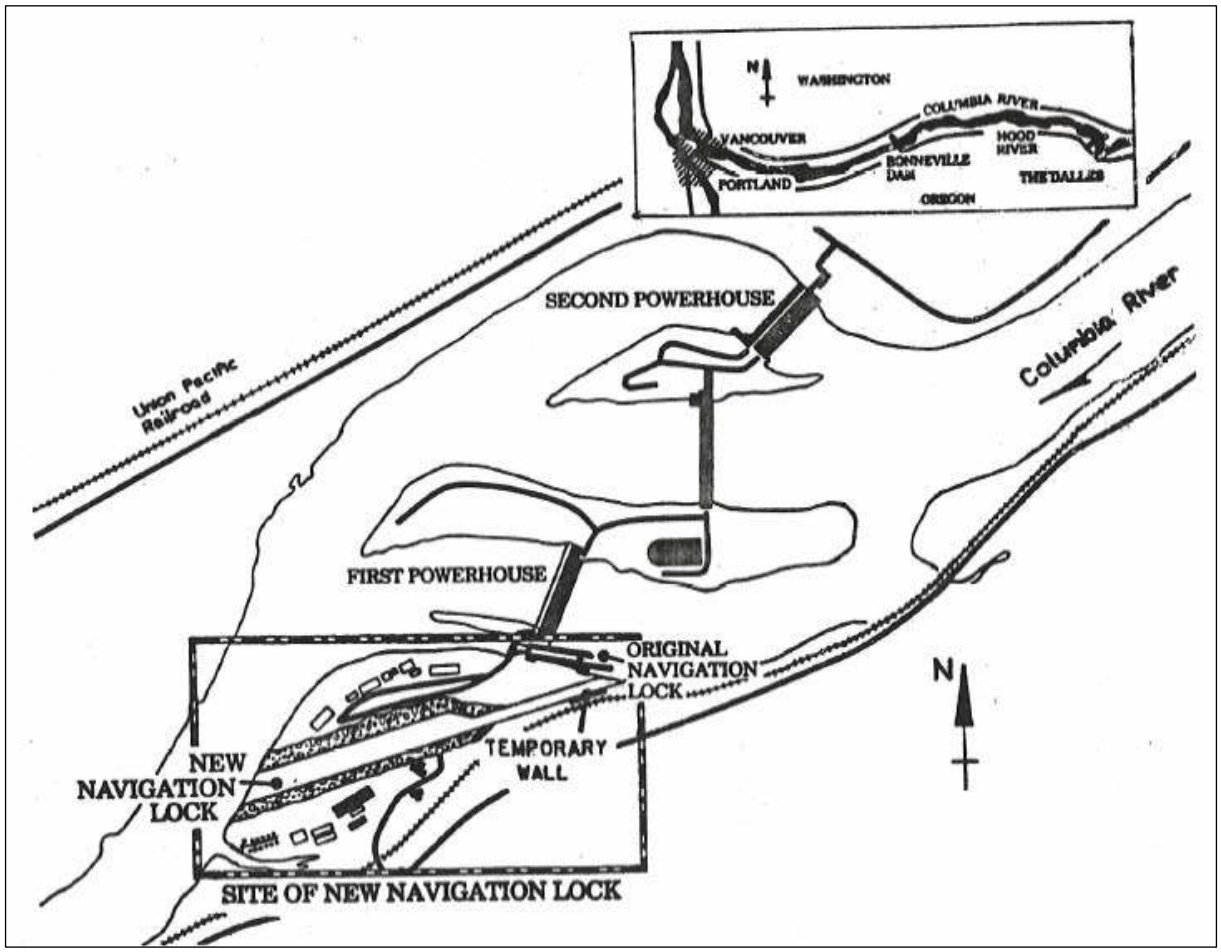

Figure 5.1. A plan view of the project site (after Knowles and Mosher 1990)

material retained by the wall is debris from the slide. The Tooth Rock Landslide is a Pleistocene Age, deep-seated slump consisting primarily of large displaced slide blocks (SB) and unconsolidated slide debris (SD). Slope stability analyses, along with evaluation of surface movement, indicated that this slide unit is stable. The slide blocks are derived mainly from the underlying weigle formation (Tw). These blocks range from tens to hundreds of feet across. The slide debris is a mixture of decomposed clayey rock materials ranging from granular deposits to boulders. River work and erosion on the SD have produced a new distinct material called reworked slide debris (RSD), a medium-dense granular deposit. RSD is a heterogeneous mixture of gravels, cobble- to boulder-size rounded rocks, and a mixture of

fine sands and silts. Ancient flood deposits of silt and sand cover much of the ground surface above the RSD. Beneath the Tooth Rock Landslide are two intact rock units: (a) the Tw, a sedimentary, “soft rock” material consisting of volcanic derived mudstone, siltstone, and claystone, and (b) the Bonney rock intrusive (Ti), a large, irregular diabase unit with columnar jointing intruding the older weigle formation. A geologic profile at the wall section under study was developed from boring logs and section profiles. This profile is shown in Figure 5.2.

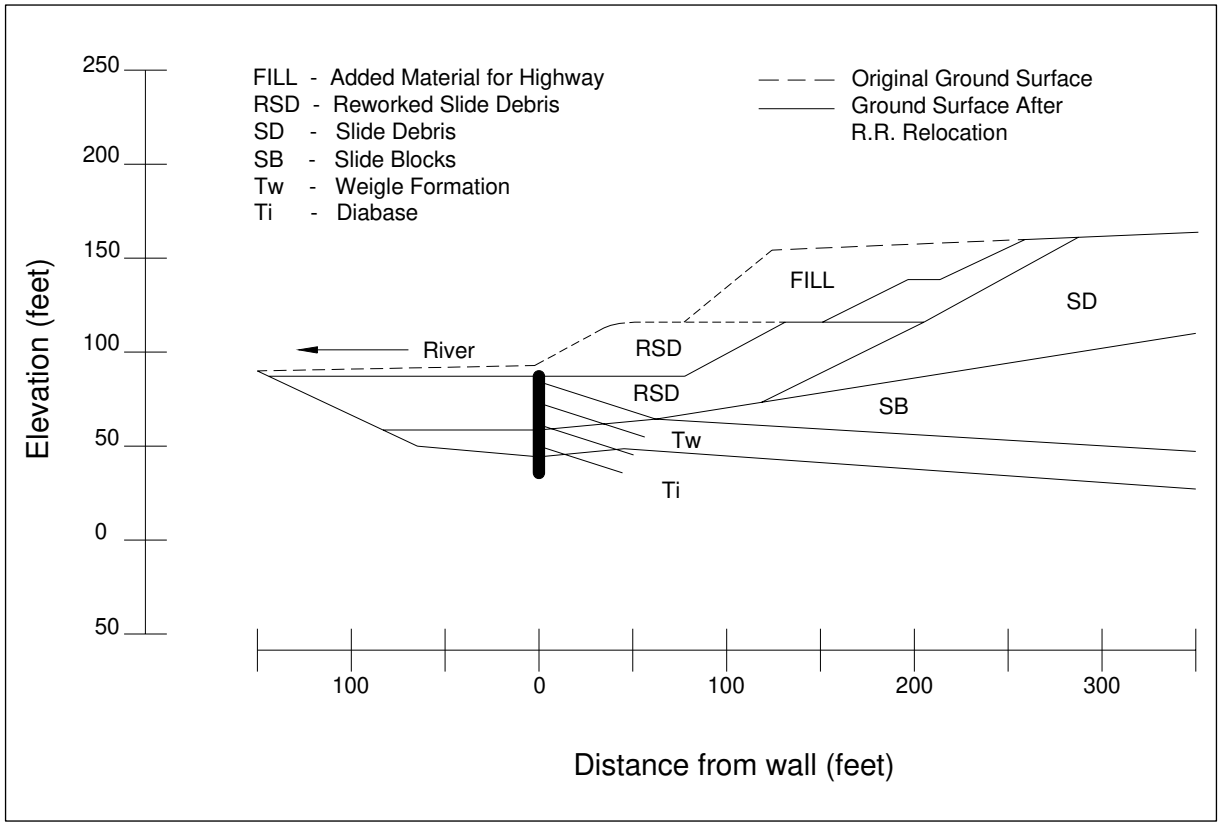

Figure 5.2. Geologic profile at Panel 6 (after Knowles and Mosher 1990)

5.1.3 Design Criteria

In order to prevent settlement of the nearby railroad foundation and to eliminate the possibility of initiating a landslide in the construction area, the maximum allowable horizontal wall deflection under normal loads was set to 0.1 ft (1.2 in.) toward the river at points along

the height of the wall. The design failure surfaces were determined using slope stability limit equilibrium procedures with a factor of safety equal to 1.5 for static load conditions. The unbonded lengths of the tendons were set so the bonded zones were beyond the design failure surfaces. A factor of safety of 2.0 was applied to the ultimate grout to soil bond stress to determine required bonded lengths. The tendons were sized using ACI 318-83 with one exception to section 18.5.l(c). The tendon loads were not to exceed 75 percent, instead of the normal 80 percent, of the ultimate tensile strength during anchor testing. Maximum performance and proof testing loads were 1.5 times the design load. Reinforced concrete was designed using ACI 318-83. The maximum allowable horizontal wall deflection of 1.2 in. was used as a limiting value in both the two-dimensional (2-D) and three-dimensional (3-D) finite element analyses.

5.1.4 Wall Description

The temporary tieback retaining wall is approximately 440 ft long. It was constructed in two phases: a 180-ft-long section and a 260-ft-long section. The heights of the panels range from 20 to 110 ft, depending on the depth to the diabase. The top of each panel in this section is at elevation (el) 89 ft. Each panel was seated at least 2 ft in the diabase for stability and seepage control. Dewatering efforts upstream and behind the wall were done to minimize seepage effects.

The diaphragm wall was constructed by the slurry trench method. In this method, each of the panels was individually built according to the following procedure. A 3- by 20-ft concrete form was placed at the ground surface in the location of the panel. This form guided a clamshell bucket as it excavated soil for the panel construction. As excavation progressed, a bentonite slurry head was maintained in the hole. Excavation continued until a minimum of

2 ft of diabase was recovered from the bottom of the hole. A crane then placed the steel reinforcing cage into the slurry-filled excavation and concrete was tremmied in, displacing the slurry.

After the wall was completed, excavation for the lock and channel was initiated. Soil was removed on the north face of the wall from the ground surface down to the top of the diabase. The material removed consisted mainly of RSD and varying amounts of the weigle. Pre-stressed anchors were installed as excavation progressed. Panel 6 of this wall's 50-ft-tall panel was instrumented with strain gages and a slope inclinometer. The data from these instruments was used to evaluate wall performance and provided information for future construction. Instrumentation results of bending moments (computed from strain measurements) and wall movement for the end of construction is shown in Figure 5.3.

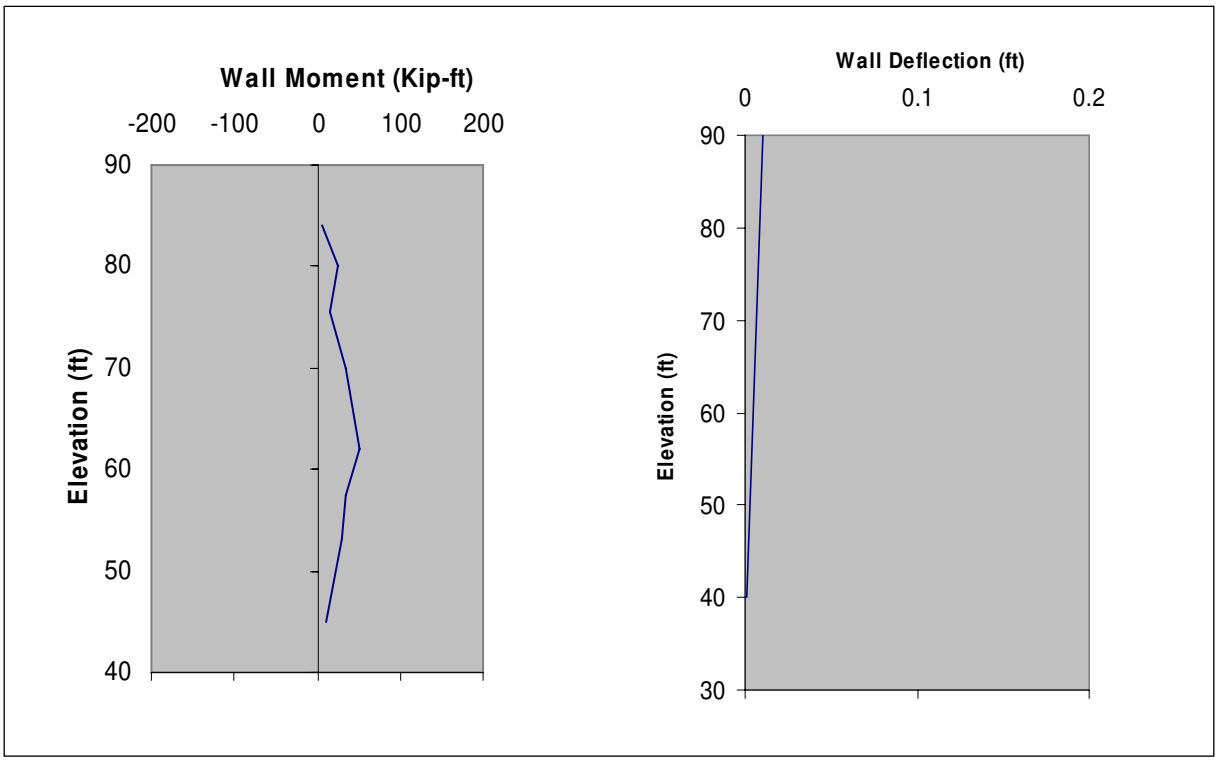

Figure 5.3. Instrumentation results for Panel 6 at end of construction

5.1.5 Tieback Anchors

Tiebacks were installed in a grid pattern of approximately 12 ft horizontal by 11 ft vertical. All anchors at the same elevation were installed before anchors at the next lower row were installed. The installation procedure consisted of drilling, grouting, prestressing, and lockoff. The tiebacks consisted of 7-strand, high-strength steel tendons. The anchorage in the soil was formed by pressure grouting. The unbonded length of the tie varied from 37 to 74 ft with each anchor, depending on the distance past the critical slip plane, was determined from limit equilibrium methods. The minimum bonded length is 30 ft for anchorage in the RSD and 35 ft in Tw. Tieback corrosion protection includes cement-grout protection over the bonded length and a grease-filled sheath over the unbonded length. All grout strengths tested above the minimum design strength of 3,000 psi. Each anchor was prestressed for a proof test and creep test by the application of a load 50 percent above the design load (DL) of the anchor. The design loads are approximately one-half (safety factor = 2) of the ultimate load capacities for the anchors as determined by the field tests detailed in the Tieback Test Program, Phase II Report (U.S. Army Corps of Engineers (USACE), Portland 1986). The design bond stress for RSD is 60 psi and 35 psi for the weigle. Figure 5.4 shows a cross section view of the wall at Panel 6. Following the prestressing, anchors were locked off at loads near their design load. Table 5.1 provides information on the four levels of anchors in Panel 6.

5.2 RESULTS OF CURRENT 2-D DESIGN METHODOLOGIES FOR "STIFF" TIEBACK WALL SYSTEMS

As presented in Chapter 4 and described in Strom and Ebeling (2001), there are various tieback wall design and analysis procedures for stiff wall systems. The case study temporary tieback wall described above is a stiff wall system in which the excavation that took place prior to tieback installation occurs to a depth of 5.5 ft below the tieback location. This

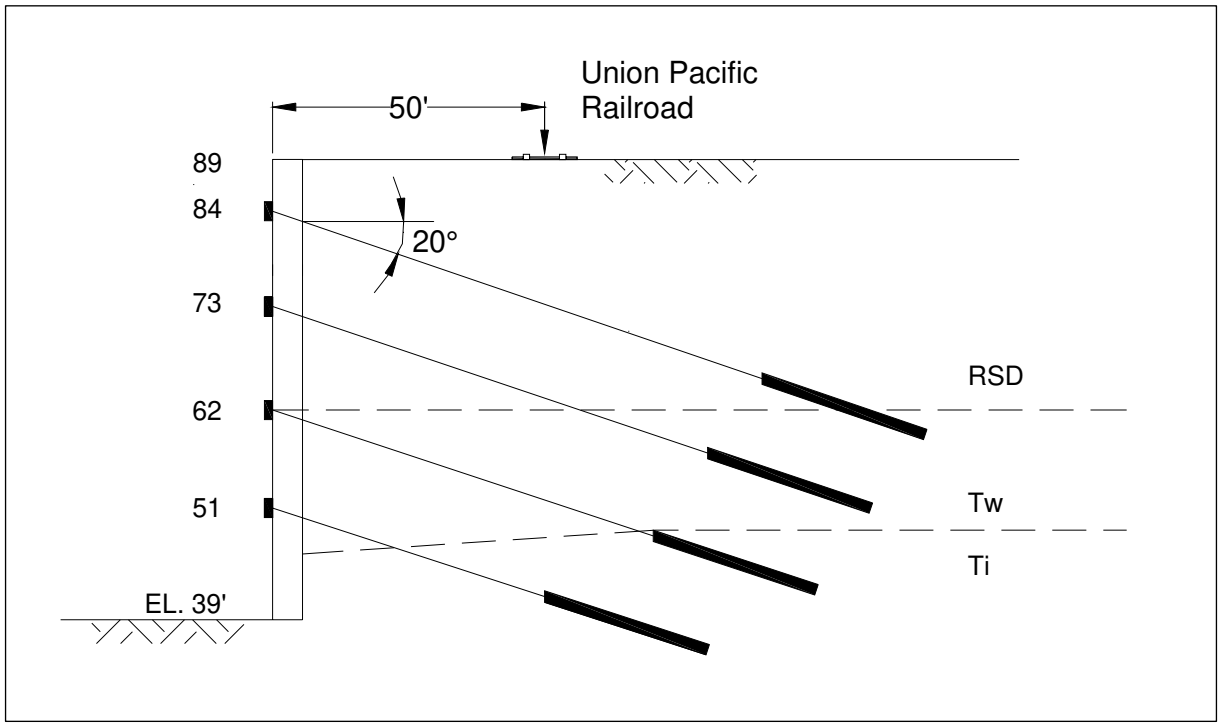

Figure 5.4. Section view of Panel 6 (after Knowles and Mosher 1990)

Table 5.1. Panel 6 Anchor Loads

Anchor Elevation ft	Design Load (DL) Kips	Prestress Load 150% DL (Kips)	Lock-off Load Kips
84	281	421.5	272
73	281	421.5	292
62	281	421.5	290
51	358	537.0	356

suggests that the largest force demands (moments and shears) on the wall will occur at intermediate construction stages rather than at the final excavation stage and, as such, only those analysis procedures considering construction sequencing will provide reasonable results. Therefore, three of these procedures (identified as Rigid 1, Rigid 2, and Winkler 1) that directly or indirectly consider the construction process were used to evaluate the “stiff” case study tieback wall. The stages of construction for the wall are described in Table 5.2.

Table 5.2. Construction Process for "Stiff" Tieback Wall

Stage	Description
1	Construct surcharge to pre-excavation grade (four increments)
2	Excavate for railroad relocation
3	Construct slurry trench temporary tieback wall
4	Excavate in front of wall to Elevation 78.5 **(Stage 1 Excavation)**
5	Install upper tieback anchor at Elevation 84 and prestress to 150% of the design load
6	Excavate in front of wall to Elevation 67.5 and lock-off upper anchor at design load. **(Stage 2 Excavation)**
7	Install second tieback anchor at Elevation 73 and prestress to 150% of the design load
8	Excavate in front of wall to Elevation 56.5 and lock-off second anchor at design load. **(Stage 3 Excavation)**
9	Install third tieback anchor at Elevation 62 and prestress to 150% of the design load
10	Excavate in front of wall to Elevation 45 and lock-off third anchor at design load. **(Stage 4 Excavation)**
11	Install forth tieback anchor at Elevation 51 and prestress to 150% of design load
12	Excavate to bottom of wall at Elevation 39 and lock-off forth anchor at design load. **(Stage 5 Excavation)**

The analysis results consisting of wall computed maximum displacements, wall maximum bending moments, and maximum anchor forces for each excavation stage for the Rigid 1, Rigid 2, and Winkler 1, were tabulated in Table 5.3. These current 2-D design/ analysis procedures were compared with the results from both 2-D and 3-D nonlinear finite element analyses, as well as available instrumentation measurements, as a means to evaluate the simplified 2-D procedures.

5.2.1 Rigid 1 Analysis Description and Results

The procedure labeled as Rigid 1 is an equivalent beam on rigid supports analysis in which the tieback wall modeled as a continuous beam on rigid supports and is loaded with an

Table 5.3. Summary of Analysis Results for Excavation Stages 1 thru 5

	RIGID 1	RIGID 2	WINKLER 1 Cmultianc	2-D Plaxis FEM	3-D Plaxis FEM
Stage 1 Excavation					
Max. Anchor Load (Kips)	NA	NA	NA	NA	NA
Max. Moment (Ft-Kips/ft run of wall)	NA	26.2	35.2	28	22.3
Max. Computed Displ. (in.)	NA	NA	-0.21	-0.15	-0.12
Stage 2 Excavation					
Max. Anchor Load (Kips)	NA	89.6	359.4	272	272
Max. Moment (Ft-Kips/ft run of wall)	NA	39.5	115	122	161
Max. Computed Displ. (in.)	NA	NA	-0.25	0.22	0.31
Stage 3 Excavation					
Max. Anchor Load (Kips)	NA	310.0	361.2	292	292
Max. Moment (Ft-Kips/ft run of wall)	NA	56.7	138.1	158	172.5
Max. Computed Displ. (in.)	NA	NA	-0.39	0.37	0.44
Stage 4 Excavation					
Max. Anchor Load (Kips)	NA	545.8	360	290	290
Max. Moment (Ft-Kips/ft run of wall)	NA	98.8	114.6	167	172.5
Max. Computed Displ. (in.)	NA	NA	-0.36	0.41	0.46
Stage 5 Excavation					
Max. Anchor Load (Kips)	237.8*	393.9	358.8	288	288
Max. Moment (Ft-Kips/ft run of wall)	21.3*	37.3	69.7	96.4	106.1
Max. Computed Displ. (in.)	NA	NA	-0.32	0.37	0.43
* For comparison purposes only and not used in design.					

apparent pressure diagram. Apparent pressures are intended to represent a load envelope and not the actual loads that might exist on the wall at any time. The analysis, therefore, is a final-excavation analysis that indirectly considers the effects of construction sequencing. This approach provides good results for flexible walls constructed in competent soils where

excavation below the point of tieback prestress application is minimal (± 1.5 ft). However, many designers of stiff wall systems believe that the use of apparent pressure diagrams for the design of stiff wall systems is ill advised (Kerr and Tamaro 1990). Therefore, the Rigid 1 approach is not expected to provide valid results for the Bonneville tieback wall, which is characterized as a stiff wall system. However, the Rigid 1 method can be used as a preliminary design tool to estimate upper anchor loads in order to determine if these anchors are overstressed (Strom and Ebeling 2002). Table 5.4 shows a comparison of maximum anchor forces (design forces) for the anchors in the upper row of anchors computed by the Rigid 1 method, the other simplified 2-D procedures and the 2-D and 3-D nonlinear finite element analyses. The apparent pressure diagram used was based on a total load approach in accordance with procedures presented in FHWS-RD-98-066. At-rest earth pressure coefficients were the basis for determining the total load, since tiebacks will be sized and prestressed to minimize wall movement. A complete summary of the Rigid 1 analysis of this wall system is presented in Appendix A.

Table 5.4. Comparison of Maximum Discrete Anchor Forces in the Upper Row of Anchors

Rigid 1	Rigid 2	Winkler 1 (Cmultianc)	2-D Plaxis FEM	3-D Plaxis FEM
Anchor Force (Kips)	Anchor Force (Kips)	Anchor Force (Kips)	Anchor Force (Kips)	Anchor Force (Kips)
186.8	89.6	359.4	272	272
Note: The Rigid 1 method computes a larger maximum anchor force than the Rigid 2 method and a smaller force than the Winkler 1 and 2-D and 3-D FEM. The maximum anchor force occurred at excavation Stage 2 for Rigid 2, Winkler 1, 2-D and 3-D FEM.				

5.2.2 Rigid 2 Analysis Description

The use of the beam on rigid supports (Rigid) method for evaluating various loading conditions encountered during construction is described in Kerr and Tamaro (1990), Ratay

(1996), and FHWA-RD-81-150. In the Rigid method, a vertical strip of the wall is treated as a multi-span beam on rigid supports that are located at tieback points. The analysis is a construction-sequencing analysis in which the earth loads are applied according to classical earth pressure theory. An equivalent cantilever beam method is used to evaluate wall-bending moments for the initial excavation (cantilever) stage of construction. For subsequent stages of excavation, where the wall is anchored, it is assumed that the depth of penetration below grade is sufficient to cause the point of contraflexure to coincide with the point of zero net pressure intensities. This allows the use of an equivalent beam supported at anchor locations and at the point of zero net earth pressure where the wall moment can be assumed to be zero. In this Rigid 2 analysis of the case study wall, the driving side earth pressures are assumed to be equal to at-rest pressure, since tiebacks will be sized and prestressed to minimize wall movement. A complete summary of the Rigid 2 analysis of this wall system is presented in Appendix A.

5.2.3 Winkler 1 Analysis Description

The Winkler 1 analysis is a beam on elastic foundation analysis where the soil springs are based on the referenced deflection method in accordance with FHWA-RD-98-066. Wall deflections greater than the reference deflections are considered to be plastic (nonrecoverable) movements. The earth pressure-deflection curves (R-y curves) are shifted following each excavation stage to account for those nonrecoverable displacements that are larger than the active state yield displacement. For cohesionless soils, active state yielding is considered to occur whenever the wall displacement exceeds 0.05 in. The shifted R-y curve approach is used to capture the buildup of earth pressure in the upper sections of the wall. Tiebacks are represented by anchor springs in the Winkler 1 analysis. Anchor loads are initially applied to

determine the wall displacement at lock off. The wall displacement at the anchor lock-off load is used to establish the anchor load with respect to zero wall displacement. With this information, the anchor spring can then be properly introduced into the Winkler analysis. The computer program CMULTIANC (Dawkins, Strom, and Ebeling 2003) was used for the Winkler 1 analysis. A complete summary of the Winkler 1 analysis of this wall system is presented in Appendix A.

5.3 RESULTS OF 2-D NONLINEAR FINITE ELEMENT METHODS (NLFEM) OF ANALYSIS

5.3.1 2-D Plaxis FEM Results

The NLFEM is one of the general methods used in the analysis and design of tieback wall systems. As previously mentioned in Chapter 4, Section 4.3, progressive type analyses (starting with the simplest design tool and progressing to more comprehensive design tools when necessary) are recommended for tieback wall analysis and design. Therefore, a 2-D NLFEM was initially performed on this case study wall. The results from this analysis were compared to the current 2-D methodologies and provided a basis for investigating the wall system behavior in the more comprehensive 3-D analysis. Plaxis Version 8.2 was utilized in the 2-D SSI analysis. There were some key 2-D Plaxis features used in the plain strain analysis including: (1) the use of 15 node triangular elements to model the soil, (2) plates (i.e., special beam elements) to model the diaphragm wall, (3) node to node bar elements along with geogrid elements to model the tieback anchors, and (4) interface elements to model SSI between the wall and adjacent soil elements. A total of 17,487 nodes and 2,146 elements containing 25,752 stress points were used to define the finite element mesh shown in Figure 5.5. Table 5.5 summarizes the calculation phases used in the 2-D SSI analysis to model the construction process that was listed in Table 5.2. Engineering properties for the wall,

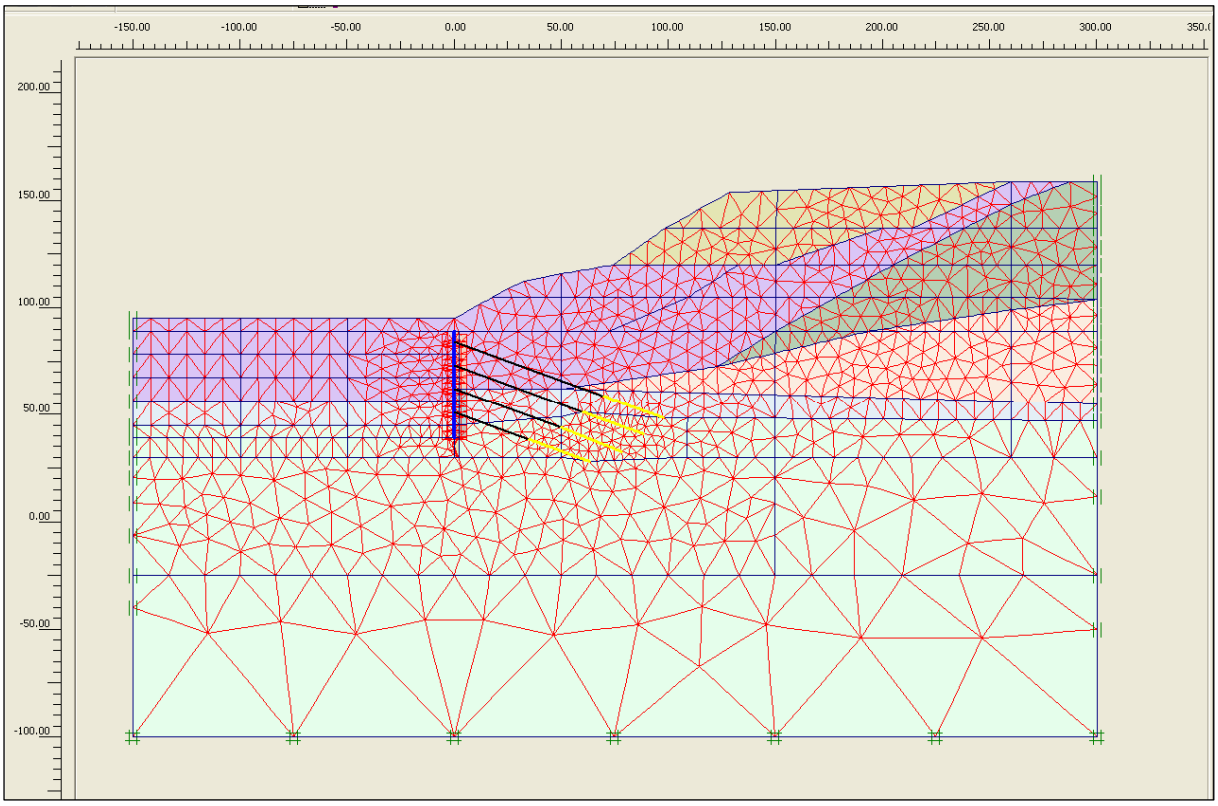

Figure 5.5. Finite element mesh used in the 2-D SSI analysis of stiff tieback wall

anchor and grouted zone are summarized in Tables 5.6 through 5.8. Loading phases 0 through 5 were used in the SSI analysis to establish the initial effective stress state condition existing prior to the construction of the wall. Loading phases 6 through 19 were used to model placing the wall, excavation for anchor placement, and the various stages of prestressing and locking off of the anchors.

Figure 5.6 shows the various soil clusters used to define regions of common soil properties for six categories of soil within the finite element mesh, i.e., fill material, reworked slide debris, slide debris, slide block, weigle formation, and diabase. Section 5.2.1 described the geological characterization of these soils. A key aspect of this SSI study was to investigate the effective soil stress conditions and the long-term behavior of the wall system. Soil stiffness and strength properties obtained from soil testing based on these conditions would

Table 5.5. Calculation Phases of 2-D Nonlinear Finite Element Analysis of Case Study Wall 1

Phase	Ph-No.	Calculation Type	Load Input
Initial phase	0		-
Build Natural Slope 1st incre.	1	Plastic analysis	Staged construction
Build Natural Slope 2nd incre.	2	Plastic analysis	Staged construction
Build Natural Slope 3rd incre.	3	Plastic analysis	Staged construction
Build Natural Slope 4th incre	4	Plastic analysis	Staged construction
Excavate for R.R. relocation	5	Plastic analysis	Staged construction
Place Wall & Interface	6	Plastic analysis	Staged construction
Excavate to El 78.5	7	Plastic analysis	Staged construction
Prestress Upper tieback	8	Plastic analysis	Staged construction
Lock off upper tieback to field load	9	Plastic analysis	Staged construction
Excavate to El 67.5	10	Plastic analysis	Staged construction
Prestress second tieback	11	Plastic analysis	Staged construction
Lock off second tieback to field load	12	Plastic analysis	Staged construction
Excavate to El 56.5	13	Plastic analysis	Staged construction
Prestress third tieback	14	Plastic analysis	Staged construction
Lock of third tieback to field load	15	Plastic analysis	Staged construction
Excavate to El 45	16	Plastic analysis	Staged construction
Prestess fourth tieback	17	Plastic analysis	Staged construction
Lock off fourth tieback to field load	18	Plastic analysis	Staged construction
Excavate to El 39	19	Plastic analysis	Staged construction

Table 5.6. Material Properties for the Diaphragm Wall

Identification	EA [lb/ft]	EI [lbft²/ft]	w [lb/ft/ft]	ν [-]
Diaphragm Wall	3.00E+09	2.25E+09	54.6	0.2

Table 5.7. Material Properties for the Grouted Zone

Identification	EA [lb/ft]	ν [-]
Tieback grout	3670916	0

Table 5.8. Material Properties for the Anchor

Identification	EA [lb]	|Fmax,comp| [lb]	|Fmax,tens| [lb]	L spacing [ft]
Anchor (tieback)	44050000	1.00E+15	1.00E+15	12

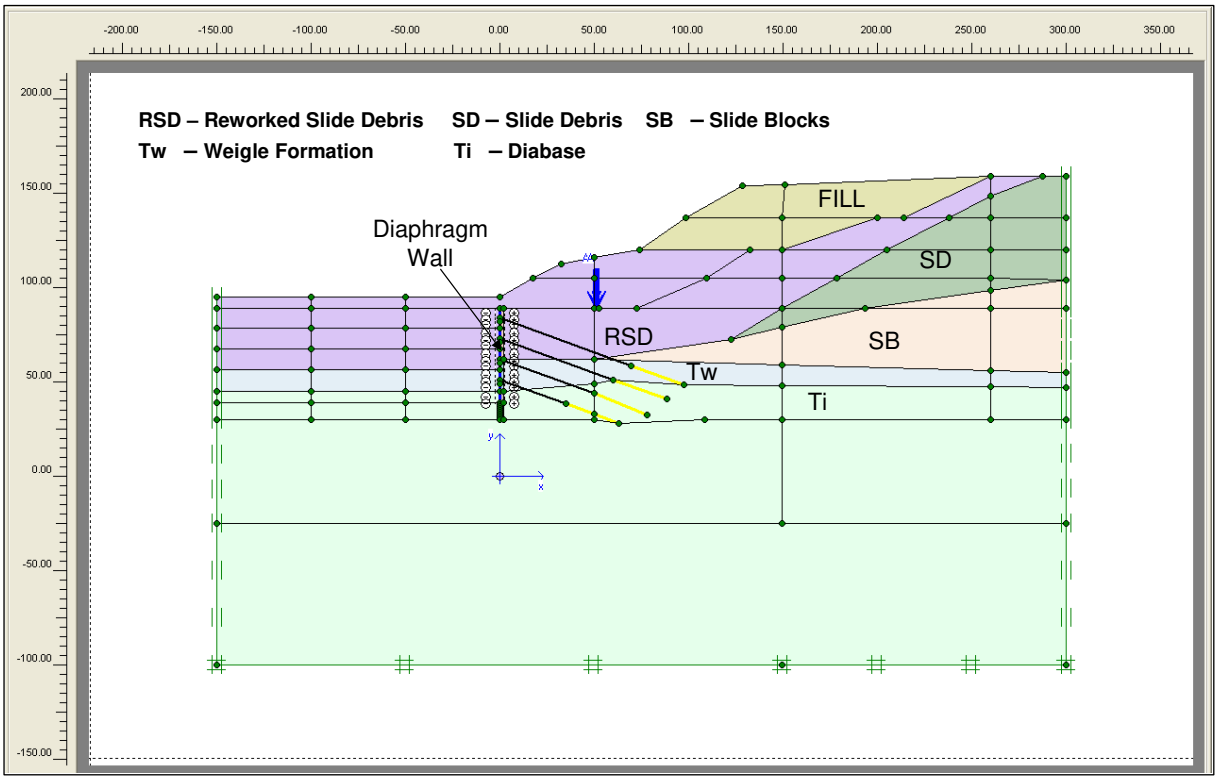

Figure 5.6. Two-dimensional cross-section model used to define soil regions and used in SSI analysis

provide the best estimate of input parameters for the Plaxis nonlinear Hardening Soil (HS) constitutive model utilized in the study. However, there was a limited amount of laboratory testing performed on the soils at this site. Triaxial tests are one of the most reliable methods of determining stiffness and strength properties of soil. A series of Isotropic Consolidated-Drained (ICD) triaxial testing of the weigle slide block material was attempted with limited success (USACE 1986). Only one sample contained enough of the weigle material to run more than one test to develop a strength envelope. Additionally, test materials were too variable to allow samples taken from different depths to be tested at varying confining pressures to determine reasonable failure envelopes. Typically, three specimens from a sample are used to develop strength and failure envelopes. The results of triaxial tests performed on two specimens of the weigle slide block were reported. These results were used to calibrate the HS parameters used to model the stress-stress behavior of the weigle slide block. A summary of the process used to calibrate the HS model constitutive parameters from the ICD triaxial tests is described in Appendix B. The HS model parameters for the remaining soil types were estimated based on available parameter correlations cited in the literature, Plaxis author's recommendations (Brinkgreve 2005), and a literature database of model parameters used in Plaxis analyses for similar soil types and properties. Table 5.9 summarizes the engineering material properties and the HS parameters assigned to the various soil types.

5.3.1.1 Initial Stress Conditions

The initial stresses in a soil body are influenced by the weight of the material and the history of the soil formation. The stress state is usually characterized by the initial vertical effective stress, σ'_v .The initial horizontal effective stress, σ'_h, related to the initial vertical effective stress by the coefficient of lateral earth pressure, K_o.

Table 5.9. Hardening Soil Parameters Used for Stiff Tieback Wall

Parameter	Symbol	Units	Weigle Slide Debris	Reworked Slide Debris	Slide Debris	Weigle Formation	Fill	Diabase
Unit Weight	γ	lb/ft^3	131	125	125	130	125	175
Cohesion	*c*	lb/ft^2	120	0	0	10000	0	100000
Friction Angle	Φ'	[°]	37.7	34	34	30	34	0
Dilation Angle	ψ	[°]	7.7	0	0	0	0	0
Secant Stiffness in standard triaxial test	E_{50}^{ref}	lb/ft^2	255200	1006000	312077	1028591	312077	20571825
Tangent Stiffness for primary oedometer loading 0.8*(E50ref)	$Eoed^{ref}$	lb/ft^2	204160	804800	249661	822873	249661	16457460
Unloading /Reloading Stiffness 3*(E_{50}^{ref})	E_{UR}^{ref}	lb/ft^2	765600	3018000	936230	3085774	936230	61715476
Power for stress level dependency of stiffness	*m*	[·]	0.8	0.8	0.8	0.8	0.8	0.8
Poisson's Ratio for Unloading /Reloading	□	[·]	0.2	0.2	0.2	0.2	0.2	0.2
Failure Ratio	R_f	[·]	0.7	0.7	0.7	0.7	0.7	0.7
Interface reduction Fator	R_{int}	[·]	0.9	0.9	0.9	0.9	0.9	0.9

$$\sigma'_h = K_o \, \sigma'_v \qquad \text{Equation 5.1}$$

The value of K_o is based on Jaky's equation:

$$K_o = 1 - sin\,\varphi' \qquad \text{Equation 5.2}$$

The original ground surface of the finite element mesh was horizontal at el 89 ft. In Plaxis, initial stresses were computed by the K_o procedure. An important aspect of the effective stress system is that the mobilized shear stress computed at strain integration points within the finite elements be less than the shear strength of the soil. The ratio of mobilized shear stress to maximum available shear stress represents the percentage of mobilized shear strength. The resulting computed fraction of mobilized shear strength (referred to as relative shear stress in Plaxis output) for the resulting initial stress condition is shown in Figure 5.7. As shown, the fraction of mobilized shear strength is less than or equal to 0.96 for all soil types. Additionally, a Plaxis Phi/C reduction procedure was performed and it resulted in a computed factor of safety against shear failure of 1.5. This computed factor of safety was

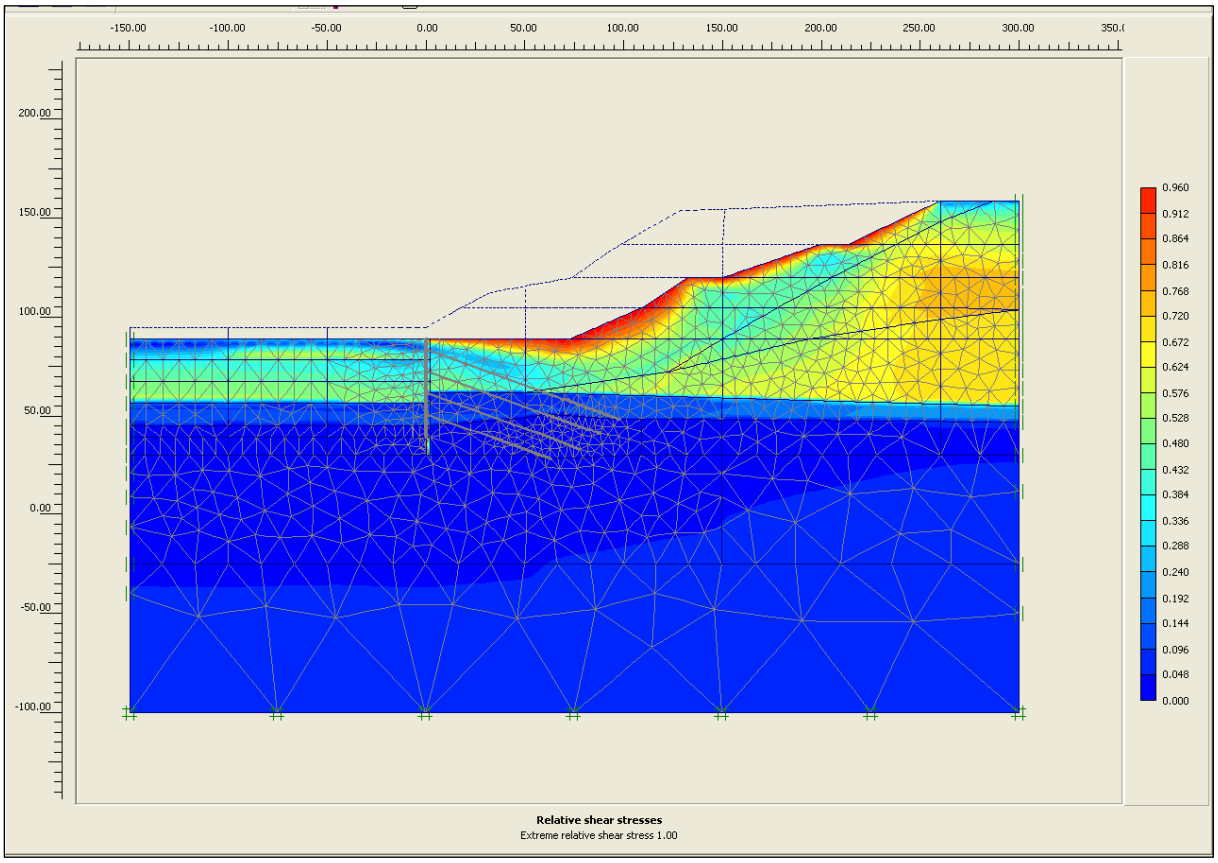

Figure 5.7. Fraction of mobilized shear strength for initial stress conditions

comparable to initial slope stability analyses performed by the designers that indicated that this slide unit is stable.

5.3.1.2 Selected Stage Construction Results

Table 5.3 listed the computed wall maximum displacements, wall maximum bending moments, and maximum anchor forces using the current 2-D analysis/design procedures for stiff tieback wall systems (i.e., Rigid 1, Rigid 2, and Winkler 1) methods for each excavation stage. Additionally, both 2-D and 3-D nonlinear finite element analyses were used as a means to access these procedures. A key construction stage for tieback design is the cantilever excavation stage (excavation stage just prior to installation and lock-off of the uppermost anchor). This stage is key because over-excavation below the ground anchor supports may

produce wall movements and wall and anchor force demands that are larger than tolerable. In this case study wall, an over-excavation of 5.5 ft was used in the analyses. Therefore, an evaluation of selected construction sequence stages was performed to determine if maximum wall movements and force demands on the wall and tiebacks occurred at intermediate stages of construction rather than for the final permanent loading condition. Figure 5.8 shows the computed 2-D FEM results of horizontal displacements of the wall after the cantilever excavation stage. The computed maximum displacement (Ux) was equal to 0.15 in., which was less than the design maximum allowable horizontal wall deflection under normal loads which is equal to 1.2 in. The corresponding wall bending moments after the cantilever excavation stage (with a maximum moment equal to 27.36 Kip*ft/ft) is shown in Figure 5.9. As shown in Table 5.3, the maximum displacement of the wall (0.41 in.) computed by the 2-D FEM occurred at the cantilever excavation stage (Stage 4) and the maximum bending moment (167.7 Kip*ft/ft) also occurred at excavation stage (Stage 4). These results demonstrate the importance of performing a construction sequencing analysis in the design of "stiff"' tieback wall systems. Maximum bending moments computed by the 2-D FEM for excavation Stages 2 through 5 were greater than those computed by the simplified 2-D procedures and thus indicated for this analysis that the simplified 2-D procedures were un-conservative in computing bending moments. Figure 5.10 shows the axial force distribution per foot run of wall that is transferred to the anchor bond zone for the upper tieback anchor. The discrete axial force is obtained by multiplying axial force distribution per foot run of wall by the plan spacing of the anchor. As shown, the largest amount of axial force is initially transferred to the top of the anchor bond zone and it decreases toward the bottom of the bond zone.

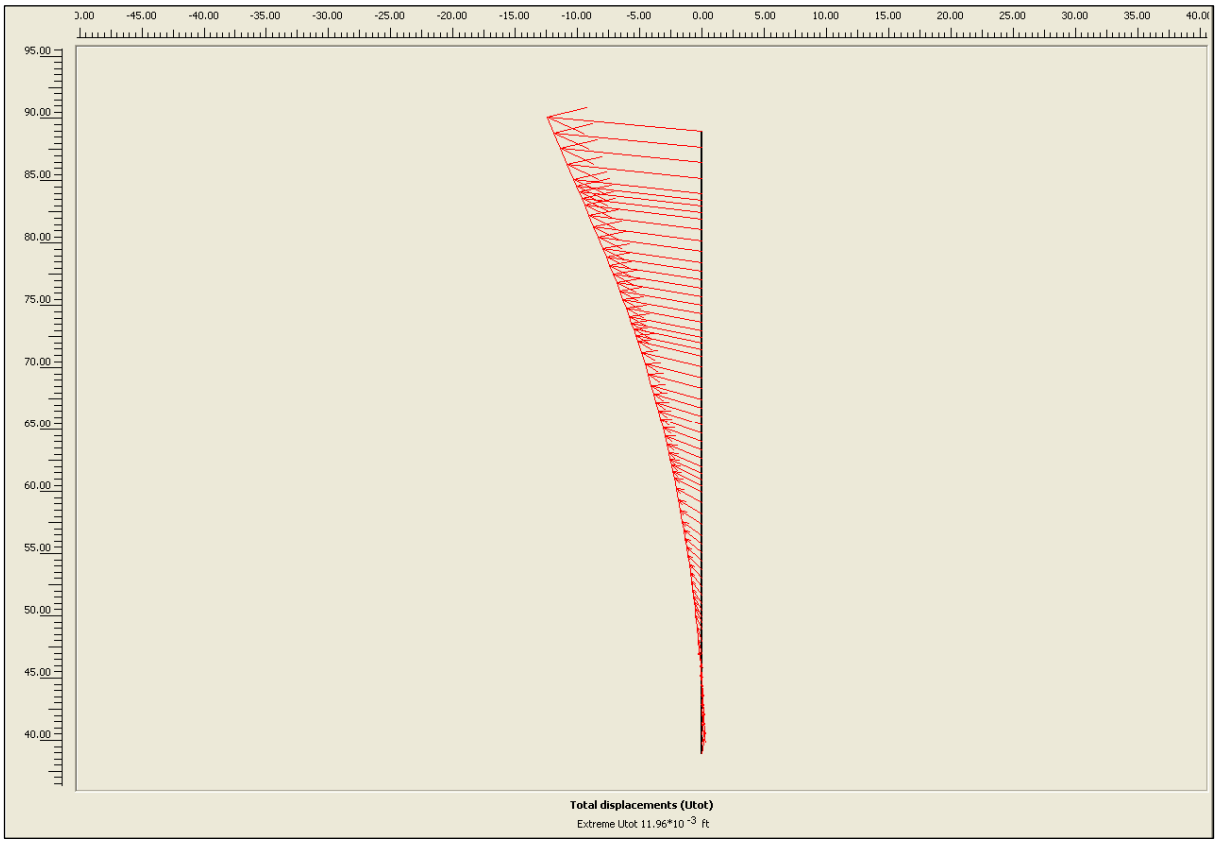

Figure 5.8. Wall displacement after Stage 1 excavation (Max Ux = - 0.0119 ft = 0.15 in.)

5.4 RESULTS 3-D NONLINEAR FINITE ELEMENT METHODS (NLFEM) OF ANALYSIS

5.4.1 3-D Plaxis FEM Results

The final analytical method used in the assessment of the "stiff" case study wall system was the more comprehensive 3-D NLFEM. It was envisioned that the 3-D NLFEM would provide (1) a means to quantify 3-D features that are not considered in current conventional 2-D procedures, (2) additional insight on the overall wall system behavior, and (3) be used to validate or enhance current simplified 2-D limit equilibrium procedures of the case study retaining wall system.

Plaxis 3-D Tunnel Version 2 was utilized to perform the comprehensive 3-D analyses. There were some key 3-D Plaxis features used in the analyses including: (1) the use of

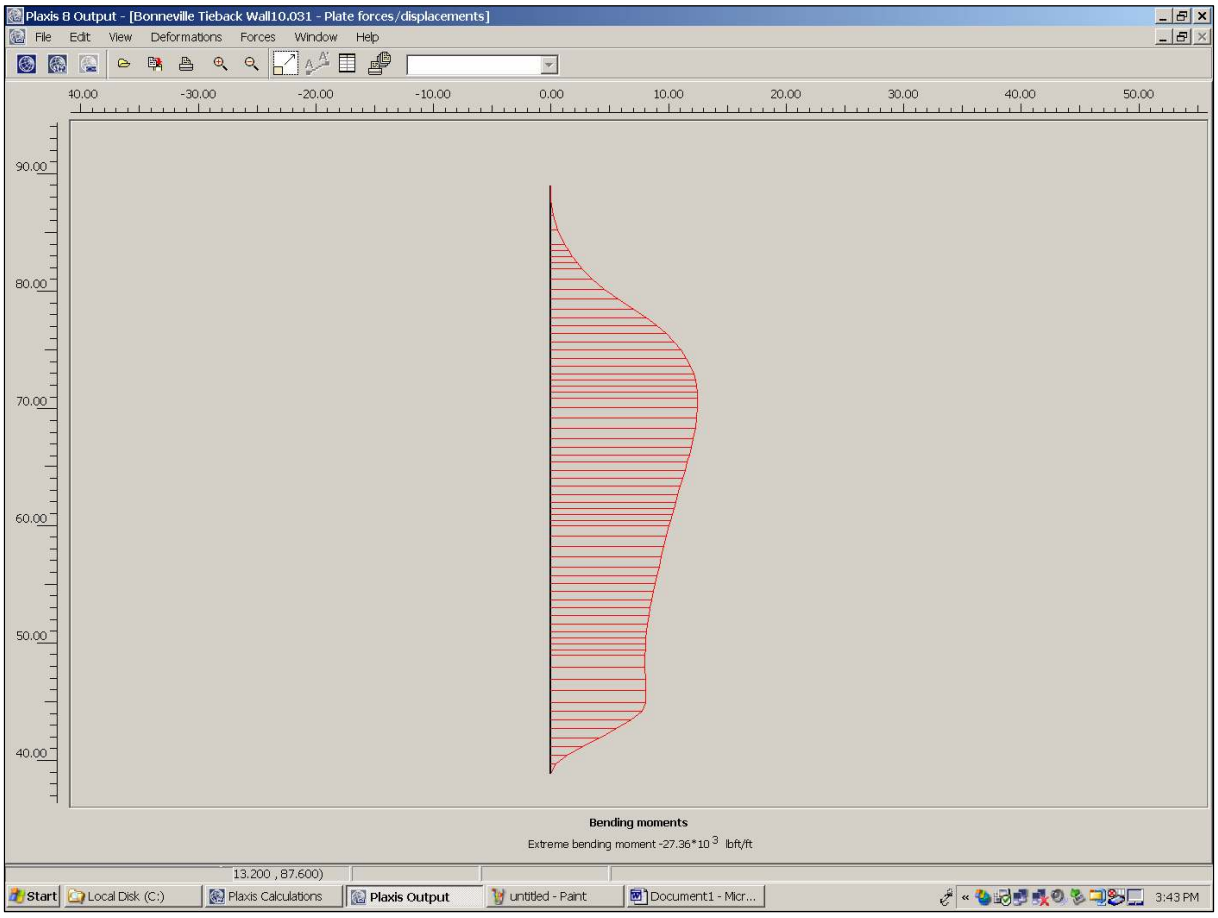

Figure 5.9. Wall bending moments after Stage 1 excavation (Max = 27.36 Kip*ft/ft)

15 node wedge elements to model the soil, (2) plate elements (i.e., special beam elements) to model the diaphragm wall, (3) node to node bar elements along with geogrid elements to model the tieback anchors, and (4) interface elements to model SSI between the wall and adjacent soil elements. A total of 56,753 nodes and 20,088 elements containing 120,528 stress points were used to define the finite element mesh shown in Figure 5.11. An initial 2-D finite element mesh cross section was extruded in the out of plane direction (z-direction) to form the 3-D model. This primary model consists of three additional vertical planes (C, F, and Rear) with an identical mesh configuration as the initial 2-D mesh cross section. The vertical planes were spaced equally to the plan spacing of the anchors, i.e., 12 ft as shown in Figure 5.12. The

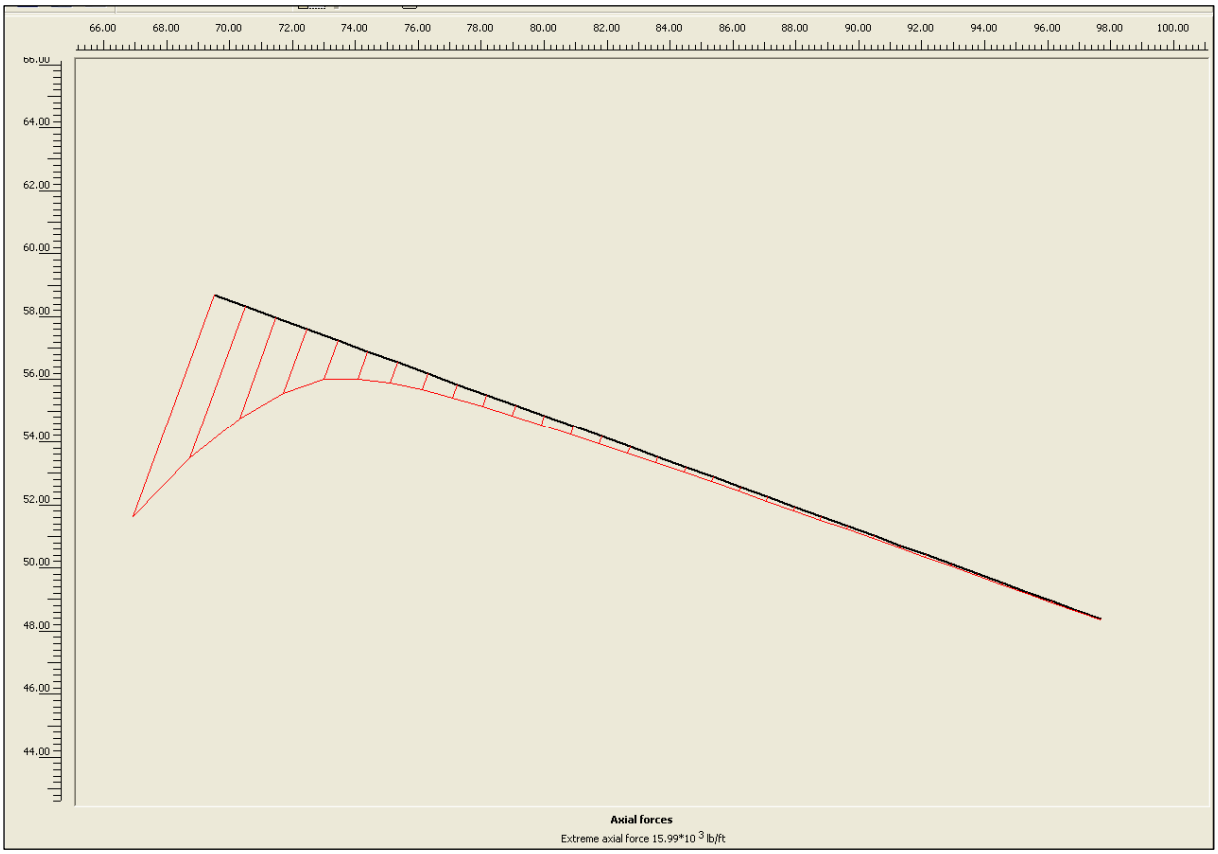

Figure 5.10. Axial forces in grouted zone after Stage 1 excavation (Max = 16 Kip/ft)

interior Plane C (z coordinate = -12 ft) was selected as a representative cross section of the wall system for use in the FEM assessment. The response of this wall section in this plane is influenced by the soil-structure interaction that occurs between the wall sections in the planes in front and behind (i.e., Front Plane, z coordinate = 0 ft and Plane F, z coordinate = -24 ft).

The same calculation phases used in the 2-D FEM analysis were also used to model the construction process in the 3-D analysis (Table 5.3). Likewise as in the 2-D analysis, loading phases 0 through 5 were used in the 3-D FEM analysis to establish the initial effective stress state condition existing prior to the construction of the wall and loading phases 6 through 19 were used to model placing the wall, excavating for anchor placement and the various stages of prestressing, and locking off of the anchors.

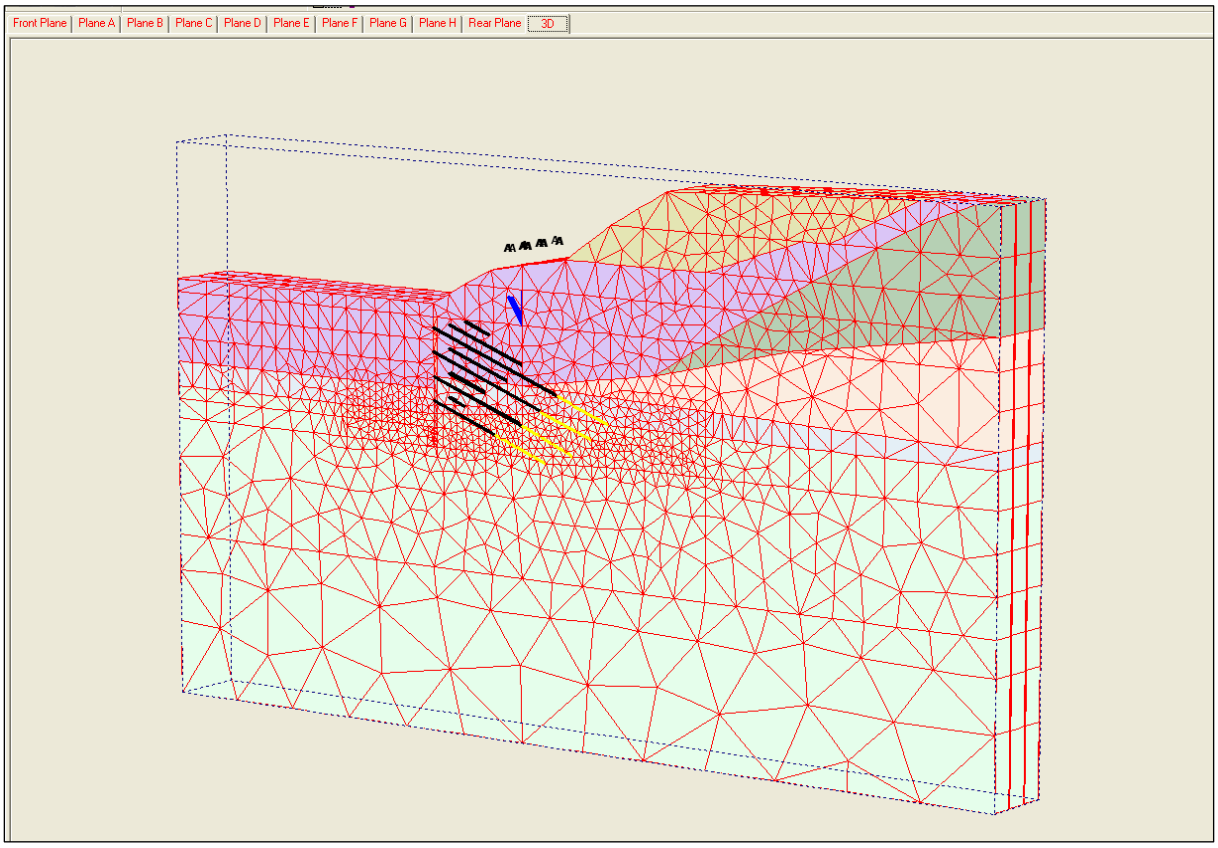

Figure 5.11. Finite element mesh used in the 3-D SSI analysis of "stiff" tieback wall

5.4.1.1 Initial Stress Conditions

As previously mentioned, an important aspect of the effective stress system is that the computed mobilized shear stress within the finite elements be less than the shear strength of the soil. The resulting 3-D computed fraction of mobilized shear strength (referred to as relative shear stress in Plaxis output) from the resulting initial stress condition is shown in Figure 5.13. As shown, the fraction of mobilized shear strength is less than or equal to 0.96 for all soil types as was indicated in the 2-D results.

5.4.1.2 Selected 3-D Stage Construction Results

Table 5.3 summarized computed wall maximum displacements, wall maximum bending moments, and maximum anchor forces using the current 2-D analysis/design procedures for

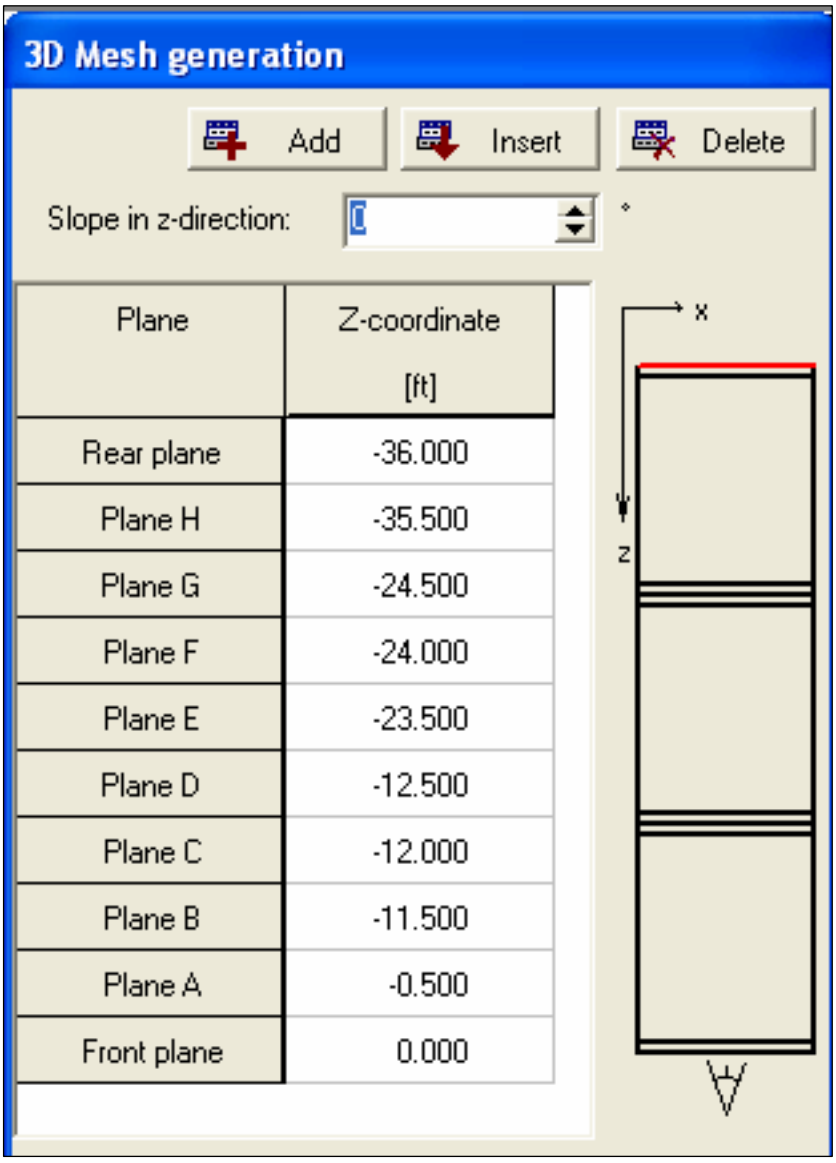

Figure 5.12. Plan spacing of planes for "stiff wall" 3-D model

stiff tieback wall systems methods as well as 2-D and 3-D NLFEM of analyses for each excavation stage. As previously described, a key construction stage for tieback design is the cantilever excavation stage. This construction stage is important because over-excavation below the ground anchor supports may produce wall movements and wall and anchor force demands that are larger than tolerable. Figure 5.14 shows plot of the 3-D FEM results of horizontal displacements of the wall after the cantilever excavation stage. The computed

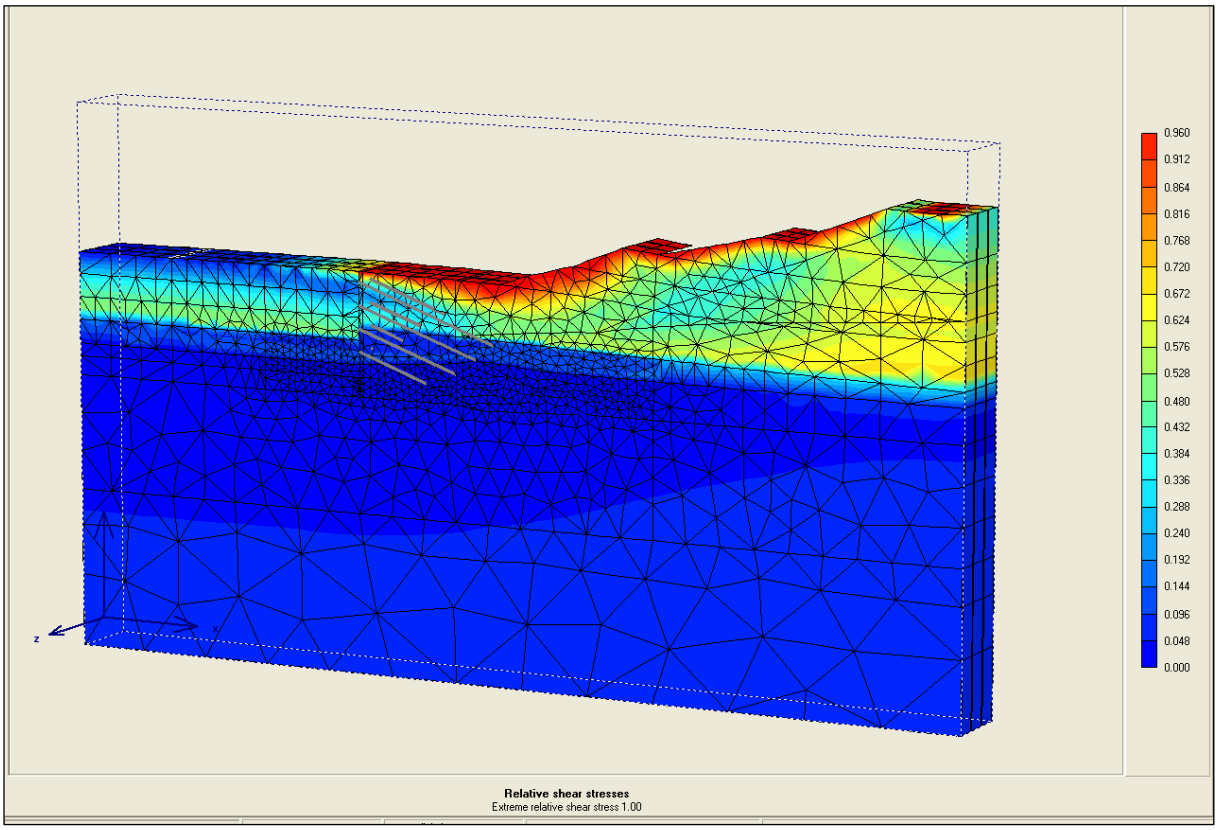

Figure 5.13. 3-D fraction of mobilized shear strength for initial stress conditions

maximum wall displacement (Ux) was equal to 0.12 in., which is less than the design maximum allowable horizontal wall deflection equal to 1.2 in. The corresponding wall bending moments per foot run of wall after the cantilever excavation stage with a maximum moment equal to 22.23 Kip*ft/ft is shown in Figure 5.15.

An evaluation of construction sequence stages was also performed to determine if the maximum wall movements and force demands on the wall and tiebacks occurred at intermediate excavation stage of construction rather than for the final permanent loading condition. As was shown in Table 5.3, the maximum computed 3-D FEM wall displacement for all excavation stages was equal to 0.46 in. and it occurred at the intermediate fourth excavation stage. Table 5.10 shows the comparison of maximum bending moments per foot run of wall computed by the 3-D FEM at various planes in the longitudinal direction and

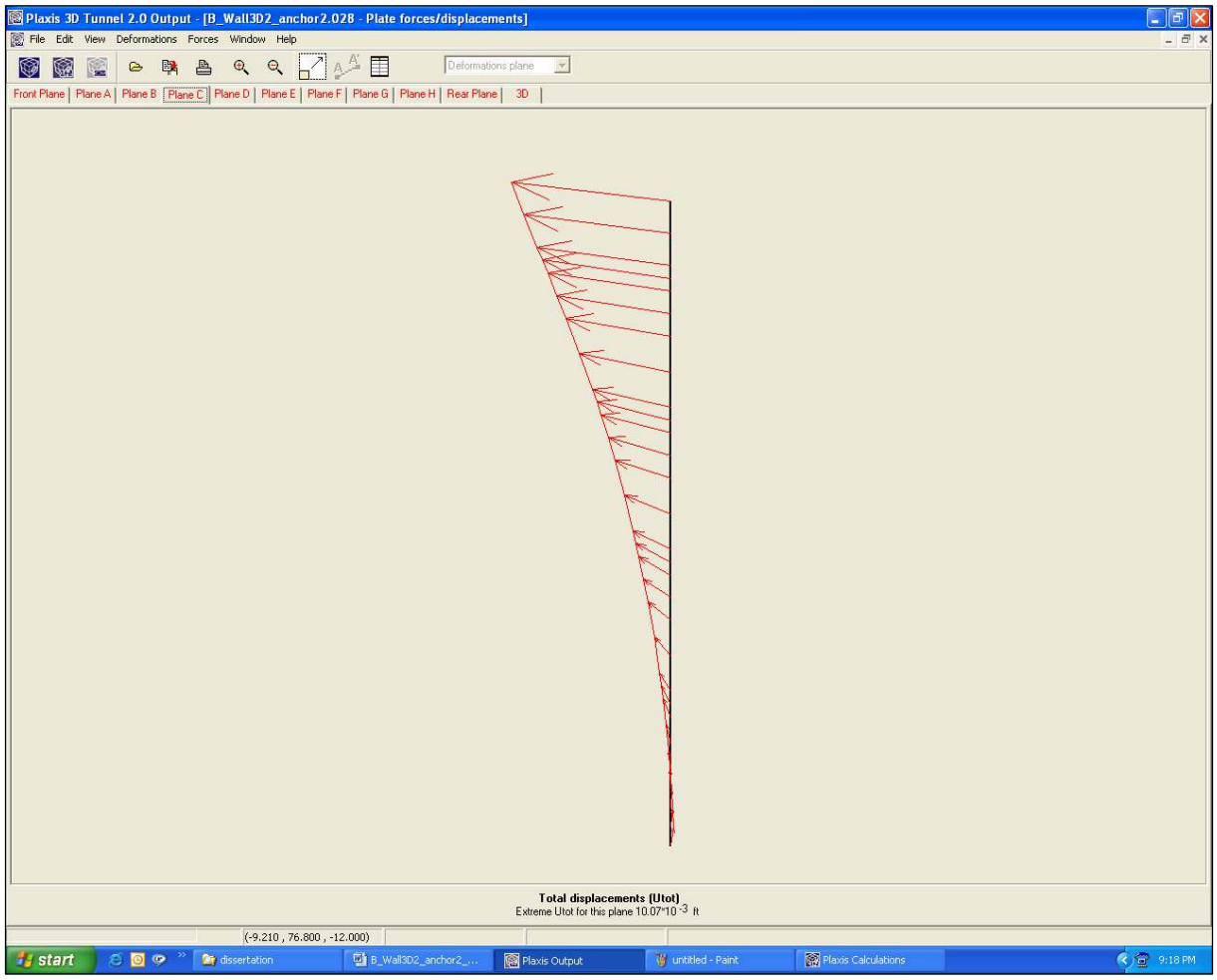

Figure 5.14. 3-D wall displacement after Stage 1 excavation (Max = 0.12 in.)

maximum bending moments computed by the 2-D FEM. The bending moment results at the interior Planes C and F are approximately the same and the moment results for the Front Plane and the Rear Plane are also approximately the same. These results show that the FEM model computes symmetric results about the center plane of symmetry. Table 5.10 also shows that the 3-D FEM computed moments per foot run of wall are generally greater than those computed by the 2-D FEM. These 3-D results further indicate that the simplified 2-D procedures may be un-conservative in computing bending moments. The computed maximum bending moment per foot run of wall for the wall occurred at the intermediate excavation

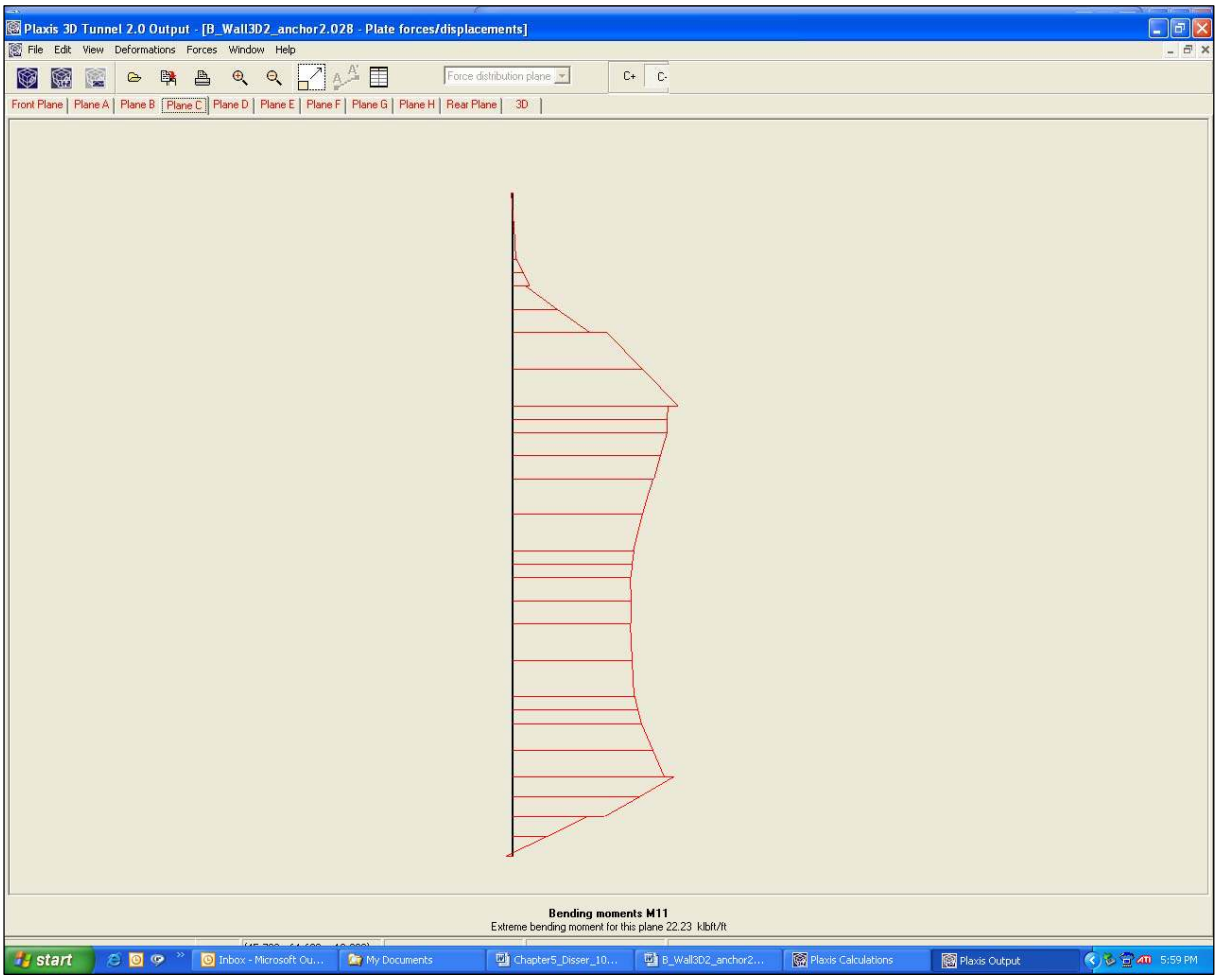

Figure 5.15. Wall bending moments after Stage 1 excavation (Max = 22.23 Kip*ft/ft)

Table 5.10. Comparison of Maximum Bending Moments

Excavation Stage	**Plaxis 2-D**	**Plaxis 3-D**			
	Kip*ft/ft	Front Plane Z=0 Kip*ft/ft	Plane C Z=-12 Kip*ft/ft	Plane F Z=-24 Kip*ft/ft	Rear Plane Z= -36 Kip*ft/ft
1	28	22.2	22.23	22.2	22.2
2	122	160.9	160.9	161.2	168.9
3	158	180.5	172.7	172.8	180.5
4	166.8	181.1	172.5	172.6	181.1
5	96.38	120.2	106.1	104.7	120.2
		Note: Plan Spacing 12 ft.			

stage (Stage 4). These results also demonstrate the importance of performing a construction sequencing analysis in the design of “stiff”‘ tieback wall systems.

As described in Chapter 4, for stiff tieback walls, a 3-D geometrical effect is the presence of discrete or finite constraints along the out of plane direction. The actual response of the wall to loading is influenced by each constraint. The tieback anchors are modeled in Plaxis as a combination on node-to-node anchors and geogrid elements. In the Plaxis 3-D Tunnel software the geogrid element is used to model the grout zone around the anchor. This element extends from the anchor-to-anchor plane in the full z-direction of the model and the actual discrete grout (shown in yellow) response is smeared over this anchor-to-anchor spacing as shown in Figure 5.16. This modeling feature is also used in the Plaxis 2-D software. In order to approximate the actual discrete response of the grouted zone and anchors, thin vertical sections (referred to as slices in Plaxis input) were defined at small distances in front of and behind the planes that had installed anchors (Figure 5.12). The “slices” in these small regions were activated and the remaining grout between the anchors remained deactivated. This modeling technique leads to discrete strips to approximate the cylindrical grout region around the anchors as shown in Figure 5.17. It is believed that this modeling feature is a better approximation of the actual discrete 3-D anchor grout zone than the anchor grout zone being smeared over the full z-direction in between the anchors. Table 5.11 shows comparison of discrete axial forces (design forces) in anchor grout zone for the upper anchor. In the 3-D analysis, the total grout spacing for planes A and C is equal to 1 ft. The total spacing is equal to 0.5 ft in front and 0.5 ft behind of the plane where the anchor is installed to model the discrete grout zone. However, for the front and rear planes, there is no grout spacing in front of planes where the anchor is installed (i.e., mesh boundaries) and thus the grout spacing for

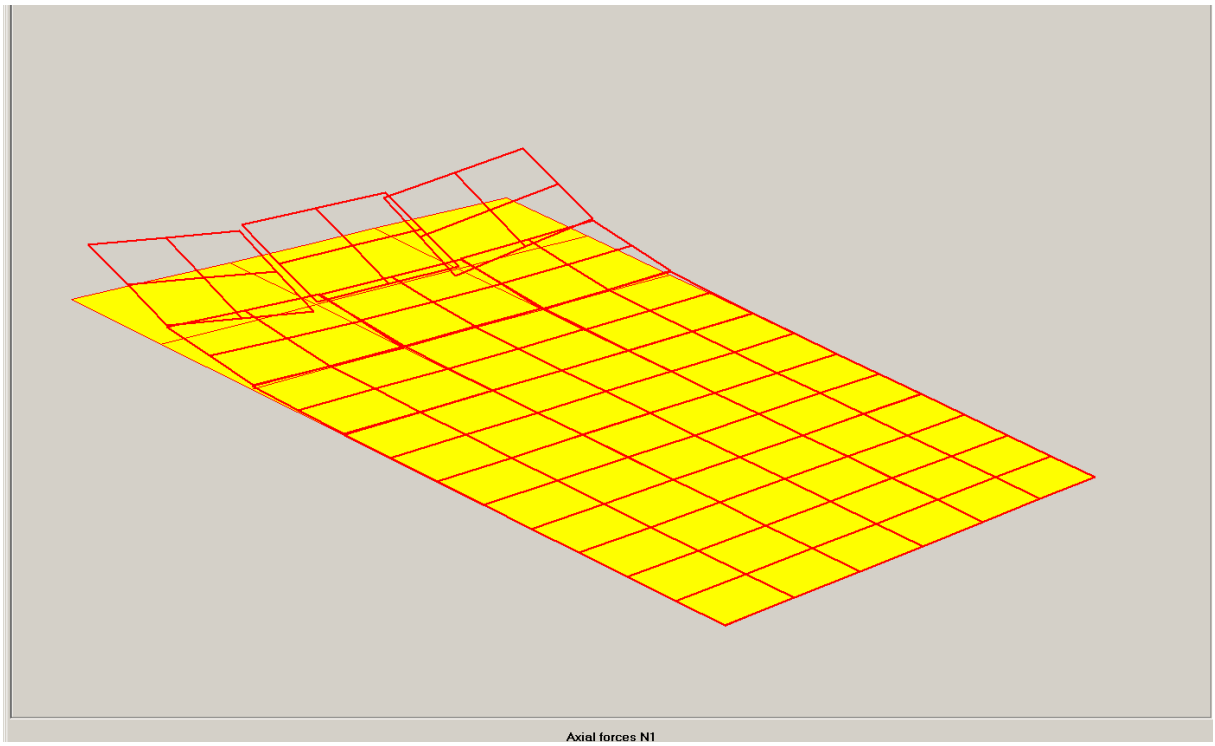

Figure 5.16. 3-D smeared modeling of anchor grout zone

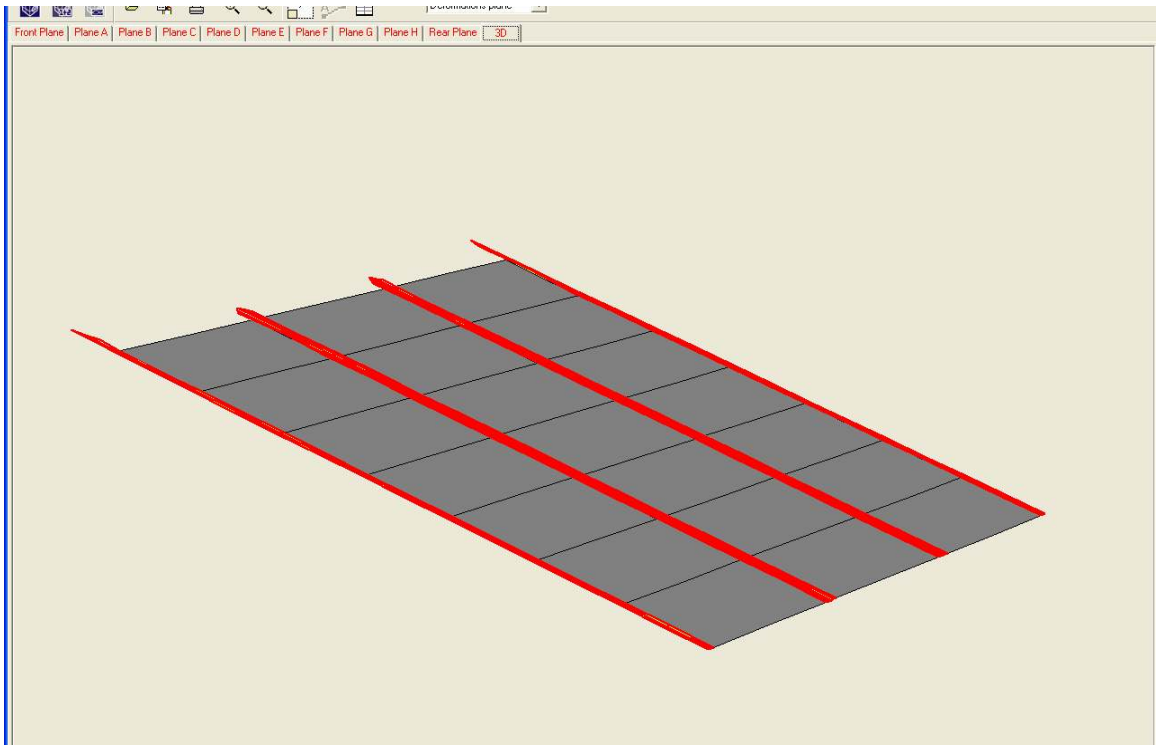

Figure 5.17. 3-D discrete modeling of anchor grout zone

Table 5.11. Comparison of Design Anchor Force in Upper Anchor

Excavation Stage	Plaxis 2-D Upper Anchor Grout Force (Kips/ft)	Grout Spacing (ft)	Design Upper Grout Force (Kips)
1	NA	NA	NA
2	16.36	12	196.32
3	16.14	12	193.68
4	16.08	12	192.96
5	16.08	12	192.96
Front Plane Z= 0	**Plaxis 3-D**		
Excavation Stage	Upper Anchor Grout Force Kip/ft	Grout Spacing (ft)	Design Upper Grout Force (Kips)
1	NA	NA	NA
2	540	0.5	270
3	540	0.5	270
4	540	0.5	270
5	540	0.5	270
Plane C Z= -12.0	**Plaxis 3-D**		
Excavation Stage	Upper Anchor Grout Force Kip/ft	Grout Spacing (ft)	Design Upper Grout Force (Kips)
1	NA	NA	NA
2	270.5	1	270.5
3	269.3	1	269.3
4	269.1	1	269.1
5	268.9	1	268.9
Plane F Z= -24	**Plaxis 3-D**		
Excavation Stage	Upper Anchor Grout Force Kip/ft	Grout Spacing (ft)	Design Upper Grout Force (Kips)
1	NA	NA	NA
2	266.7	1	266.7
3	265.6	1	265.6
4	265.6	1	265.6
5	268.9	1	268.9
Rear Plane Z= -36	**Plaxis 3-D**		
Excavation Stage	Upper Anchor Grout Force Kip/ft	Grout Spacing (ft)	Design Upper Grout Force (Kips)
1	NA	NA	NA
2	540	0.5	270
3	540	0.5	270
4	540	0.5	270
5	540	0.5	270

these planes is equal to 0.5 ft. Figure 5.18 shows the axial force distribution that is transferred to the anchor bond zone for the upper tieback anchor for excavation Stage 2. As shown, the force is transferred from the top of the anchor bond zone toward the bottom of the grout zone. Table 5.12 shows a comparison of axial force distribution in the grout zone for each row of anchors. As shown, the 3-D FEM of analysis computes significantly more force transfer to grout zone and shear transfer to the surrounding soil regions than those computed by the 2-D FEM of analysis. This excavation stage results in the largest computed anchor force for the upper anchor.

Table 5.13 shows a comparison of discrete anchor forces for each row of anchors. The 2-D and 3-D FEM of analysis computes consistent anchor forces. Figure 5.19 shows a plot of the relative shear stress in the grout region surrounding the upper anchor. As shown, the fraction of mobilized shear strength is less than or equal to 0.8 for soil surrounding the anchor

Figure 5.18. Axial forces in grouted zone after Stage 2 (Max = 540.3 Kips/ft)

Table 5.12. Comparison of Axial Force Results in Grouted Zone (2-D and 3-D FEM)

			Plaxis 2-D		
		Upper Grout Force	2nd Grout Force	Third Grout Force	Lower Grout Force
Excavation Stage		Kips	Kips	Kips	Kips
	1	NA	NA	NA	NA
	2	196.3	NA	NA	NA
	3	193.7	170.4	NA	NA
	4	192.9	170.4	72	NA
	5	192.9	170.3	72.3	124.8
Plane	Z-Coord.		Plaxis 3-D		
Front	0				
		Upper Grout Force	2nd Grout Force	Third Grout Force	Lower Grout Force
Excavation Stage		Kips	Kips	Kips	Kips
	1	NA	NA	NA	NA
	2	270	NA	NA	NA
	3	270	272.6	NA	NA
	4	270	272.8	89.4	NA
	5	270	272.8	86.9	149.1
Plane	Z-Coord.		Plaxis 3-D		
C	-12				
		Upper Grout Force	2nd Grout Force	Third Grout Force	Lower Grout Force
Excavation Stage		Kips	Kips	Kips	Kips
	1	NA	NA	NA	NA
	2	270.15	NA	NA	NA
	3	269.25	244.8	NA	NA
	4	269.05	245.1	84.7	NA
	5	266.45	245	84.7	153.6
Plane	Z-Coord.		Plaxis 3-D		
F	-24				
		Upper Grout Force	2nd Grout Force	Third Grout Force	Lower Grout Force
Excavation Stage		Kips	Kips	Kips	Kips
	1	NA	NA	NA	NA
	2	266.65	NA	NA	NA
	3	265.6	240.8	NA	NA
	4	265.55	241	83.8	NA
	5	268.95	244	84.6	151.2
Plane	Z-Coord.		Plaxis 3-D		
Rear	-36				
		Upper Grout Force	2nd Grout Force	Third Grout Force	Lower Grout Force
Excavation Stage		Kips	Kips	Kips	Kips
	1	NA	NA	NA	NA
	2	270	NA	NA	NA
	3	270	272.6	NA	NA
	4	270	272.7	86.9	NA
	5	270	272.6	86.9	148.6
			Note: Plan Spacing 12 ft.		

Table 5.13. Comparison of Discrete Anchor Force Results (2-D and 3-D FEM)

			Plaxis 2-D		
		Upper Anchor Force	2nd Anchor Force	Third Anchor Force	Lower Anchor Force
Excavation Stage		Kips	Kips	Kips	Kips
	1	NA	NA	NA	NA
	2	272	NA	NA	NA
	3	265.9	291.9	NA	NA
	4	264.2	290	290	NA
	5	263.5	288	286.8	355.2
Plane	Z-Coord.		Plaxis 3-D		
Front	0				
		Upper Anchor Force	2nd Anchor Force	Third Anchor Force	Lower Anchor Force
Excavation Stage		Kips	Kips	Kips	Kips
	1	NA	NA	NA	NA
	2	272	NA	NA	NA
	3	267.7	292	NA	NA
	4	265.2	289.1	290	NA
	5	264.8	287.2	286.4	356
Plane	Z-Coord.		Plaxis 3-D		
C	-12				
		Upper Anchor Force	2nd Anchor Force	Third Anchor Force	Lower Anchor Force
Excavation Stage		Kips	Kips	Kips	Kips
	1	NA	NA	NA	NA
	2	272	NA	NA	NA
	3	266.8	292	NA	NA
	4	265.2	289.4	290	NA
	5	264.7	287.5	286.6	356
Plane	Z-Coord.		Plaxis 3-D		
F	-24				
		Upper Anchor Force	2nd Anchor Force	Third Anchor Force	Lower Anchor Force
Excavation Stage		Kips	Kips	Kips	Kips
	1	NA	NA	NA	NA
	2	272	NA	NA	NA
	3	266.8	292	NA	NA
	4	265.2	289.4	290	NA
	5	264.7	287.5	286.6	356
Plane	Z-Coord.		Plaxis 3-D		
Rear	-36				
		Upper Anchor Force	2nd Anchor Force	Third Anchor Force	Lower Anchor Force
Excavation Stage		Kips	Kips	Kips	Kips
	1	NA	NA	NA	NA
	2	272	NA	NA	NA
	3	266.8	292	NA	NA
	4	265.2	289.1	290	NA
	5	264.8	287.2	286.5	356
			Note: Plan Spacing 12 ft.		

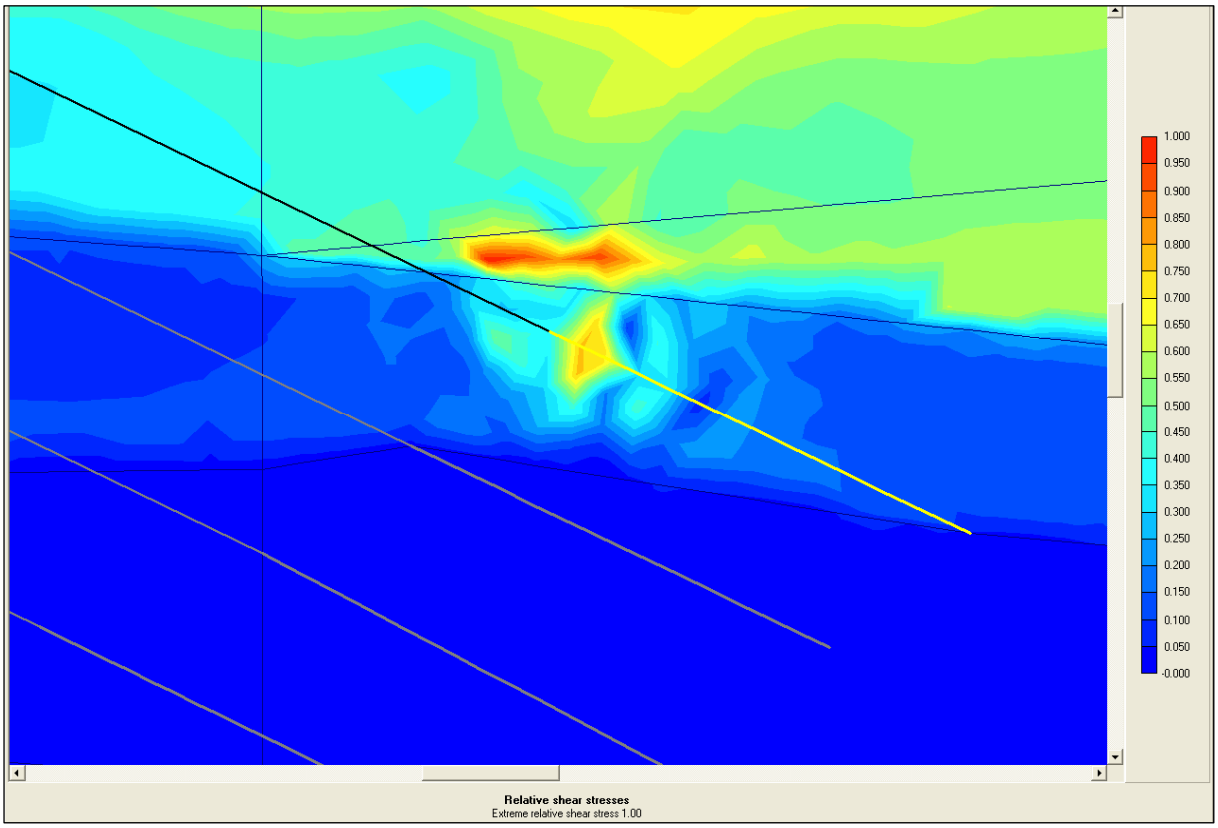

Figure 5.19. Relative shear stress in grouted zone for upper anchor after excavation Stage 2

grout region. This value indicates available shear strength in the soil region surrounding the upper anchor.

Figure 5.20 shows a plot of the 3-D FEM results of horizontal displacements of the wall after the final excavation stage (Stage 5). The computed maximum wall displacement (Ux) was equal to 0.43 in. toward the soil which is comparable to the instrumentation results (0.67 in.) for this stage of construction. The corresponding wall bending moments per foot run of wall for this stage of construction with a maximum moment equal to 106.23 Kip*ft/ft is shown in Figure 5.21. The resulting computed fraction of mobilized shear strength for the final excavation stage is shown in Figure 5.22. As shown, the fraction of mobilized shear strength is still less than or equal to 0.96 for all soil types and this value indicates available shear strength for the soil.

Figure 5.20. 3-D wall displacement after excavation Stage 5 (Max = 0.43 in.)

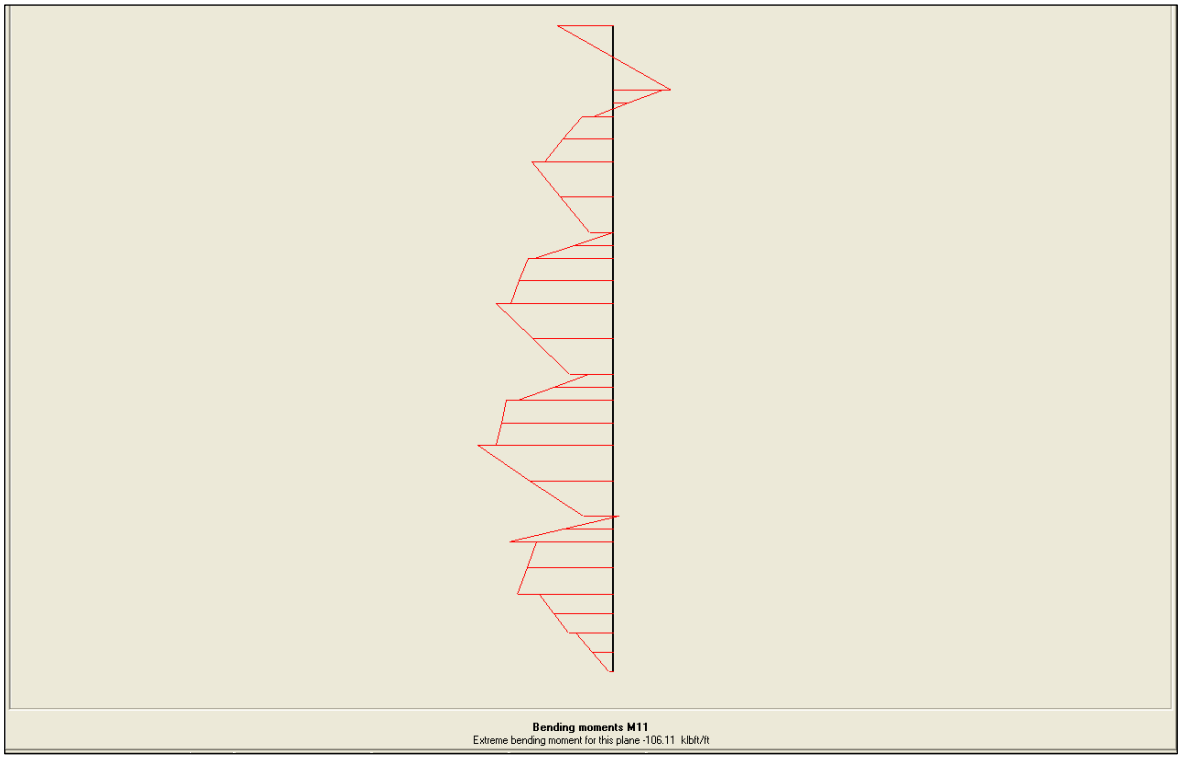

Figure 5.21. Wall bending moments after excavation Stage 5 (Max = 106 Kip*ft/ft)

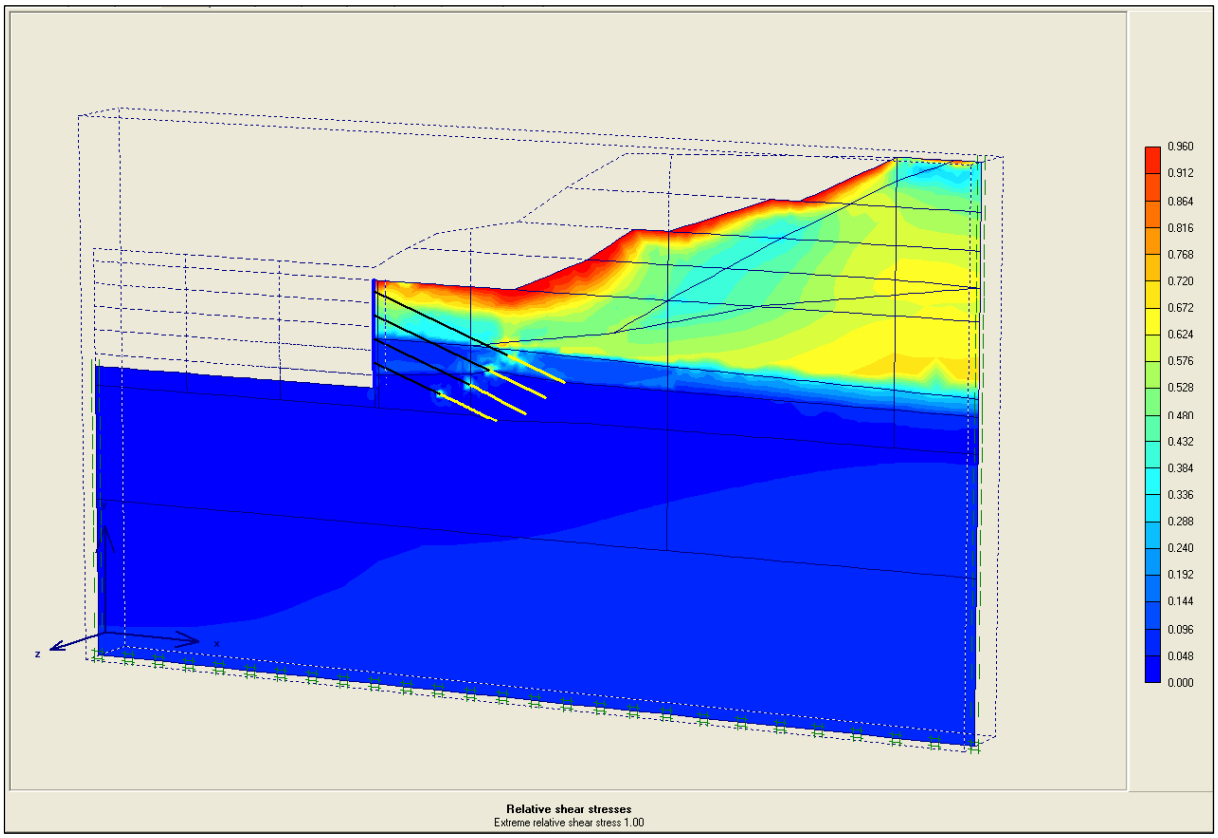

Figure 5.22. 3-D fraction of mobilized shear strength for excavation Stage 5

5.4.1.3 Engineering Assessment Observations

Based on an extensive literature review, it was determined that this was the first Corps of Engineers research effort utilizing 3-D nonlinear FEM procedures as a means to assess different 2-D analysis/design procedures for a full-scale instrumented "stiff" tieback wall system with multiple rows of prestressed anchors. In the comprehensive 3-D nonlinear FEM procedure, there were some key modeling features used that are vital in capturing 3-D effects of this "stiff" tieback wall system. A key 3-D geometrical effect was found to be the presence of discrete anchors. The actual response of the wall to loading is influenced by each anchor. The discrete anchors were modeled in Plaxis as a combination on node-to-node anchors and geogrid elements (for modeling grouted zone). Additionally, in order to approximate the actual discrete response of the grouted zone and anchors, a special modeling feature was

incorporated: thin vertical sections (referred to as slices in Plaxis input) were defined at small distances in front of and behind the planes that had installed anchors. This modeling technique allowed for discrete strips to approximate the cylindrical grout region around the anchors (Refer to Figure 5.17). It is believed that modeling discrete anchors and their grout region is a better approximation of the actual discrete 3-D anchor and grout zone than the 2-D approximation of averaging the anchor and grout zone model parameters over the plan spacing between the anchors.

Additionally, 3-D interface elements were used to simulate the soil-structure interaction that occurs at the interface between the wall and adjacent soil elements. Utilizing interface elements is an important feature that allows the soil regime to move independent of the structural regime. SSI FEM analyses utilizing interface elements typically result in more accurate computations of shear and normal acting on the tieback walls.

The 3-D nonlinear FEM analysis also modeled the construction process that was performed in the actual field construction of the stiff tieback wall. Modeling the construction sequence is a key aspect of SSI procedures in order to accurately compute the responses of the wall system due to the nonlinear stress-strain behavior of soils. Additionally, for this case study tieback the excavation that took place prior to tieback installation occurred to a depth of as much as 5.5 ft below the tieback elevation. This suggests that the largest force demands (moments and shears) on the wall would occur at an intermediate construction stage rather than at the final excavation stage and this model behavior further supports the importance of modeling the complete construction process .

The 3-D FEM model for the “stiff” tieback wall was calibrated by performing a parametric study on the key HS constitutive parameter, the secant stiffness (E_{50}^{ref}), that

would produce results which best matched to the available instrumentation results for different stages of construction. Also, triaxial tests were conducted on one soil type, the weigle slide block material. The results of triaxial tests were used to determine the HS parameters used to model the stress-stress behavior of the weigle slide block (See Appendix B). The HS model parameters for the remaining soil types were estimated based on available parameter correlations cited in the literature, Plaxis author's recommendations (Brinkgreve 2005), and a literature database of model parameters used in Plaxis analyses for similar soil types.

Another important aspect of 3-D nonlinear FEM model validation is the ability to observe symmetric results computed about planes of symmetry. Symmetric results were computed during the 3-D FEM staged construction analyses and were reported in Table 5.10. These results give confidence that this 3-D FEM SSI analysis can model the key 3-D features of this "stiff" tieback wall system.

With the robust modeling of the above-mentioned 3-D features, coupled with comprehensive simulation of the field construction process and calibration of the constitutive model to instrumentation results, lends confidence that the 3-D FEM methodology is a viable procedure for capturing key 3-D features and responses of a stiff tieback wall system that are not considered in 2-D FEM and 2-D limit equilibrium procedures. Therefore, an assessment of computed results (with 3-D FEM analysis used as the basis of comparison) of this stiff tieback is deemed reasonable and are presented.

The analysis results (computed maximum wall displacements, maximum bending moments per foot run of wall, and anchor forces) from the 2-D and 3-D FEM were compared with the current 2-D analysis/design procedures as a means to assess the procedures. This

information was provided in Table 5.3. A positive displacement indicates movement toward the retained soil and a negative displacement toward the excavation. The tabulated maximum bending moments per foot run of wall were reported as the maximum absolute values and used in the design of the wall section. The reported maximum anchor forces may also be used in the design. Note, that the 3-D and 2-D finite element analysis computed responses are at working load levels and not at ultimate loads. Additionally, the response of the anchors in the grouted zones was compared between the 2-D and 3-D FEM.

The comparison of results between the 2-D FEM and the simplified 2-D design/analysis procedures for this specific case study wall indicated that the simplified 2-D procedures underestimate bending moment demands on the wall and the wall displacements. Of the simplified 2-D procedures, the Winkler 1 procedure using the program CMULTIANC provided the best estimate of moment demand for a stiff wall system. The 2-D FEM showed that the maximum bending moments per foot run of wall and maximum wall displacements occurred at an intermediate stage of excavation. These results demonstrate the importance of performing a construction sequencing analysis in the design of "stiff" tieback wall systems. The 2-D FEM also computes force transfer to grout zone that is not included in the current 2-D simplified analysis and design procedures.

The comparison of results between the 2-D and 3-D FEM indicated an overall consistency. The computed 3-D bending moments per foot run of wall and the wall displacements were greater than those computed by the 2-D FEM for each stage of excavation. These results also demonstrated the importance of performing a construction sequencing analysis in the design of "stiff" tieback wall systems because the maximum bending moment per foot run of wall for the wall occurred at an intermediate stage of

excavation. Discrete maximum anchor force results from the 2-D and 3-D FEM were approximately the same. However, the 3-D FEM analysis computed significantly more force transfer to grout zone and shear force transfer to the surrounding soil regions than computed by the 2-D FEM. This assessment indicated that the 3-D effect of the discrete anchors affects the overall system behavior of a "stiff" tieback wall system analytical model. These effects are not accounted for in the 2-D simplified procedures used in analysis and design of these wall systems.

3-D FEM results indicated the potential for enhancements to be made to one of the 2-D simplified design procedures (Rigid 2). The Rigid 2 procedure uses a factor of safety equal to one applied to the shear strength of the soil below the excavation level (i.e., a passive limit state). The plot of mobilized shear indicated that there is reserve passive resistance available in the soil. Therefore, the Rigid 2 procedure could be modified by applying a passive factor of safety greater than one (1.5 is recommended in pile design) and reanalyzing the wall system to compute wall forces and displacements. A second series of parametric Rigid 2 analyses were conducted with the results summarized in Appendix D. The Rigid 2 procedure with a FSp(ave) equal to 1.4 generally computes slightly larger maximum bending moments than the Rigid 2 procedure with FSp equal to one for these intermediate construction stages. However, for stages 2 and 3, the Rigid 2 procedure with a FSp(ave) equal to 1.4 computed much smaller bending moments as compared to the simplified Winkler 1 procedure, and 2-D and 3-D FEM results. Recall, that the simplified Rigid 2 procedure is based on the assumption that a point of fixity in the soil below the excavation elevation occurs at a depth of zero net pressure for the second and all subsequent construction stages. These results indicate that the simplified approach used to estimate the depth to fixity might be a key reason for the disparity in results.

CHAPTER 6

ENGINEERING ASSESSMENT OF CASE STUDY RETAINING WALL NO. 2

6.1 BACKGROUND

6.1.1 Test Site Description

A 25-ft-high, instrumented, full-scale, tieback, H-beam and wood lagging wall supported by pressure-injected ground anchors was constructed at the Texas A&M University National Science Foundation (NSF) designated site for geotechnical experimentation. This full-scale test program was a part of a four-part study that focused on the improved design of permanent ground anchor walls for highway applications. A 25-ft-high wall was chosen for this test program because most highway walls are of similar height. A test section wall contained a section supported by one row of ground anchors and a section supported by two rows of anchors. Each wall section was divided into a driven beam and a drilled-beam portion. A total of eight soldier beams in the wall were instrumented and studied. A driven wall section supporting two rows of anchors was used in the engineering assessment of case study wall No. 2.

6.1.2 Project Site Geology

The wall was constructed in an alluvial sand deposit. A series of in situ and laboratory tests were performed to characterize the soil at the site. The in situ tests included: Standard Penetration (SPT) borings, Cone Penetrometer (CPT) soundings, Preboring Pressuremeter (PBPMT) borings, a Dilatometer (DMT) boring, and a Borehole Shear Test (BHST) hole. Locations for the in situ tests are shown on the site plan for the wall in Figure 6.1. Laboratory tests were used to determine the natural moisture contents, the particle size distributions, the

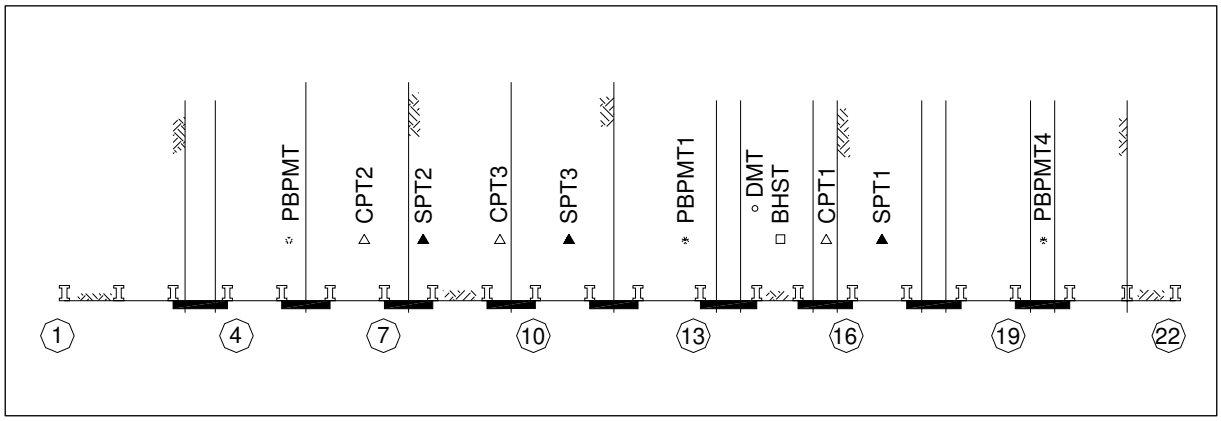

Figure 6.1. Site plan and in situ test locations

Atterberg limits, and the Unified Soil Classification for disturbed samples obtained from the SPT borings.

The SPT borings were denoted as SPT 1, SPT 2, and SPT 3. The average SPT values and cross-sectional view showing the soil profile at the center of the wall are shown in Figure 6.2. The soils at the wall were classified as a loose clayey sand or a silty sand from depth 0 to 10 ft; a medium dense, clean, poorly graded sand from depth 10 to 25 ft; a medium dense, clayey sand from depth 25 to 40 ft and a hard clay below depth 40 ft. Using the SPT tests, the angle of internal friction, φ' was estimated to be between 29° and 33° and the total unit weight, γ was estimated to be between 113 and 118 pcf.

The CPT test soundings were taken from the ground surface. The soil classifications based on the CPT logs were determined using relationships developed by Schmertmann (1970). The angle of internal friction, φ' was estimated to be between 30° and 32º using the correlation developed by Trofimenkov (1974). The relative density was estimated to be between 40 and 60 percent using the correlation developed by Schmertmann (1977). These soil classifications, internal friction angles, and relative densities were similar to those determined from the SPT tests.

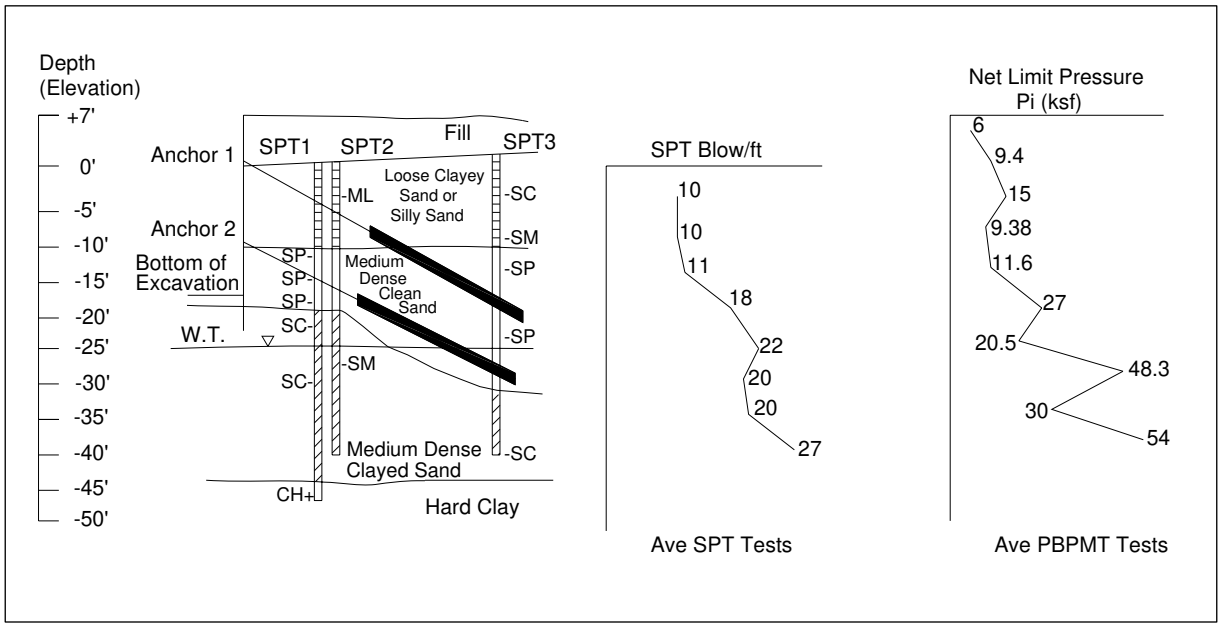

Figure 6.2. Wall cross section and in situ test results

The BHST tests indicated that the soil at the test site had an angle of internal friction between 30º and 33º, and the soil had an average cohesion of 0.34 psi. The average net limit pressures from the PBPMT tests are also shown in Figure 6.2. Based on the results of these various tests, the soil at the test site was assigned a total unit weight, γ, of 115 pcf and an angle of internal friction, φ' of 32º.

6.1.3 Design Criteria

Soldier beams and the ground anchors for the two tier tieback wall were designed to support the 25H (H is wall height) trapezoidal apparent earth pressure diagram are shown in Figure 6.3. A 5-ft-long toe embedment was selected for the wall. This embedment was selected based on experience with similar walls that indicated a 5-ft toe was adequate to support the lateral and vertical loads applied to the soldier beam. The soldier beams were assumed to be continuous over the upper row of anchors and hinged at the second row of anchors and at the bottom of the excavation. Soldier beams were designed to resist bending

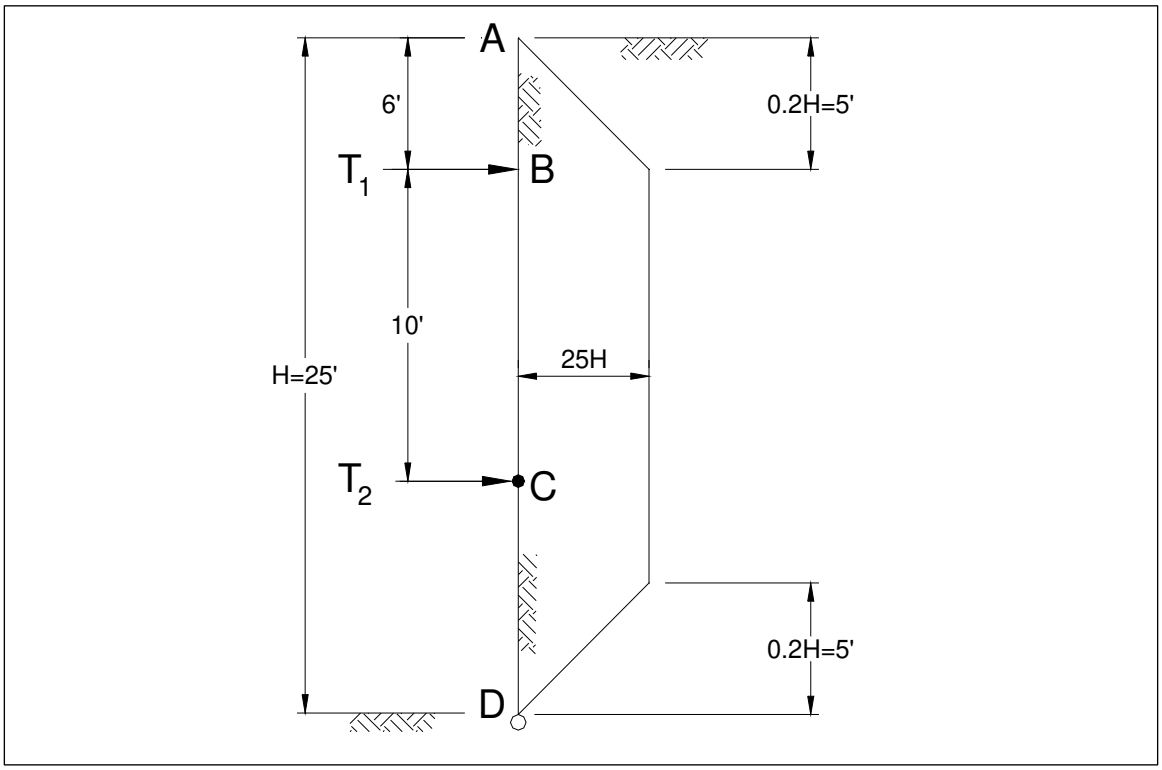

Figure 6.3. Apparent earth pressure diagram and calculation for two-tier wall

moments but they were not designed for combined axial and bending stresses. Soldier beam bending moment and ground anchor load were calculated based on force and moment equilibrium.

Internal stability of the wall was checked to ensure that the ground anchors would develop their load-carrying capacity behind the critical failure surface. A Rankine failure surface extending from the bottom of the excavation up at an angle of 45 + φ'/2 was used define the critical failure surface. Federal Highway Administration (FHWA) guidelines Cheney (1988) recommend that the unbonded length be extended behind the critical failure surface a minimum distance of 5 ft or 20 percent of the wall height. Applying FHWA guidelines, the minimum unbonded lengths for the two-tiered wall were 14.5 ft for the upper anchor and 10 ft for the lower anchor. The unbonded lengths for the test wall were extended

beyond the minimums. An unbonded length of 18 ft was selected for the upper anchor and an unbonded length of 15 ft for the lower anchor of the two-tier wall.

The anchor bond was selected so the ultimate ground anchor capacity was at least twice the ground anchor design load, i.e., factor of safety (FS) ≥ 2.0. The maximum ground anchor design load was 106.5 Kips. Pressure-injected ground anchors in medium dense sand develop ultimate load-carrying capacities that were estimated to be 10 Kips/linear ft. Therefore, anchor bond lengths of 24 ft were selected with an approximate ultimate capacity of 240 Kips.

The ground anchors had to be long enough to satisfy external stability. External stability criteria were satisfied when all failure surfaces passing behind the backs of the anchors had a FS ≥ 1.3. A 29-ft-long upper anchor and a 21-ft-long lower anchor satisfied the external stability requirements for the two-tier wall. Total anchor lengths for the two-tier wall were 42 ft for the upper anchor and 39 ft for the lower anchor were used.

6.1.4 Wall Description

A two-tier segment of the test wall with driven soldiers beam sections was utilized in the assessment of a “flexible” tieback wall system. Soldier beams designated as 7 and 8 were instrumented in the driven test section and these beam sections were used in this study. Figure 6.4 shows an elevation view of the wall and Figure 6.5 shows a plan view. To protect the vibrating wire strain gauges from damage during installation of the soldier beams, structural angles were welded over the gauges. Soldier beams 7 to 10 had 3 × 3 × 5/16 angles welded to the WF 6 × 25 beams. The composite WF 6 × 25 beams had moments of inertia of 132.9 $in.^4$ Figure 6.6 shows a section view through the two-tier section. Soldier beams 7 and 8 were driven to the desired depth using an air hammer. Three-inch-thick wood lagging was used to support the soil between the soldier beams.

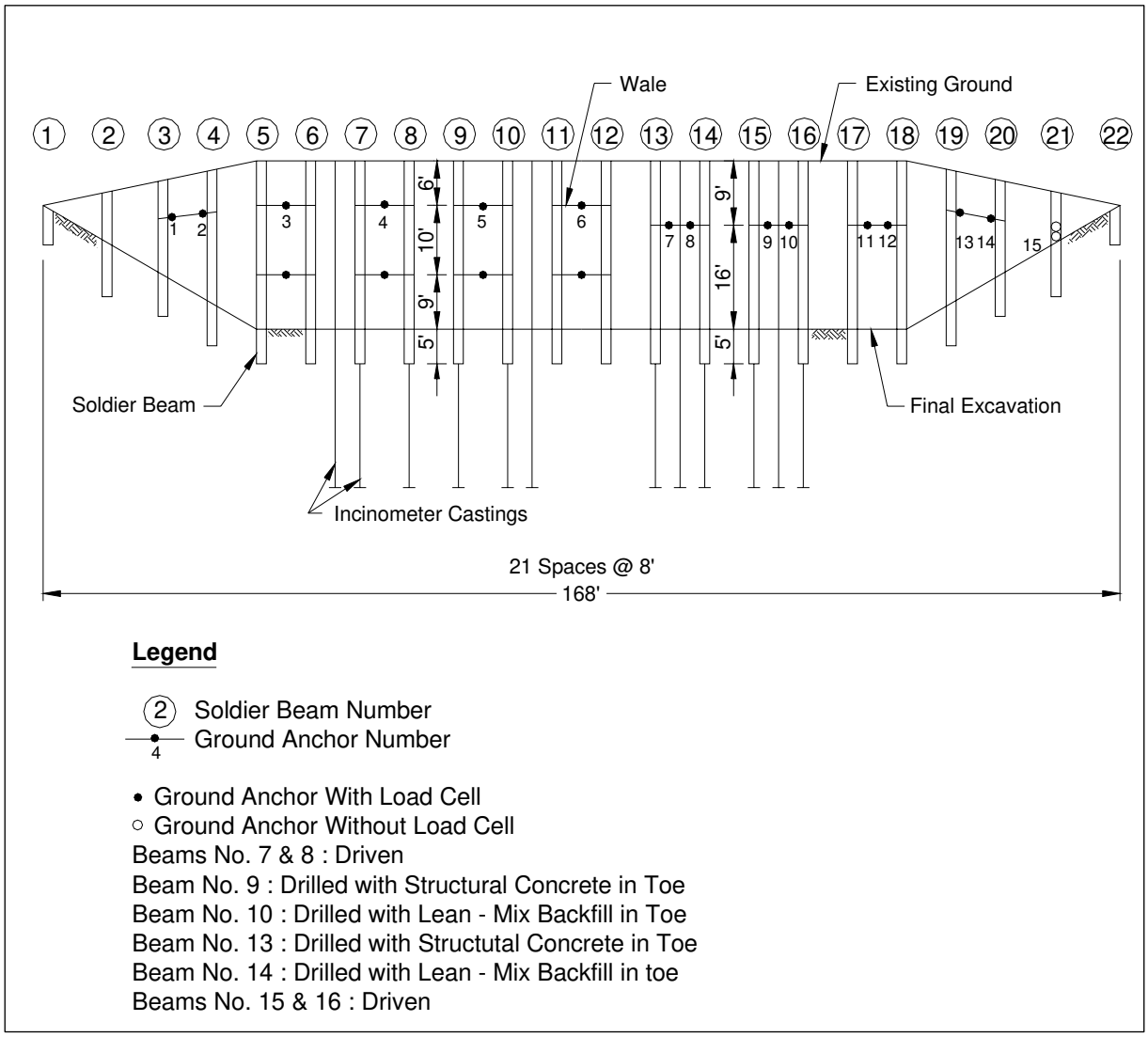

Figure 6.4. Elevation view of wall

6.1.5 Tieback Anchors

Pressure-injected ground anchors were used to support the wall. The ground anchor angle was selected to be 30º from the horizontal so the ground anchors would apply a significant downward load on the soldier beams. Table 6.1 lists the ground anchor schedule for the wall. The anchors were installed by driving a closed-end, 3.5-in. casing into the ground. After the casing reached the desired depth, then the ground anchor tendon was inserted in the casing and the closure point driven off. Cement grout was pumped down the casing as the casing was

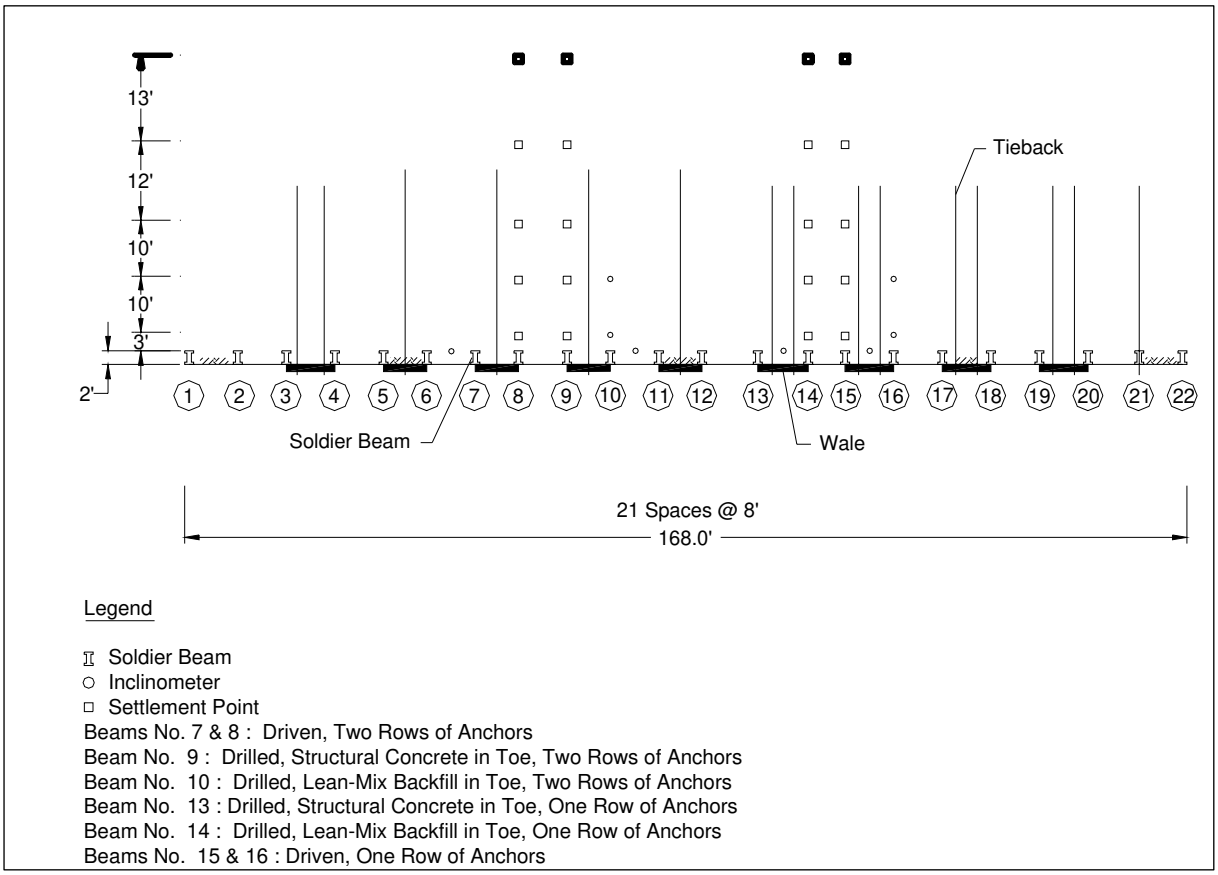

Figure 6.5. Plan view of the wall

extracted. The grout surrounding the bond length was placed at pressures exceeding 200 psi. The top row of anchors had an 18-ft unbonded length and the bottom row of anchors had a 15-ft unbonded length. A plastic tube was used as a bond breaker over the unbonded length. Each anchor was tested and stressed three days after the anchors were installed. Test loads were 133 percent of the design loads and the lock-off loads were 75 percent of the design loads.

6.1.6 Wall Instrumentation and Measured Results

The instrumentation for the wall consisted of strain gauges, embedment strain gauges, load cells, inclinometers, and settlement points. Surface-mounted vibrating wire strain gauges were used on the soldier beams. Twenty-eight strain gauges were installed (at approximately

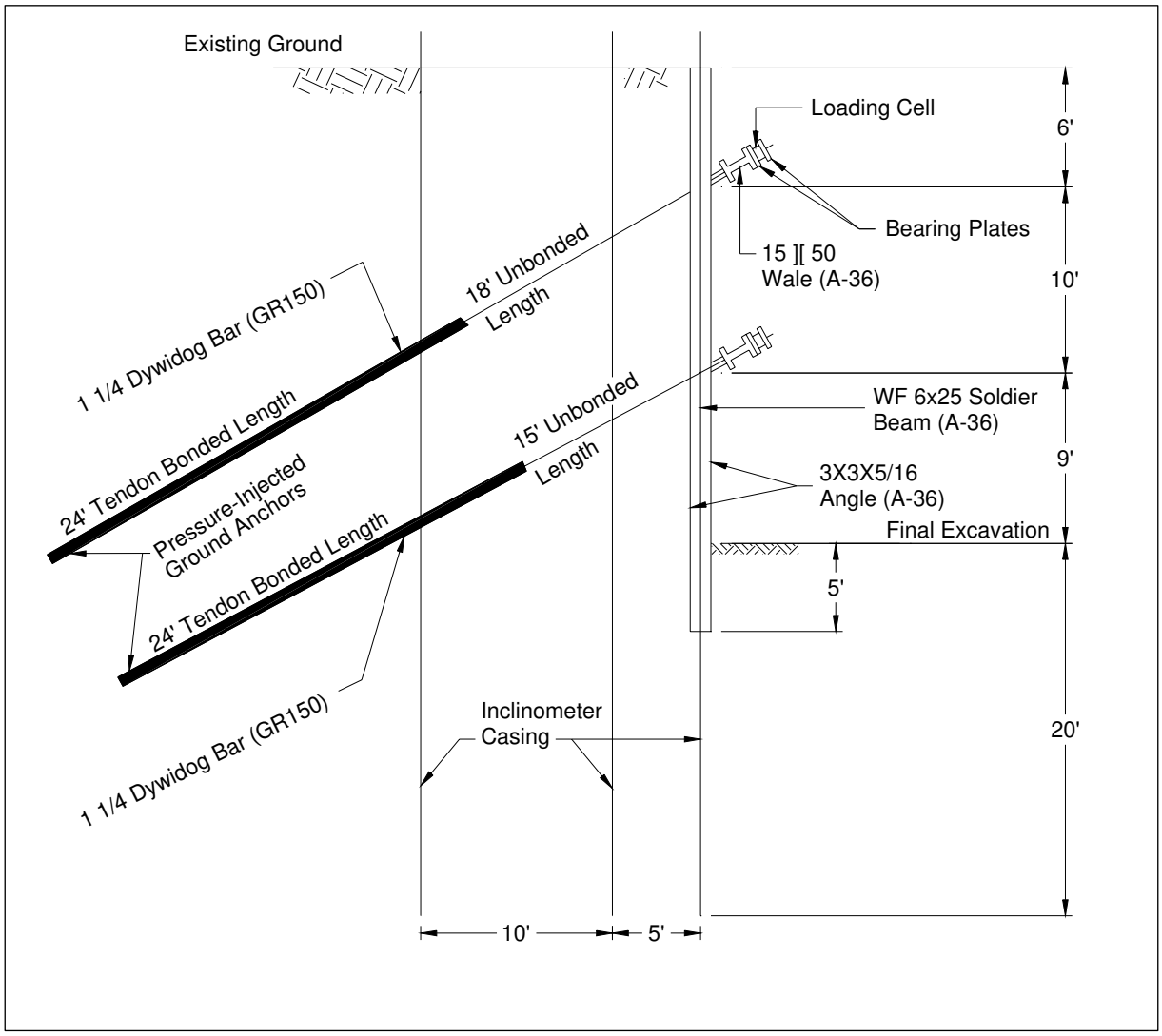

Figure 6.6. Section view through the two-tier wall

Table 6.1. Ground Anchor Schedule

Anchor No.	Tendon Size Diameter (in.)	Design Load (Kips)	Lock-off Load (Kips)
1	1-3/8	25.5	19.1
2	1-3/8	49.0	36.8
3-6	1-1/4	106.5	82.0
7-12	1-1/4	90.0	67.5
13	1-3/8	49.0	36.8
14	1-3/8	25.4	19.1
15	1-1/4	20.0	15.0
16-19	1-1/4	96.0	72.0

1-ft spacing along the beams) on the extreme fibers of each flange. Vibrating load cells were installed on each ground anchor supporting an instrumented soldier beam. The locations of the load cells were shown in Figure 6.4. Two-inch-thick bearing plates were used on each side of the load cells to minimize errors resulting from eccentric loading. Inclinometer casings were installed at each instrumented soldier beam, between the instrumented beams, and behind the wall face at the locations as were shown in Figure 6.5. The inclinometer casings were installed by driving a 3.5-in. closed-end casing into the ground to ensure that no ground was lost during installation. Figure 6.7 shows scaled instrumentation results for the final excavation stage.

6.2 RESULTS OF THE CURRENT 2-D DESIGN METHODOLOGY FOR THE "FLEXIBLE" TIEBACK WALL SYSTEM

As presented in Chapter 4 and described in Ebeling, Azene, and Strom, (2002), an equivalent beam on rigid support method of analysis using apparent earth pressure envelopes (identified as Rigid 1 method) is most often used in the design and analysis of "flexible" tieback wall systems. Soil arching, construction-sequencing effects, stressing of the ground anchors, and the lagging flexibility all caused the earth pressures behind flexible walls to redistribute to and concentrate at anchor support locations (FHWA-RD-98-066). The apparent earth pressure diagrams used in the Rigid 1 method were developed from measured loads and thus include the effects of soil arching, construction-sequencing effects, stressing of the ground anchors, and the lagging flexibility. These apparent pressures can provide an indication of the strength performance of the flexible tieback wall system. The case study wall described above is a flexible tieback wall system consisting of a flexible soldier beams with wood lagging. Therefore, the Rigid 1 method was used to evaluate the "flexible" case study tieback wall. The stages of construction for the wall are described in Table 6.2.

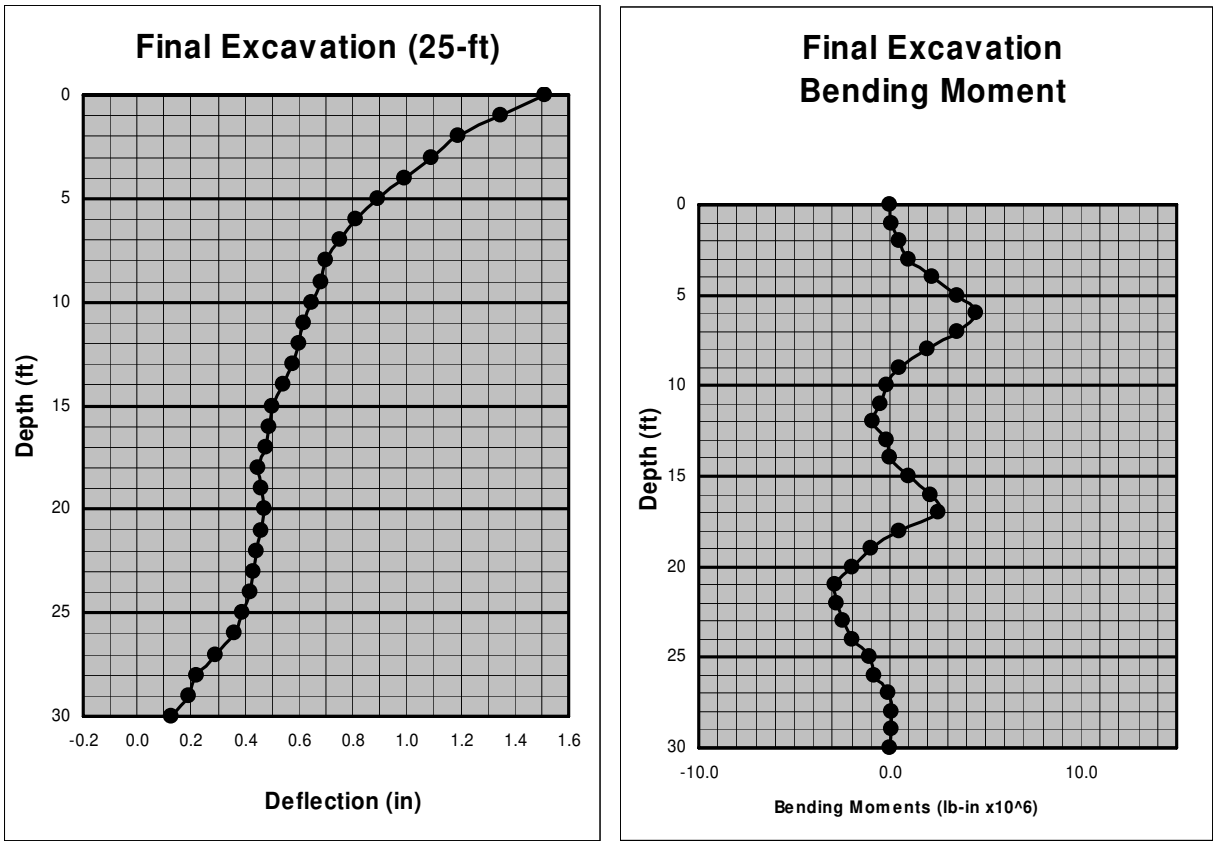

Figure 6.7. Flexible wall instrumentation results for final excavation stage

Table 6.2. Construction Process for "Flexible" Tieback Wall

Stage	Description
1	Place Soldier Beam
2	Excavate in front of wall to Elevation 17.0 **(Stage 1 Excavation)**
3	Install upper tieback anchor at Elevation 19 and prestress to 133 percent of the design load
4	Lock-off upper anchor at 75 percent of the design load
5	Excavate in front of wall to Elevation 8.0 **(Stage 2 Excavation)**
6	Install lower tieback anchor at Elevation 9 and prestress to 133 percent of the design load
7	Lock-off lower anchor at 75 percent of the design load
8	Excavate in front of wall to Elevation 0.0 **(Stage 3 Excavation)**

The analysis results consisting of wall computed maximum displacements, wall maximum bending moments, and maximum anchor forces for each excavation stage for the Rigid 1 method were tabulated in Table 6.3. This current 2-D design/analysis procedure was compared with the results from both 2-D and 3-D nonlinear finite element analyses, as well as available instrumentation results, as a means to evaluate the simplified Rigid 1 procedure.

6.2.1 Rigid 1 Analysis Results

The Rigid 1 procedure is an equivalent beam on rigid supports analysis in which the tieback wall modeled as a continuous beam on rigid supports and is loaded with an apparent pressure diagram. This procedure using the apparent earth pressure approach results in "hand calculations" of ground anchor loads and bending moments (refer to Figures 4.13 and 4.14). These diagrams are intended to represent a loading envelope used to design the structural components of flexible tieback wall system reflecting the entire construction and in service history. This approach provides good results for flexible walls constructed in competent soils

Table 6.3. Summary of Analysis Results for Excavation Stages 1 thru 3

	RIGID 1	2-D Plaxis FEM	3-D Plaxis FEM	Instrument.
Stage 1 Excavation (El. +17)				
Max. Anchor Load (Kips)	NA	NA	NA	NA
Max. Moment (ft-Kips)	NA	24	10	17
Max. Computed Displ. (in.)	NA	-0.45	-0.40	-0.5
Stage 2 Excavation (El. +8)				
Max. Anchor Load (Kips)	NA	80	67.8	NA
Max. Moment (ft-Kips)	NA	40	33.6	37.5
Max. Computed Displ. (in.)	NA	-0.3	-1.0	-0.7
Stage 3 Excavation (El. 0)				
Max. Anchor Load (Kips)	52.9	95.6	74.7	72
Max. Moment (ft-Kips)	49.2	42	36	37.5
Max. Computed Displ. (in.)	NA	-0.7	-1.7	-1.5

where excavation below the point of tieback prestress application is minimal (± 1.5 ft). Table 6.3 listed the maximum wall displacements, wall maximum bending moments, and maximum anchor forces for each excavation stage for the Rigid 1. A complete summary of the Rigid 1 analysis of this wall system is presented in Appendix C.

6.3 RESULTS OF 2-D NONLINEAR FINITE ELEMENT METHODS (NLFEM) OF ANALYSIS

6.3.1 2-D Plaxis FEM Results

As previously mentioned, the NLFEM is one of the general methods used in the analysis and design of tieback wall systems. Also as mentioned in Chapter 4, progressive type analyses (starting with the simplest design tool and progressing to more comprehensive design tools when necessary) are recommended for tieback wall analysis and design. Again, a 2-D NLFEM SSI analysis utilizing Plaxis Version 8.2 was initially performed on this case study wall. The results from this analysis were compared to the current 2-D methodology and provided a basis for investigating the wall system behavior in the more comprehensive 3-D analysis. Recalling, there were some key 2-D Plaxis features used in the plain strain analysis including: (1) the use of 15 node triangular elements to model the soil, (2) plates (i.e., special beam elements) to model the soldier beams, (3) node to node bar elements along with geogrid elements to model the tieback anchors, and (4) interface elements to model SSI between the wall and adjacent soil elements. A total of 12,599 nodes and 1,533 elements containing 18,396 stress points were used to define the finite element mesh shown in Figure 6.8. Table 6.4 summarizes the calculation phases used in the 2-D SSI analysis to model the construction process that was listed in Table 6.2. Engineering properties for the soldier beams, grouted zone and anchor are summarized in Tables 6.5 through 6.7.

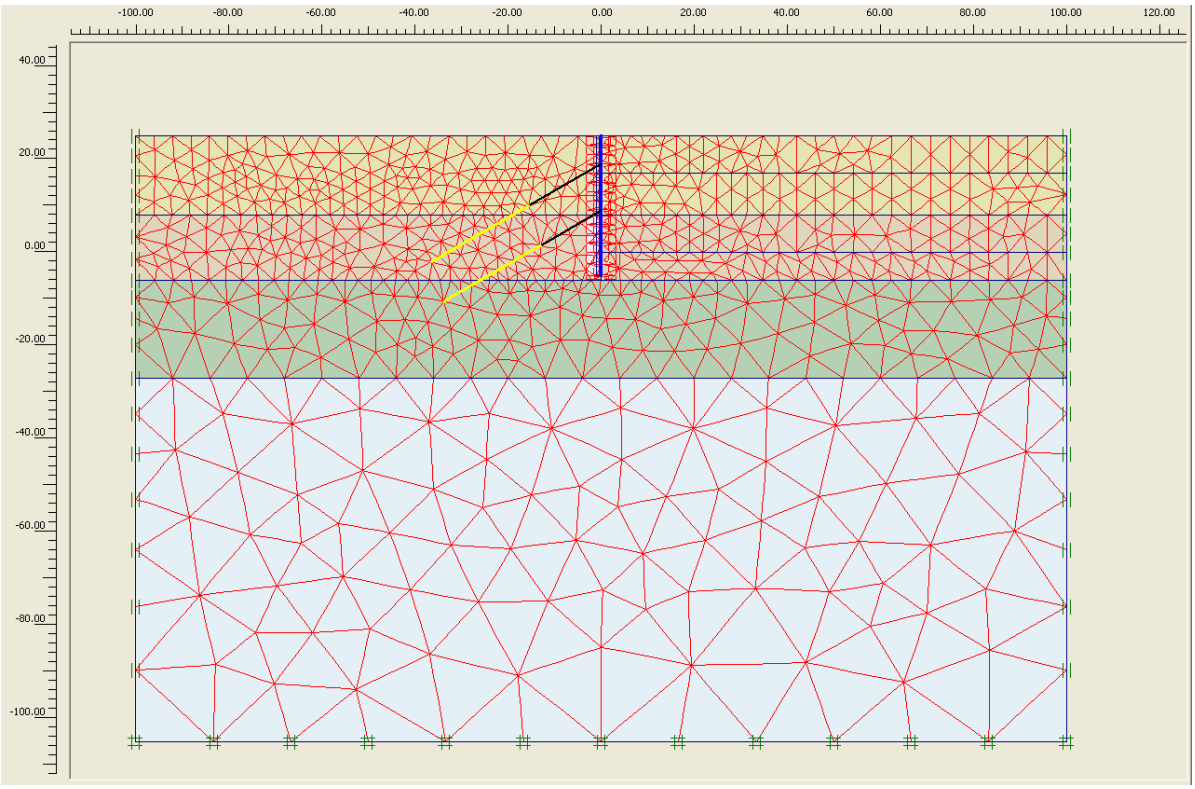

Figure 6.8. Finite element mesh used in the 2-D SSI analysis of flexible tieback wall

Table 6.4. Calculation Phases of 2-D Nonlinear Finite Element Analysis of Case Study Wall 2

Phase	Ph-No.	Calculation Type	Load Input
Initial phase	0		-
Place Wall & Interface	1	Plastic analysis	Staged construction
Excavate to El 17.0	2	Plastic analysis	Staged construction
Prestress Upper tieback	3	Plastic analysis	Staged construction
Lock off upper tieback to 75 percent of design load	4	Plastic analysis	Staged construction
Excavate to El 8.0	5	Plastic analysis	Staged construction
Prestress lower tieback	6	Plastic analysis	Staged construction
Lock off lower tieback to 75 percent of design load	7	Plastic analysis	Staged construction
Excavate to El 0.0	8	Plastic analysis	Staged construction

Table 6.5. Material Properties for the Soldier Beams

Identification	EA [lb/ft]	EI [lbft²/ft]	w [lb/ft/ft]	ν [-]
Soldier Beam	4.09E+07	3.46E+06	25.0	0.2

Table 6.6. Material Properties for the Grouted Zone

Identification	EA [lb/ft]	ν [-]
Tieback grout	2340000	0

Table 6.7. Material Properties for the Anchor

Identification	EA [lb]	|Fmax,comp| [lb]	|Fmax,tens| [lb]	L spacing [ft]
Anchor (tieback)	18750000	1.00E+15	1.00E+15	8

Figure 6.9 shows the various soil clusters used to define regions of common soil properties for four categories of soil within the finite element mesh, i.e., silty sand, medium dense sand, medium dense clayey sand, and hard clay. Section 6.1.2 described the geological characterization of these soils. A key aspect of this SSI study was to investigate the effective soil stress conditions and the long-term behavior of the wall system. Soil stiffness and strength properties obtained from soil testing based on these conditions would provide the best estimate of input parameters for the Plaxis nonlinear Hardening Soil (HS) constitutive model utilized in the study. There was a limited amount of in situ tests and laboratory tests performed on the soils at this site. The in situ tests provided estimates of angle of internal friction, total units weights, and information that could be used in relative density correlations to obtain estimates of soil stiffness. The laboratory tests were used to determined information such as Atterberg limits and the soil classification.

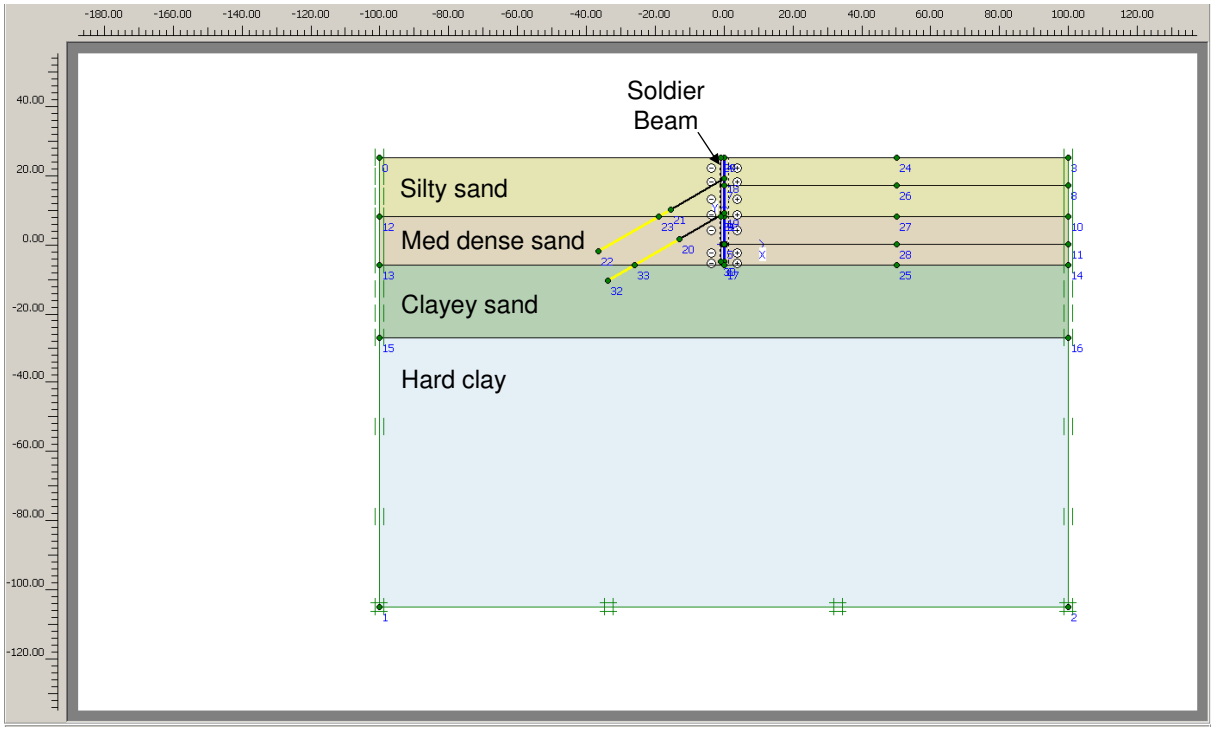

Figure 6.9. Two-dimensional cross-section model used to define soil regions and used in SSI analysis of the flexible tieback wall

However, triaxial tests are one of the most reliable methods of determining stiffness and strength properties for input in nonlinear Hardening Soil (HS) constitutive model utilized in the study. There were no triaxial testing preformed on soils at the test site. Therefore, a parametric study was performed on the key HS constitutive parameter, the secant stiffness (E_{50}^{ref}) that would produce results, which best matched to the available instrumentation results for this case study wall . Other HS constitutive parameters used in the parametric study were estimated based on available parameter correlations sited in the literature, Plaxis author's recommendations (Brinkgreve 2005), and a literature database of model parameters used in Plaxis analyses for similar soil types and properties. A summary of the range of values of E_{50}^{ref} for sands from the above-mentioned resources is shown in Table 6.8.

Table 6.8. Summary of Estimates of Secant Stiffness E_{50}^{ref} (psf) for Sands

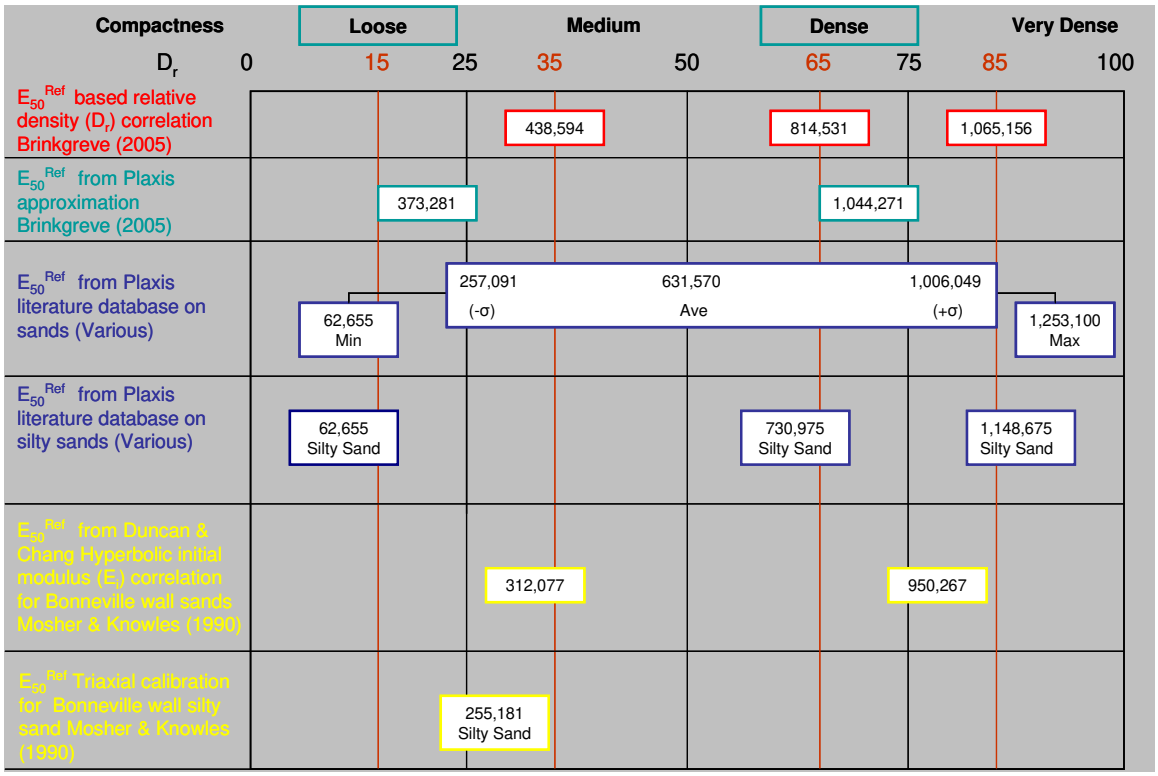

Tables 6.9 to 6.11 show Plaxis 2-D FEM parametric results for variations in E_{50}^{ref} at selected construction stages. These computed results were compared to the measured results as a mean to calibrate the HS constitutive model for both the 2-D and 3-D analyses. Tables 6.9 and 6.10 show as E_{50}^{ref} decreased the corresponding wall deflection and bending moments decreased for the initial cantilever construction stage and the final construction stage. Table 6.11 show further refinement in the parametric study by means of variation in both E_{50}^{ref} for silty sand and the medium dense sand in an attempt to better approximate the measured results. There is good agreement in results for both construction stages except for the final stage wall deflection. It was noted that a strong storm occurred at the end of the wall testing period that may have caused an increase in pore water pressures therefore increased

Table 6.9. Stiffness Variations for Silty Sand and the Resulting Computed Deformations and Moments

	Varation of E_{50}^{Ref} Silty Sand (psf)			
	255,181	501,250	631,570	
I. Cantilever Stage				**Measured**
a. Wall Deflection (in)	1	0.72	0.61	0.5
b. Max. Moment (Kips*ft)	28.6	25.6	24.8	20
II. Final Stage				**Measured**
a. Wall Deflection (in)	0.96	0.88	0.63	1.5
b. Max. Moment (Kips*ft)	56	52	40	45

Table 6.10. Stiffness Variations for Medium Dense Sand and the Resulting Computed Deformations and Moments

	Variation of E_{50}^{Ref} Med Dense Sand (psf)			
	814,531	501,250	631,570	
I. Cantilever Stage				**Measured**
a. Wall Deflection (in.)	1	0.58	NA	0.5
b. Max. Moment (Kips*ft)	28.6	24.8	NA	20
II. Final Stage				**Measured**
a. Wall Deflection (in.)	0.96	0.65	NA	1.5
b. Max. Moment (Kips*ft)	56	40.8	NA	45

Table 6.11. Stiffness Variations for Silty Sand and Medium Dense Sand and the Resulting Computed Deformations and Moments

	Silty Sand	**Med Dense Sand**	**Silty Sand**	**Med Dense Sand**	**Silty Sand**	**Med Dense Sand**	
	313,281	438,594	814,531	313,281	730,975	313,281	
I. Cantilever Stage							**Measured**
a. Wall Deflection (in)	0.88		0.42		0.46		0.5
b. Max. Moment (Kips*ft)	27.1		23.92		24		20
II. Final Stage							**Measured**
a. Wall Deflection (in)	0.74		0.7		0.7		1.5
b. Max. Moment (Kips*ft)	41.2		42.56		42		45

the horizontal pressures on the wall over a short duration. Additionally, there was good agreement in results at other intermittent construction stages. The values of E_{50}^{ref} equal to 730,975 psf and 313,281 psf were selected for silty sand and medium dense sand, respectively. The stiffness values were used as basis for both the 2-D and 3-D assessments and these values were within the range of values found in the literature for similar soils (Refer to Table 6.8).

Table 6.12 summarizes the engineering material properties and the HS parameters assigned to the various soil types.

6.3.1.1 Initial Stress Conditions

The original ground surface of the finite element mesh was horizontal at el 25 ft. In Plaxis, initial stresses were computed by the K_o (i.e., at-rest) procedure. As previously mentioned, an important aspect of the effective stress domain is that the mobilized shear stress computed at strain integration points within the finite elements be less than the shear strength

Table 6.12. Hardening Soil Parameters Used for Flexible Tieback Wall

	Parameter	Symbol	Units	Silty Sand	Medium Dense Sand	Clayey Sand	Hard Clay
	Unit Weight	γ	lb/ft^3	115	115	125	130
	Cohesion	c	lb/ft^2	0	0	10	10000
	Friction Angle	Φ'	[°]	32	32	32	30
	Dilation Angle	ψ	[°]	2	2	0	0
	Secant Stiffness in standard triaxial test	E_{50}^{ref}	lb/ft^2	730975	313281	313281	1028591
	Tangent Stiffness for primary oedometer loading 1.0*(E50ref)	$Eoed^{ref}$	lb/ft^2	730975	313281	313281	1028591.27
	Unloading /Reloading Stiffness $3*(E_{50}^{ref})$	E_{UR}^{ref}	lb/ft^2	2192925	939843	939843	3085774
	Power for stress level dependency of stiffness	m	[]	0.8	0.8	0.8	0.8
	Poisson's Ratio for Unloading /Reloading	υ	[]	0.2	0.2	0.2	0.2
	Failure Ratio	R_f	[]	0.7	0.7	0.7	0.7
	Interface reduction Fator	R_{int}	[]	0.9	0.9	0.9	0.9

of the soil. The ratio of mobilized shear stress to maximum available shear stress represents the percentage of mobilized shear strength. The resulting computed fraction of mobilized shear strength (referred to as relative shear stress in Plaxis output) for the resulting initial stress condition is shown in Figure 6.10. As shown, the fraction of mobilized shear strength is less than or equal to 0.68 for all soil types which indicates stability of soil. The uniform shading for the silty sand, medium dense sand and the clayey sand is attributed to them having essentially the same strength properties.

6.3.1.2 Selected Stage Construction Results

Table 6.3 listed the computed wall maximum displacements, wall maximum bending moments, and maximum anchor forces using the current 2-D analysis/design procedure for flexible tieback wall system i.e., Rigid 1 method for each excavation stage. Additionally, both 2-D and 3-D nonlinear finite element analyses were used as a means to access this procedure.

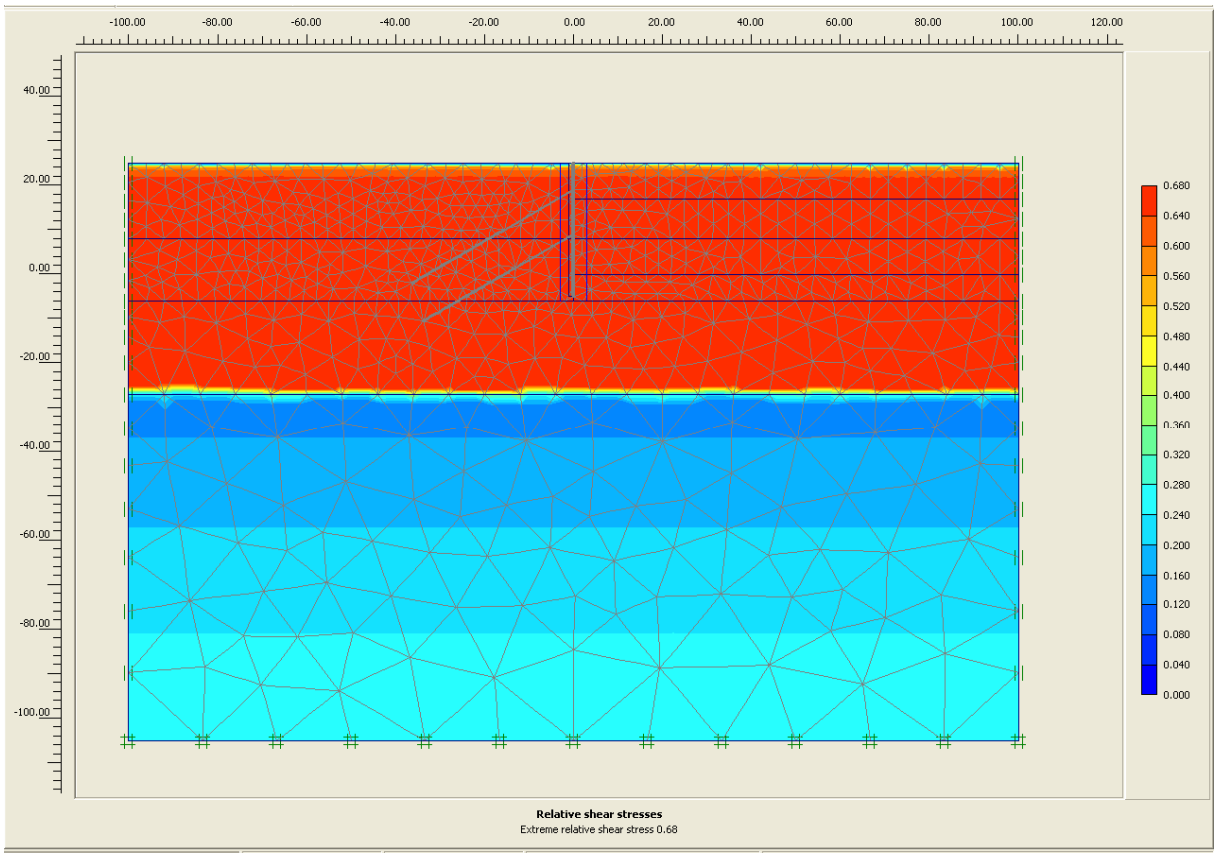

Figure 6.10. Fraction of mobilized shear strength for initial stress conditions

A key construction stage for tieback design is the cantilever excavation stage (excavation stage just prior to installation and lock-off of the uppermost anchor). This stage is key because over-excavation below the ground anchor supports may produce wall movements and wall anchor force demands that are larger than tolerable. For this case study wall, an over-excavation of 2.0 ft was used in the analyses. An evaluation of selected construction sequence stages was performed to determine if maximum wall movements and force demands on the wall and tiebacks occurred at intermediate stages of construction rather than for the final permanent loading condition. Figure 6.11 shows the computed 2-D FEM results of horizontal displacements of the wall after the cantilever excavation stage. The computed maximum displacement (Ux) was equal to 0.46 in. compared to 0.5 in. from inclinometer measurements.

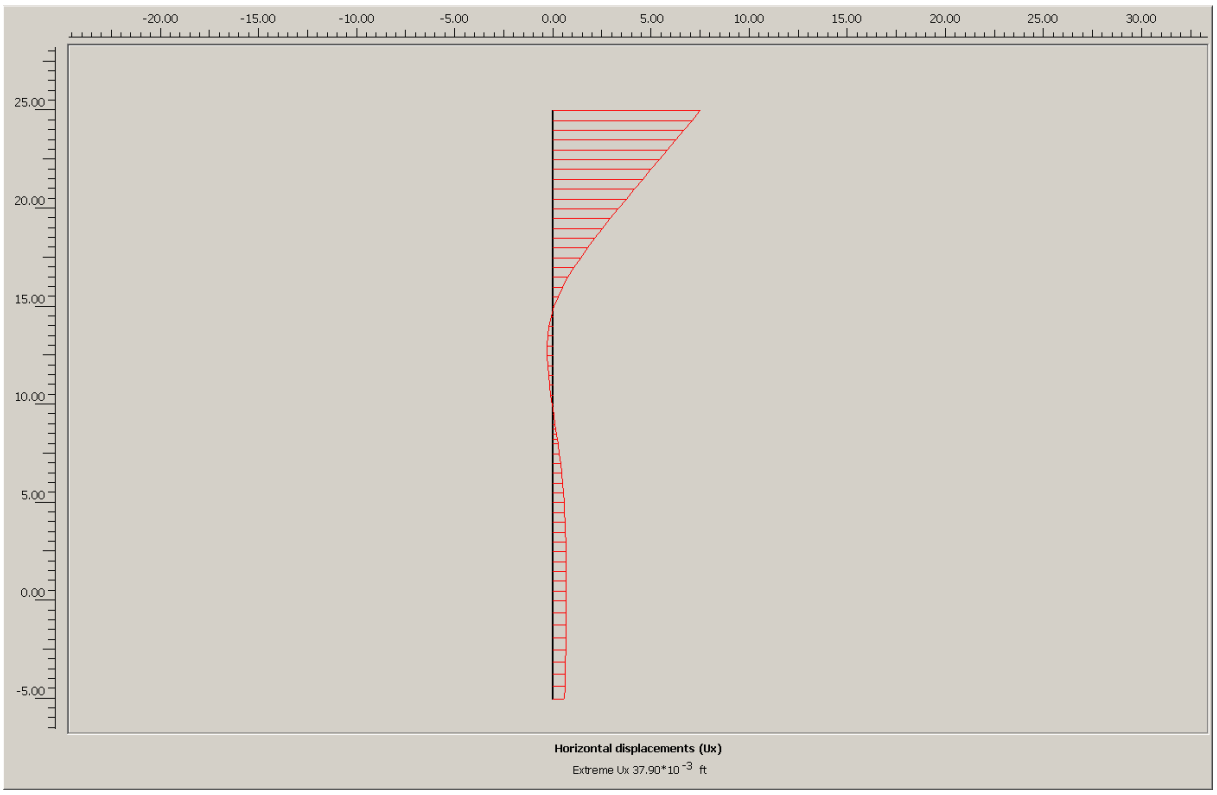

Figure 6.11. 2-D FEM horizontal displacements of the wall after the cantilever excavation stage (Ux (Max) = 0.46 in.)

The corresponding wall bending moments after the cantilever excavation stage (with a maximum moment equal to 3.1 Kip*ft/per ft run of wall) is shown in Figure 6.12. This 2-D FEM moment computed was comparable to 2.5 Kip*ft/per ft run of wall computed from strain gauge measurements. Discrete values of bending moments for the soldier beams can be derived from these "smeared" bending moments per foot run of wall based on the following relationships:

$$\theta_{\text{soldier beam}} \text{ (per ft run)} = M_{\text{soldier beam}} \text{ (per ft run)/ } EI_{\text{soldier beam}} \text{ (per ft run)} \qquad \text{Equation 6.1}$$

where θ = soldier beam rotation; EI = bending stiffness

$$EI_{\text{soldier beam}} \text{ (per ft run)} = EI_{\text{soldier beam}} \text{ (Discrete)/Plan Spacing} \qquad \text{Equation 6.2}$$

$$M_{\text{soldier beam}} \text{ (Discrete)} = \boldsymbol{\theta}_{\text{plate}} \text{ (per ft run)} * EI_{\text{plate}} \text{ (Discrete)} \qquad \text{Equation 6.3}$$

Substituting Equations 6.1 and 6.2 into 6.3 yields

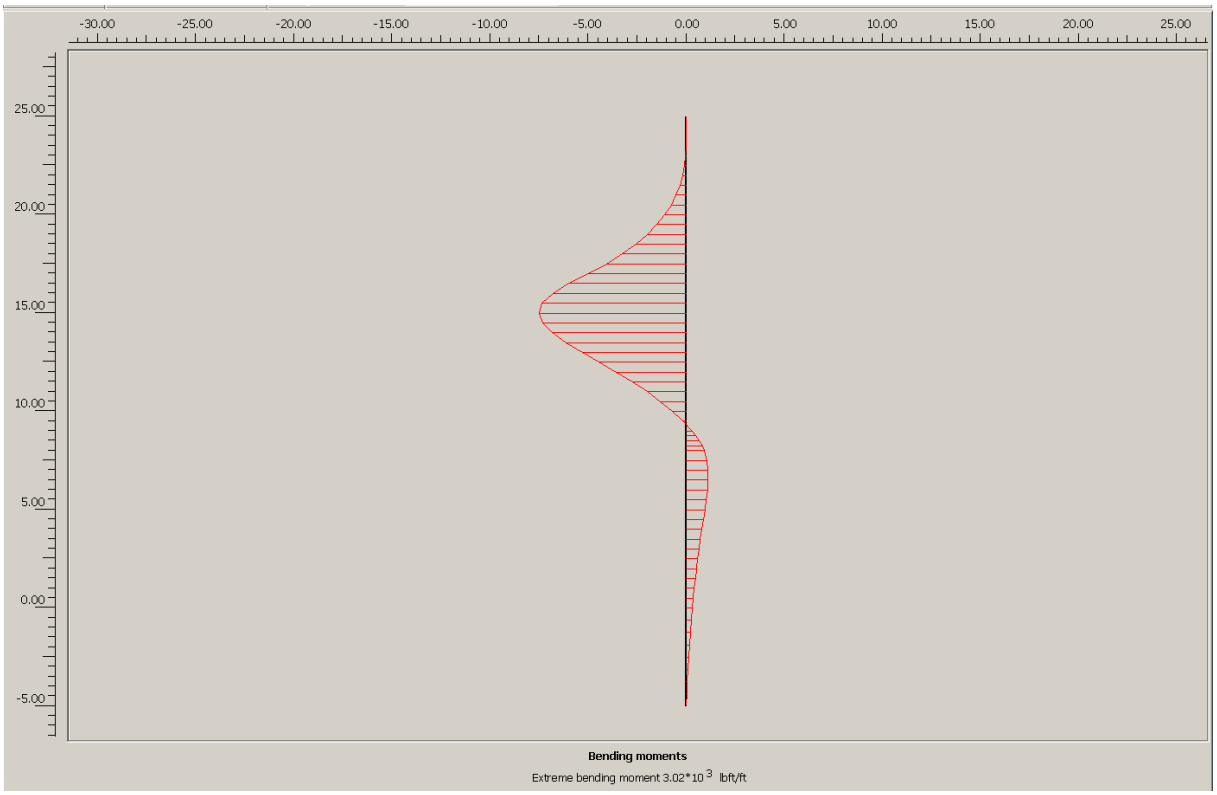

Figure 6.12. 2-D FEM bending moment results (moment max = 3.1 Kip*ft/ft run of wall)

$$M_{\text{soldier beam}} \text{ (Discrete)} = M_{\text{soldier beam}} \text{ (per ft run)} * \text{Plan Spacing} \qquad \text{Equation 6.4}$$

Figure 6.13 shows the computed 2-D FEM results of horizontal displacements of the wall after the final excavation stage. The computed maximum displacement (Ux) was equal to 0.70 in. compared to 1.5 in. from inclinometer measurements. It was noted that a strong storm occurred at the end of the wall testing period that may have caused an increase in pore water pressures therefore increased the horizontal.

The corresponding wall bending moments after the final excavation stage (with a maximum moment equal to 5.25 Kip*ft/per ft run of wall) is shown in Figure 6.14 compared well to 5.63 Kip*ft/per ft run of wall computed from strain gauge measurements.

Figure 6.15 shows the axial force distribution per foot run of wall that is transferred to the anchor bond zone for the upper tieback anchor. The discrete axial force is obtained by

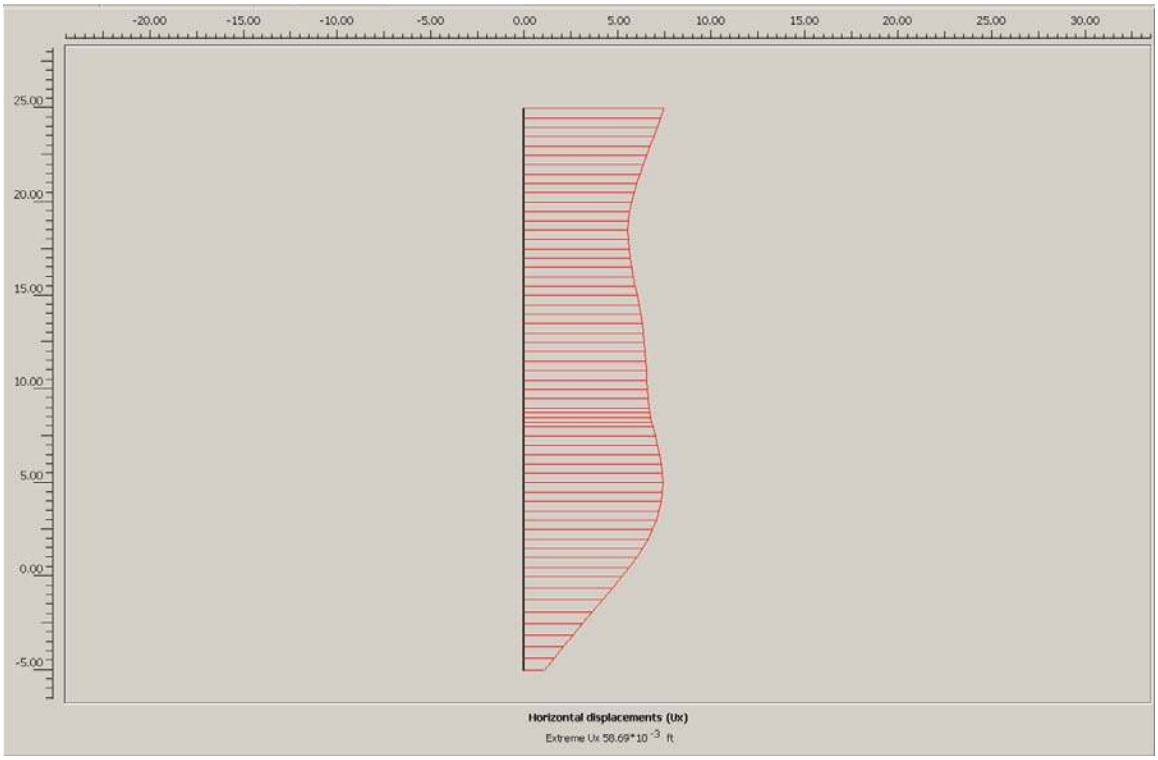

Figure 6.13. 2-D FEM horizontal displacements of the wall after the final excavation stage (Ux (Max) = 0.70 in.)

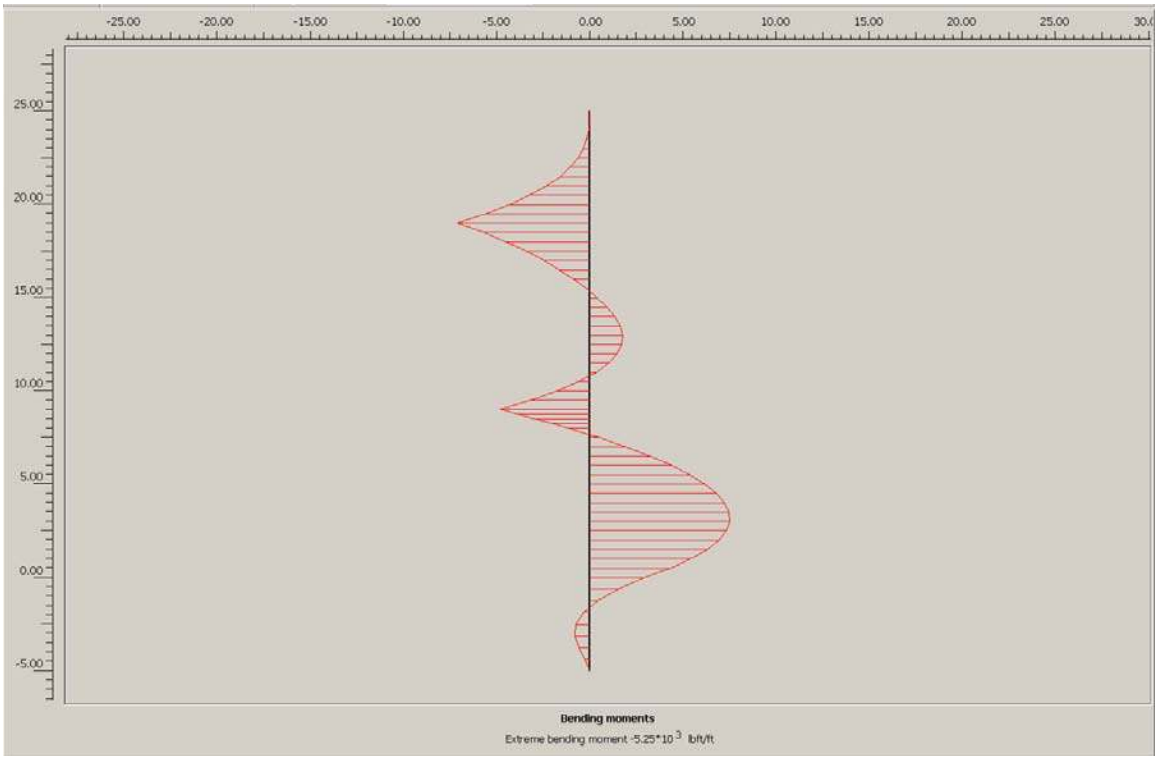

Figure 6.14. 2-D FEM bending moment results (moment max = 5.25 Kip*ft/ft run of wall)

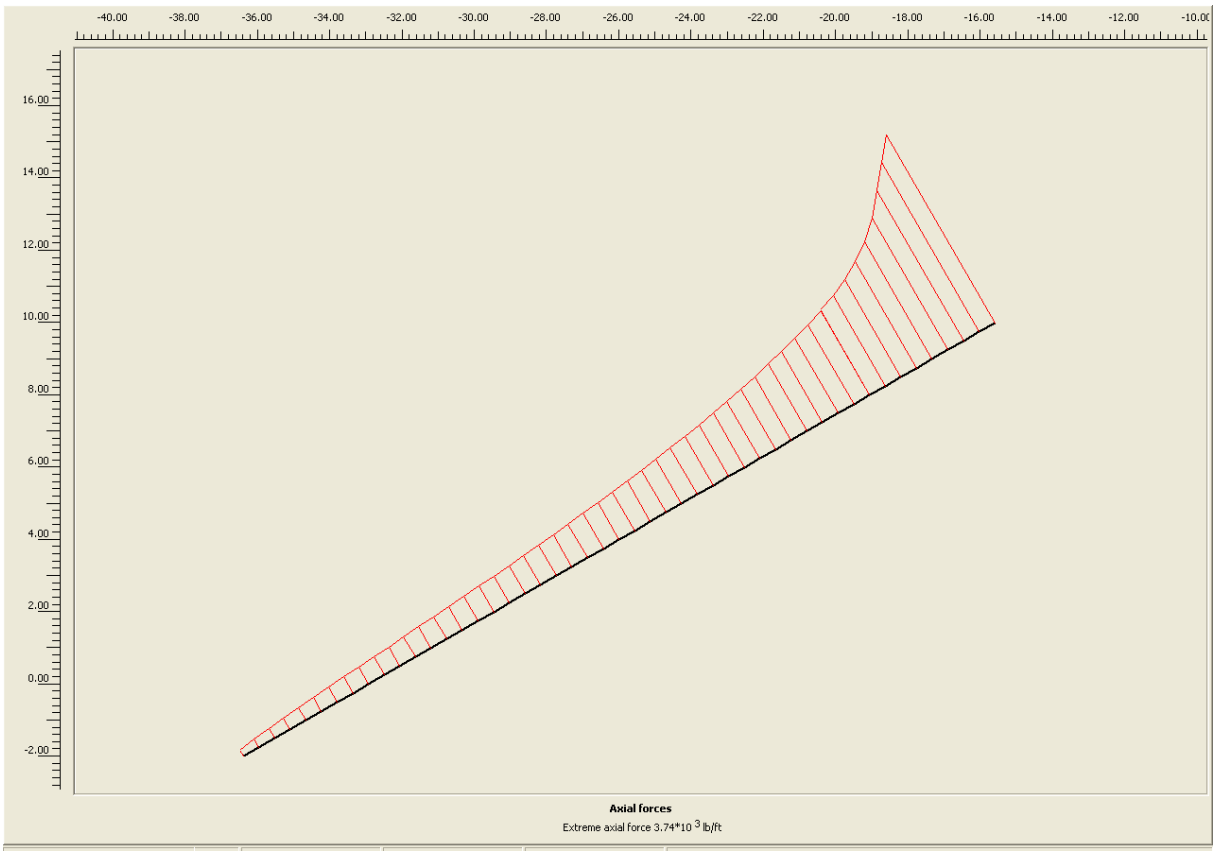

Figure 6.15. Axial forces in grouted zone after Stage 1 excavation (Max = 3.74 Kip/ft)

multiplying axial force distribution per foot run of wall by the plan spacing of the anchor. As shown, the largest amount of axial force is initially transferred to the top of the anchor bond zone and it decreases in magnitude toward the bottom of the bond zone.

6.4 RESULTS 3-D NONLINEAR FINITE ELEMENT METHOD (NLFEM) OF ANALYSIS

6.4.1 3-D Plaxis FEM Results

As with the "stiff" case study wall system, the final analytical method used in the engineering assessment of the "flexible" case study wall system was the more comprehensive 3-D NLFEM. It was also envisioned that the 3-D NLFEM of the flexible case study wall would provide: (1) a means to quantify 3-D features that are not considered in current conventional 2-D procedures, (2) additional insight on the overall wall system behavior, and

(3) a way to assess simplified 2-D limit equilibrium procedures of the case study retaining wall system.

Plaxis 3-D Tunnel Version 2 was also utilized to perform the comprehensive 3-D analyses. There were some key 3-D Plaxis features used in the analyses including: (1) the use of 15 node wedge elements to model the soil, soldier beams, and the wale seats, (2) plate elements (i.e., special beam elements) to model the wood lagging, wales, hinges at the interface of the soldier beam and lagging, and for computing bending moments in the soldier beams, (3) node to node bar elements along with geogrid elements to model the tieback anchors, and (4) interface elements to model SSI between the wall and adjacent soil elements. A total of 69,830 nodes and 24,710 elements containing 148,260 stress points were used to define the finite element mesh shown in Figure 6.16. An initial 2-D finite element mesh cross section was extruded in the out of plane direction (z-direction) to form the 3-D model. The interior Planes C (z-coordinate = -4.5 ft) at the center plane of soldier beam 7, Plane G (z-coordinate = -8.5) at the ground anchor location, and Plane K (z-coordinate = -12.5) at the center plane of soldier beam 8 were selected as key representative cross sections of the wall system for use in the FEM assessment (Figure 6.17).

6.4.1.1 Special 3-D Plaxis Modeling Features

The flexible case study wall consisted of discrete soldier beams with horizontally placed wood lagging to support the soil between the beams (Refer to Figure 6.5). The soldier beams were steel beam sections. These discrete beams were modeled with 3-D volume elements using the linear elastic material model. Modeling the discrete soldier beams with volume elements was due to the extrusion procedure used to develop the full 3-D model within Plaxis 3-D tunnel so that Plaxis could extrude a plate element over the full z-direction of the finite

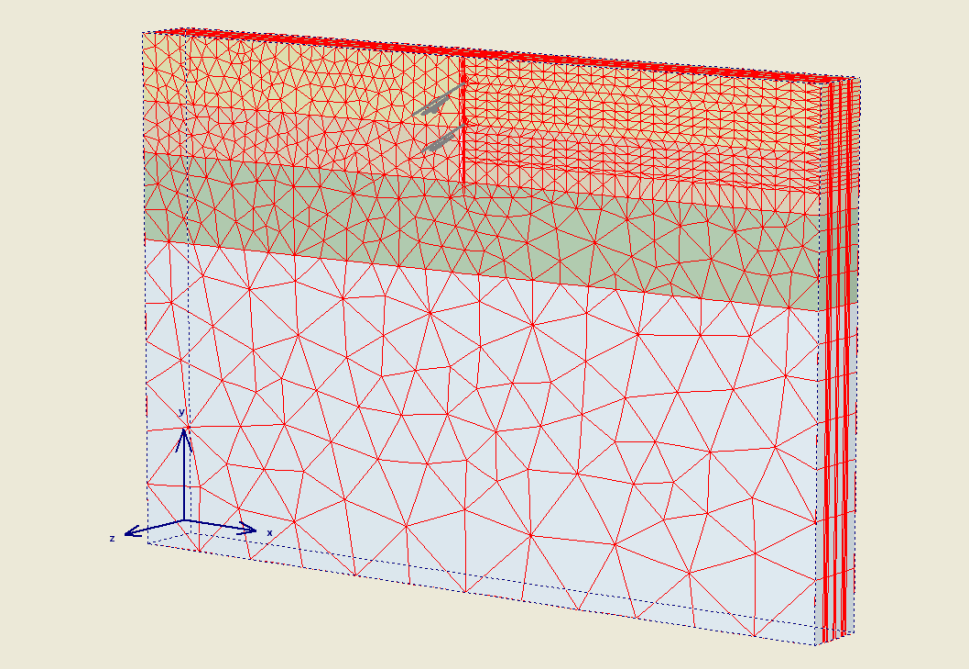

Figure 6.16. Finite element mesh used in the 3-D SSI analysis of the flexible tieback wall

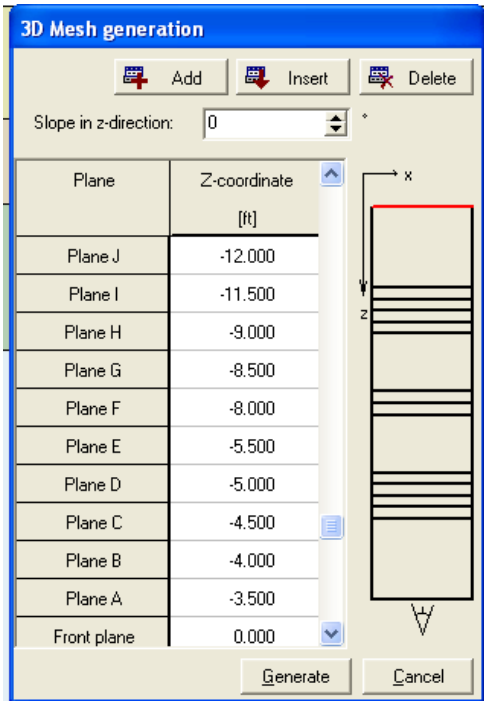

Figure 6.17. Plan spacing of planes for "flexible wall" 3-D model

element model. Vertical plate elements were inserted at the center widths of the volume elements used to model the soldier beams in order to compute bending moments within the volume elements.

The plate elements were assigned a very small bending stiffness (1E-6 times the actual stiffness of the soldier beams) to prevent the plate elements from influencing the deformations of the soldier beams via volumetric elements. The 3-D Plaxis bending moment per ft run of wall in the soldier beam is determined from the properties of the soldier beam and plate element as well as the moment computed by Plaxis in the plate element. The value for $M_{soldier\ beam}$ is determined using the following relationships:

$$M_{soldier\ beam} = \theta_{soldier\ beam} * (EI)_{soldier\ beam} \quad \text{Equation 6.5}$$

$$\theta_{plate\ element} = M_{plate\ element} / (EI)_{plate\ element} \quad \text{Equation 6.6}$$

$$\theta_{soldier\ beam} = \theta_{plate\ element} \quad \text{Equation 6.7}$$

$$M_{soldier\ beam} = (EI)_{soldier\ beam} / (EI)_{plate\ element} * M_{plate\ element} \quad \text{Equation 6.8}$$

where θ = rotation; EI = bending stiffness.

Equation 6.8 describes the soldier beam bending moment per ft run of wall in the Plaxis 3-D FEM analysis. The remaining components of a typical soldier beam and lagging tieback wall and their effects on the wall system behavior are described below. These components and their effects are not included in 2-D FEM analysis nor in 2-D simplified procedure Rigid 1. Recalling, one objective of this study was to investigate the effects of 3-D features that are not considered in current conventional 2-D procedures.

Lagging consisting of horizontally placed panels of wood members were modeled with rows plate elements extending in the z-direction. Wood lagging provide support to the soil between the soldier beams and transfers a portion of the soil load to the soldier beam. Wood

lagging is commonly installed behind the front flange of the I-beams adjacent to the excavation side of the wall.

The lagging is not rigidly attached to the soldier beam flange and thus there is no bending moments transferred (hinge connection). Plaxis 3-D Tunnel currently does not support a hinge connection. However, hinge connections were approximated by defining plate elements over small slices in front and behind of each soldier beam (in the z-direction). The hinge plates had the same stiffness properties as wood lagging, but the hinge plates were modeled with the elasto-plastic material model and assigned a very small plastic bending moment. A parametric study was performed to determine a plastic moment value to assign to the hinge plate and maintain a numerically stable model. This series of computations resulted in a plastic moment value of 7.5 ft*lb assigned to the hinge plate elements. This value is approximately 0.1 percent of an estimated bending moment corresponding to first yield of the extreme fibers of the wood lagging (5,400 ft*lb). The bending moment at yield for the wood lagging was based on the allowable bending stress and section properties for a typical (3 in. × 12 in.) timber section.

The test section beams designated as 7 and 8 had discrete wales spanning between the soldier beams (Figure 6.18). These wales were also modeled with plate elements. Wales are horizontal stiffeners that transfer loads from the soldier beams to the ground anchors. The wales used at this test site are typically single steel channel section. This type of soldier beam and lagging tieback wall system with discrete wales is not typically used in Corps of Engineers designs. Corps of Engineers designed soldier beam and lagging tieback walls typically have pairs of C-channel wales that span continuously over the wall system. Wales are often placed on discrete offsets called “seats” along the soldier beams to form a gap

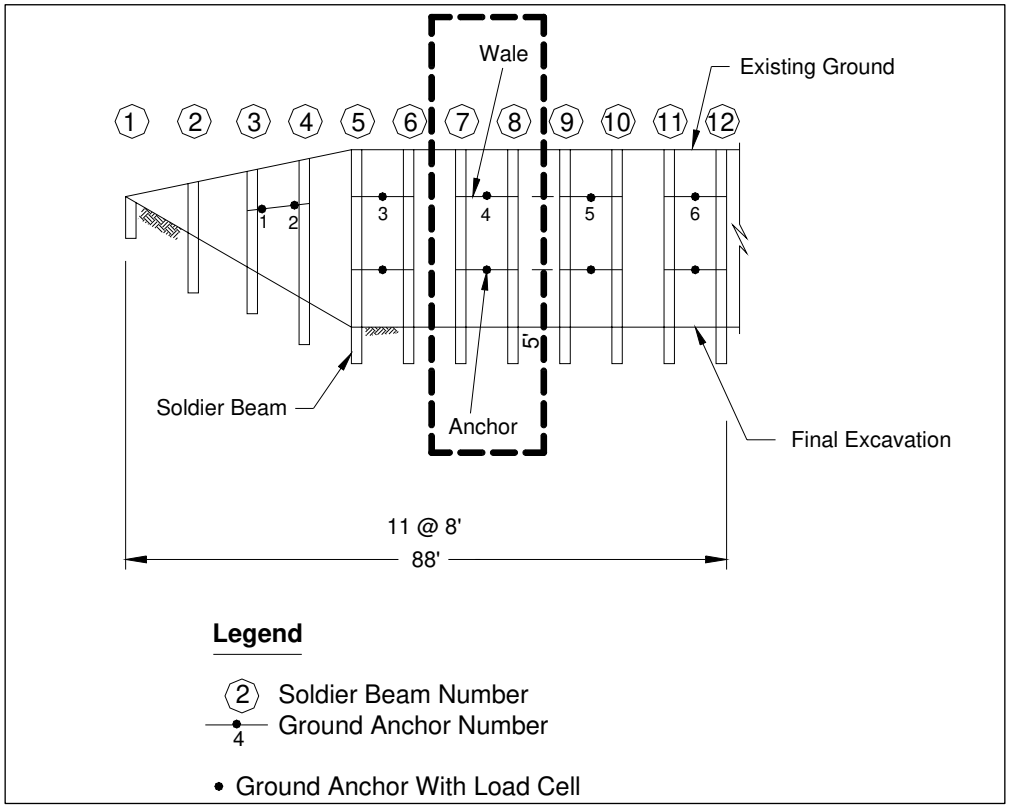

Figure 6.18. Wall test section showing discrete wales

between the lagging and the wales. The purpose of offsetting the wales on the seats is to prevent load transfer between the lagging and the wales. Figure 6.19 shows a 3-D FEM model with above-mentioned components identified.

The same major construction process steps used in the 2-D FEM analysis of this flexible wall system were also used to model the construction process in the 3-D analysis (Refer to Table 6.2). However, additional construction steps were included to model placing the wood lagging and placing the wales and wale seats in order to determine their 3-D effects on the wall system. This type of wall system is usually constructed using the top-down construction procedure, where the soldier piles are driven first followed by an alternating pattern of excavation of soil and installing the lagging. This construction process was simulated in the

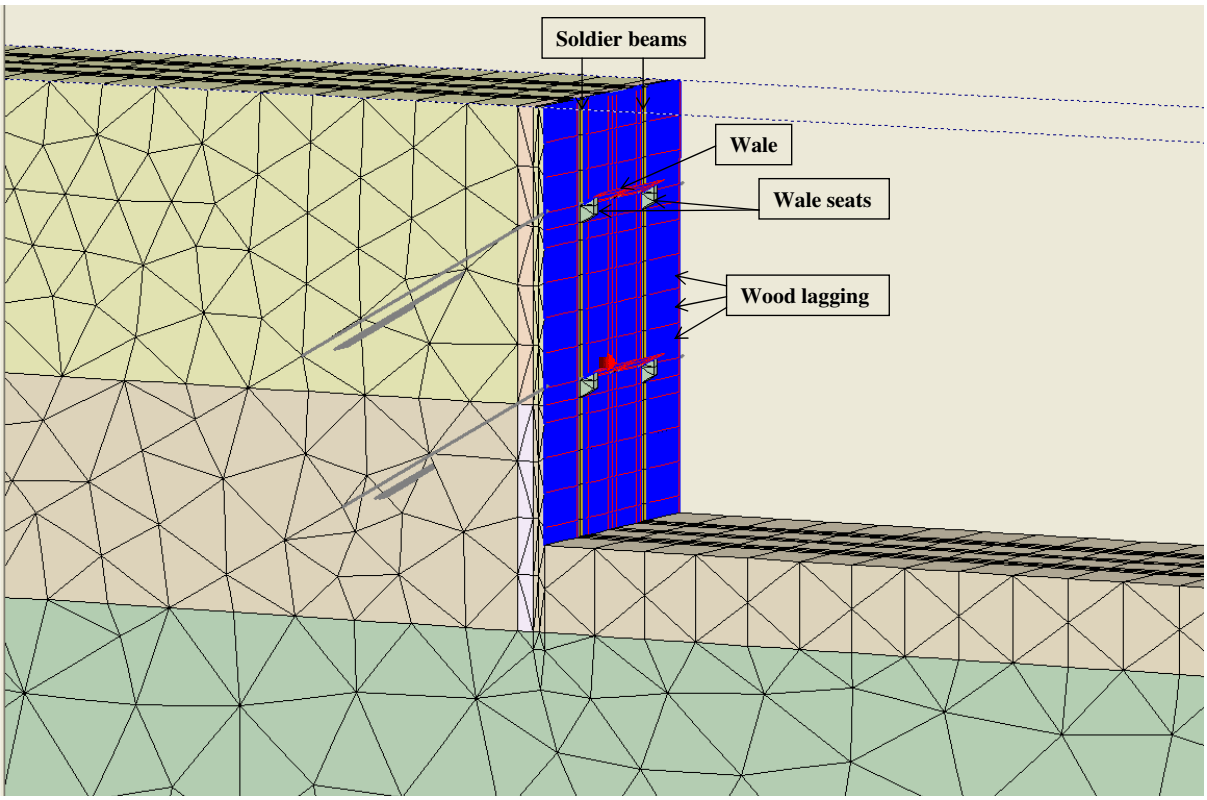

Figure 6.19. Components of flexible tieback wall used in 3-D FEM model

3-D FEM analysis. Table 6.13 lists the loading phases used in the 3-D FEM analysis to model the complete construction process.

6.4.1.2 Initial Stress Conditions

As previously mentioned, an important aspect of the effective stress system is that the computed mobilized shear stress within the finite elements be less than the shear strength of the soil. The resulting 3-D computed fraction of mobilized shear strength (referred to as relative shear stress in Plaxis output) from the resulting initial stress condition is shown in Figure 6.20. As shown, the fraction of mobilized shear strength is less than or equal to 0.68 for all soil types and thus indicates a stable initial soil stress condition. This condition was also indicated in the 2-D FEM results.

Table 6.13. Calculation Phases of 2-D Nonlinear Finite Element Analysis of Case Study Wall 2

Phase	Ph-No.	Calculation Type	Load Input
Initial phase	0		-
Place Soldier Beam & Interface	1	Plastic analysis	Staged construction
Excavate to El 23.0	2	Plastic analysis	Staged construction
Excavate to El 21.0 & Place Lagging to El 23	3	Plastic analysis	Staged construction
Excavate to El 19.0 & Place Lagging to El 21	4	Plastic analysis	Staged construction
Excavate to El 17.0 & Place Lagging to El 19	5	Plastic analysis	Staged construction
Place Lagging to El 17	6	Plastic analysis	Staged construction
Place Upper Wale Seat and Wale	7	Plastic analysis	Staged construction
Prestress Upper tieback to 133 percent of Design load	8	Plastic analysis	Staged construction
Lock off Upper tieback to 75 percent of design load	9	Plastic analysis	Staged construction
Excavate to El 15.0	10	Plastic analysis	Staged construction
Excavate to El 13.0 & Place Lagging to El 15	11	Plastic analysis	Staged construction
Excavate to El 11.0 & Place Lagging to El 13	12	Plastic analysis	Staged construction
Excavate to El 9.0 & Place Lagging to El 11	13	Plastic analysis	Staged construction
Excavate to El 7.0 & Place Lagging to El 9	14	Plastic analysis	Staged construction
Place Lagging to El 7	15	Plastic analysis	Staged construction
Place Lower Wale Seat and Wale	16	Plastic analysis	Staged construction
Prestress Lower tieback to 133 percent of Design load	17	Plastic analysis	Staged construction
Lock off Upper tieback to 75 percent of design load	18	Plastic analysis	Staged construction
Excavate to El 5.0	19	Plastic analysis	Staged construction
Excavate to El 3.0 & Place Lagging to El 5	20	Plastic analysis	Staged construction
Excavate to El 1.0 & Place Lagging to El 3	21	Plastic analysis	Staged construction
Excavate to El 0.0 & Place Lagging to El 1	22	Plastic analysis	Staged construction
Excavate to El 0.0	23	Plastic analysis	Staged construction

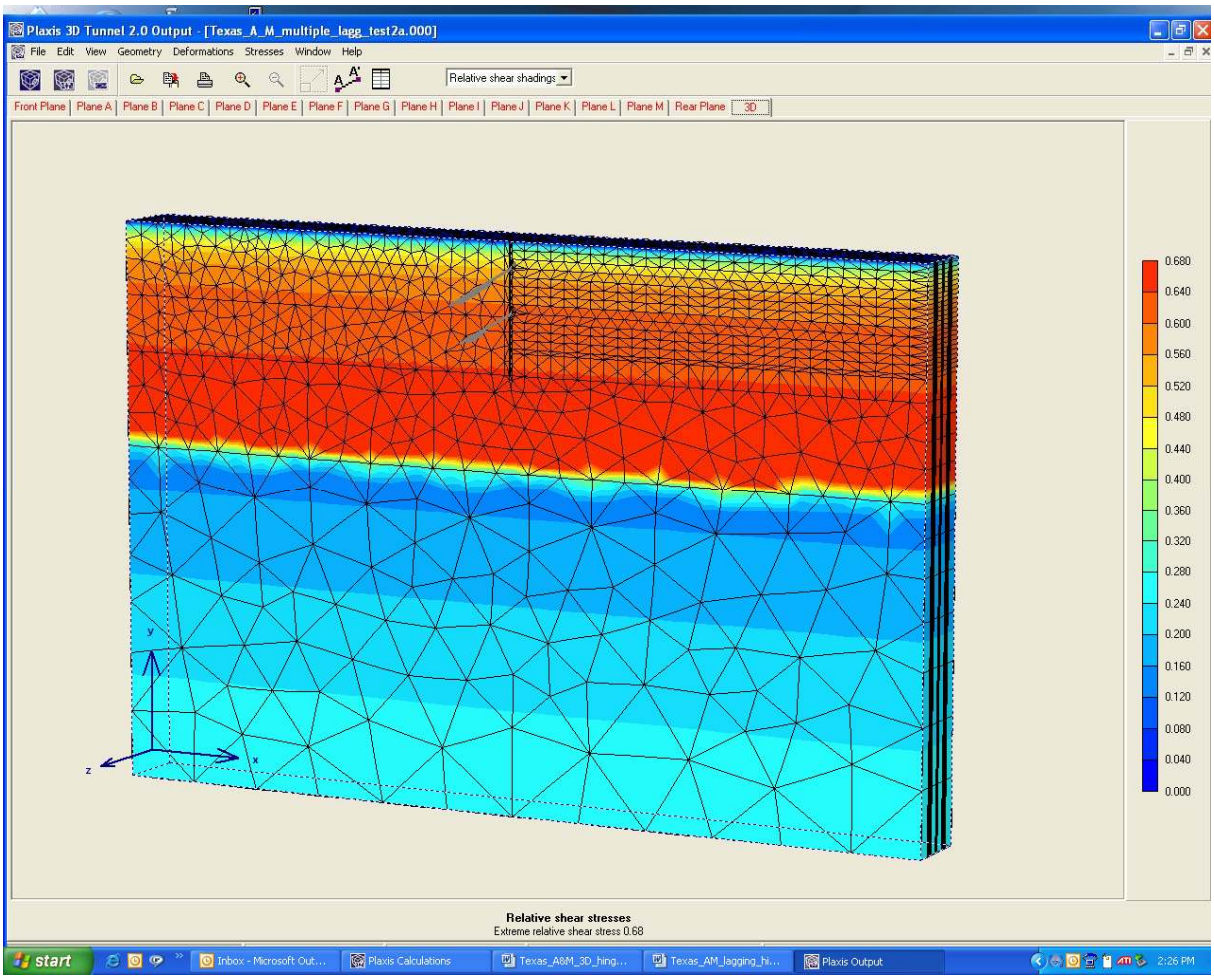

Figure 6.20. 3-D fraction of mobilized shear strength for initial stress conditions

6.4.1.3 Selected 3-D Stage Construction Results

A preliminary assessment of results was performed to evaluate the 3-D model utilized in this study. As shown in Figure 6.19, there is an axis of symmetry in the model at the centerline of the lagging between the soldier beams. The ground anchors were also installed at this location (Plane G in the model). Therefore, the model should compute symmetric responses about the ground anchor location. Table 6.14 shows displacement results at different planes along the z-direction for various stages of construction. As shown, there are generally symmetric displacement results at the different planes for each of the construction stages. An example is the cantilever excavation stage, Planes F and H have approximately the

same results, and likewise Plane E and I, etc. It is noted that the displacement results for the Front Plane (z = 0), Plane G (z = -8.5) and the Rear Plane (z = -17) have approximately symmetric for the first construction stage. However, for the remaining construction stages Plane G results deviate from the results for the Front and Rear planes. This difference can be attributed to the localized effects due to the presence of the anchor (z = -8.5) and the effects of prestress loads applied to the anchors.

Table 6.15 shows the corresponding bending moments at these previously described planes along the z-direction for same stages of construction. There are generally symmetric bending moment results at the planes at equal distances from Plane G (anchor location). The bending moments computed at Plane G also deviates from the results for the Front and Rear planes. These differences also can be attributed to the localized effects due to the presence of the anchor and the effects of prestress loads applied to the anchors.

The behavior of the lagging and the hinge (both modeled with plate elements) are key features of the 3-D assessment. An initial hypothesis was that the more flexible lagging (compared to the soldier beam) would undergo deformation due to the soil loading and result in the 3-D stress flow (arching) of soil. Figure 6.21 shows a 3-D deformed shape (shown in red) of a single panel of wood lagging extending along the z-direction. The lagging between the two soldier beams (shown in gray) undergoes a “bulging” type deformation where the maximum deformation is at the center of the panel. Additionally, Figure 6.21 shows the formation of the plastic hinges before and after the soldier beams that prevent the transfer of bending moments from the lagging to the soldier beam. The results of this preliminary assessment give confidence that this 3-D FEM model can model the key 3-D features of this flexible wall system.

Table 6.14. Displacement Results for Flexible Wall at Various Construction Stages

													ANCHOR											
Z-Coord	0		-3.5		-4.0		-5.0		-5.5		-8.0		-8.5		-9.0		-11.5		-12.0		-13.0		-13.5		-17.0
Construction Stage	Front Plane	Ave	Plane A	Ave	Plane B	Ave	Plane D	Ave	Plane E	Ave	Plane F	Ave	Plane G	Ave	Plane H	Ave	Plane I	Ave	Plane J	Ave	Plane L	Ave	Plane M	Ave	Rear Plane
Cantilever Excavation EL 17	0.023	0.0205	0.018	0.015	0.012	0.012	0.012	0.0155	0.019	0.0205	0.022	0.022	0.022	0.022	0.022	0.0205	0.019	0.0155	0.012	0.012	0.012	0.0155	0.019	0.021	0.023
Prestress Anchor	0.032	0.0205	0.009	0.0235	0.038	0.043	0.048	0.0275	0.007	0.015	0.023	0.0235	0.024	0.0235	0.023	0.015	0.007	0.0275	0.048	0.043	0.038	0.0235	0.009	0.0205	0.032
2nd Stage Excavation EL 8	0.069	0.0565	0.044	0.03	0.016	0.021	0.026	0.033	0.04	0.0485	0.057	0.057	0.057	0.057	0.057	0.049	0.041	0.0335	0.026	0.0205	0.015	0.0295	0.044	0.057	0.07
Prestress Anchor	0.074	0.0615	0.049	0.032	0.015	0.0215	0.028	0.0365	0.045	0.053	0.061	0.061	0.061	0.061	0.061	0.0535	0.046	0.036	0.026	0.0205	0.015	0.0325	0.05	0.0625	0.075
Final Excavation EL 0	0.134	0.1215	0.109	0.084	0.059	0.0535	0.048	0.0765	0.105	0.0585	0.012	0.0665	0.121	0.1205	0.12	0.113	0.106	0.0775	0.049	0.0545	0.06	0.085	0.11	0.122	0.134

Table 6.15. Bending Moment Results of Flexible Wall at Various Construction Stages

													ANCHOR												
Z-Coordinate	0	-3.5		-4.0		-5.0		-5.5		-8.0		-8.5		-9.0		-11.5		-12.0		-13.0		-13.5		-17.0
Construction Stage	Front Plane	Plane A		Plane B		Plane D		Plane E		Plane F		Plane G		Plane H		Plane I		Plane J		Plane L		Plane M		Rear Plane
		+	-	+	-	+	-	+	-	+	-	+	-	+	-	+	-	+	-	+	-	+	-	
Cantilever Excavation EL 17	14.44	16.25	3.5	3.22	0	0	3.03	3.5	15.16	13.88	13.39	12.83	12.92	13.62	13.91	14.9	3.5	3.05	0	0	3.65	3.55	15.88	14.88
Prestress Anchor	58.78	72.46	1.2	3.79	0	0	2.98	0.87	77.65	43.12	59.28	60.4	60.21	58.69	42.59	80.71	0.87	2.96	0	0	3.83	1.18	67.43	61.54
2nd Stage Excavation EL 8	12.01	88.1	1.73	0.95	0	0	2.97	0.76	100.3	33.8	19.67	18.8	18.72	19.55	33.96	99.1	4.79	3.78	0	0	3.14	1.55	86.45	11.32
Prestress Anchor	15.71	88.28	1.24	3.29	0	0	3.35	1.03	99.94	45.37	28.28	27.97	27.58	27.18	42.77	98.54	0.28	2.51	0	0	3.39	1.1	86.36	13.84
Final Excavation EL 0	20.2	90.87	0.59	2.58	0	0	2.74	0.19	102.6	49.83	32.41	32.14	31.94	31.34	46.93	99.56	2.76	5.41	0	0	1.75	0.59	90	19.94

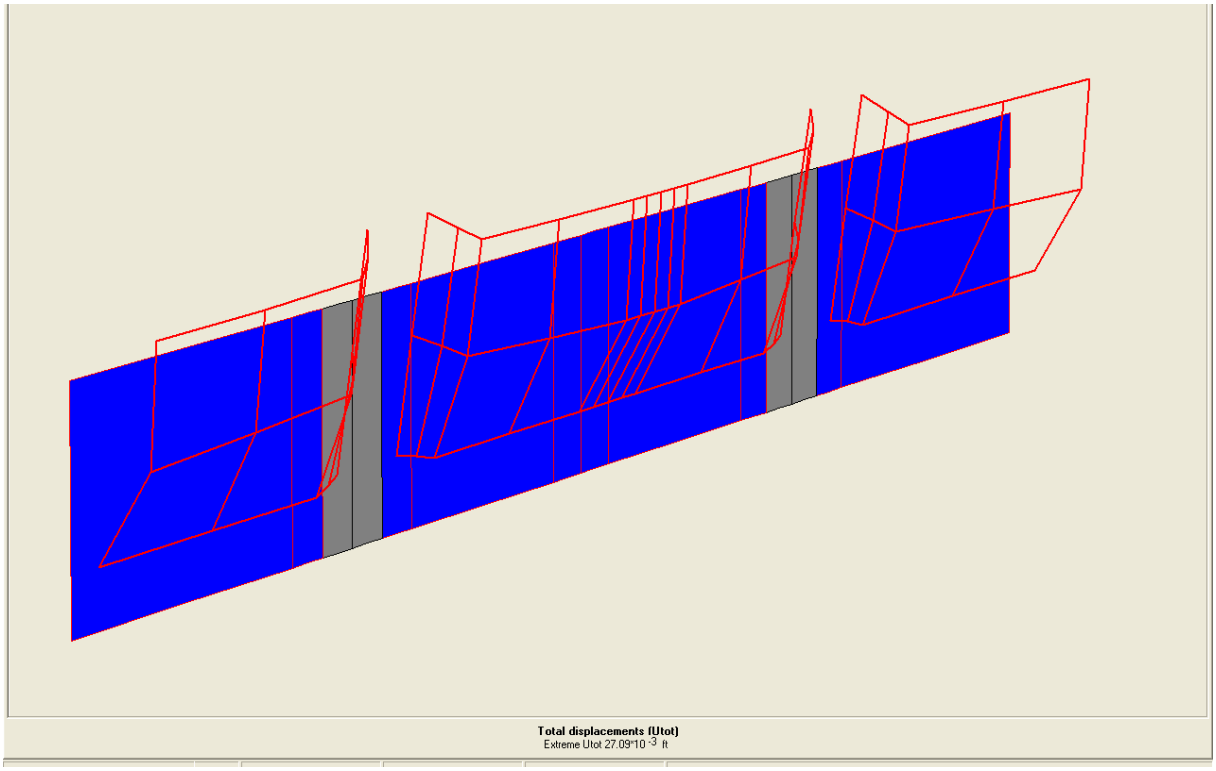

Figure 6.21. Deformed shape of a horizontal lagging panel after cantilever excavation stage

Table 6.3 summarized computed wall maximum displacements, wall maximum bending moments, and maximum anchor forces using the 2-D analysis/design procedure Rigid 1 for flexible tieback wall systems as well as 2-D and 3-D NLFEM of analyses for various excavation stages. As previously mentioned, a key construction stage for tieback wall design is the cantilever excavation stage. This construction stage is important because over-excavation below the ground anchor supports may produce wall movements and wall and anchor force demands that are larger than tolerable. Figure 6.22 shows plot of the 3-D FEM results of horizontal displacements of the wall after the cantilever excavation stage. The computed maximum wall displacement (Ux) was equal to 0.40 in., compared to an approximate instrumentation value equal to 0.5 in. The maximum displacement computed by the 3-D FEM occurred at the top of the wall and it occurred at same location as the

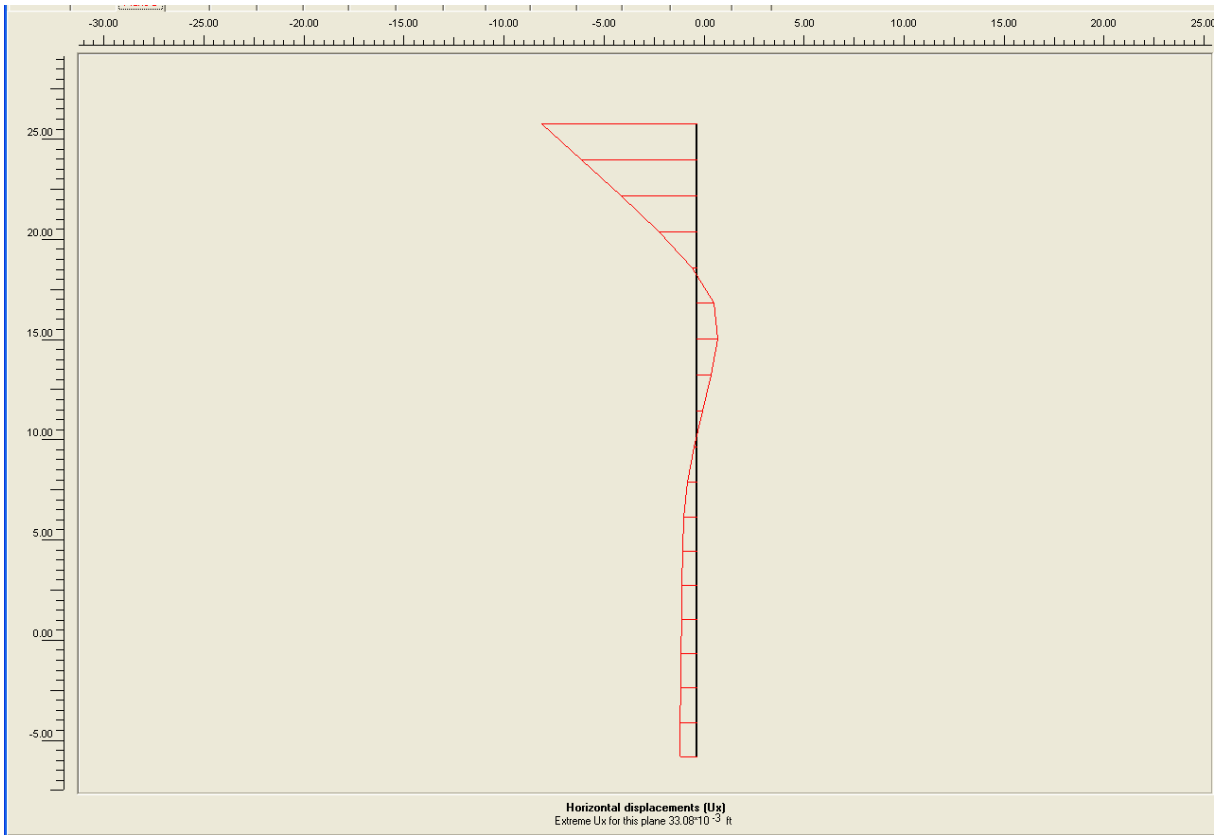

Figure 6.22. 3-D wall displacement after Stage 1 excavation (Max = 0.40 in.)

instrumentation results. The corresponding computed soldier beam bending moments per foot run of wall for this construction stage with a maximum moment equal to 10.0 Kip*ft/ft is shown in Figure 6.23. Recalling, a plate element with a very low bending stiffness was used to compute bending moments in the soldier beam. 3-D Plaxis reports the bending moments per ft run of wall in the plate element. The bending moment in the soldier beam is computed using Equation 6.8.

Additionally, the discrete bending moments in the soldier beam in units of Kip*ft are the same as the bending moment in the plate per ft run because the equivalent soldier beam with (in z-direction) was specified as 1 ft in the volumetric element. Figure 6.24 shows a plot of the 3-D FEM results of horizontal displacements of the wall after the final excavation stage

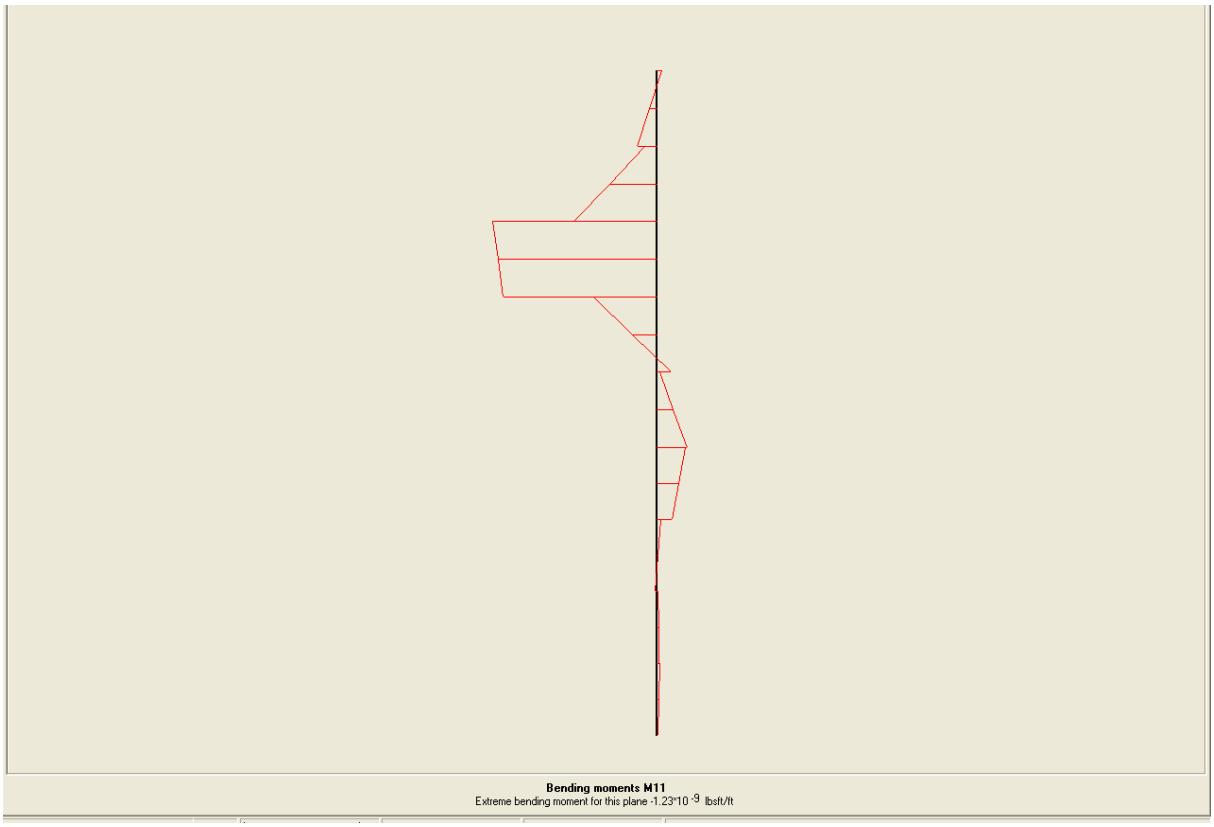

Figure 6.23. Wall bending moments after Stage 1 excavation (Max = 10.0 Kip*ft/ft)

(Stage 3). The computed maximum wall displacement (Ux) was equal to 1.7 in. compared to the instrumentation results (1.5 in.) for this stage of construction. The corresponding wall bending moments for this stage of construction with a maximum moment equal to 36.0 Kip*ft/ft is shown in Figure 6.25. The resulting computed fraction of mobilized shear strength for the final excavation stage is shown in Figure 6.26. As shown, the fraction of mobilized shear strength is still less than or equal to 0.96 for all soil types and this value indicates available shear strength for the soil.

An evaluation of construction sequence stages was also performed to determine if the maximum wall movements and force demands on the wall and tiebacks occurred at intermediate excavation stage of construction rather than for the final permanent loading condition. As was shown in Table 6.3, the maximum computed 3-D FEM soldier beam

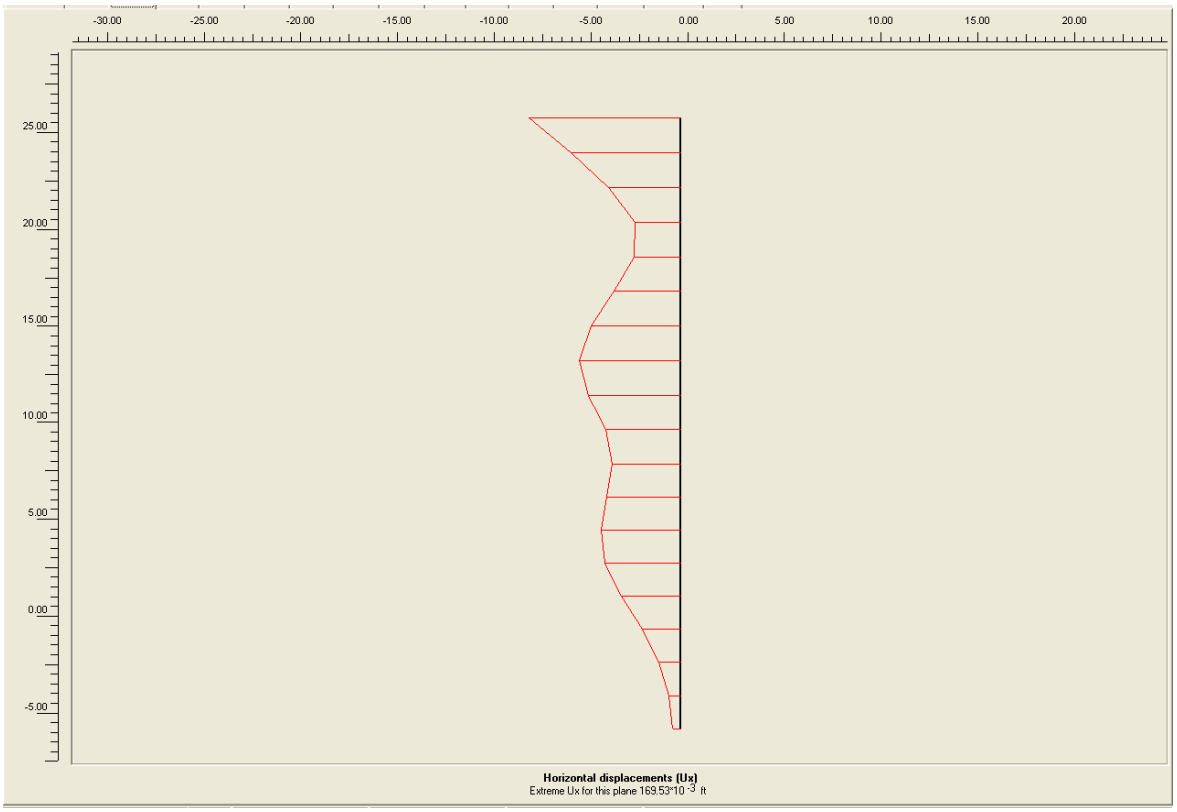

Figure 6.24. 3-D wall displacement after final excavation (Max = 1.7 in.)

displacement and corresponding maximum bending moment for all excavation stages were equal to 1.7 in. and 36 Kip*ft, respectively. These maximums did occur at the final excavation stage for this specific wall. However, for flexible tieback walls it is recommended to check all construction sequence stages in order to determine maximum wall movements and force demands on the wall.

Table 6.3 also showed that the maximum bending moments in the soldier beam computed by the 3-D FEM are generally smaller than those computed by the 2-D FEM. These 3-D results further indicate that the simplified 2-D procedures may over-predict bending moment demand on the wall. As described in Chapter 4, for flexible tieback walls, a 3-D geometrical effect is the presence of discrete or finite constraints along the out of plane direction. The actual response of the wall to loading is influenced by each constraint. Recalling, that tieback

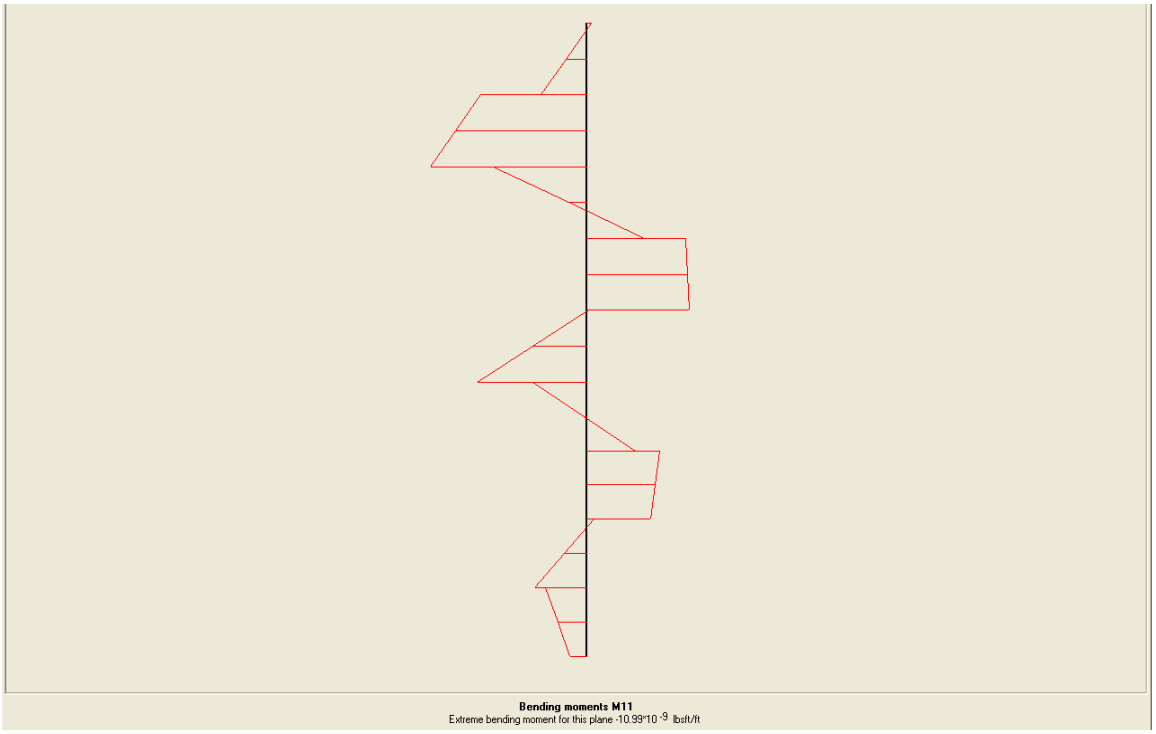

Figure 6.25. Wall bending moments after final excavation stage (Max = 36 Kip*ft/ft)

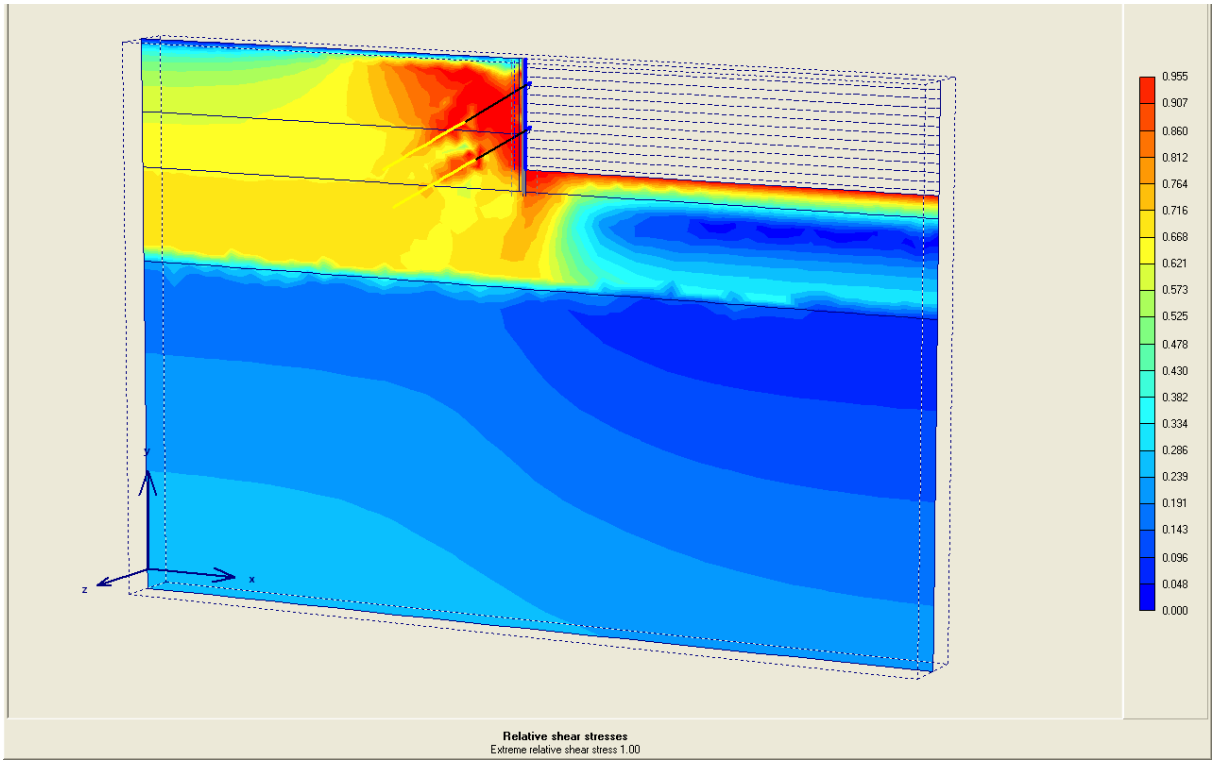

Figure 6.26. Relative shear stress after final excavation stage

anchors are modeled in Plaxis 3-D Tunnel as a combination on node-to-node anchors and geogrid elements. The same procedure used to model discrete grouted regions for the stiff tieback wall by defining small "slices" in front of and behind the planes that had anchors installed was also utilized for the flexible tieback wall.

Again, this modeling technique leads to discrete strips to approximate the cylindrical grout region around the anchors and it is believed that this modeling feature is a better approximation of the actual discrete 3-D anchor grout zone. Figure 6.27 shows the axial force distribution that is transferred to the anchor bond zone for the upper tieback anchor for the final stage of excavation (elevation 0.0). As shown, the axial force is transferred from the top of the anchor bond zone toward the bottom of the grout zone. Table 6.16 shows a summary of axial force distribution in the grout zone for the upper anchor. As shown, the 3-D FEM analysis computes significantly more force transfer to grout zone and shear transfer to the surrounding soil regions than those computed by the 2-D FEM analysis.

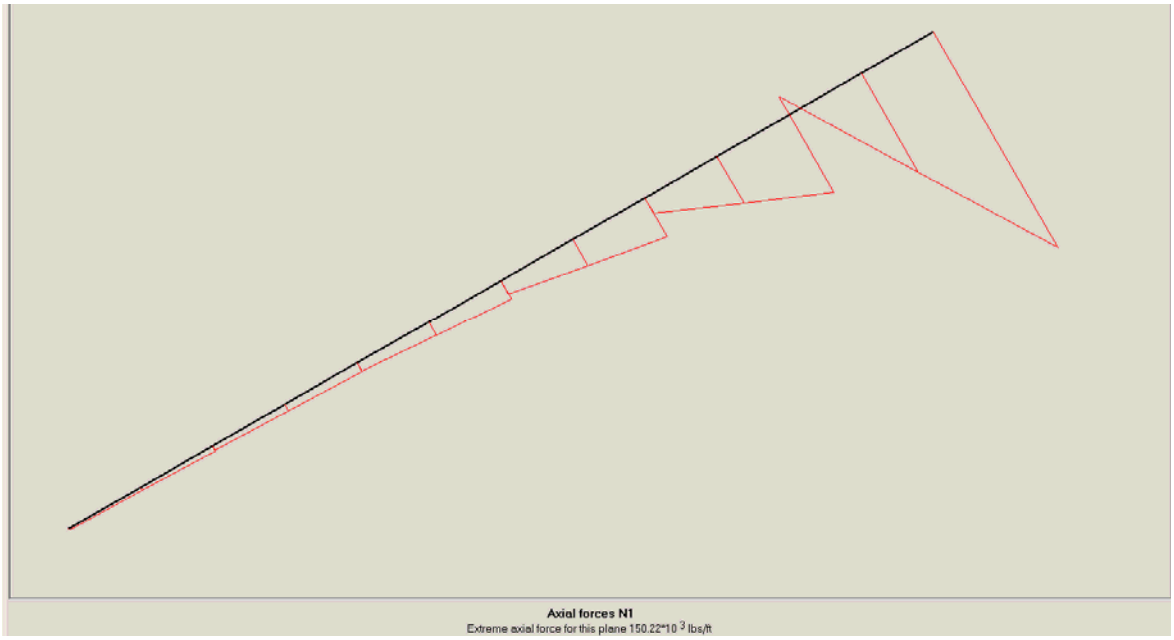

Figure 6.27. Axial forces in grouted zone for upper anchor after final excavation stage

Table 6.16. Axial Force Distribution in the Grout Zone
for the Upper Anchor

	Plaxis 2-D		
Excavation Stage	Upper Anchor Grout Force (Kips/ft)	Grout Spacing (ft)	Design Upper Grout Force (Kips)
1	NA	NA	NA
2	3.74	8	29.92
3	4.25	8	34
Plane G Z= -8.5	**Plaxis 3-D**		
Excavation Stage	Upper Anchor Grout Force Kip/ft	Grout Spacing (ft)	Design Upper Grout Force (Kips)
1	NA	NA	NA
2	147	0.5	73.5
3	150	0.5	75

Table 6.17 shows a comparison of discrete anchor forces for each row of anchors. The 3-D FEM analysis computes lower anchor forces compared to the 2-D analysis. As was shown in Table 6.16 the 3-D FEM analysis computed significantly more force transfer to grout zone and shear force transfer to the surrounding soil regions than those computed by the 2-D FEM.

As previously described in Chapter 1, one means of assessing the state of stress in soil from FEM analyses is to relate computed stresses to earth pressure coefficients. The ratio of horizontal stress σ_h to overburden pressure (γ*H), (σ_h/ γ*H) is defined as the horizontal earth pressure coefficient (K_h). The three general soil stress states considered in soil-structure systems are: at rest, active, and passive. These soil stress states can be described in terms of earth pressure coefficients K_o, K_a, and K_p, respectively.

Table 6.17. Comparison of Discrete Anchor Forces for Each Row of Anchors

Excavation Stage	**Plaxis 2-D** Upper Anchor Force (Kips)	Lower Anchor Force (Kips)
1	NA	NA
2	80	NA
3	80.2	95.5
Plane G Z= -8.5	**Plaxis 3-D**	
Excavation Stage	Upper Anchor Force (Kips)	Lower Anchor Force (Kips)
1	NA	NA
2	67.8	NA
3	67.4	74.7

Figure 6.28 shows the variation in K_h with depth adjacent to the centerline of the soldier beam (Plane C) for various stages of construction. The value of K_h was computed by the following equation:

$$K_h = \sigma_{xx}(\text{computed by Plaxis})/\gamma H \qquad \text{Equation 6.9}$$

where; γ is the unit weight of soil and H is the depth below ground surface. As shown, the magnitude of K_h generally decreases from a K_o stress condition down to a minimum active stress state for the cantilever excavation stage, except for points at shallow depths. The values of K_h for intermittent and final construction stages are between minimum active and maximum passive earth pressure coefficients. To view lateral earth pressure σ_{xx} in terms of earth pressure coefficient is most convenient for cohesionless soils. In this analysis, the soil is a frictional-cohesive material with a low cohesion value equal to 100 psf, which allows for convenient interpretation of results for presentation purposes via Equation 6.9 for all except shallow depths. For shallow depths, it is more reasonable to plot the actual horizontal earth

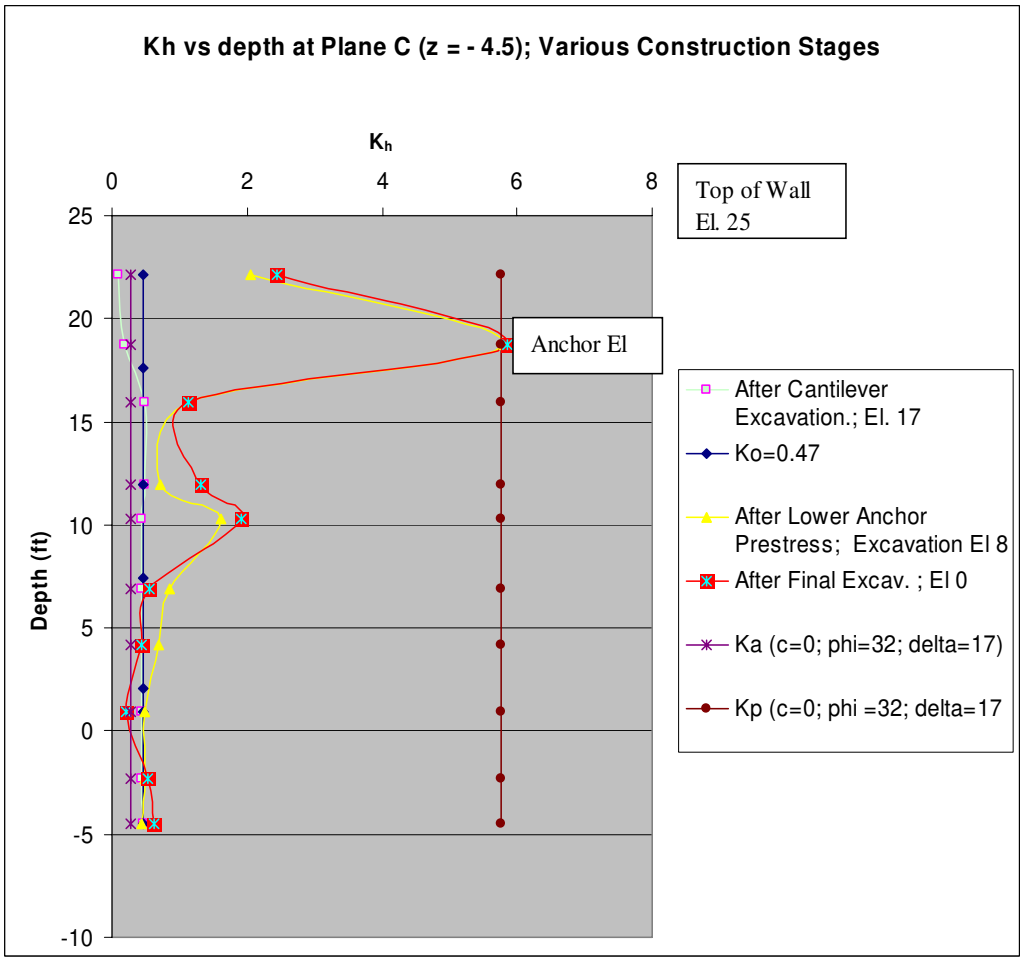

Figure 6.28. Distribution of earth pressure coefficient (K_h) on the soldier beam (z = -4.5 ft) for various construction stages

pressure versus the horizontal component of the active earth pressure. Active earth pressure of a frictional-cohesive soil can be approximated by the method described in Jumikis (1984). The following equation was used to compute the active earth pressures (Bowles 1997).

$$\sigma_a = \gamma H * K_a - 2c * \sqrt{K_a} \qquad \text{Equation 6.10}$$

where; K_a is the Coulomb's earth pressure coefficient based on the following equation:

$$K_a = \frac{\cos^2(\phi)}{\{\cos(\delta)\} \cdot \left[1 + \sqrt{\frac{\{\sin(\phi+\delta)\} \cdot \{\sin(\phi)\}}{\{\cos(\delta)\}}}\right]^2} \qquad \text{Equation 6.11}$$

where; ϕ is soil angle of internal friction and δ is wall-to-soil friction angle. 3-D Plaxis results indicated an average value of (δ) equal to 17 degrees.

Lastly, the horizontal component of the active earth pressure is computed by the following equation:

$$\sigma_{a(hor)} = \sigma_a * cos(\delta) \qquad \text{Equation 6.12}$$

Figure 6.29 shows a plot horizontal earth pressure on the soldier beam at depths of 2.83 ft and 6.23 ft below the ground surface versus the horizontal component of the active earth pressure. The computed lateral stress is greater than the minimum horizontal component of the limiting active pressure for these depths, as expected. The variation in K_h at the centerline of the wood lagging (Plane G) for various stages of construction is shown in Figure 6.30. All computed values of K_h shown in the figure are less than K_p of 6.8 (line not shown in the figure). As shown, the magnitude of K_h decreases from an initial value K_o down to values less than or equal to the reference K_a for a cohesionless soil. A lateral earth pressure gradient equal to 32 psf per ft depth was computed using the approximate procedure by Jumkis. The horizontal component of the active pressure $\sigma_{a(hor)}$ for the shallow depth of 2.83 ft below the ground using the Jumikis approximation was 14.3 psf and the corresponding lateral stress (σ_{xx}) computed by Plaxis was 0.2 psf. When viewed in terms an equivalent depth with an active pressure increase of 32 psf per ft depth, the error corresponds an error of 0.5 ft. This error is considered acceptable for this numerical procedure. The program activates tension cut-off in active zone above this depth. Moreover, Plaxis performs load redistribution that could lead to the 0.5 ft error in the computed results. These reduced pressure results indicate that a portion of initial soil pressures exerted on the flexible wood lagging may be redistributed to the stiffer soldier beams due the (3-D) stress flow of the retained soil.

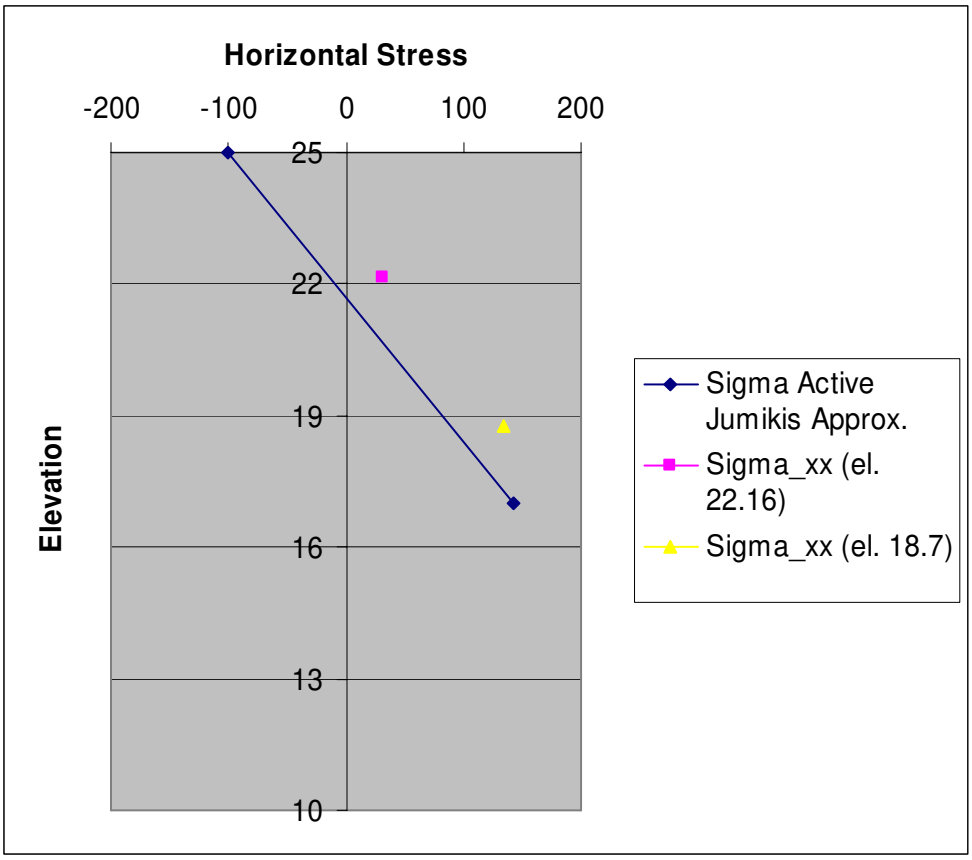

Figure 6.29. Comparison of horizontal earth pressure and horizontal component of the active earth pressure on the soldier beam

As described above, for shallow depths, it is reasonable to plot the actual horizontal earth pressure versus the horizontal component of the active earth pressure. Figure 6.31 shows a plot horizontal earth pressure on the lagging at depths of 2.83 ft and 6.23 ft below the ground surface versus the horizontal component of the active earth pressure. As expected, the computed lateral stress is greater than the minimum horizontal component of the limiting active pressure for these depths.

Lastly, Figure 6.32 shows the distribution of K_h at constant elevation (el. 22.1 ft) in the longitudinal direction (z-direction) for three stages of construction. The centerline of the soldier beams are at z coordinates of -4.5 ft and -12.5 ft and the center of the lagging is at a

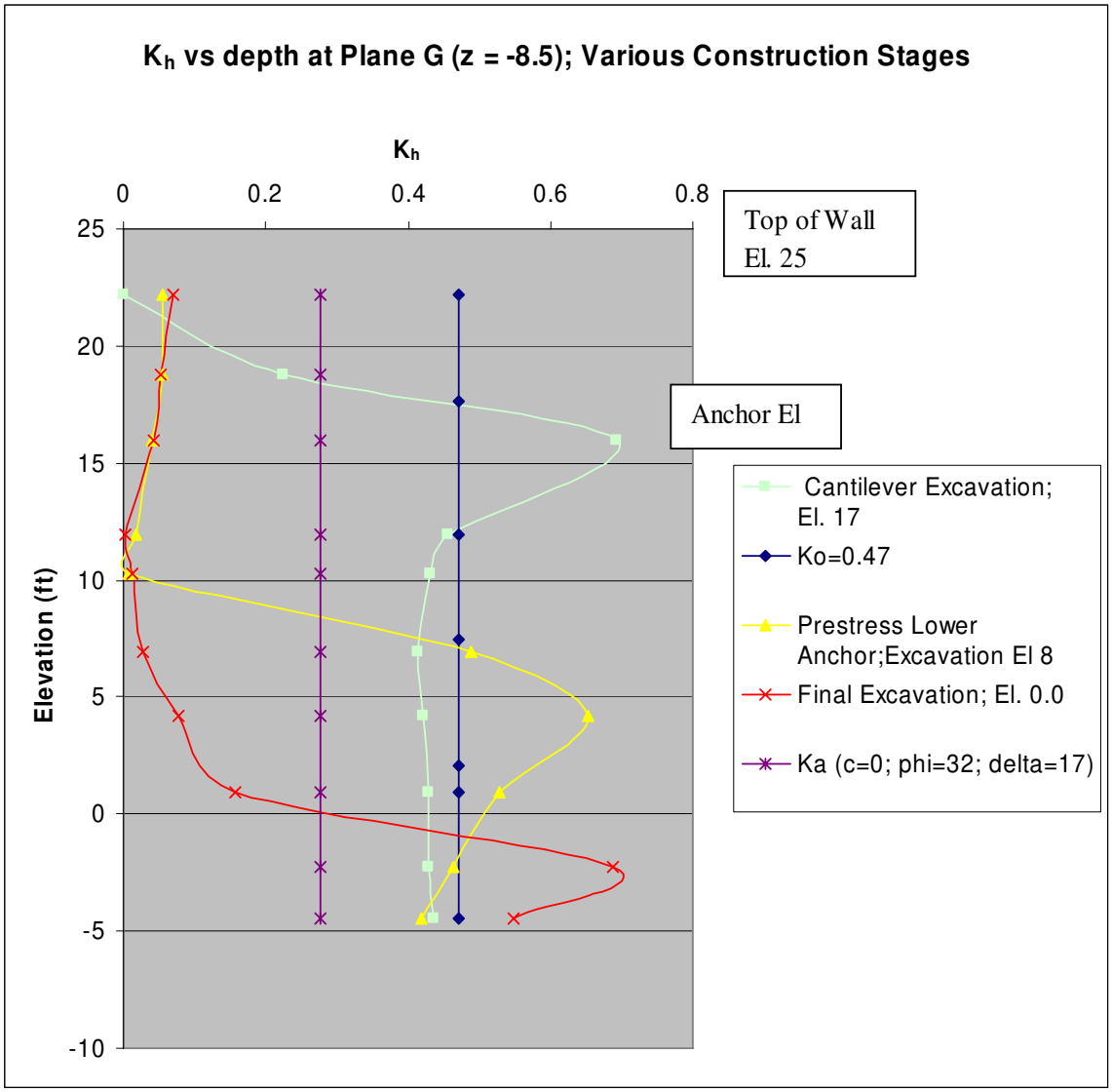

Figure 6.30. Distribution of earth pressure coefficient (K_h) in lagging (z = -8.5 ft) for various construction stages

z coordinate of -8.5 ft. As shown, the magnitude of K_h exerted on the lagging is much less, than the magnitude exerted on the soldier beams. The flexible lagging undergoes large deformations and the earth pressure on the lagging is reduced. The larger magnitude of K_h exerted on the stiffer soldier beams further indicate that a portion of the soil pressures is redistributed to soldier beams due the 3-D stress flow (arching) of the retained.

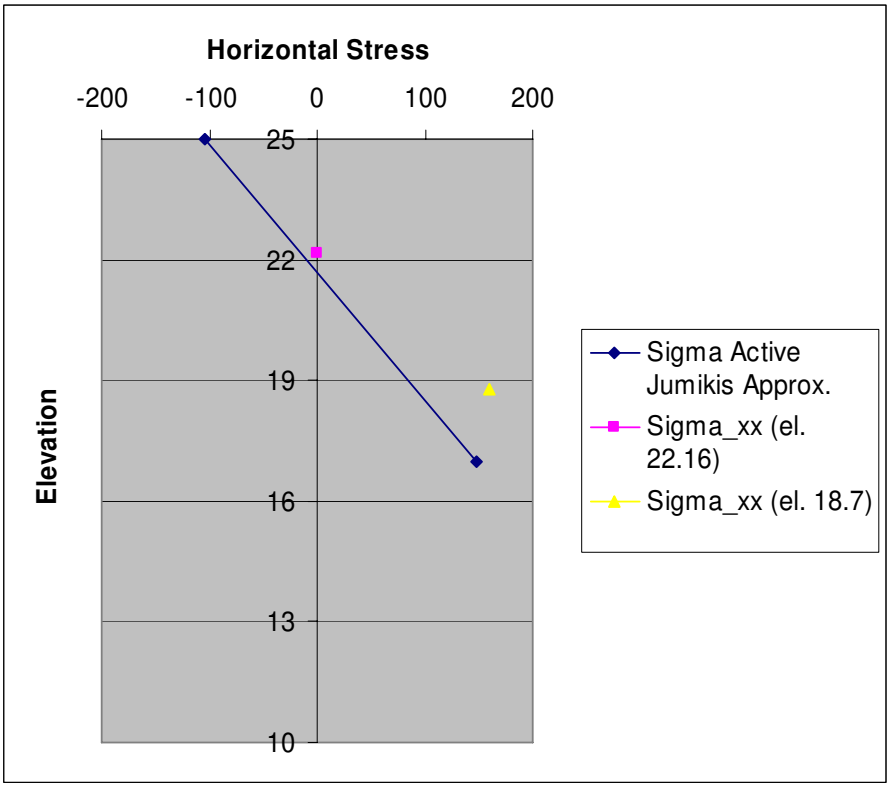

Figure 6.31. Comparison of horizontal earth pressure and horizontal component of the active earth pressure on the lagging

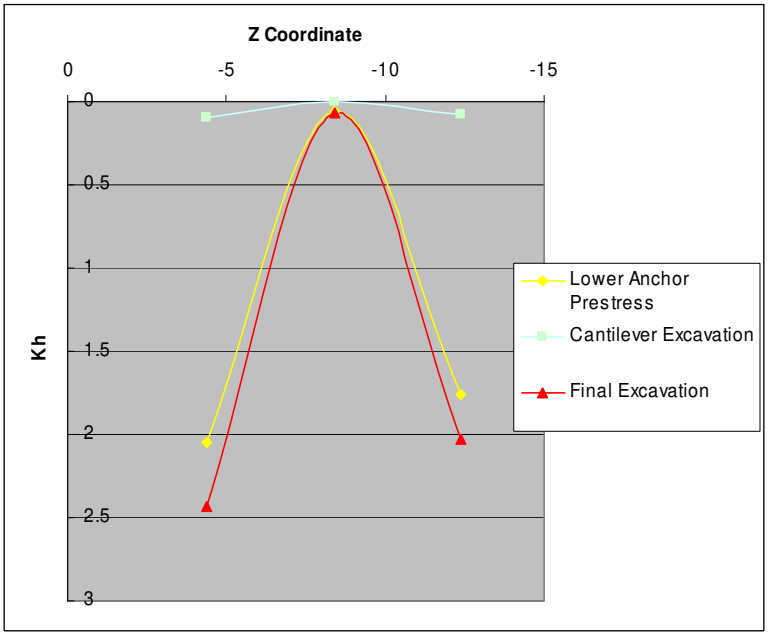

Figure 6.32. Variation of K_h at constant elevations in the longitudinal direction

6.4.1.4 Engineering Assessment Observations of the Flexible Wall

Just as was discovered in a literature review of stiff tieback walls, this was also the first Corps of Engineers research effort that utilized 3-D nonlinear FEM procedures as a means to assess different 2-D analysis/design procedures for a full-scale instrumented "flexible" tieback wall system with multiple rows of prestressed anchors. In the comprehensive 3-D nonlinear FEM procedure, there were some key modeling features used to capture 3-D effects of this "flexible" tieback wall system that are not included in 2-D analysis and design procedures. A key 3-D geometrical effect was found to be the presence of discrete anchors. The actual response of the wall to loading is influenced by each anchor. Again, discrete anchors were modeled in 3-D Plaxis as a combination on node-to-node anchors and geogrid elements (for modeling grouted zone). Additionally, in order to approximate the actual discrete response of the grouted zone and anchors, a special modeling feature was incorporated: thin vertical sections (referred to as slices in Plaxis input) were defined at small distances in front of and behind the planes that had installed anchors. This modeling technique allowed for discrete strips to approximate the cylindrical grout region around the anchors. It is believed that modeling discrete anchors and their grout region is a better approximation of the actual discrete 3-D anchor and grout zone model parameters than the 2-D approximation of averaging the anchor and grout zone over the plan spacing between the anchors.

Additionally, 3-D interface elements were used to simulate the soil-structure interaction that occurs at the interface between the wall and adjacent soil elements. Utilizing interface elements is an important feature that allows the soil regime to move independent of the structural regime. SSI FEM analyses utilizing interface elements typically result in more accurate computations of shear and normal acting on the tieback walls.

The discrete soldier beams were modeled with 3-D volume elements using the linear elastic material model. Vertical plate elements were inserted at the center widths of the volume elements used to model the soldier beams in order to compute bending moments within the volume elements. The plate elements were assigned a very small bending stiffness (1E-6 times the actual stiffness of the soldier beams) to prevent the plate elements from influencing the deformations of the soldier beams via volumetric elements. The 3-D Plaxis bending moment per ft run of wall in the soldier beam is determined from the properties of the soldier beam and plate element as well as the moment computed by Plaxis in the plate element. The value for is the $M_{soldier\ beam}$ is determined using Equations 6.5 to 6.8.

Additional components of a typical soldier beam and lagging tieback wall and their effects on the wall system behavior were modeled in the 3-D FEM procedure. These components and their effects are not included in 2-D FEM analysis nor in 2-D simplified procedure Rigid 1.

Lagging consisting of horizontally placed panels of wood members were modeled with rows plate elements extending in the z-direction. Wood lagging provide support to the soil between the soldier beams and helps transfers a portion of the soil load to the soldier beam. The lagging is not rigidly attached to the soldier beam flange and thus there is no bending moment transferred (i.e., a hinge connection). Hinge connections were approximated in Plaxis 3-D Tunnel by defining plate elements over small slices in front and behind of each soldier beam (in the z-direction). The hinge plates had the same stiffness properties as wood lagging, but the hinge plates were modeled with the elasto-plastic material model and assigned a very small plastic bending moment. A parametric study was performed to determine a plastic moment value to assign to the hinge plate while maintaining a numerically stable model. The

behavior of the lagging and the hinge (both modeled with plate elements) are key features of the 3-D modeling effort. An initial hypothesis was that the more flexible lagging (compared to the soldier beam) would undergo greater deformations due to the soil loading and result in the 3-D stress flow towards the soldier beams with arching of soil between the soldier beams. Figure 6.21 showed a 3-D deformed shape (shown in red) of a single panel of wood lagging extending along the z-direction. The lagging between the two soldier beams (shown in gray) undergoes a "bulging" type deformation where the maximum deformation is at the center of the panel. The deformation of the lagging resulted in decreased earth pressure acting on the lagging. A portion of the initial earth pressures acting on the lagging was redistributed to the surrounding soil and soldier beams during the deformation of the soil and soldier beams. Therefore, the 3-D FEM results indicated that a 3-D stress flow did occur. This response is not captured in 2-D modeling procedures.

The test section soldier beams that were analyzed using 3-D nonlinear FEM procedure had discrete wales spanning between the soldier beams (See Figure 6.18). Wales are horizontal stiffeners that transfer loads from the soldier beams to the ground anchors. Modeling the wales is an important feature in order to capture the force transfer to the ground anchors and grouted zone. Additionally, wales are often placed on discrete offsets called "seats" along the soldier beams to form a gap between the lagging and the wales. The purpose of offsetting the wales on the seats is to prevent load transfer between the lagging and the wales. Wale seats were also modeled using the 3-D nonlinear FEM procedure.

The 3-D nonlinear FEM analysis also simulated the construction process that was performed in the actual field construction of the flexible tieback wall. Modeling the construction sequence is a key aspect of SSI procedures in order to accurately compute the

responses of the wall system due to the nonlinear stress-strain behavior of soils. The 3-D nonlinear FEM procedure was able simulated construction steps that were not able to be considered in 2-D FEM and 2-D limit equilibrium procedures. These construction steps unique to the 3-D FEM included modeling an alternating pattern of excavation of soil and installing the wood lagging, the wales and wale seats. Additionally, for this flexible wall system an evaluation of construction sequence stages results was also performed to determine if the maximum wall movements and force demands on the wall and tiebacks occurred at an intermediate excavation stage of construction or at the final permanent loading stage.

The 3-D FEM constitutive model for the "flexible" tieback wall was calibrated by performing a parametric study on the key HS constitutive parameter, the secant stiffness (E_{50}^{ref}), that would produce results which best matched to the available instrumentation results for different stages of construction. Other HS constitutive parameters used in the parametric study were estimated based on available parameter correlations sited in the literature, Plaxis author's recommendations (Brinkgreve 2005), and a literature database of model parameters used in Plaxis analyses for similar soil types.

Another important aspect of 3-D nonlinear FEM model validation is the ability to observe symmetric results computed about planes of symmetry. Symmetric bending moment and displacement results were computed by the 3-D FEM analysis and reported in Tables 6.14 and 6.15. These results give confidence that this 3-D FEM SSI analysis can model the key 3-D features of this "flexible" tieback wall system.

With the robust modeling of the above-mentioned 3-D features, coupled with comprehensive simulation of the field construction process and calibration of the constitutive model to instrumentation results, lends confidence that the 3-D FEM methodology is a viable

procedure for capturing key 3-D features and responses of a flexible tieback wall system that are not considered in 2-D FEM and 2-D limit equilibrium procedures. Therefore, an assessment of computed results (with 3-D FEM analysis used as the basis of comparison) of this flexible tieback is deemed reasonable and are presented.

The analysis results (computed maximum wall displacements, discrete maximum soldier beam bending moments, and anchor forces) from the 2-D and 3-D FEM were compared with the simplified 2-D design/analysis procedure RIGID 1 as a means to assess this procedure. This information was provided in Table 6.3. The tabulated maximum discrete bending moments were reported as the maximum absolute values and used in the design. Recall that the 3-D and 2-D FEM computed responses are at working load levels and not ultimate loads. The maximum anchor forces may also be used in the design. Additionally, the response of the anchors in the grouted zones was compared between the 2-D and 3-D FEM.

The comparison of results between the 2-D FEM and the RIGID 1 procedure for this case study wall indicated that the RIGID 1 procedure is conservative in estimating bending moment demands on the wall but it underestimates the wall anchor forces. The RIGID 1 procedure computes moment demand based on loads distributed over a tributary area. The 2-D FEM showed that the maximum discrete bending moments of the wall and maximum wall displacements occurred at the final stage of excavation. However, for flexible tieback walls it is recommended to check all construction sequence stages in order to determine maximum wall movements, force and moment demands on the walls. The 2-D FEM also computes anchor force transfer to grout zone that is not explicitly considered in the simplified 2-D design/analysis procedure RIGID 1. The comparison of results between the 2-D and 3-D FEM indicated an overall consistent behavior. The computed 3-D discrete bending moments

on the wall were less than those computed by the 2-D FEM for each stage of excavation. This is attributed to 3-D modeling features such as the modeling of the flexible lagging that leads to 3-D stress flow and the modeling of discrete anchor response in lieu of a smeared response as done in all 2-D models. The displacement results computed by the 3-D FEM were generally larger than those computed by the 2-D FEM. The deformation of the flexible wood lagging resulted in stress redistribution to the stiffer soldier beams in the 3-D analysis due the (3-D) stress flow of the retained soil. The incorporation of discrete soldier beams in the 3-D model contributes to this behavior. This increased pressure exerted on the soldier beams leads to increased displacements that were consistent with instrumentation results. This type of response is not accounted for in current 2-D methodologies (due, in part, to the smearing of the soldier beam stiffness over the tributary length). The anchor forces computed by the 3-D FEM were less than those computed by the 2-D FEM. The 3-D FEM analysis computed significantly more anchor force transfer to grout zone and shear force transfer to the surrounding soil regions than those computed by the 2-D FEM. The 3-D anchor force results were comparable with available instrumentation results. These results indicate the importance of modeling the 3-D effect of the discrete anchors. This engineering assessment of a flexible tieback wall with multiple rows of prestress anchors showed that 3-D effects of stress flow and the presence of discrete anchors have an impact on deformation and anchor response of the wall system. Due to 3-D geometrical effects of the wall and nonlinear stress-strain behavior of the soil, wall displacements in SSI systems is the most difficult parameter to accurately compute. The 3-D nonlinear LFEM analysis resulted in computed wall displacements, closest to the value recorded in the field, 1.7 in. compared to 1.5 in. The 2-D nonlinear FEM analysis computed a final displacement of 0.7 in.

CHAPTER 7

CONCLUSIONS AND RECOMMENDATIONS

This research endeavor had two primary objectives. The first objective was to perform an engineering assessment of key 3-D SSI aspects of two tieback retaining wall systems with multiple rows of prestressed anchors that are not considered in conventional 2-D analysis/ design procedures. The assessment was done by performing comprehensive SSI analyses using 3-D nonlinear FEM procedures. These two retaining wall systems have the potential for use on Corps of Engineers projects. The second objective was to assess the simplified 2-D limit equilibrium and simplified 2-D computer-aided procedures for these wall systems utilizing the results from the comprehensive 3-D FEM analyses. It was noted that based on an extensive literature review, this was the first Corps of Engineers research effort that utilized 3-D nonlinear FEM procedures as a means to assess different 2-D analysis/design procedures for a full-scale instrumented "stiff" and "flexible" tieback wall systems with multiple rows of prestressed anchors.

For the "stiff" case study tieback wall, the comprehensive 3-D nonlinear FEM procedure incorporated some key modeling features that are vital in capturing 3-D effects of this "stiff" tieback wall system. A key 3-D geometrical effect was found to be the presence of discrete anchors. The actual response of the wall to loading is influenced by each anchor. The discrete anchors were modeled as a combination on node-to-node anchors and geogrid elements (for modeling grouted zone). Additionally, in order to approximate the actual discrete response of the grouted zone and anchors, a special modeling feature was incorporated: thin vertical sections were defined at small distances in front of and behind the planes that had anchors

installed. This modeling technique allowed for discrete strips to approximate the cylindrical grout region around the anchors. It is believed that modeling discrete anchors and their grout region is a better approximation of the actual discrete 3-D anchor and grout zone than the 2-D approximation of averaging the anchor and grout zone model parameters over the plan spacing between the anchors.

Additionally, 3-D interface elements were used to simulate the soil-structure interaction that occurs at the interface between the wall and adjacent soil elements. Utilizing interface elements is an important feature that allows the soil regime to move independent of the structural regime. SSI FEM analyses utilizing interface elements typically result in more accurate computations of shear and normal stresses acting on the tieback walls.

The 3-D nonlinear FEM analysis also modeled the construction process that was performed in the actual field construction of the stiff tieback wall. Modeling the construction sequence is a key aspect of SSI procedures in order to accurately compute the responses of the wall system due to the nonlinear stress-strain behavior of soils. Additionally, for this case study tieback wall, the excavation that took place prior to tieback installation occurred to a depth of as much as 5.5 ft below the tieback elevation. This suggests that the largest force demands (moments and shears) on the wall would occur at an intermediate construction stage rather than at the final excavation stage and this model behavior further supports the importance of modeling the complete construction process .

The 3-D FEM model for the "stiff" tieback wall was calibrated by performing a parametric study on the key HS constitutive parameter, the secant stiffness (E_{50}^{ref}), that would produce results which best matched to the available instrumentation results for different stages of construction. Also, triaxial tests were conducted on one soil type, the

weigle slide block material. The results of triaxial tests were used to determine the HS parameters used to model the stress-stress behavior of the weigle slide block. The HS model parameters for the remaining soil types were estimated based on available parameter correlations cited in the literature, Plaxis author's recommendations (Brinkgreve 2005), and a literature database of model parameters used in Plaxis analyses for similar soil types.

Another important aspect of 3-D nonlinear FEM model validation is the ability to observe symmetric results computed about planes of symmetry. Symmetric results were computed during the 3-D FEM staged construction analyses and were reported in Table 5.10. These results give confidence that this 3-D nonlinear FEM SSI analysis can model the key 3-D features of this "stiff" tieback wall system.

With the robust modeling of the above-mentioned 3-D features, coupled with comprehensive simulation of the field construction process and calibration of the constitutive model to instrumentation results, lends confidence that the 3-D FEM methodology is a viable procedure for capturing key 3-D features and responses of a stiff tieback wall system that are not considered in 2-D FEM and 2-D limit equilibrium procedures. Therefore, an assessment of computed results (with 3-D FEM analysis used as the basis of comparison) of this stiff tieback is deemed reasonable and was performed.

The analysis results (computed maximum wall displacements, maximum bending moments per foot run of wall, and anchor forces) from the 2-D and 3-D FEM were compared with the current 2-D analysis/design procedures as a means to assess the procedures. This information was provided in Table 5.3. The tabulated maximum bending moments per foot run of wall were reported as the maximum absolute values and used in the design of the wall section. The reported maximum anchor forces may also be used in the design. Note, that the

3-D and 2-D finite element analysis (FEA) computed responses are at working load levels and not at ultimate loads. Additionally, the response of the anchors in the grouted zones was compared between the 2-D and 3-D FEM.

The comparison of results between the 2-D FEM and the simplified 2-D analysis/design procedures for this specific case study wall indicated that the simplified 2-D procedures underestimate both bending moment demands on the wall and wall displacements. Of the simplified 2-D procedures, the Winkler 1 procedure using the program CMULTIANC provided the best estimate of moment demand for a stiff tieback wall system. The 2-D FEM showed that the maximum bending moments per foot run of wall and maximum wall displacements occurred at an intermediate stage of excavation. These results further demonstrate the importance of performing a construction sequencing analysis in the design of "stiff" tieback wall systems. The 2-D FEM also computes force transfer to grout zone that is not included in the current 2-D simplified analysis and design procedures.

The comparison of results between the 2-D and 3-D FEM indicated an overall consistency. The computed 3-D bending moments per foot run of wall and the wall displacements were greater than those computed by the 2-D FEM for each stage of excavation. These results also demonstrated the importance of performing a construction sequencing analysis in the design of "stiff" tieback wall systems because the maximum bending moment per foot run of wall for the wall occurred at an intermediate stage of excavation. Discrete maximum anchor force results from the 2-D and 3-D FEM were approximately the same. However, the 3-D FEM analysis computed significantly more force transfer to grout zone and shear force transfer to the surrounding soil regions than computed by the 2-D FEM. This assessment indicated that the 3-D effect of the discrete anchors affects

the overall system behavior of a "stiff" tieback wall system analytical model. These effects are not accounted for in the 2-D simplified procedures used in analysis and design of these wall systems.

3-D FEM results indicated the potential for enhancements to be made to one of the 2-D simplified design procedures (RIGID 2). The RIGID 2 procedure uses a factor of safety equal to one applied to the shear strength of the soil below the excavation level (i.e., a passive limit state). The plot of mobilized shear indicated that there is reserve passive resistance available in the soil. Therefore, the RIGID 2 procedure could be modified by applying a passive factor of safety greater than one (1.5 is recommended in pile design) and reanalyzing the wall system to compute wall forces and displacements. A second series of parametric Rigid 2 analyses were conducted with the results summarized in Appendix D. The Rigid 2 procedure with a $FS_{p(ave)}$ equal to 1.4 generally computes slightly larger maximum bending moments than the Rigid 2 procedure with FS_p equal to one for these intermediate construction stages. However, for stages 2 and 3, Rigid 2 procedure with a $FS_{p(ave)}$ equal to 1.4 computes much smaller bending moments as compared to the simplified Winkler 1 procedure, and 2-D and 3-D FEM results. Recall, that the simplified Rigid 2 procedure is based on the assumption that a point of fixity in the soil below the excavation elevation occurs at a depth of zero net pressure for the second and all subsequent construction stages. These results indicate that the simplified approach used to estimate the depth to fixity might be a key reason for the disparity in results.

For the "flexible" case study tieback wall, the comprehensive 3-D nonlinear FEM procedure, incorporated some key modeling features unique to this type of tieback wall

system that are vital in capturing 3-D effects and are not included in 2-FEM nor in the 2-D simplified procedure Rigid 1.

The discrete soldier beams were modeled with 3-D volume elements using the linear elastic material model. Vertical plate elements were inserted at the center widths of the volume elements were used to model the soldier beams in order to compute bending moments within the volume elements. The plate elements were assigned a very small bending stiffness (1E-6 times the actual stiffness of the soldier beams) to prevent the plate elements from influencing the deformations of the soldier beams via volumetric elements. The 3-D Plaxis bending moment per ft run of wall in the soldier beam was determined from the properties of the soldier beam and plate element as well as the moment computed by Plaxis in the plate element. The value for $M_{soldier\ beam}$ is determined using Equations 6.5 to 6.8.

Lagging consisting of horizontally placed panels of wood members were modeled with rows of plate elements extending in the z-direction. Wood lagging provide support to the soil between the soldier beams and helps transfers a portion of the soil load to the soldier beam. The lagging is not rigidly attached to the soldier beam flange and thus there is no bending moment transferred (i.e., a hinge connection). Hinge connections were approximated in Plaxis 3-D Tunnel by defining plate elements over small slices in front and behind of each soldier beam (in the z-direction). The hinge plates had the same stiffness properties as wood lagging, but the hinge plates were modeled with the elasto-plastic material model and assigned a very small plastic bending moment. A parametric study was performed to determine a plastic moment value to assign to the hinge plate while maintaining a numerically stable model. The behavior of the lagging and the hinge (both modeled with plate elements) are key features of the 3-D modeling effort. An initial hypothesis was that the more flexible lagging (compared to

the soldier beam) would undergo greater deformations due to the soil loading and result in the 3-D stress flow towards the soldier beams with arching of soil between the soldier beams. Figure 6.21 showed a 3-D deformed shape (shown in red) of a single panel of wood lagging extending along the z-direction. The lagging between the two soldier beams (shown in gray) undergoes a "bulging" type deformation where the maximum deformation is at the center of the panel. The deformation of the lagging resulted in decreased earth pressure acting on the lagging. A portion of the initial earth pressures acting on the lagging was redistributed to the surrounding soil and soldier beams during the deformation of the soil and soldier beams. Therefore, the 3-D FEM results indicated that a 3-D stress flow did occur. This response is not captured in 2-D modeling procedures.

The test section soldier beams that were analyzed using the 3-D nonlinear FEM procedure had discrete wales spanning between the soldier beams. Wales are horizontal stiffeners that transfer loads from the soldier beams to the ground anchors. Modeling the wales is an important feature in order to capture the force transfer to the ground anchors and grouted zone. Additionally, wales are often placed on discrete offsets called "seats" along the soldier beams to form a gap between the lagging and the wales. The purpose of offsetting the wales on the seats is to prevent load transfer between the lagging and the wales.

The 3-D nonlinear FEM procedure was able to simulate construction steps that were not able to be considered in 2-D FEM and 2-D limit equilibrium procedures. These construction steps unique to the 3-D FEM included modeling an alternating pattern of excavation of soil and installing the wood lagging, the discrete wales and wale seats. Additionally, for this flexible wall system an evaluation of construction sequence stages results was also performed to determine if the maximum wall movements and force demands on the wall and tiebacks

occurred at an intermediate excavation stage of construction or at the final permanent loading stage.

The 3-D FEM constitutive model for the "flexible" tieback wall was calibrated by performing a parametric study on the key HS constitutive parameter, the secant stiffness (E_{50}^{ref}), that would produce results which best matched to the available instrumentation results for different stages of construction. Other HS constitutive parameters used in the parametric study were estimated based on available parameter correlations sited in the literature, Plaxis author's recommendations (Brinkgreve 2005), and a literature database of model parameters used in Plaxis analyses for similar soil types.

Another important aspect of 3-D nonlinear FEM model validation is the ability to observe symmetric results computed about planes of symmetry. Symmetric bending moment and displacement results were computed by the 3-D FEM analysis and reported in Tables 6.14 and 6.15. These results give confidence that this 3-D FEM SSI analysis can model the key 3-D features of this "flexible" tieback wall system.

With the robust modeling of the above-mentioned 3-D features, coupled with comprehensive simulation of the field construction process and calibration of the constitutive model to instrumentation results, lends confidence that the 3-D FEM methodology is a viable procedure for capturing key 3-D features and responses of a flexible tieback wall system that are not considered in 2-D FEM and 2-D limit equilibrium procedures. Therefore, an assessment of computed results (with 3-D FEM analysis used as the basis of comparison) of this flexible tieback is deemed reasonable and were presented.

The analysis results (computed maximum wall displacements, discrete maximum soldier beam bending moments, and anchor forces) from the 2-D and 3-D FEM were compared with

the simplified 2-D design/analysis procedure RIGID 1 as a means to assess this procedure. This information was provided in Table 6.3. The tabulated maximum discrete bending moments were reported as the maximum absolute values and used in the design. The maximum computed anchor forces may also be used in the design. Recall, that the 3-D and 2-D FEM computed responses are at working load levels and not ultimate loads.

The comparison of results between the 2-D FEM and the RIGID 1 procedure for this case study wall indicated that the RIGID 1 procedure is conservative in estimating bending moment demands on the wall but it underestimates the wall anchor forces. Recall, the RIGID 1 procedure computes moment demand based on loads distributed over a tributary area. The 2-D FEM showed that the maximum discrete bending moments of the wall and maximum wall displacements occurred at the final stage of excavation. However, for flexible tieback walls it is recommended to check all construction sequence stages in order to determine maximum wall movements, force and moment demands on the walls. The 2-D FEM also computes anchor force transfer to grout zone that is not explicitly considered in the simplified 2-D analysis/design procedure RIGID 1.

The comparison of results between the 2-D and 3-D FEM indicated an overall consistent behavior. The computed 3-D discrete bending moments on the wall were less than those computed by the 2-D FEM for each stage of excavation. This is attributed to 3-D modeling features such as the modeling of the flexible lagging that leads to 3-D stress flow and the modeling of discrete anchor response in lieu of a smeared response as done in all 2-D models. The displacement results computed by the 3-D FEM were generally larger than those computed by the 2-D FEM. The deformation of the flexible wood lagging resulted in stress redistribution to the stiffer soldier beams in the 3-D analysis due the (3-D) stress flow of the

retained soil. The incorporation of discrete soldier beams in the 3-D model contributes to this behavior. This increased pressure exerted on the soldier beams leads to increased displacements that were consistent with instrumentation results. This type of response is not accounted for in current 2-D methodologies (due, in part, to the smearing of the soldier beam stiffness over the tributary length). The anchor forces computed by the 3-D FEM were less than those computed by the 2-D FEM. The 3-D FEM analysis computed significantly more anchor force transfer to grout zone and shear force transfer to the surrounding soil regions than those computed by the 2-D FEM. The 3-D anchor force results were comparable with available instrumentation results. These results indicate the importance of modeling the 3-D effect of the discrete anchors. This engineering assessment of a flexible tieback wall with multiple rows of prestress anchors showed that 3-D effects of stress flow and the presence of discrete anchors have an impact on deformation and anchor response of the wall system. Due to 3-D geometrical effects of the wall and nonlinear stress-strain behavior of the soil, wall displacements in SSI systems is the most difficult parameter to accurately compute. The 3-D nonlinear FEM analysis resulted in computed wall displacements, closest to the value recorded in the field, 1.7 in. compared to 1.5 in. The 2-D nonlinear FEM analysis computed a final displacement of 0.7 in. Lastly, the 3-D FEM results indicate that the bending stiffness and anchor stiffness used in the current simplified 2-D design procedure for flexible tieback walls may need to be adjusted in order to consider these 3-D effects in an appropriate manner.

7.1 RECOMMENDATIONS FOR FUTURE RESEARCH

This engineering assessment utilizing 3-D FEM has shown that there are 3-D effects that are not considered in current 2-D design and analysis procedures for stiff and flexible tieback wall systems with multiple rows of prestressed anchors. A recommendation for future

research is to perform additional 3-D FEM analyses for both flexible and stiff tieback wall systems with various soil types in order develop a database of wall system responses. It is believed that tieback walls system responses computed by the comprehensive 3-D FEM approach provides useful information analyses to help validate or possibly enhance simplified 2-D analysis/design methodologies.

REFERENCES

Abraham, K. (1995). Analysis of a sheet pile wall system using classical and soil structure interaction methods. Thesis, Mississippi State University.

Ann, T., Hai, O., Lum, C. (2004). "Simulation of soil nail's dynamic pullout response," Plaxis Bulletin Issue no. 15, pg 10.

Ann,T., Hai, O., Lum, C., and Tan, D. "Finite element analysis of a soil nailed slope-some recent experience," pg 189.

Ann, T., Hoe, C., and Chiat, C. (2000). "Modeling of a reinforced soil wall subject to blast," Plaxis Bulletin Issue no. 9, pg 6.

ASCE/SEI. (2000). "Effective analysis of diaphragm walls," Joint Technical Committee on Performance of Structure During Construction, American Society of Civil Engineering Institute, Reston, VA.

Baggett, J.K., and Buttling, S. (1977). "Design and in situ performance of a sheet-pile wall," Proceedings ninth international conference on soil mechanics and foundation engineering, pp 3-7.

Bathe, K.J. (1982). Finite element analysis in engineering analysis, Prentice Hall, New Jersey.

Bergado, D.T., Youwai, S., Teerawattanasuk, C., and Visudmedanukul P. (2003). "The interaction mechanism and behavior of hexagonal wire mesh reinforced embankment with silty sand backfill on soft clay," *Computers and Geotechnics* 30 (2003)517-534, pg 523.

Bowles, J.E. (1996). Foundation Analysis and Design, 5th ed., McGraw-Hill

Brinkgreve, R. (2005). "Selection of soil models and parameters for geotechnical engineering application," ASCE Evaluation, Selection, and Calibration.

Brinkgreve, R. (1999). "Finite element simulation of the soil-structure interaction for a navigable lock," Plaxis Bulletin Issue no. 11, pg 4.

Brinkgreeve, R., Broere, W., and Waterman, D., ed. (2001). Plaxis 3D. Tunnel-Version 2, Delft University of Technology and Plaxis B.V., The Netherlands.

Britto, A.M., and Gunn, M.J. (1987). "Critical state soil mechanics via finite elements," Ellis Horwood Limited.

Caliendo, J.A., Anderson, L.R., and Gordon, W.J. (1990). "A Field Study of a Tieback Excavation with a Finite Element Analysis," Geotechnical Special Publication no. 25, ASCE, New York, NY, pp 747-763.

Cheang, W.L., Tan, S. A., and Yong K.Y. (2003). "Finite element modelling of a deep excavation supported by jack-in anchors," Plaxis Bulletin, pg 17.

Cheney, R.S. (1988). Permanent Ground Anchors, Federal Highway Administration Report, FHWA-DP-68-1R.

Clough, G.W., and Duncan, J.M. (1969). "Finite element analyses of Port Allen and Old River Locks," Report No. TE 69-3, College of Engineering, Office of Research Services, University of California, Berkeley, CA.

Dawkins, W.P. (1994a). "User's guide: Computer program for Winkler soil-structure interaction analysis of sheet-pile walls (CWALSSI)," Instruction Report ITL-94-1, U.S. Army Engineer, Waterways Experiment Station, Vicksburg, MS.

_____. (1994b). "User's guide: Computer program for analysis of beam column structures with nonlinear supports (CBEAMC)," Technical Report ITL-94-6, U.S. Army Engineer, Waterways Experiment Station, Vicksburg, MS.

Dawkins, W.P., Strom, R.W., and Ebeling, R.M. (2003) "User's Guide: Computer Program for Simulation of Construction Sequence for Stiff Wall Systems with Multiple Levels of Anchors (CMULTIANC)," Instruction Report ITL- U.S. Army Engineer Research and Development Center, Vicksburg, MS.

Ebeling, R.M., Azene, M., and Strom, R.W. (2002). "Simplified procedures for the design of tall, flexible anchored tieback walls," Technical Report ERDC/ITL TR-02-9, U.S. Army Engineer Research and Development Center, Vicksburg, MS.

Ebeling, R.M., and Mosher, R.L. (1996). "Red River U-frame Lock No. 1 backfill-structure-foundation interaction," ASCE, *Journal of Geotechnical Engineering* 122(30), 216-25.

Ebeling, R.M., Peters, J.F., and Clough, G.W. (1990). "User's guide for the incremental construction soil-structure interaction program SOILSTRUCT," Technical Report ITL-90-6, U.S. Army Engineer Waterways Experiment Station, Vicksburg, MS.

Ebeling, Mosher, Abraham, K. and Peters, J.F. (1993). "Soil structure interaction study of Red River Lock and Dam No. 1 subjected to sediment loading, " Technical Report ITL-93-3, U.S. Army Engineer Waterways Experiment Station, Vicksburg, MS.

Ebeling, R.M., Peters, J.F., and Mosher, R.L. (1997). "The role of non-linear deformation analysis in the design of a reinforced soil berm at Red River U-frame Lock No 1," *International Journal for Numerical and Analytical Methods in Geomechanics* 21, 753-87.

Ebeling, R.M., and Wahl, R.E. (1997). "Soil-structure-foundation interaction analysis of new roller-compacted concrete North Lock Wall at McAlpine Locks," Technical Report ITL-90-5, U.S. Army Engineer Waterways Experiment Station, Vicksburg, MS.

FHWA-RD-75-128. “Lateral support systems and underpinning” [Goldberg, Jaworski, and Gordon 1975].

FHWA-RD-81-150. “Permanent, ground anchors, Soletanche design criteria” [Pfisher, Evens, Guillaud, and Davision 1982].

FHWA-RD-97-130.”Design manual for permanent ground anchor walls” [Weatherby 1998].

FHWA-RD-98-065. “Summary report of research on permanent ground anchor walls; Vol I, Current practice and limit equilibrium analysis” [Long, Weatherby, and Cording 1998].

FHWA-RD-98-066, “Summary report of research on permanent ground anchor walls; Vol II, Full-scale wall tests and a soil structure interaction model” [Weatherby, Chung, Kim, and Briaud 1998].

FHWA-RD-98-068. “Summary report of research on permanent ground anchor walls; Vol IV, Conclusions and recommendations” [Weatherby 1998].

FHWA-SA-99-015. “Ground anchors and anchored systems,” Geotechnical Engineering Circular No. 4 [Sabatini, Pass, and Bachus 1999].

Gourvenec, S.M., and Powrie, W. (2000). “Three-dimensional finite element analyses of embedded retaining walls supported by discontinuous berms,” *Canadian Geotechnical Journal* 37, pp 1062–1077.

Gysi, H.J., Morri, G., Gysi, L., and Zurich, A.G. (2001). “Cut and cover tunnel with sheet pile walls used as anchor walls in Switzerland,” Plaxis Bulletin Issue no. 11, pg 11.

Hakman, P., and Buser, W. M. (1962). “Bulkhead test program at Port of Toledo, Ohio,” *Journal of the Soil Mechanics and Foundations Division*, Proceedings American Society of Civil Engineers, pp 151-184.

Hasen, L.A. (1980). “Prediction of the behavior of braced excavation in anisotropic clay,” Stanford University, Stanford, CA, 439p.

Headquarters, Department of the Army. (1987). “Bonneville Navigation Lock, Geology, Excavation, and Foundation,” Design Memorandum No. 3, Supplement 1, Washington, DC.

Headquarters, U.S. Army Corps of Engineers. (1989). “Retaining and flood walls,” Engineer Manual 1110-2-2502, Washington, DC.

Headquarters, U.S. Army Corps of Engineers. (1994). “Design of sheet pile walls,” Engineer Manual 1110-2-2504, Washington DC.

Hoefsloot, F.J.M. and Verwij, F. (2005). “4D grouting pressure model of a bored tunnel in 3D tunnel,” Plaxis Bulletin, Issue no. 18, pg 7.

Idaho National Engineering and Environmental Laboratory. (2003). "OU 7-13/14 In situ grouting project foundation grouting study," Project no. 23 833, pg 39.

Jumikis, A.R. (1984). Soil Mechanics, Robert E. Krieger, Florida.

Kerr, W. C., and Tamaro G.J. (1990) "Diaphragm walls—Update on design and performance." Proceedings, ASCE specialty conference on design and performance of earth retaining structures, Geotechnical Special Publication 25. American Society of Civil Engineers, Reston, VA.

Konstantakos, D., Whittle, A., Scharner, B., and Ragalado, C. (2005). "Control of ground movements for a multi-level-anchored diaphragm wall during excavation," Plaxis Bulletin Issue no. 17, pg 5.

Lasebnik, G.Y. (1961). "Investigation of anchored sheet-pile bulkheads," Thesis presented to the Kieu Polytechnical Institute, at Kieu, USSR, in 1961, in partial fulfillment of the requirements for the degree of Doctor of Philosophy.

Lengkeek, H.J. (2003). "Estimation of sand stiffness parameters from cone resistance," Plaxis Bulletin Issue no. 13, pg 15.

Liao, H.J., and Hsieh, P.G. (2002). "Tied-Back excavations in alluvial soil of Taipei," *Journal of the Geotechnical and Geo-environmental Engineering*, Technical Notes, American Society of Civil Engineers, pp 435-441.

Liew, S.S., Tan, Y.C., Ng, H.B., and Lee, P.T. (2003). "New approached of using jacked anchors as reinforcements in soil stabilization works for a cut-and-cover tunne1 with 17-m deep excavation," ICOF. Dundee, Scotland, pg 4.

Liu, Y. (1998). "Lecture notes: introduction to finite element method," University of Cincinnati.

Long, J.H., Weatherby, D.E., and Cording, E.J. (1998). "Summary report of research on permanent ground anchor walls; I, Current practice and limiting equilibrium analyses," Report FHWA-RD-98-065, Federal Highway Administration, McLean, VA.

Matich, M.A., Henderson, R.P., and Oates, D.B. (1964). "Performance measurements on two new anchored bulkheads," *Canadian Geotechnical Journal*, Vol. I, no. 3, pp. 167-178.

Mosher, R.L., and Knowles, V.R., (1990). "Finite analysis study of tieback wall for Bonneville navigation lock," Technical Report ITL-90-4, U.S. Army Engineer Waterways Experiment Station, Vicksburg, Ms.

Ratay, R. T. (1996). Handbook of temporary structures in construction. McGraw Hill, New York.

Rowe, P.W. (1957). "Anchored sheet-pile walls," Proceedings Institution Civil Engineers, Paper No. 5788, pp 27-69.

Schweiger, F. (2002). “Benchmarking 11,” Plaxis Bulletin Issue no. 12, pg 12.

Schertmann, J.H. (1970). “Static Cone to Compute Static Settlement Over Sand,” Proceedings ASCE, J. Soil Mechs. And Found. Engrg. Div., Vol. 96, No. SM3, May, pp. 1011-1048.

Schertmann, J.H. (1977). Guidelines for CPT Performance and Design, Pub. No. FHWA-TS-78-209, Federal Highway Adminstration, Washington, DC.

Sellountou, E.A., O’Neill, M.W., and Vipulanandan, C. (2005). “Construction effects on acip piles behavior in Texas coastal soils,” ASCE, GSP 132 advances in deep foundations.

Strom, R.W., and Ebeling, R.M. (2001). “State of practice in the design of tall, stiff, and flexible tieback retaining walls,” Technical Report ERDC/ITL TR-01-1, U.S Army Engineer Research and Development Center, Vicksburg, MS.

Strom, R.W., and Ebeling, R.M. (2002a). “Simplified procedures for the design of tall, stiff tieback walls,” Technical Report ERDC/ITL TR-02-10, U.S Army Engineer Research and Development Center, Vicksburg, MS.

_____. (2002b). “Methods used in tieback wall design and construction to prevent local anchor failure, progressive anchor failure, and ground mass stability failure,” Technical Report ERDC/ITL TR-02-11, U.S Army Engineer Research and Development Center, Vicksburg, MS.

Sabatini, P.I., Pass, D.G., and Bachus, R.C. (1990).”Ground anchors and anchored systems,” Geotechnical Engineering Circular No. 4, FHWA-SA-99-015, Federal Highway Administration, Washington, DC.

Terzaghi, K. (1959). “Theoretical soil mechanics,” John Wiley & Sons, New York.

Terzaghi, K., and Peck, R.B. (1967). Soil Mechanics in Engineering Practice, John Wiley & Sons, New York.

Trofimenkov, J.G. (1974). “Penetration Testing in USSR,” State-of-the-Art Report, European Symp. Penetration Testing, Stockholm, Vol. I.

Tschebotarioff, G.P. (1948). “Large scale earth pressure tests with model flexible bulkhead,” Final Report, Bureau of Yards and Dock, Department of Navy, pp 1-112.

Viggiani, G., and Tamagnini, C. (2000). “Ground movements around excavations in granular soils: a few remarks on the influence of the constitutive assumptions on FE predictions,” Mechanics of cohesive-frictional materials, pg 407.

Vermeer, P.A. (2001). “New developments,” Plaxis Bulletin Issue no. 10, pg 5.

Vermeer, P.A. (1997). “Editorial,” Plaxis Bulletin Issue no. 4, pg 2.

Vermeer, P.A. (1997). “Column Vermeer,” Plaxis Bulletin Issue no. 2, pg 1.

Wehnert, M. and, Vermeer P.A. (2004). “Numerical analyses of load test on bored piles,” NUMOG 9, pg 3.

Woods, R., and Rahim, A. (2002). SAGE CRISP Technical Manual.

Yassar, E. (1998). “Settlement behavior of a large clinker silo on soft ground,” Plaxis Bulletin Issue no. 5, pg 3.

APPENDIX A

SUMMARY OF RESULTS USING CURRENT 2-D PROCEDURES FOR CASE STUDY WALL NO. 1

A.1. RIGID 1 ANALYSIS

An equivalent beam on rigid supports analysis loaded with an apparent pressure diagram is used for the RIGID 1 analysis. For this analysis the total load used to construct the apparent pressure diagram is based on at-rest earth pressures (i.e., approximate factor of safety of 1.5 on the shear strength of the soil) (see discussion in Strom and Ebeling, 2001). The resulting apparent pressure diagram is shown in Figure A.1. Anchor forces and wall bending moment calculations follow.

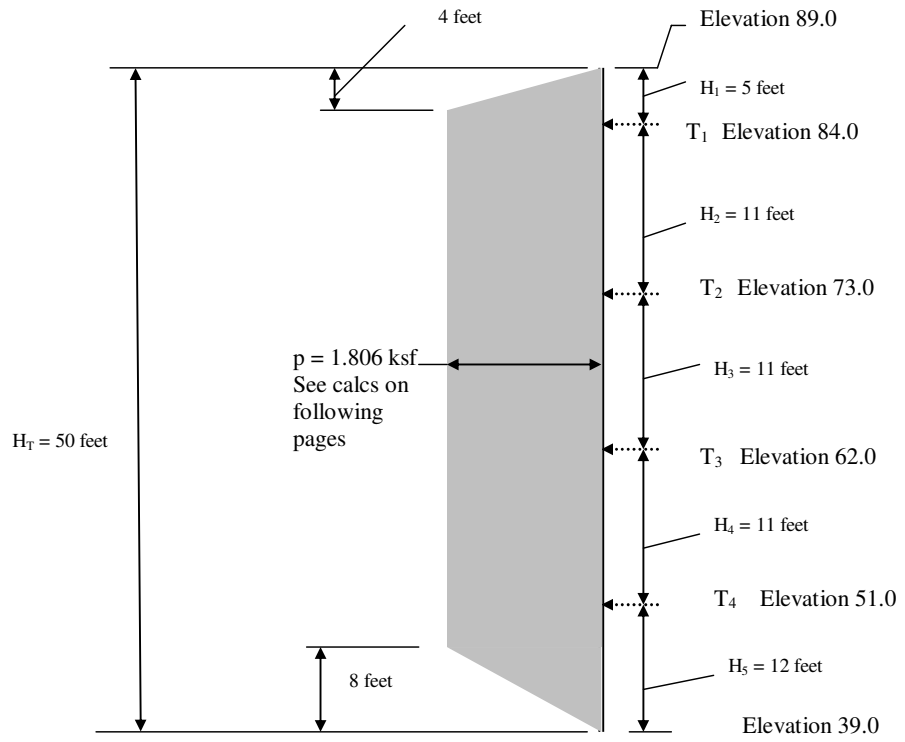

Figure A.1 Apparent pressure and surcharge loading on Bonneville tieback wall

I. Compute the static soil pressure. Active pressure coefficient (K_a) based on Coulomb equations. Passive earth pressure coefficients (K_p) are per Caquot and Kerisel (1973). (Figure A.2 and the calculations below). The following computations for K_a and K_p are used in subsequent calculations.

$\phi := 30 \cdot deg \qquad \beta := 0 \cdot deg$
$\theta := 0 \cdot deg \qquad \delta := 0 \cdot deg$

$$K_a := \frac{\cos(\phi - \theta)^2}{\cos(\theta)^2 \cdot \cos(\theta + \delta) \cdot \left[1 + \sqrt{\frac{(\sin(\phi + \delta) \cdot \sin(\phi - \beta))}{\cos(\delta + \theta) \cdot \cos(\beta - \theta)}}\right]^2}$$

$K_a = 0.333$ **Use K_a=0.333**

$\phi := 30 \cdot deg \qquad \theta := 0 \cdot deg$
$\beta := 0 \cdot deg \qquad \delta := 15 \cdot deg$

$$K_p := \frac{\cos(\phi + \theta)^2}{\cos(\theta)^2 \cdot \cos(\delta - \theta) \cdot \left[1 - \sqrt{\frac{(\sin(\phi + \delta) \cdot \sin(\phi + \beta))}{(\cos(\delta - \theta) \cdot \cos(\beta - \theta))}}\right]^2}$$

$K_p = 4.977$

By Log Spiral (Capout and Kerisel)

$K_{pls} := 6.5 \qquad R_{pls} := 0.746$
$K_p := R_{pls} \cdot K_{pls}$
$K_p = 4.849$

Use Kp=4.85

Driving-side at-rest earth pressure at elevations significant to the Rigid 1 and Rigid 2 analyses are shown in Figure A.3.

II. Determine total earth pressure load based on at-rest earth pressure

Soil properties
Friction Angle = 30 degrees
Total weight (γ) = 125 pcf
Ka = 0.333
Kp = 4.85

$\phi := 30 \cdot deg$

$K_0 := 1 - \sin(\phi)$ $\sin(\phi) = 0.5$ $H_T := 50$

$\gamma := 0.125$ $K_0 := 0.5$

The total load (T_L) for the apparent earth pressure diagram shown in Fig A.1 equates to

$$T_L := K_0 \cdot \left[\frac{1}{2} \cdot \gamma \cdot \left(H_T \right)^2 \right]$$

$T_L = 78.125$ kips/ft

III. Compute earth pressure to stabilize soil cut (p) which is the ordinate of the apparent earth pressure in Figure A.1

$H_T = 50$ $H_1 := 5$ $H_2 := 11$

$H_3 := 11$ $H_4 := 11$ $H_5 := 12$

$$p := \frac{T_L}{\left(H_T - 0.333 \cdot H_1 - 0.333\, H_5 \right)}$$

$p = 1.762$ ksf

IV. Calculate Bending Moment at Upper Ground Anchor (M_1)

$$M_1 := \left(\frac{13}{54} \right) \cdot H_1^{\,2} \cdot p$$

$M_1 = 10.605$ ft.kip per ft. run of wall

Calculate the Ground Anchor Loads by the Tributary Area Method

$$T_1 := \left[\left(\frac{2}{3}\right)\cdot H_1 + \left(\frac{1}{2}\right)\cdot H_2\right]\cdot p$$

$T_1 = 15.564$ kips per ft run of wall

$$T_2 := \left[\left(\frac{1}{2}\right)\cdot H_2 + \left(\frac{1}{2}\right)\cdot H_3\right]\cdot p$$

$T_2 = 19.382$ kips per ft run of wall

$$T_3 := \left[\left(\frac{1}{2}\right)\cdot H_3 + \left(\frac{1}{2}\right)\cdot H_4\right]\cdot p$$

$T_3 = 19.382$ kips for ft run of wall

$$T_4 := \left[\left(\frac{1}{2}\right)\cdot H_4 + \left(\frac{23}{48}\right)\cdot H_5\right]\cdot p$$

$T_4 = 19.822$ kips for ft run wall

Calculate the subgrade reaction at base of wall (R_B)

$$R_B := \left[\left(\frac{3}{16}\right)\cdot H_5\right]\cdot p$$

$R_B = 3.964$ kips per ft run of wall

Calculate the Maximum Bending Moment Below the Upper Anchor

$$MM_1 := \left(\frac{1}{10}\right)\cdot H_2^{\,2}\cdot(p)$$

$MM_1 = 21.32$ ft. kips per ft run of wall

Note Rigid 1 Analysis of "Stiff" Bonneville Wall

Apparent pressures are intended to represent a load envelopes and not actual loads that might exist on the wall at any time. This procedure is a final-excavation analysis that indirectly considers the effects of construction sequences. Other researchers, (Kerr and Tamaro 1990) believed that use of apparent pressure diagrams for designs of stiff walls is ill-advised. However, the procedure can be used to compare to other methods to ensure that upper tieback is not over-stressed.

A.2. RIGID 2 ANALYSES

The RIGID 2 analysis is an equivalent beam on rigid supports excavation sequencing analysis. Earth pressures, however, are in accordance with classical earth pressure theory, assuming a wall retaining nonyielding soil backfill (at-rest earth pressure distribution). The Computer-Aided Structural Engineering (CASE) computer program CBEAMC was utilized to compute wall bending moments and shears.

A.2.1. FIRST-STAGE excavation analysis

The first-stage net pressure conditions are illustrated in Figure A.4. Calculations for quantities of interest follow, along with a CBEAMC analysis used to determine wall bending moments and shears.

For the cantilevered section of tieback wall (uppermost section), the minimum penetration (maximum moment condition) was determined based on Figure 2-3 Andersen's "Substructure Analysis and Design" 2nd Edition.

$$Po := \frac{(3.125)}{50} \quad Po = 0.063 \quad \text{kips/ft.}$$

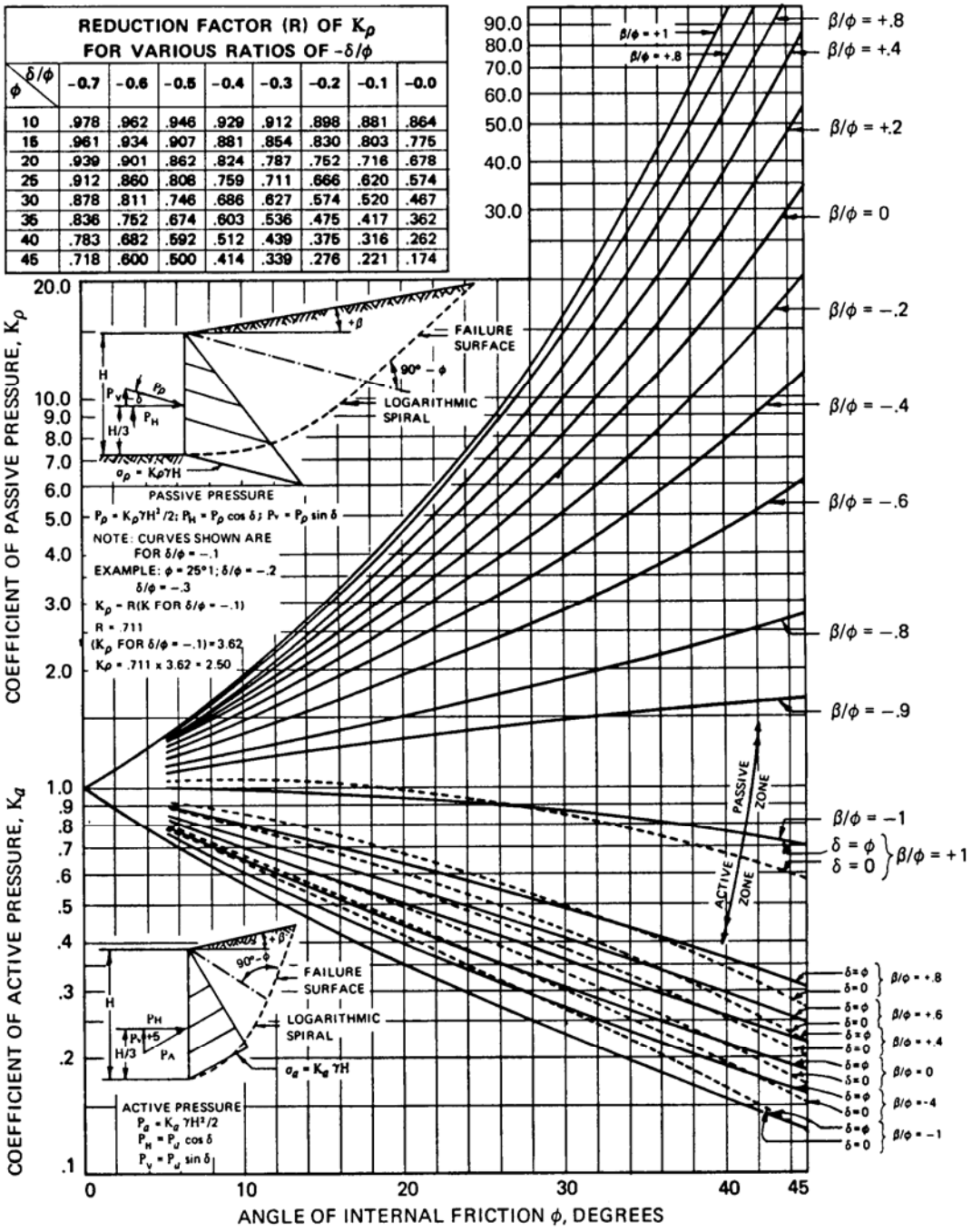

ϕ \ δ/ϕ	-0.7	-0.6	-0.5	-0.4	-0.3	-0.2	-0.1	-0.0
10	.978	.962	.946	.929	.912	.898	.881	.864
15	.961	.934	.907	.881	.854	.830	.803	.775
20	.939	.901	.862	.824	.787	.752	.716	.678
25	.912	.860	.808	.759	.711	.666	.620	.574
30	.878	.811	.746	.686	.627	.574	.520	.467
35	.836	.752	.674	.603	.536	.475	.417	.362
40	.783	.682	.592	.512	.439	.375	.316	.262
45	.718	.600	.500	.414	.339	.276	.221	.174

Figure A.2. Active and passive coefficients
(after Caquot and Kerisel, 1973)

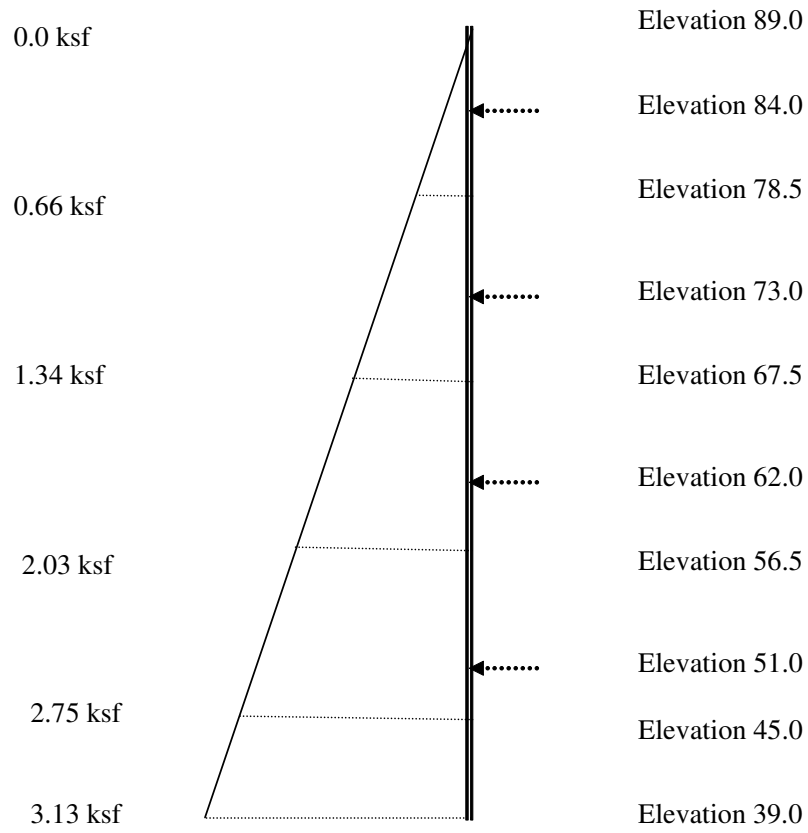

Figure A.3. Excavation and tieback locations driving side earth pressures at excavation levels

Po is the at-rest pressure with depth on the driving side of the wall. The rate of increase of Po is reported on figure A.3.

$\gamma := 0.125$ kips/ft.

$Kp := 4.85$ After Caquot and Kerisel

$Pp := Kp \cdot \gamma$ $\quad Pp := 0.606$ kips/ft.

$m_1 := \frac{0.656}{Pp - Po}$ $\quad m_1 = 1.207$ Feet

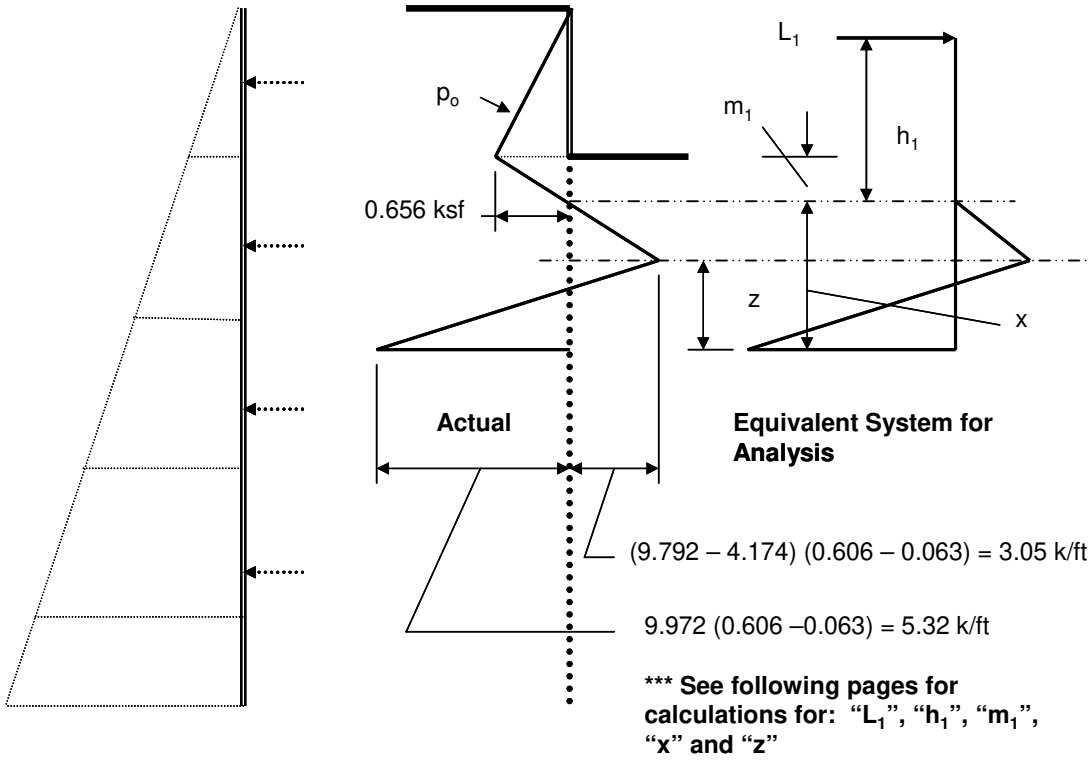

Figure A.4. Excavate to elevation 78.5 - first stage excavation

$$L_1 := \left(0.656 \cdot 10.5 \cdot \frac{1}{2}\right) + 0.656 \cdot \frac{m_1}{2} \qquad L_1 = 3.84 \quad \text{kips}$$

$$h_1 := \left[0.656 \cdot (10.5) \cdot \left(\frac{1}{2}\right) \cdot \left[10.5 \cdot \left(\frac{1}{3}\right) + m_1\right] + 0.656 \cdot \left(\frac{m_1}{2}\right) \cdot \left(2 \cdot \frac{m_1}{3}\right)\right] \cdot \frac{1}{L_1}$$

$h_1 = 4.305$ Feet

Try various values of "x"
The correct value of "x" is when Y=0

Try $x := 9.7916$ Feet

$$Y := x^4 - \left(\frac{8 \cdot L_1}{Pp - Po}\right) \cdot x^2 - \frac{\left(12 \cdot L_1 \cdot h_1\right)}{(Pp - Po)} \cdot x - \left(\frac{2 \cdot L_1}{Pp - Po}\right)^2$$

$Y = -0.035$ Approximately equal to zero okay

$$z := \left(\frac{x}{2}\right) - \frac{L_1}{(Pp - Po)\cdot x} \qquad z = 4.174 \quad \text{feet}$$

Use x= 9.7916 ft. For x, refer to Figure A.4.

The net earth pressure diagram based on classical methods, established by the above calculations and illustrated in Figure 3.5, is used in a beam-column analysis (CBEAMC analysis) to determine wall bending moments and shears. In the CBEAMC analysis, the wall is provided with a fictitious support. This support is fixed against translation and rotation to provide stability for the beam column solution. The support is located at a distance equal to (89.0 - 78.5) + m_1+x, or 21.51 ft below the top of the wall. This is the point that first provides static equilibrium and thus produces the minimum penetration depth required for system stability. At this depth the moment should be zero, and provides the fictitious support depth has been properly determined, the CBEAMC analysis should confirm this. Input and output for the CBEAMC analysis are provided on the following pages.

```
'Bonneville Tieback  First Stage Excavation
BEAM  FT  KSF  FT
  0    21.51   4.750E+05   3    2.25    3    2.25
NODES  FT  FT
  0    21.51    1
LOADS DISTRIBUTED  FT  K/FT
  0    0    0    10.5    0    0.656
  10.5    0    0.656   11.71    0    0
  11.71    0    0    17.33    0   -3.05
  17.33    0   -3.05    21.51    0    5.32
FIXED  FT  FT
  21.51   0.000  0.000  0.000
FINISHED
```

```
   PROGRAM CBEAMC - ANALYSIS OF BEAM-COLUMNS WITH NONLINEAR
SUPPORTS
```

DATE: 16-MARCH-2007 TIME: 20:44:18

****
* SUMMARY OF RESULTS *
****

I.--HEADING
'Bonneville Tieback First Stage Excavation

II.—MAXIMA

	MAXIMUM POSITIVE	X-COORD (FT)	MAXIMUM NEGATIVE	X-COORD (FT)
AXIAL DISPLACEMENT (IN)	: 0.000E+00	0.00	0.000E+00	0.00
LATERAL DISPLACEMENT (IN)	: 3.489E-02	0.00	0.000E+00	0.00
ROTATION (RAD)	: 0.000E+00	0.00	-2.051E-04	0.00
AXIAL FORCE (K)	: 0.000E+00	0.00	0.000E+00	0.00
SHEAR FORCE (K)	: 3.841E+00	11.71	-7.030E+00	19.00
BENDING MOMENT (K-FT)	: 2.617E+01	15.46	0.000E+00	0.00

III.--REACTIONS AT FIXED SUPPORTS

X-C00RD (FT)	X-REACTION (K)	Y-REACTION (K)	MOMENT-REACTION (K-FT)
21.51	0.000E+00	-1.468E-02	3.051E-02

IV.--FORCES IN LINEAR CONCENTRATED SPRINGS
NONE

V.--FORCES IN NONLINEAR CONCENTRATED SPRINGS
NONE

PROGRAM CBEAMC - ANALYSIS OF BEAM-COLUMNS WITH NONLINEAR SUPPORTS
DATE: 16-MARCH-2007 TIME: 20:44:18

****
* COMPLETE RESULTS *
****

I.--HEADING
'Bonneville Tieback First Stage Excavation

II.--DISPLACEMENTS AND INTERNAL FORCES

<---------DISPLACEMENTS-------->				<--------INTERNAL FORCES------->		
X-COORD	AXIAL	LATERAL	ROTATION	AXIAL	SHEAR	MOMENT
(FT)	(IN)	(IN)	(RAD)	(K)	(K)	(K-FT)
0.00	0.000E+00	3.489E-02	-2.051E-04	0.000E+00	-4.591E-13	4.944E-13
0.95	0.000E+00	3.254E-02	-2.051E-04	0.000E+00	2.846E-02	9.056E-03
1.91	0.000E+00	3.019E-02	-2.051E-04	0.000E+00	1.139E-01	7.245E-02
2.86	0.000E+00	2.784E-02	-2.050E-04	0.000E+00	2.562E-01	2.445E-01
3.82	0.000E+00	2.549E-02	-2.046E-04	0.000E+00	4.554E-01	5.796E-01
4.77	0.000E+00	2.315E-02	-2.039E-04	0.000E+00	7.116E-01	1.132E+00
5.73	0.000E+00	2.082E-02	-2.025E-04	0.000E+00	1.025E+00	1.956E+00
6.68	0.000E+00	1.852E-02	-2.003E-04	0.000E+00	1.395E+00	3.106E+00
7.64	0.000E+00	1.624E-02	-1.969E-04	0.000E+00	1.822E+00	4.637E+00
8.59	0.000E+00	1.401E-02	-1.919E-04	0.000E+00	2.305E+00	6.602E+00
9.55	0.000E+00	1.185E-02	-1.849E-04	0.000E+00	2.846E+00	9.056E+00
10.50	0.000E+00	9.784E-03	-1.755E-04	0.000E+00	3.444E+00	1.205E+01
11.11	0.000E+00	8.536E-03	-1.681E-04	0.000E+00	3.742E+00	1.424E+01
11.71	0.000E+00	7.347E-03	-1.594E-04	0.000E+00	3.841E+00	1.654E+01
12.65	0.000E+00	5.643E-03	-1.433E-04	0.000E+00	3.603E+00	2.006E+01
13.58	0.000E+00	4.136E-03	-1.243E-04	0.000E+00	2.889E+00	2.314E+01
14.52	0.000E+00	2.856E-03	-1.030E-04	0.000E+00	1.698E+00	2.533E+01
15.46	0.000E+00	1.825E-03	-8.035E-05	0.000E+00	3.177E-02	2.617E+01
16.39	0.000E+00	1.050E-03	-5.767E-05	0.000E+00	-2.111E+00	2.524E+01
17.33	0.000E+00	5.217E-04	-3.676E-05	0.000E+00	-4.730E+00	2.207E+01
18.17	0.000E+00	2.338E-04	-2.128E-05	0.000E+00	-6.580E+00	1.725E+01
19.00	0.000E+00	8.053E-05	-1.003E-05	0.000E+00	-7.030E+00	1.146E+01
19.84	0.000E+00	1.735E-05	-3.296E-06	0.000E+00	-6.081E+00	5.882E+00
20.67	0.000E+00	1.243E-06	-4.657E-07	0.000E+00	-3.733E+00	1.682E+00
21.51	0.000E+00	0.000E+00	0.000E+00	0.000E+00	**1.468E-02**	**3.051E-02**

Note: Shear and moment values in bold are approximately equal to zero

A.2.2 SECOND-STAGE excavation analysis

The computations for the second excavation stage (Stage 2) are provided below. Second-stage excavation is at a depth of 89.0-67.5=21.5ft. In the analysis, a point of contraflexure is assumed to coincide with zero net pressure point located at a distance of "21.5 + *m* ft" below the surface. Using this assumption, the upper portion of the anchored tieback wall can be treated as an equivalent beam that is simply supported at the anchor location and at the first

point of zero net pressure intensity. The equivalent beam with net pressure loading is shown Figure A.5. As with first-stage excavation, the second-stage excavation analysis is performed using the CASE computer program CBEAMC. The CBEAMC input and output for the final stage analysis is provided below.

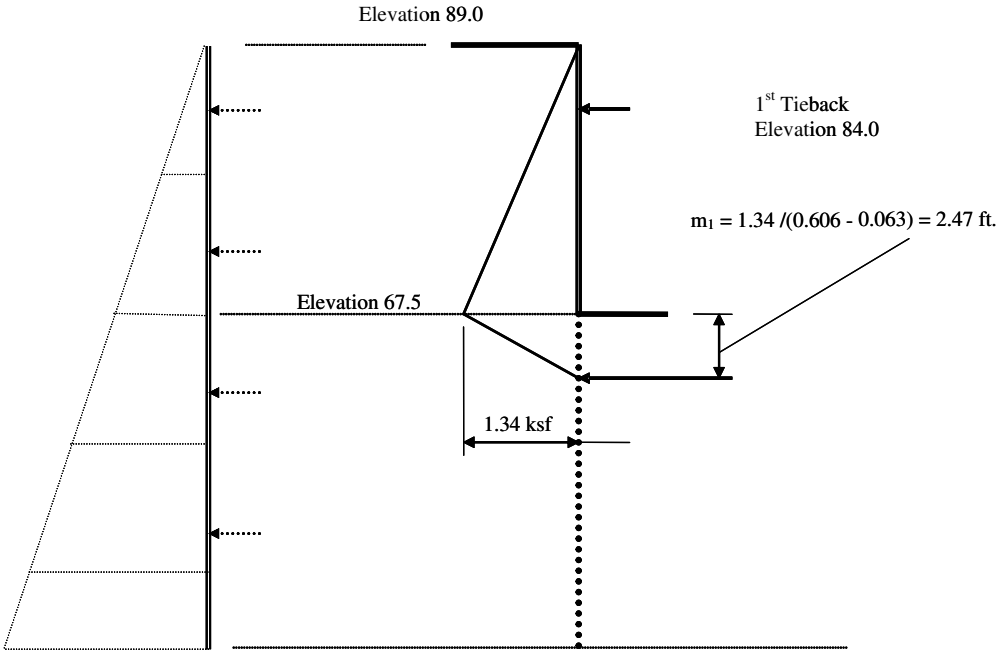

Figure A.5. Excavate to elevation 67.5 – second stage excavation

```
'Bonneville Tieback  Second Stage Excavation
BEAM  FT  KSF  FT
  0    23.97   4.750E+05   3    2.25    3    2.25
NODES  FT  FT
  0    23.97    2
LOADS DISTRIBUTED  FT  K/FT
  0    0    0    21.5    0    1.34
  21.5    0    1.34    23.97    0    0
FIXED  FT  FT
  5   0.000  0.000  FREE
  23.97   0.000  0.000  FREE
FINISHED

   PROGRAM CBEAMC - ANALYSIS OF BEAM-COLUMNS WITH NONLINEAR
SUPPORTS
```

DATE: 18-MARCH-2007 TIME: 15:18:33

****
* SUMMARY OF RESULTS *
****

I.--HEADING
'Bonneville Tieback Second Stage Excavation

II.—MAXIMA

	MAXIMUM POSITIVE	X-COORD (FT)	MAXIMUM NEGATIVE	X-COORD (FT)
AXIAL DISPLACEMENT (IN)	: 0.000E+00	0.00	0.000E+00	0.00
LATERAL DISPLACEMENT (IN)	: 1.633E-02	14.17	-1.298E-02	0.00
ROTATION (RAD)	: 2.176E-04	5.00	-2.388E-04	23.97
AXIAL FORCE (K)	: 0.000E+00	0.00	0.000E+00	0.00
SHEAR FORCE (K)	: 8.599E+00	23.97	-6.682E+00	5.00
BENDING MOMENT (K-FT)	: 1.298E+00	5.00	-3.953E+01	16.00

III.--REACTIONS AT FIXED SUPPORTS

X-C00RD (FT)	X-REACTION (K)	Y-REACTION (K)	MOMENT-REACTION (K-FT)
5.00	0.000E+00	-7.461E+00	0.000E+00
3.97	0.000E+00	-8.599E+00	0.000E+00

IV.--FORCES IN LINEAR CONCENTRATED SPRINGS
NONE
V.--FORCES IN NONLINEAR CONCENTRATED SPRINGS
NONE

PROGRAM CBEAMC - ANALYSIS OF BEAM-COLUMNS WITH NONLINEAR SUPPORTS
DATE: 18-MARCH-2007 TIME: 15:18:33

****
* COMPLETE RESULTS *
****

I.--HEADING
'Bonneville Tieback Second Stage Excavation

II.--DISPLACEMENTS AND INTERNAL FORCES
<---------DISPLACEMENTS--------> <--------INTERNAL FORCES------->

X-COORD	AXIAL	LATERAL	ROTATION	AXIAL	SHEAR	MOMENT
(FT)	(IN)	(IN)	(RAD)	(K)	(K)	(K-FT)
0.00	0.000E+00	-1.298E-02	2.161E-04	0.000E+00	1.234E-13	1.533E13
1.67	0.000E+00	-8.663E-03	2.161E-04	0.000E+00	8.656E-02	4.809E02
3.33	0.000E+00	-4.338E-03	2.164E-04	0.000E+00	3.463E-01	3.847E01
5.00	0.000E+00	0.000E+00	2.176E-04	0.000E+00	7.791E-01	1.298E+00
5.00	0.000E+00	0.000E+00	2.176E-04	0.000E+00	-6.682E+00	1.298E+00
6.83	0.000E+00	4.737E-03	2.097E-04	0.000E+00	-6.006E+00	-1.036E+01
8.67	0.000E+00	9.087E-03	1.829E-04	0.000E+00	-5.121E+00	2.060E+01
10.50	0.000E+00	1.267E-02	1.401E-04	0.000E+00	-4.026E+00	2.901E+01
12.33	0.000E+00	1.516E-02	8.461E-05	0.000E+00	-2.721E+00	3.523E+01
14.17	0.000E+00	1.633E-02	2.067E-05	0.000E+00	-1.207E+00	3.886E+01
16.00	0.000E+00	1.604E-02	-4.702E-05	0.000E+00	5.164E-01	3.953E+01
17.83	0.000E+00	1.427E-02	-1.130E-04	0.000E+00	2.449E+00	3.684E+01
19.67	0.000E+00	1.112E-02	-1.713E-04	0.000E+00	4.592E+00	3.042E+01
21.50	0.000E+00	6.840E-03	-2.150E-04	0.000E+00	6.944E+00	1.988E+01
22.74	0.000E+00	3.509E-03	-2.327E-04	0.000E+00	8.185E+00	1.045E+01
23.97	0.000E+00	0.000E+00	-2.388E-04	0.000E+00	8.599E+00	1.064E-13

II.--FORCES IN LINEAR DISTRIBUTED SPRINGS
NONE

IV.--FORCES IN NONLINEAR DISTRIBUTED SPRINGS
NONE

A.2.3. THIRD-STAGE excavation analysis

The third-stage excavation is to el 56.6. The equivalent beam with net pressure loading is shown in Figure A.6. Calculations for the third-stage excavation are performed in the same manner as for the second-stage excavation.

```
'Bonneville Tieback  Third Stage Excavation
BEAM  FT  KSF  FT
  0   36.24  4.750E+05  3   2.25   3   2.25
NODES  FT  FT
  0   36.24   2
```

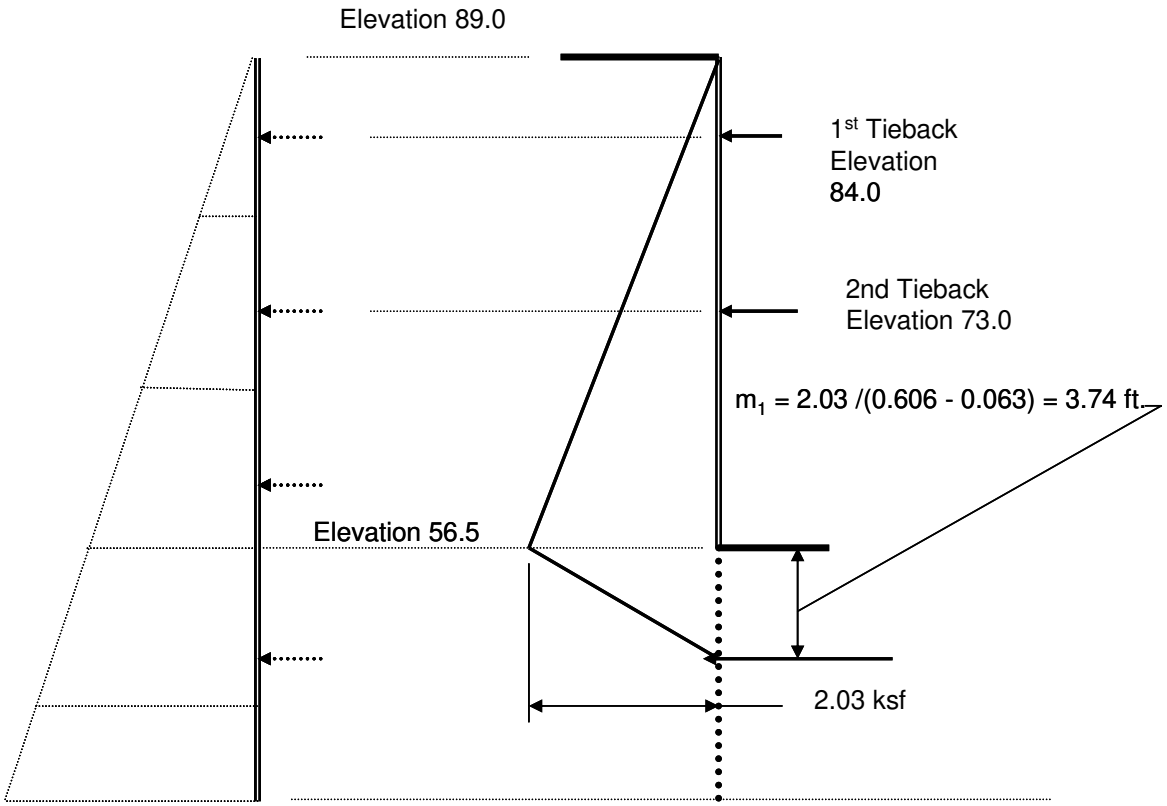

Figure A.6. Excavate to elevation 56.5 – third stage excavation

```
LOADS DISTRIBUTED  FT  K/FT
  0   0   0.0   32.5   0   2.03
  32.5   0   2.03   36.24   0   0
FIXED  FT  FT
  5   0.000  0.000  FREE
  16   0.000  0.000  FREE
  36.24   0.000  0.000  FREE
FINISHED

   PROGRAM CBEAMC - ANALYSIS OF BEAM-COLUMNS WITH NONLINEAR
SUPPORTS
   DATE: 17-MARCH-2007                    TIME: 0:00:43


                        **********************
                        * SUMMARY OF RESULTS  *
                        **********************

    I.--HEADING
```

'Bonneville Tieback Third Stage Excavation

II.—MAXIMA

	MAXIMUM POSITIVE	X-COORD (FT)	MAXIMUM NEGATIVE	X-COORD (FT)
AXIAL DISPLACEMENT (IN)	: 0.000E+00	0.00	0.000E+00	0.00
LATERAL DISPLACEMENT (IN)	: 2.319E-02	27.00	-3.412E-03	12.33
ROTATION (RAD)	: 2.429E-04	19.67	-3.404E-04	36.24
AXIAL FORCE (K)	: 0.000E+00	0.00	0.000E+00	0.00
SHEAR FORCE (K)	: 1.198E+01	36.24	-1.681E+01	16.00
BENDING MOMENT (K-FT)	: 5.442E+01	16.00	-5.696E+01	28.83

III.--REACTIONS AT FIXED SUPPORTS

X-C00RD	X-REACTION	Y-REACTION	MOMENT-REACTION
(FT)	(K)	(K)	(K-FT)
5.00	0.000E+00	1.071E+00	0.000E+00
16.00	0.000E+00	-2.587E+01	0.000E+00
36.24	0.000E+00	-1.198E+01	0.000E+00

IV.--FORCES IN LINEAR CONCENTRATED SPRINGS
NONE

V.--FORCES IN NONLINEAR CONCENTRATED SPRINGS
NONE

PROGRAM CBEAMC - ANALYSIS OF BEAM-COLUMNS WITH NONLINEAR SUPPORTS
DATE: 17-MARCH-2007 TIME: 0:00:43

****
* COMPLETE RESULTS *
****

I.--HEADING
'Bonneville Tieback Third Stage Excavation

II.--DISPLACEMENTS AND INTERNAL FORCES

	<---------DISPLACEMENTS-------->			<--------INTERNAL FORCES------->		
X-COORD	AXIAL	LATERAL	ROTATION	AXIAL	SHEAR	MOMENT

(FT)	(IN)	(IN)	(RAD)	(K)	(K)	(K-FT)
0.00	0.000E+00	3.972E-03	-6.650E-05	0.000E+00	0.000E+00	-1.404E14
1.67	0.000E+00	2.642E-03	-6.648E-05	0.000E+00	8.675E-02	4.820E02
3.33	0.000E+00	1.314E-03	-6.620E-05	0.000E+00	3.470E-01	3.856E01
5.00	0.000E+00	0.000E+00	-6.498E-05	0.000E+00	7.808E-01	1.301E+00
5.00	0.000E+00	0.000E+00	-6.498E-05	0.000E+00	1.852E+00	1.301E+00
6.83	0.000E+00	-1.382E-03	-5.951E-05	0.000E+00	2.529E+00	5.285E+00
8.67	0.000E+00	-2.560E-03	-4.602E-05	0.000E+00	3.417E+00	1.070E+01
10.50	0.000E+00	-3.328E-03	-2.174E-05	0.000E+00	4.514E+00	1.794E+01
12.33	0.000E+00	-3.412E-03	1.679E-05	0.000E+00	5.822E+00	2.739E+01
14.17	0.000E+00	-2.454E-03	7.369E-05	0.000E+00	7.339E+00	3.942E+01
16.00	0.000E+00	0.000E+00	1.537E-04	0.000E+00	9.066E+00	5.442E+01
16.00	0.000E+00	0.000E+00	1.537E-04	0.000E+00	-1.681E+01	5.442E+01
17.83	0.000E+00	4.220E-03	2.216E-04	0.000E+00	-1.487E+01	2.535E+01
19.67	0.000E+00	9.410E-03	2.429E-04	0.000E+00	-1.272E+01	3.015E02
21.50	0.000E+00	1.461E-02	2.241E-04	0.000E+00	-1.037E+01	2.117E+01
23.33	0.000E+00	1.903E-02	1.728E-04	0.000E+00	-7.798E+00	3.785E+01
25.17	0.000E+00	2.204E-02	9.706E-05	0.000E+00	-5.021E+00	4.963E+01
27.00	0.000E+00	2.319E-02	5.568E-06	0.000E+00	-2.034E+00	5.613E+01
28.83	0.000E+00	2.224E-02	-9.227E-05	0.000E+00	1.162E+00	5.696E+01
30.67	0.000E+00	1.915E-02	-1.864E-04	0.000E+00	4.569E+00	5.174E+01
32.50	0.000E+00	1.414E-02	-2.661E-04	0.000E+00	8.186E+00	4.008E+01
34.37	0.000E+00	7.492E-03	-3.210E-04	0.000E+00	1.103E+01	2.181E+01
36.24	0.000E+00	0.000E+00	-3.404E-04	0.000E+00	1.198E+01	4.961E14

A.2.4. FOURTH-STAGE excavation analysis

Fourth-stage excavation is to el 45.0. The equivalent beam with net pressure loading is shown in Figure A.7. Calculations for the third-stage excavation are performed in the same manner as for the second and third stages. The CBEAMC input and output for the final stage analysis is provided below.

```
'Bonneville Tieback  Fourth Stage Excavation
BEAM  FT  KSF  FT
  0    49.06   4.750E+05   3    2.25    3    2.25
NODES  FT  FT
  0    49.06    3
```

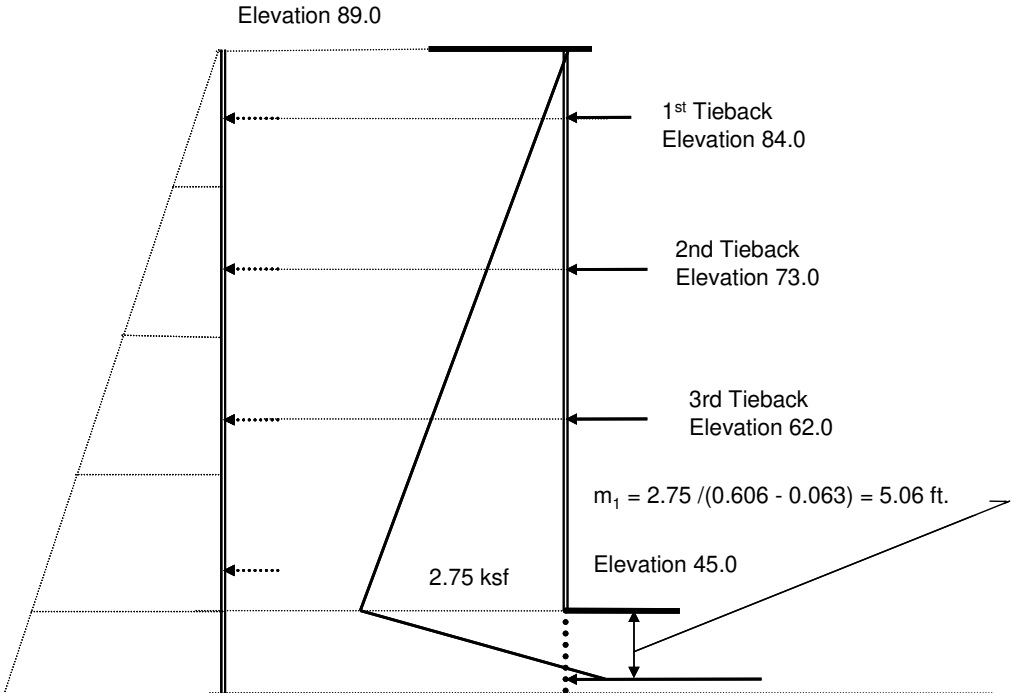

Figure A.7. Excavate to elevation 45 – fourth stage excavation

LOADS DISTRIBUTED FT K/FT
0 0 0.0 44 0 2.75
44 0 2.75 49.06 0 0
FIXED FT FT
5 0.000 0.000 FREE
16 0.000 0.000 FREE
27 0.000 0.000 FREE
49.06 0.000 0.000 FREE
FINISHED

PROGRAM CBEAMC - ANALYSIS OF BEAM-COLUMNS WITH NONLINEAR SUPPORTS
DATE: 17-MARCH-2007 TIME: 0:09:51

****
* SUMMARY OF RESULTS *
****

I.--HEADING
'Bonneville Tieback Fourth Stage Excavation

II.—MAXIMA

	MAXIMUM POSITIVE	X-COORD (FT)	MAXIMUM NEGATIVE	X-COORD (FT)
AXIAL DISPLACEMENT (IN)	: 0.000E+00	0.00	0.000E+00	0.00
LATERAL DISPLACEMENT (IN)	: 4.445E-02	38.33	-4.746E-03	24.25
ROTATION (RAD)	: 4.158E-04	29.83	-5.988E-04	49.06
AXIAL FORCE (K)	: 0.000E+00	0.00	0.000E+00	0.00
SHEAR FORCE (K)	: 1.791E+01	27.00	-2.757E+01	27.00
BENDING MOMENT (K-FT)	: 9.884E+01	27.00	-9.278E+01	41.17

III.--REACTIONS AT FIXED SUPPORTS

X-C00RD (FT)	X-REACTION (K)	Y-REACTION (K)	MOMENT-REACTION (K-FT)
5.00	0.000E+00	-4.780E+00	0.000E+00
16.00	0.000E+00	-9.385E-02	0.000E+00
27.00	0.000E+00	-4.548E+01	0.000E+00
49.06	0.000E+00	-1.711E+01	0.000E+00

IV.--FORCES IN LINEAR CONCENTRATED SPRINGS
NONE

V.--FORCES IN NONLINEAR CONCENTRATED SPRINGS
NONE

PROGRAM CBEAMC - ANALYSIS OF BEAM-COLUMNS WITH NONLINEAR SUPPORTS
DATE: 17-MARCH-2007 TIME: 0:09:51

****
* COMPLETE RESULTS *
****

I.--HEADING
'Bonneville Tieback Fourth Stage Excavation

II.--DISPLACEMENTS AND INTERNAL FORCES

	<---------DISPLACEMENTS-------->			<--------INTERNAL FORCES------->		
X-COORD (FT)	AXIAL (IN)	LATERAL (IN)	ROTATION (RAD)	AXIAL (K)	SHEAR (K)	MOMENT (K-FT)

0.00	0.000E+00	-2.651E-03	4.388E-05	0.000E+00	0.000E+00	2.262E-14
2.50	0.000E+00	-1.334E-03	4.397E-05	0.000E+00	1.953E-01	1.628E-01
5.00	0.000E+00	0.000E+00	4.540E-05	0.000E+00	7.812E-01	1.302E+00
5.00	0.000E+00	0.000E+00	4.540E-05	0.000E+00	-3.999E+00	1.302E+00
7.75	0.000E+00	1.407E-03	3.576E-05	0.000E+00	-2.903E+00	-8.296E+00
10.50	0.000E+00	2.136E-03	5.849E-06	0.000E+00	-1.335E+00	-1.423E+01
13.25	0.000E+00	1.691E-03	-3.322E-05	0.000E+00	7.065E-01	-1.520E+01
16.00	0.000E+00	0.000E+00	-6.701E-05	0.000E+00	3.220E+00	-9.911E+00
16.00	0.000E+00	0.000E+00	-6.701E-05	0.000E+00	3.126E+00	-9.911E+00
18.75	0.000E+00	-2.483E-03	-7.807E-05	0.000E+00	6.113E+00	2.684E+00
21.50	0.000E+00	-4.675E-03	-4.560E-05	0.000E+00	9.572E+00	2.414E+01
24.25	0.000E+00	-4.746E-03	5.488E-05	0.000E+00	1.350E+01	5.576E+01
27.00	0.000E+00	0.000E+00	2.512E-04	0.000E+00	1.791E+01	9.884E+01
27.00	0.000E+00	0.000E+00	2.512E-04	0.000E+00	-2.757E+01	9.884E+01
29.83	0.000E+00	1.187E-02	4.158E-04	0.000E+00	-2.254E+01	2.774E+01
32.67	0.000E+00	2.636E-02	4.115E-04	0.000E+00	-1.700E+01	-2.840E+01
35.50	0.000E+00	3.841E-02	2.797E-04	0.000E+00	-1.097E+01	-6.814E+01
38.33	0.000E+00	4.445E-02	1.809E-04	0.000E+00	2.608E+00	-9.278E+01
44.00	0.000E+00	3.238E-02	-4.077E-04	0.000E+00	1.015E+01	-7.482E+01
46.53	0.000E+00	1.766E-02	-5.484E-04	0.000E+00	1.537E+01	-4.181E+01
49.06	0.000E+00	0.000E+00	-5.988E-04	0.000E+00	1 .711E+01	9.804E-14

A.2.5 THIRD-STAGE excavation analysis

Final excavation is to el 39.0. The equivalent beam with net pressure loading is shown in Figure 3. 10. Calculations for final-stage excavation are similar to those performed in Stages 2 through 4.

```
'Bonneville Tieback  Final Stage Excavation
BEAM  FT  KSF  FT
  0    50   4.750E+05   3    2.25    3    2.25
NODES  FT  FT
  0    50    3
LOADS DISTRIBUTED  FT  K/FT
  0    0    0.0    50    0    3.125
FIXED  FT  FT
  5   0.000  0.000  FREE
  16   0.000  0.000  FREE
  27   0.000  0.000  FREE
  38   0.000  0.000  FREE
  50   0.000  0.000  FREE
FINISHED
```

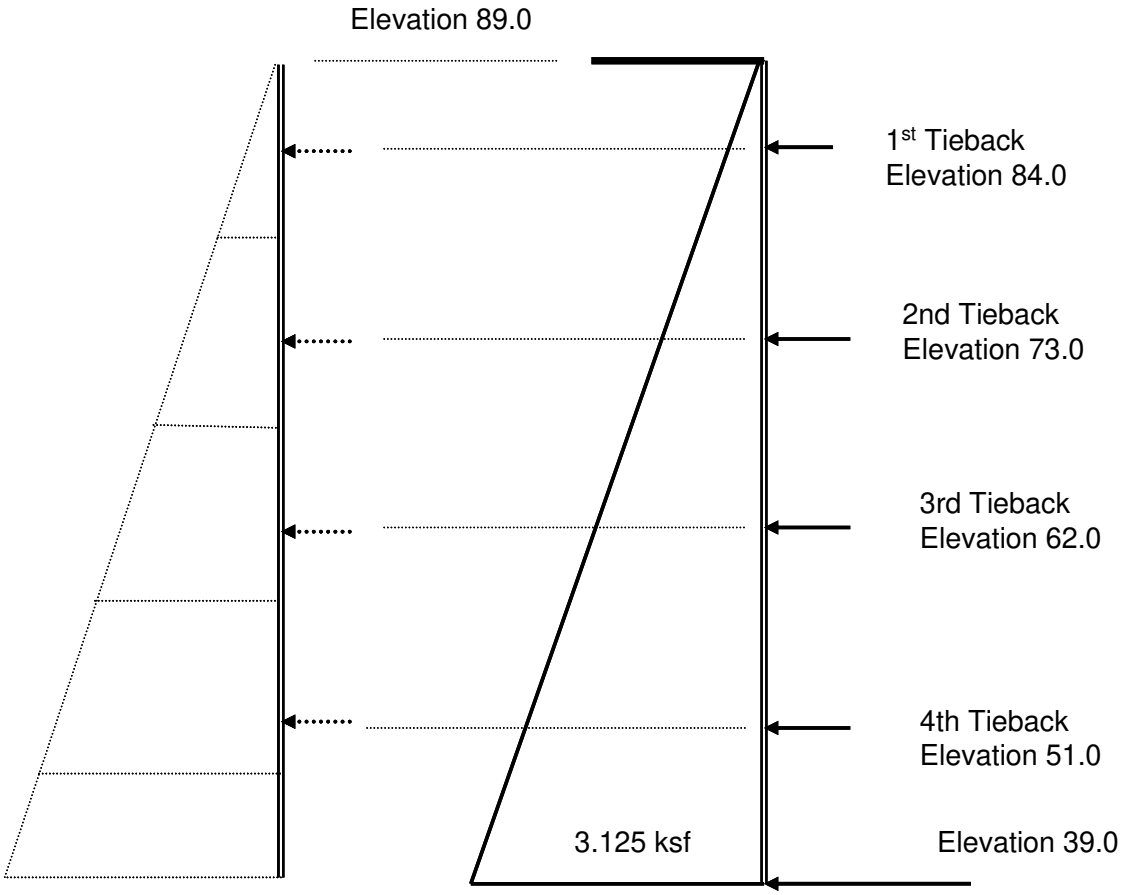

Figure A.8 Excavate to elevation 39.0 – fifth stage excavation

PROGRAM CBEAMC - ANALYSIS OF BEAM-COLUMNS WITH NONLINEAR SUPPORTS
DATE: 17-MARCH-2007 TIME: 0:21:25

****
* SUMMARY OF RESULTS *
****

I.--HEADING
'Bonneville Tieback Final Stage Excavation

II.--MAXIMA

	MAXIMUM POSITIVE	X-COORD (FT)	MAXIMUM NEGATIVE	X-COORD (FT)
AXIAL DISPLACEMENT (IN)	: 0.000E+00	0.00	0.000E+00	0.00
LATERAL DISPLACEMENT (IN)	: 4.572E-03	44.00	-4.508E-04	0.00

ROTATION (RAD)	: 7.952E-05	41.00	-1.172E-04	50.00
AXIAL FORCE (K)	: 0.000E+00	0.00	0.000E+00	0.00
SHEAR FORCE (K)	: 1.415E+01	50.00	-1.885E+01	38.00
BENDING MOMENT (K-FT)	: 3.726E+01	38.00	-3.087E+01	44.00

III.--REACTIONS AT FIXED SUPPORTS

X-C00RD	X-REACTION	Y-REACTION	MOMENT-REACTION
(FT)	(K)	(K)	(K-FT)
5.00	0.000E+00	-2.837E+00	0.000E+00
16.00	0.000E+00	-1.175E+01	0.000E+00
27.00	0.000E+00	-1.656E+01	0.000E+00
38.00	0.000E+00	-3.283E+01	0.000E+00
50.00	0.000E+00	-1.415E+01	0.000E+00

IV.--FORCES IN LINEAR CONCENTRATED SPRINGS
NONE

V.--FORCES IN NONLINEAR CONCENTRATED SPRINGS
NONE

PROGRAM CBEAMC - ANALYSIS OF BEAM-COLUMNS WITH NONLINEAR SUPPORTS
DATE: 17-MARCH-2007 TIME: 0:21:25

****
* COMPLETE RESULTS *
****

I.--HEADING
'Bonneville Tieback Final Stage Excavation

II.--DISPLACEMENTS AND INTERNAL FORCES

	<---------DISPLACEMENTS-------->			<--------INTERNAL FORCES------->		
X-COORD	AXIAL	LATERAL	ROTATION	AXIAL	SHEAR	MOMENT
(FT)	(IN)	(IN)	(RAD)	(K)	(K)	(K-FT)
0.00	0.000E+00	-4.508E-04	7.209E-06	0.000E+00	0.000E+00	0.000E+00
2.50	0.000E+00	-2.340E-04	7.304E-06	0.000E+00	1.953E-01	1.628E-01
5.00	0.000E+00	0.000E+00	8.732E-06	0.000E+00	7.812E-01	1.302E+00
5.00	0.000E+00	0.000E+00	8.732E-06	0.000E+00	-2.055E+00	1.302E+00
7.75	0.000E+00	2.727E-04	5.963E-06	0.000E+00	-9.597E-01	-2.952E+00
10.50	0.000E+00	3.207E-04	-3.317E-06	0.000E+00	6.087E-01	-3.543E+00

13.25	0.000E+00	1.030E-04	-8.012E-06	0.000E+00	2.650E+00	8.292E-01
16.00	0.000E+00	0.000E+00	6.321E-06	0.000E+00	5.163E+00	1.146E+01
16.00	0.000E+00	0.000E+00	6.321E-06	0.000E+00	-6.590E+00	1.146E+01
18.75	0.000E+00	4.665E-04	1.589E-05	0.000E+00	-3.603E+00	-2.660E+00
21.50	0.000E+00	7.699E-04	2.349E-07	0.000E+00	-1.443E-01	-7.921E+00
24.25	0.000E+00	4.726E-04	-1.616E-05	0.000E+00	3.787E+00	-3.020E+00
27.00	0.000E+00	0.000E+00	-5.477E-06	0.000E+00	8.192E+00	1.334E+01
27.00	0.000E+00	0.000E+00	-5.477E-06	0.000E+00	-8.367E+00	1.334E+01
29.75	0.000E+00	1.062E-04	4.863E-06	0.000E+00	-3.490E+00	-3.070E+00
32.50	0.000E+00	5.112E-05	-9.216E-06	0.000E+00	1.859E+00	-5.421E+00
35.25	0.000E+00	-3.556E-04	-9.861E-06	0.000E+00	7.681E+00	7.589E+00
38.00	0.000E+00	0.000E+00	4.413E-05	0.000E+00	1.398E+01	3.726E+01
38.00	0.000E+00	0.000E+00	4.413E-05	0.000E+00	-1.885E+01	3.726E+01
41.00	0.000E+00	2.610E-03	7.952E-05	0.000E+00	-1.145E+01	-8.336E+00
44.00	0.000E+00	4.572E-03	1.891E-05	0.000E+00	-3.480E+00	-3.087E+01
47.00	0.000E+00	3.622E-03	-7.062E-05	0.000E+00	5.051E+00	-2.865E+01
50.00	0.000E+00	0.000E+00	-1.172E-04	0.000E+00	1 .415E+01	1.486E-14

II.--FORCES IN LINEAR DISTRIBUTED SPRINGS
NONE

IV.--FORCES IN NONLINEAR DISTRIBUTED SPRINGS
NONE

A.3 WINKLER 1 CONSTRUCTION SEQUENCING ANALYSIS

A construction sequencing analysis using beam on elastic foundation techniques (Winkler spring analysis) was performed for the “stiff” case study tieback wall. The analysis was performed using the computer program CMULTIANC (Dawkins, 2002). Following each excavation stage of the analysis the soil load – displacement curves (R-y curves) were shifted to account for active state plastic yielding that occurs in the soil as the wall moves towards the excavation. This R-y curve shifting is necessary to assure that as the wall is pulled back into the soil by the upper ground anchor prestress force, soil pressures behind the wall immediately increase above active earth pressure. The soil springs are based on the reference deflection method per Weatherby et al, 1998. According to Weatherby, et al, 1998 these reference deflection values do not change with effective overburden pressure. For

cohesionless soils the reference displacement indicating active state first yield is 0.05 in. and the reference deflection indicating passive state first yield is 0.50 in. Ground anchors are represented as springs that are preloaded to produce a lock-off load at a wall deflection consistent with that obtained when the lock-off load is applied as a force. Several analyses were required to perform the construction sequencing analysis for all five-excavation stages. These occur internally within the CMULTIANC program and are summarized in Table A-1.

Table A.1 CMULTIANC steps used in construction sequencing analysis

Internal Analysis Step	Description
1	Develop soil springs and wall stiffness from input data and run Winker analysis to determine wall displacements and forces for the first stage excavation (excavation to elevation 78.5)
2	Shift R-y curves in locations where displacements exceed active state yielding, i.e. 0.05-in. for cohesionless soils. Rerun first stage excavation analysis with the shifted R-y curves to verify force results are consistent with Step 1.
3	Apply the Anchor 1 lock-off load (lock-off load provided as input) as a concentrated force and run the Winker analysis to determine the wall displacement at the Anchor 1 location.
4	Replace the anchor lock-off load with a concentrated anchor spring and repeat Steps 1 through 4 for the remaining excavation stages. The concentrated anchor spring is fitted to the lock-off load/wall displacement point obtained from Step 3 using the anchor spring stiffness and yield plateau information supplied as input.

The coordinate system for the CMULTIANC construction sequencing analysis is as shown in Figure A.9. The distributed soil springs representing the R-y curves are shifted at those locations where displacements from the Step 1 analysis indicate active state yielding has occurred. The analysis is rerun (Step 2) using the shifted R-y curves to assure the results are

consistent with the Step 1 analysis. In Step 3 the anchor load at lock-off (28.1 kips/ft) is applied as a concentrated force. The wall configuration for Step 3 is as shown in Figure A-10.

The displacement from the Step 3 analysis is used to establish the anchor force at a zero wall displacement. With this information, an anchor spring can be developed and inserted into the Step 4 analysis as a replacement for the Step 3 anchor force. This is illustrated in Figure A-11.

The CMULTIANC program provides results for each of the steps described in Table A-1. These results are provided for each excavation stage. The input for the analysis and the results for each excavation stage are shown below.

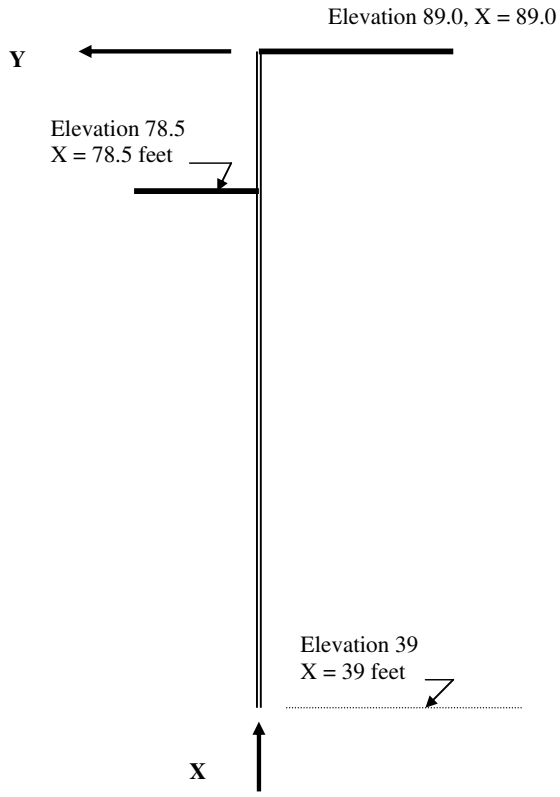

Figure A.9 Excavate to elevation 78.5 – first stage excavation

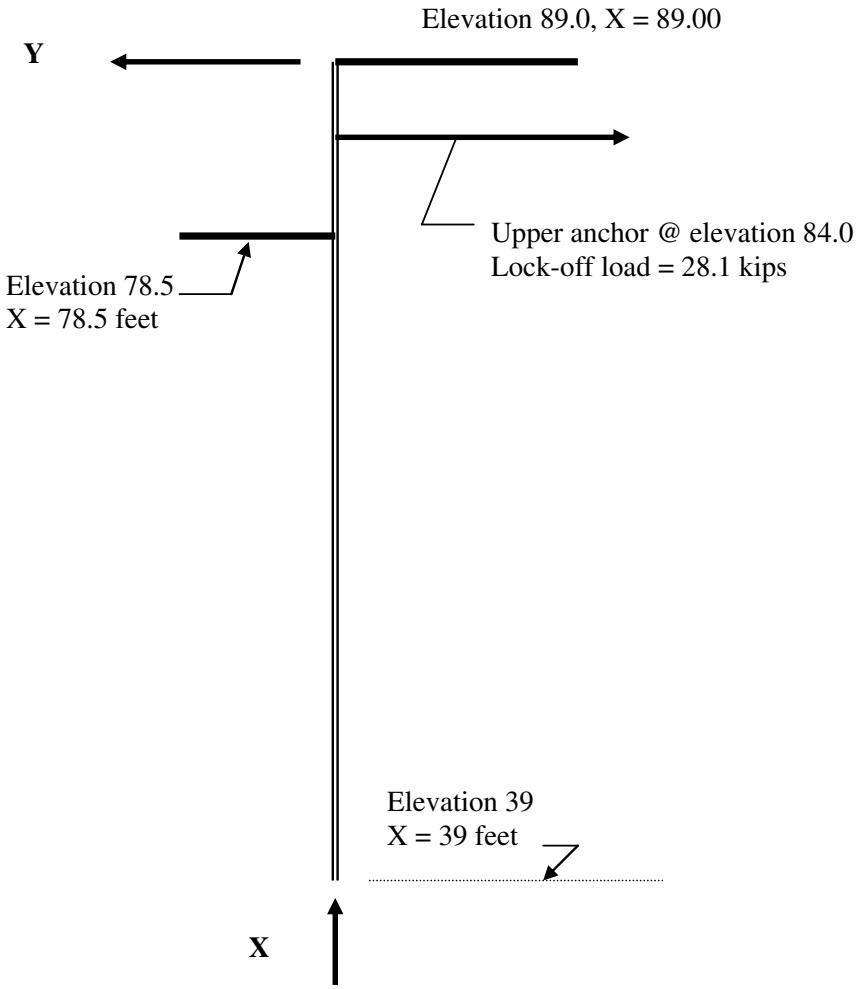

Figure A.10 Upper anchor as concentrated force

CMULTIANC: SIMULATION OF CONSTRUCTION SEQUENCE FOR STIFF WALL SYSTEMS
WITH MULTIPLE LEVELS OF ANCHORS
DATE: 14-MARCH-2007 TIME: 16:14:52

****
* RESULTS FOR INITIAL SSI CURVES *
****

I.--HEADING
'BONNEVILLE TIEBACK WALL

SOIL PRESSURES DETERMINED BY COULOMB COEFFICIENTS
AND THEORY OF ELASTICITY EQUATIONS FOR SURCHARGE LOADS.

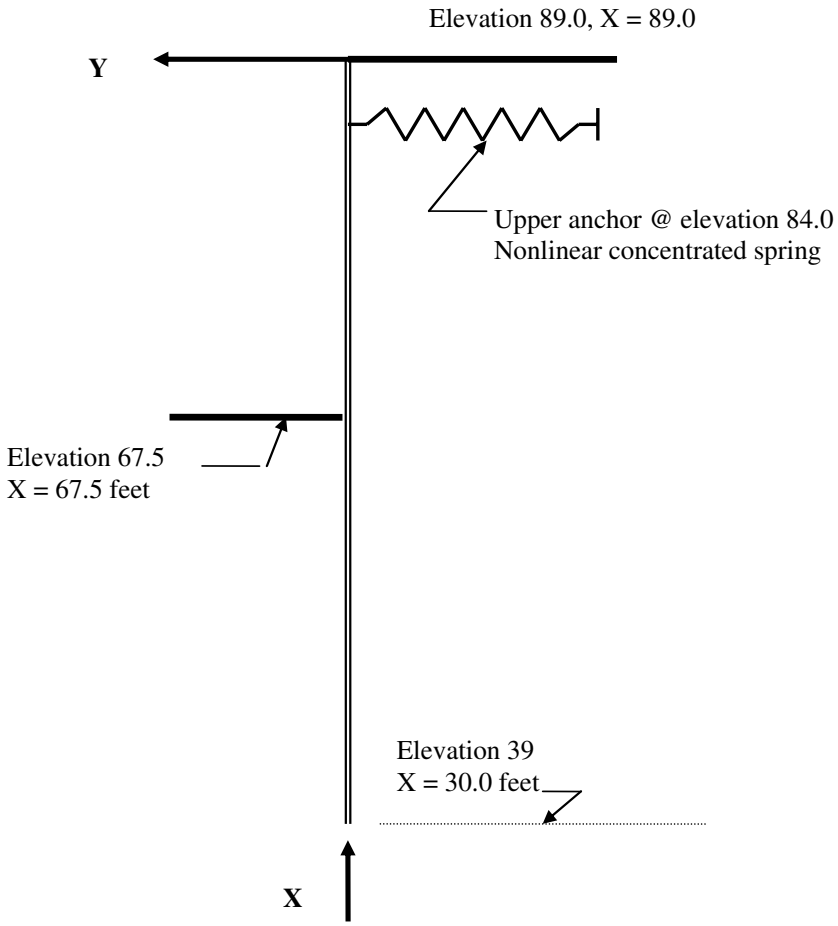

Figure A.11 Excavate to elevation 67.5 and anchor modeled as nonlinear concentrated spring

II.--MAXIMA

	MAXIMUM	MINIMUM
DEFLECTION (FT)	: 1.729E-02	0.000E+00
AT ELEVATION (FT)	89.00	39.00
BENDING MOMENT (LB-FT)	: 3.516E+04	-7.420E+03
AT ELEVATION (FT)	: 67.00	44.00
SHEAR (LB)	: 3557.44	-2708.90
AT ELEVATION (FT)	: 39.00	56.50
RIGHTSIDE SOIL PRESSURE (PSF)	: 4625.15	
AT ELEVATION (FT)	: 39.00	
LEFTSIDE SOIL PRESSURE (PSF)	: 607.62	
AT ELEVATION (FT)	: 9.00	

III.--ANCHOR FORCES

ELEVATION AT ANCHOR (FT)	ANCHOR STATUS	TOTAL ANCHOR FORCE (LB)
84.00	INACTIVE	
73.00	INACTIVE	
62.00	INACTIVE	
51.00	INACTIVE	

IV.--COMPLETE RESULTS

ELEV. (FT)	DEFLECTION (FT)	SHEAR FORCE (LB)	BENDING MOMENT (LB-FT)	<-SOIL PRESS. (PSF)-> LEFT	RIGHT
89.00	1.729E-02	0.00	0.00	0.00	0.00
88.00	1.662E-02	20.83	6.94	0.00	41.67
87.00	1.595E-02	83.33	55.56	0.00	83.33
86.00	1.528E-02	187.50	187.50	0.00	125.00
85.00	1.461E-02	333.33	444.44	0.00	166.67
84.00	1.395E-02	520.83	868.06	0.00	208.33
83.00	1.328E-02	750.00	1500.00	0.00	250.00
82.00	1.262E-02	1020.83	2381.94	0.00	291.67
81.00	1.195E-02	1333.33	3555.56	0.00	333.33
80.00	1.129E-02	1687.50	5062.50	0.00	375.00
79.00	1.064E-02	2083.33	6944.44	0.00	416.67
78.00	9.991E-03	2520.83	9243.06	0.00	458.33
77.00	9.352E-03	2895.40	11964.27	206.60	500.00
76.00	8.724E-03	3112.72	14978.88	397.87	541.67
75.00	8.110E-03	3187.86	18137.28	574.34	583.33
74.00	7.513E-03	3135.32	21304.68	736.65	625.00
73.00	6.936E-03	2968.85	24360.43	885.61	666.67
72.00	6.381E-03	2701.34	27197.23	1022.15	708.33
71.00	5.852E-03	2344.69	29720.21	1147.34	750.00
70.00	5.351E-03	1909.67	31845.85	1262.32	791.67
69.00	4.880E-03	1405.88	33500.84	1368.34	833.33
68.00	4.439E-03	841.66	34620.83	1466.66	875.00
67.50	4.231E-03	539.26	34965.51	1513.34	895.83
67.00	4.031E-03	233.31	35155.82	1558.58	952.98
66.00	3.656E-03	-342.91	35069.93	1645.34	1101.56
65.00	3.314E-03	-855.40	34440.26	1728.14	1249.73
64.00	3.004E-03	-1301.68	33332.18	1808.08	1396.44
63.00	2.724E-03	-1681.27	31812.47	1886.13	1540.86
62.00	2.475E-03	-1995.35	29947.48	1963.17	1682.31

61.00	2.253E-03	-2246.50	27801.64	2039.93	1820.29
60.00	2.058E-03	-2438.36	25436.15	2116.98	1954.49
59.00	1.886E-03	-2575.30	22908.19	2194.76	2084.76
58.00	1.736E-03	-2662.14	20270.21	2273.59	2211.13
57.00	1.604E-03	-2703.82	17569.79	2353.59	2333.77
56.50	1.545E-03	-2708.90	16214.58	2394.05	2393.78
56.00	1.489E-03	-2704.48	14859.31	2434.80	2453.00
55.00	1.388E-03	-2669.71	12157.88	2517.10	2569.27
54.00	1.298E-03	-2602.56	9508.61	2600.27	2683.14
53.00	1.218E-03	-2505.79	6942.20	2683.97	2795.30
52.00	1.143E-03	-2381.06	4487.13	2767.76	2906.49
51.00	1.073E-03	-2228.78	2170.78	2851.13	3017.53
50.00	1.005E-03	-2047.94	20.84	2933.48	3129.31
49.00	9.372E-04	-1836.05	-1933.28	3014.20	3242.72
48.00	8.675E-04	-1589.04	-3658.88	3092.61	3358.68
47.00	7.944E-04	-1301.28	-5118.42	3168.04	3478.07
46.00	7.165E-04	-965.63	-6267.92	3239.83	3601.73
45.00	6.328E-04	-573.51	-7055.51	3307.39	3730.41
44.00	5.426E-04	-115.10	-7420.09	3370.19	3864.72
43.00	4.455E-04	420.37	-7290.13	3427.87	4005.08
42.00	3.418E-04	1044.29	-6582.96	3480.21	4151.67
41.00	2.319E-04	1768.09	-5204.34	3527.30	4304.33
40.00	1.173E-04	2602.65	-3048.68	3569.50	4462.52
39.00	0.000E+00	3557.44	0.00	3607.62	4625.15

CMULTIANC: SIMULATION OF CONSTRUCTION SEQUENCE FOR STIFF WALL SYSTEMS
WITH MULTIPLE LEVELS OF ANCHORS
DATE: 14-MARCH-2007 TIME: 16:15:06

****
* RESULTS AFTER EXCAVATE TO EL 67.5 *
****

I.--HEADING
'BONNEVILLE TIEBACK WALL

II.--MAXIMA

	MAXIMUM	MINIMUM
DEFLECTION (FT)	: 7.613E-03	-2.124E-02
AT ELEVATION (FT)	: 63.00	89.00
BENDING MOMENT (LB-FT)	: 9.215E+03	-1.150E+05

AT ELEVATION (FT)	:	84.00	73.00
SHEAR (LB)	:	7529.41	-22954.21
AT ELEVATION (FT)	:	61.00	84.00
RIGHTSIDE SOIL PRESSURE (PSF)	:	4625.15	
AT ELEVATION (FT)	:	39.00	
LEFTSIDE SOIL PRESSURE (PSF)	:	2746.80	
AT ELEVATION (FT)	:	43.00	

III.--ANCHOR FORCES

ELEVATION AT ANCHOR (FT)	ANCHOR STATUS (LB)	TOTAL ANCHOR FORCE*
84.00	ACTIVE	359415
73.00	INACTIVE	
62.00	INACTIVE	
51.00	INACTIVE	

* ALONG ANCHOR LINE OF ACTION

IV.--COMPLETE RESULTS

ELEV. (FT)	DEFLECTION (FT)	SHEAR FORCE (LB)	BENDING MOMENT (LB-FT)	<-SOIL PRESS. (PSF)-> LEFT	RIGHT
89.00	-2.124E-02	0.00	0.00	0.00	0.00
88.00	-1.954E-02	246.23	85.29	0.00	482.82
87.00	-1.784E-02	946.35	653.41	0.00	907.77
86.00	-1.613E-02	2042.46	2129.29	0.00	1274.81
85.00	-1.443E-02	3476.63	4879.98	0.00	1583.87
84.00	-1.271E-02	5190.76	9214.54	0.00	1834.72
84.00	-1.271E-02	-22954.21	9214.54	0.00	1834.72
83.00	-1.100E-02	-21018.38	-12761.15	0.00	2027.25
82.00	-9.293E-03	-18918.56	-32709.60	0.00	2162.76
81.00	-7.619E-03	-16710.61	-50495.28	0.00	2243.63
80.00	-5.992E-03	-14447.64	-66037.32	0.00	2273.00
79.00	-4.426E-03	-12179.31	-79306.37	0.00	2254.64
78.00	-2.934E-03	-9951.19	-90320.78	0.00	2192.89
77.00	-1.526E-03	-7804.33	99142.30	0.00	2092.51
76.00	-2.099E-04	-5774.82	-105871.32	0.00	1958.61

75.00	1.007E-03	-3893.52	-110641.72	0.00	1796.54
74.00	2.121E-03	-2185.87	-113615.58	0.00	1611.79
73.00	3.128E-03	-671.82	-114977.65	0.00	1409.88
72.00	4.029E-03	634.22	-114929.84	0.00	1196.27
71.00	4.822E-03	1723.20	-113685.76	0.00	976.31
70.00	5.509E-03	2609.28	-111465.37	0.00	791.67
69.00	6.091E-03	3421.78	-108453.31	0.00	833.33
68.00	6.573E-03	4275.95	-104607.91	0.00	875.00
67.50	6.777E-03	4718.66	-102359.70	0.00	895.83
67.00	6.957E-03	5149.70	-99891.17	88.69	916.67
66.00	7.247E-03	5907.76	-94350.10	271.38	958.33
65.00	7.449E-03	6522.40	-88122.08	458.48	1000.00
64.00	7.569E-03	6990.75	-81352.53	646.99	1041.67
63.00	7.613E-03	7312.72	-74188.31	834.25	1083.33
62.00	7.588E-03	7490.74	-66775.00	1017.93	1125.00
61.00	7.500E-03	7529.41	-59254.63	1196.04	1166.67
60.00	7.357E-03	7435.12	-51763.64	1366.94	1208.33
59.00	7.165E-03	7215.77	-44431.25	1529.31	1250.00
58.00	6.932E-03	6880.38	-37378.17	1682.19	1291.67
57.00	6.663E-03	6438.80	-30715.62	1824.88	1333.33
56.50	6.518E-03	6181.31	-27560.41	1892.27	1354.17
56.00	6.366E-03	5901.21	-24539.74	1956.99	1375.00
55.00	6.046E-03	5278.73	-18950.94	2078.33	1416.67
54.00	5.708E-03	4581.92	-14023.80	2188.93	1458.33
53.00	5.357E-03	3821.44	-9827.26	2288.94	1500.00
52.00	4.996E-03	3007.76	-6419.66	2378.61	1541.67
51.00	4.629E-03	2151.08	-3849.00	2458.25	1583.33
50.00	4.259E-03	1261.30	-2153.27	2528.15	1625.00
49.00	3.886E-03	415.85	-1360.68	2588.52	1803.43
48.00	3.512E-03	-280.17	-1353.18	2639.47	2035.58
47.00	3.137E-03	-785.34	-1949.58	2680.96	2277.56
46.00	2.760E-03	-1080.13	-2949.38	2712.79	2529.68
45.00	2.380E-03	-1144.30	-4132.28	2734.65	2792.50
44.00	1.996E-03	-956.64	-5257.33	2746.13	3066.71
43.00	1.607E-03	-494.82	-6061.81	2746.80	3353.02
42.00	1.213E-03	264.58	-6260.05	2736.24	3652.02
41.00	8.131E-04	1345.72	-5542.52	2714.21	3963.98
40.00	4.081E-04	2772.92	-3575.22	680.75	4288.68
39.00	0.000E+00	4569.63	0.00	2636.34	4625.15

CMULTIANC: SIMULATION OF CONSTRUCTION SEQUENCE FOR STIFF WALL SYSTEMS

WITH MULTIPLE LEVELS OF ANCHORS

DATE: 14-MARCH-2007 TIME: 16:15:13

****
* RESULTS AFTER EXCAVATE TO EL 56.5 *
****

I.--HEADING
'BONNEVILLE TIEBACK WALL

II.--MAXIMA

	MAXIMUM	MINIMUM
DEFLECTION (FT)	1.393E-02	-3.318E-02
AT ELEVATION (FT)	56.50	89.00
BENDING MOMENT (LB-FT)	1.188E+04	-1.381E+05
AT ELEVATION (FT)	84.00	59.00
SHEAR (LB)	12389.65	-20770.56
AT ELEVATION (FT)	39.00	84.00
RIGHTSIDE SOIL PRESSURE (PSF)	4625.15	
AT ELEVATION (FT)	39.00	
LEFTSIDE SOIL PRESSURE (PSF)	2039.47	
AT ELEVATION (FT)	44.00	

III.--ANCHOR FORCES

ELEVATION AT ANCHOR (FT)	TOTAL ANCHOR STATUS	ANCHOR FORCE* (LB)
84.00	ACTIVE	351874
73.00	ACTIVE	361234
62.00	INACTIVE	
51.00	INACTIVE	

* ALONG ANCHOR LINE OF ACTION

IV.--COMPLETE RESULTS

ELEV. (FT)	DEFLECTION (FT)	SHEAR FORCE (LB)	BENDING MOMENT (LB-FT)	<-SOIL PRESS. (PSF)-> LEFT	RIGHT
89.00	-3.318E-02	0.00	0.00	0.00	0.00
88.00	-3.109E-02	300.43	100.14	0.00	600.87

87.00	-2.900E-02	1192.79	801.16	0.00	1180.28
86.00	-2.692E-02	2623.33	2682.44	0.00	1669.60
85.00	-2.483E-02	4509.53	6233.33	0.00	2091.58
84.00	-2.273E-02	6783.91	11875.79	0.00	2445.94
84.00	-2.273E-02	-20770.56	11875.79	0.00	2445.94
83.00	-2.063E-02	-18175.74	-7590.26	0.00	2732.43
82.00	-1.853E-02	-15327.90	-24323.89	0.00	2952.03
81.00	-1.646E-02	-12292.98	-38105.48	0.00	3106.67
80.00	-1.442E-02	-9134.78	-48780.41	0.00	3198.76
79.00	-1.243E-02	-5914.46	-56256.57	0.00	3231.12
78.00	-1.049E-02	-2690.27	-60501.62	0.00	3206.73
77.00	-8.603E-03	482.56	-61539.93	0.00	3128.65
76.00	-6.774E-03	3551.78	-59449.60	0.00	2999.81
75.00	-5.001E-03	6467.95	-54359.46	0.00	2822.84
74.00	-3.279E-03	9184.07	-46446.48	0.00	2599.96
73.00	-1.599E-03	11655.02	-35933.54	0.00	2332.76
73.00	-1.599E-03	-16632.37	-35933.54	0.00	2332.76
72.00	4.269E-05	-14450.01	-51375.23	0.00	2023.03
71.00	1.637E-03	-12596.30	-64793.89	0.00	1675.76
70.00	3.171E-03	-11105.73	-76536.79	0.00	1297.10
69.00	4.633E-03	-10006.51	-86982.59	0.00	893.46
68.00	6.014E-03	-9121.78	-96534.93	0.00	875.00
67.50	6.672E-03	-8679.07	-100985.58	0.00	895.83
67.00	7.306E-03	-8225.95	-105212.27	0.00	916.67
66.00	8.498E-03	-7288.45	-112972.94	0.00	958.33
65.00	9.586E-03	-6309.28	-119775.28	0.00	1000.00
64.00	1.056E-02	-5288.45	-125577.61	0.00	1041.67
63.00	1.142E-02	-4225.95	-130338.29	0.00	1083.33
62.00	1.216E-02	-3121.78	-134015.62	0.00	1125.00
61.00	1.277E-02	-1975.95	-136567.96	0.00	1166.67
60.00	1.325E-02	-788.45	-137953.64	0.00	1208.33
59.00	1.361E-02	440.72	-138130.97	0.00	1250.00
58.00	1.383E-02	1711.55	-137058.31	0.00	1291.67
57.00	1.393E-02	3024.05	-134693.98	0.00	1333.33
56.50	1.393E-02	3695.93	-133014.42	0.00	1354.17
56.00	1.390E-02	4345.44	-131001.79	131.05	1375.00
55.00	1.375E-02	5480.24	-126071.12	390.41	1416.67
54.00	1.348E-02	6400.74	-120114.19	642.50	1458.33
53.00	1.310E-02	7116.24	-113341.43	883.27	1500.00
52.00	1.262E-02	639.99	-105951.93	1108.93	1541.67
51.00	1.203E-02	7988.79	-98129.70	1316.09	1583.33
50.00	1.135E-02	8182.68	-90040.23	1501.70	1625.00
49.00	1.059E-02	8244.58	-81827.46	1663.08	1666.67
48.00	9.755E-03	8199.86	-73611.10	1797.95	1708.33
47.00	8.849E-03	8076.01	-65484.35	1904.40	1750.00
46.00	7.881E-03	7902.24	-57512.00	1980.88	1791.67

45.00	6.859E-03	7709.13	-49728.87	2026.19	1833.33
44.00	5.791E-03	7528.29	-42138.59	2039.47	1875.00
43.00	4.683E-03	7392.04	-34712.78	2020.20	1916.67
42.00	3.543E-03	7510.50	-27390.50	1968.15	2315.77
41.00	2.378E-03	8261.68	-19720.61	1883.44	3047.68
40.00	1.194E-03	9865.16	-10886.48	1766.62	3818.96
39.00	0.000E+00	12389.65	0.00	1618.80	4625.15

CMULTIANC: SIMULATION OF CONSTRUCTION SEQUENCE FOR STIFF WALL SYSTEMS
WITH MULTIPLE LEVELS OF ANCHORS
DATE: 14-MARCH-2007 TIME: 16:15:20

****
* RESULTS AFTER EXCAVATE TO EL 45 *
****

I.--HEADING
'BONNEVILLE TIEBACK WALL

II.--MAXIMA

		MAXIMUM	MINIMUM
DEFLECTION (FT)	:	7.901E-03	-2.993E-02
AT ELEVATION (FT)	:	52.00	89.00
BENDING MOMENT (LB-FT)	:	1.148E+04	-1.146E+05
AT ELEVATION (FT)	:	84.00	50.00
SHEAR (LB)	:	24056.37	-21023.75
AT ELEVATION (FT)	:	39.00	84.00
RIGHTSIDE SOIL PRESSURE (PSF)	:	4625.15	
AT ELEVATION (FT)	:	39.00	
LEFTSIDE SOIL PRESSURE (PSF)	:	555.02	
AT ELEVATION (FT)	:	39.00	

III.--ANCHOR FORCES

ELEVATION AT ANCHOR (FT)	TOTAL ANCHOR STATUS (LB)	ANCHOR FORCE*
84.00	ACTIVE	352426

73.00	ACTIVE	357590
62.00	ACTIVE	360206
51.00	INACTIVE	

* ALONG ANCHOR LINE OF ACTION

IV.--COMPLETE RESULTS

ELEV. (FT)	DEFLECTION (FT)	SHEAR FORCE (LB)	BENDING MOMENT (LB-FT)	<-SOIL PRESS. (PSF)-> LEFT	RIGHT
89.00	-2.993E-02	0.00	0.00	0.00	0.00
88.00	-2.835E-02	296.90	100.14	0.00	590.28
87.00	-2.676E-02	1159.43	790.57	0.00	1125.62
86.00	-2.518E-02	2529.82	2606.62	0.00	1606.00
85.00	-2.359E-02	4353.05	6028.66	0.00	2031.29
84.00	-2.200E-02	6573.91	11482.00	0.00	2401.23
84.00	-2.200E-02	-21023.75	11482.00	0.00	2401.23
83.00	-2.040E-02	-18460.74	-8261.10	0.00	2715.58
82.00	-1.881E-02	-15610.67	-25288.61	0.00	2975.38
81.00	-1.724E-02	-12527.15	-39340.75	0.00	3182.57
80.00	-1.571E-02	-9261.57	-50210.31	0.00	3339.66
79.00	-1.422E-02	-5862.64	-57740.20	0.00	3449.51
78.00	-1.279E-02	-2376.07	-61820.59	0.00	3515.16
77.00	-1.141E-02	1155.46	-62385.82	0.00	3539.69
76.00	-1.009E-02	4692.26	-59411.36	0.00	3526.00
75.00	-8.829E-03	8197.39	-52910.88	0.00	3476.62
74.00	-7.615E-03	11636.14	-42933.79	0.00	3393.50
73.00	-6.440E-03	14975.35	-29563.20	0.00	3277.81
73.00	-6.440E-03	-13026.72	-29563.20	0.00	3277.81
72.00	-5.297E-03	-9819.05	-40916.87	0.00	3130.63
71.00	-4.192E-03	-6772.46	-49139.91	0.00	2955.90
70.00	-3.132E-03	-3912.20	-54407.06	0.00	2758.28
69.00	-2.123E-03	-1258.99	-56915.93	0.00	2542.12
68.00	-1.167E-03	1170.60	-56882.67	0.00	2311.38
67.50	-7.085E-04	2296.70	-56006.15	0.00	2191.63
67.00	-2.633E-04	3371.30	-54581.73	0.00	2105.75
66.00	5.894E-04	5406.99	-50141.60	0.00	1962.18
65.00	1.396E-03	7295.44	-43739.30	0.00	1811.44
64.00	2.161E-03	9029.43	-35525.56	0.00	1653.42
63.00	2.894E-03	10601.22	-25658.40	0.00	1487.19
62.00	3.602E-03	12001.71	-14304.05	0.00	1310.90
62.00	3.602E-03	-16205.21	-14304.05	0.00	1310.90
61.00	4.294E-03	-14965.28	-29845.72	0.00	1166.67

60.00	4.957E-03	-13777.78	-44220.72	0.00	1208.33
59.00	5.579E-03	-12548.61	-57387.39	0.00	1250.00
58.00	6.148E-03	-11277.78	-69304.06	0.00	1291.67
57.00	6.652E-03	-9965.28	-79929.06	0.00	1333.33
56.50	6.877E-03	-9293.40	-84744.17	0.00	1354.17
56.00	7.082E-03	-8611.11	-89220.73	0.00	1375.00
55.00	7.428E-03	-7215.28	-97137.40	0.00	1416.67
54.00	7.684E-03	-5777.78	-103637.40	0.00	1458.33
53.00	7.843E-03	-4298.61	-108679.07	0.00	1500.00
52.00	7.901E-03	-2777.78	-112220.74	0.00	1541.67
51.00	7.853E-03	-1215.28	-114220.74	0.00	1583.33
50.00	7.700E-03	388.89	-114637.41	0.00	1625.00
49.00	7.439E-03	2034.72	-113429.08	0.00	1666.67
48.00	7.073E-03	3722.22	-110554.08	0.00	1708.33
47.00	6.603E-03	5451.39	-105970.75	0.00	1750.00
46.00	6.034E-03	7222.22	-99637.42	0.00	1791.67
45.00	5.373E-03	9034.72	-91512.42	0.00	1833.33
44.00	4.626E-03	10812.89	-81580.43	148.95	1875.00
43.00	3.804E-03	12594.78	-69922.40	277.82	2120.36
42.00	2.916E-03	14658.10	-56421.82	384.24	2675.57
41.00	1.976E-03	17208.29	-40629.91	466.43	3283.13
40.00	9.979E-04	20319.01	-22021.31	523.39	3936.09
39.00	0.000E+00	24056.37	0.00	555.02	4625.15

CMULTIANC: SIMULATION OF CONSTRUCTION SEQUENCE FOR STIFF WALL SYSTEMS WITH MULTIPLE LEVELS OF ANCHORS

DATE: 14-MARCH-2007 TIME: 16:15:27

****
* RESULTS AFTER EXCAVATE TO EL 40 *
****

I.--HEADING
'BONNEVILLE TIEBACK WALL

II.--MAXIMA

	MAXIMUM	MINIMUM
DEFLECTION (FT)	: 2.631E-03	-2.763E-02
AT ELEVATION (FT)	: 50.00	89.00
BENDING MOMENT (LB-FT)	: 1.100E+04	-6.969E+04

AT ELEVATION (FT)	:	84.00	68.00
SHEAR (LB)	:	21826.89	-21383.59
AT ELEVATION (FT)	:	39.00	84.00
RIGHTSIDE SOIL PRESSURE (PSF)	:	4625.15	
AT ELEVATION (FT)	:	39.00	
LEFTSIDE SOIL PRESSURE (PSF)	:	92.50	
AT ELEVATION (FT)	:	39.00	

III.--ANCHOR FORCES

ELEVATION AT ANCHOR (FT)	TOTAL ANCHOR STATUS (LB)	ANCHOR FORCE*
84.00	ACTIVE	353576
73.00	ACTIVE	357332
62.00	ACTIVE	357799
51.00	ACTIVE	358835

* ALONG ANCHOR LINE OF ACTION

IV.--COMPLETE RESULTS

ELEV. (FT)	DEFLECTION (FT)	SHEAR FORCE (LB)	BENDING MOMENT (LB-FT)	<-SOIL PRESS. (PSF)-> LEFT	RIGHT
89.00	-2.763E-02	0.00	0.00	0.00	0.00
88.00	-2.620E-02	286.29	98.27	0.00	564.05
87.00	-2.477E-02	1111.06	760.60	0.00	1076.96
86.00	-2.334E-02	2423.14	2499.88	0.00	1538.68
85.00	-2.191E-02	4171.31	5777.84	0.00	1949.11
84.00	-2.047E-02	6304.14	11004.92	0.00	2308.00
84.00	-2.047E-02	-21383.59	11004.92	0.00	2308.00
83.00	-1.903E-02	-18917.74	-9147.74	0.00	2615.12
82.00	-1.759E-02	-16170.12	-26685.28	0.00	2871.58
81.00	-1.618E-02	-13190.42	-41351.24	0.00	3079.39
80.00	-1.481E-02	-10026.01	-52937.81	0.00	3241.16
79.00	-1.348E-02	-6721.46	-61283.22	0.00	3359.90
78.00	-1.222E-02	-3318.18	-66268.73	0.00	3438.87
77.00	-1.101E-02	145.70	-67815.37	0.00	3481.38
76.00	-9.869E-03	3635.31	-65880.63	0.00	3490.63

75.00	-8.787E-03	7118.82	-60455.25	0.00	3469.50
74.00	-7.762E-03	10567.04	-51560.37	0.00	3420.34
73.00	-6.783E-03	13952.77	-39245.15	0.00	3344.78
73.00	-6.783E-03	-14029.09	-39245.15	0.00	3344.78
72.00	-5.846E-03	-10731.46	-51567.01	0.00	3244.40
71.00	-4.956E-03	-7544.53	-60644.46	0.00	3123.68
70.00	-4.123E-03	-4486.08	-66598.23	0.00	2987.80
69.00	-3.351E-03	-1568.81	-69564.20	0.00	2841.69
68.00	-2.644E-03	1199.27	-69688.48	0.00	2689.80
67.50	-2.315E-03	2525.22	-68749.96	0.00	2612.92
67.00	-2.001E-03	3821.71	-67158.20	0.00	2572.30
66.00	-1.422E-03	6372.30	-62030.85	0.00	2526.52
65.00	-8.995E-04	8878.36	-54376.99	0.00	2483.47
64.00	-4.278E-04	11342.59	-44239.65	0.00	2443.07
63.00	2.869E-06	13767.08	-31659.23	0.00	2404.17
62.00	4.043E-04	16152.18	-16674.66	0.00	2364.38
62.00	4.043E-04	-11866.27	-16674.66	0.00	2364.38
61.00	7.862E-04	-9522.55	-27344.14	0.00	2321.50
60.00	1.143E-03	-7221.97	-35692.12	0.00	2278.22
59.00	1.466E-03	-4963.04	-41761.88	0.00	2238.32
58.00	1.751E-03	-2740.72	-45593.33	0.00	2205.17
57.00	1.994E-03	-546.85	-47219.60	0.00	2181.57
56.50	2.099E-03	542.11	-47218.91	0.00	2174.08
56.00	2.193E-03	1628.11	-46674.70	0.00	2169.73
55.00	2.348E-03	3798.81	-43950.77	0.00	2171.04
54.00	2.463E-03	5977.55	-39055.79	0.00	2185.96
53.00	2.541E-03	8177.67	-31974.86	0.00	2213.98
52.00	2.590E-03	10411.48	-22679.94	0.00	2253.43
51.00	2.618E-03	12688.93	-11131.60	0.00	2301.36
51.00	2.618E-03	-15410.65	-11131.60	0.00	2301.36
50.00	2.631E-03	-13082.21	-25381.48	0.00	2355.48
49.00	2.622E-03	-10694.16	-37275.89	0.00	2420.67
48.00	2.577E-03	-8232.24	-46749.63	0.00	2503.35
47.00	2.490E-03	-5676.09	-53720.02	0.00	2609.32
46.00	2.352E-03	-2999.93	- 58081.09	0.00	2743.57
45.00	2.161E-03	-173.48	-59698.60	0.00	2910.11
44.00	1.914E-03	2836.94	-58406.00	0.00	3111.72
43.00	1.613E-03	6067.06	-54001.68	0.00	3349.74
42.00	1.262E-03	9553.10	-46247.61	0.00	3623.77
41.00	8.688E-04	3329.87	34869.77	0.00	3931.36
40.00	4.432E-04	17428.53	-19560.57	0.00	4267.69
39.00	0.000E+00	21826.89	0.00	92.50	4625.15

APPENDIX B

HARDENING SOIL MODEL PARAMETER CALIBRATION FROM TRIAXIAL TESTS

Recent advances in computer technology and increased computational power have led to numerical codes that use the Finite Element Method (FEMT) in the field of geotechnical engineering. The behavior of soils is implemented in these codes by means of constitutive model. These models are usually derived based on empirical relationships that are fitted to a laboratory soil test or theoretical soil mechanics. In order to incorporate a constitutive model to a specific soil, set of soil parameters relating to the model must be input into the code. The accuracy of the computed FEM results depends to a great extent on the accuracy of the soil input parameters used to characterize the constitutive model.

As mentioned in Chapter 5, a single series of Isotropic Consolidated-Drained (ICD) triaxial testing of the weigle slide block material was performed. The results of triaxial tests performed on two specimens of the weigle slide block were reported. These results were used to calibrate the HS parameters used to model the stress-stress behavior of the weigle slide block. A summary of the process used to calibrate the HS model constitutive parameters for the weigle slide block is presented.

First, values of deviator stress ($\sigma_1 - \sigma_3$) versus axial strain and volumetric strain versus axial strain were scaled off from the test report plots and new plots were developed based on these scaled values. Shear strength parameters angle of internal friction and cohesion were determined from Mohr's circles. The Mohr's circles were constructed based on the effective confining pressure and the maximum deviator stresses $(\sigma_1 - \sigma_3)_{max}$.

Second, compute the triaxial stiffness at 50 percent of the strength (E_{50}) . Recalling that the HS model has a hyperbolic relationship between the axial strain and the deviator stress and thus an initial triaxial stiffness E_o is difficult to measure and is it common to use E_{50} (refer to Figure 3.6). The stiffness E_{50} is a secant modulus and it was determined from a secant line drawn between the origin and the point on the stress strain curve corresponding to 50 percent of the maximum deviator stress $(\sigma_1 - \sigma_3)_{max}$. The resulting values of E_{50} for the two tests were 242,857 psf and 778,181 psf.

Third, computed the Plaxis input reference stiffness parameter E_{50}^{ref} . The general equation for computing E_{50} based on the confining stress for primary loading is given by the equation:

$$E_{50} = E_{50}^{ref}\left(\frac{c\cdot\cos(\phi)-\sigma_3\cdot\sin(\phi)}{c\cdot\cos(\phi)+p^{ref}\cdot\sin(\phi)}\right)^m \qquad \text{Equation B.1}$$

where E_{50}^{ref} is a reference stiffness modulus corresponding to the reference confining pressure p^{ref} and *m* is the exponent for controlling the amount of stress dependency. With the values of E_{50} and the following parameters from the ICD triaxial tests, values for E_{50}^{ref} can be computed.

Given:

$\phi 1 := 37.7\cdot deg$ $\phi 2 := 37.7\cdot deg$

$c1 := 120$ $c2 := 120$

$\sigma 1_3 := 2000$ $\sigma 2_3 := 8000$

$pref2 := 2116$ $pref1 := 2116$

$E1_{50} := 242857$ $E2_{50} := 778181$

$$E1_{50} = E_{50}^{ref}\left(\frac{c1\cdot\cos(\phi1)-\sigma1_3\cdot\sin(\phi1)}{c1\cdot\cos(\phi1)+pref1\cdot\sin(\phi1)}\right)^m$$

$$242{,}857 = E_{50}^{ref}(0.94)^m$$

$$E1_{50} = E_{50}^{ref}\left(\frac{c2\cdot\cos(\phi2)-\sigma2_3\cdot\sin(\phi2)}{c2\cdot\cos(\phi2)+pref2\cdot\sin(\phi2)}\right)^m$$

$$778{,}181 = E_{50}^{ref}(4.0)^m$$

$c1 := 242857$ $c2 := 0.94$ $c3 := 778181$ $c4 := 4.0$

$$A := \begin{bmatrix} 1 & \log(c2) \\ 1 & \log(c4) \end{bmatrix} \qquad B := \begin{bmatrix} \log(c1) \\ \log(c3) \end{bmatrix}$$

$$\text{lsolve}(A, B) = \begin{bmatrix} 5.407 \\ 0.804 \end{bmatrix}$$

$10^{5.407} = 2.553\cdot10^5$

The computed value for the reference stiffness E_{50}^{ref} was 255,300 psf and the exponent for controlling the amount of stress dependency *m* was 0.8. These values were used in Plaxis triaxial test simulation to calibrate the HS model parameters for the weigle slide block.

A triaxial test was modeled in Plaxis by means of geometry of unit dimensions (1ft x 1ft) as shown in Figure B.1. These dimensions are unrealistic, but they were selected based on simplicity of the model. The dimensions of the model do not influence the results, provided the soil weight in not taken into account. The simulation of the initial confining pressure was done by applying distributed loads equal to the principal stress σ_1' (load A) and principal stress σ_3' (load B) for the initial stage construction phase. For subsequent construction phases,

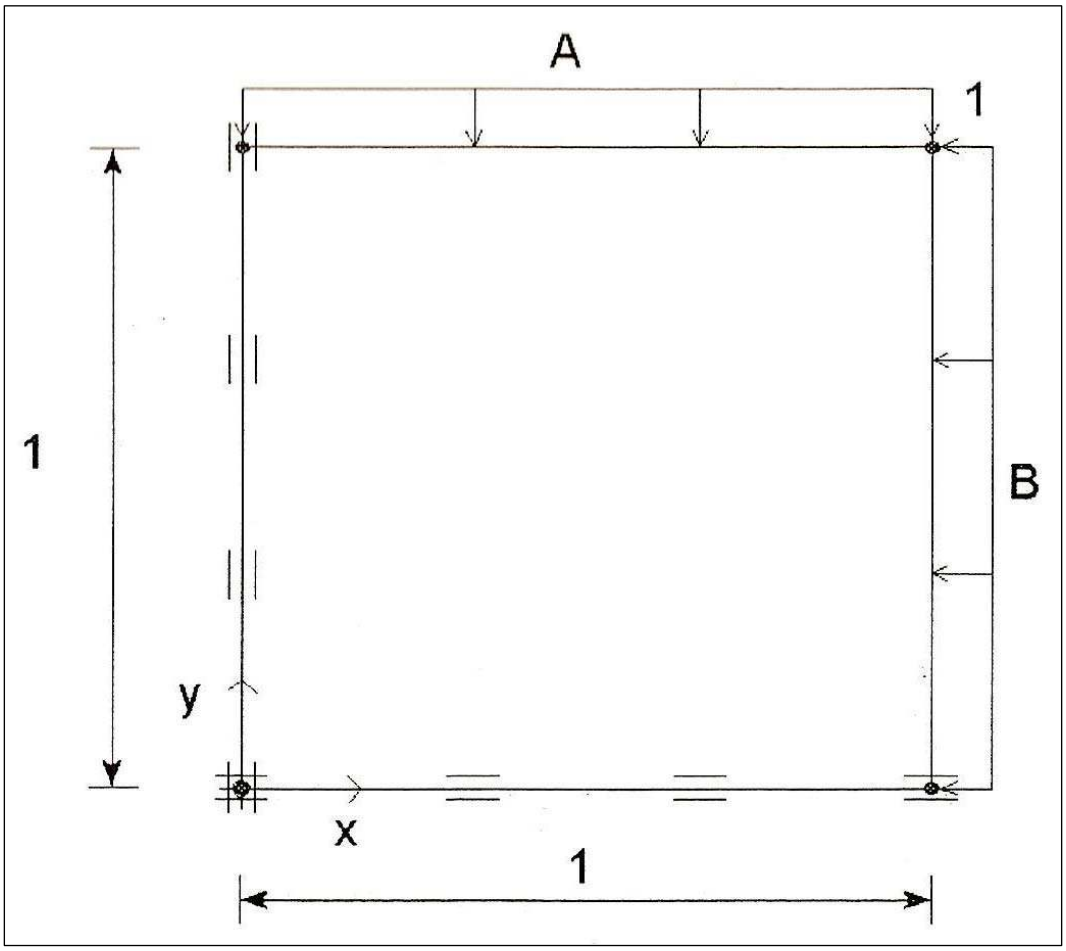

Figure B.1. Plaxis triaxial test model

σ_1' is increased to the corresponding test value of $\Delta\sigma_1'$ while the horizontal pressure σ_3' remained constant. A parametric study was performed using Plaxis to simulate ICD triaxial tests in order to obtain a combination of key HS constitutive parameters e.g., (E_{oed}^{ref}), dilation angle, and R_f that produced stress-strain responses that best matched the laboratory results. Figures B.2 to B.4 show Plaxis simulated triaxial tests results for the two tests and the scaled laboratory results. Based on the Plaxis parametric study, the combination of E_{oed}^{ref} = 0.8 E_{50}^{ref} , R_f = 0.7 and dilation angle (ψ) = 7.7 (based on correlation $\psi = \varphi - 30°$) produced

the best match to the laboratory results. These HS constitutive parameters for the weigle slide block were utilized the 2-D and 3-D FEM analyses of case study wall No. 1.

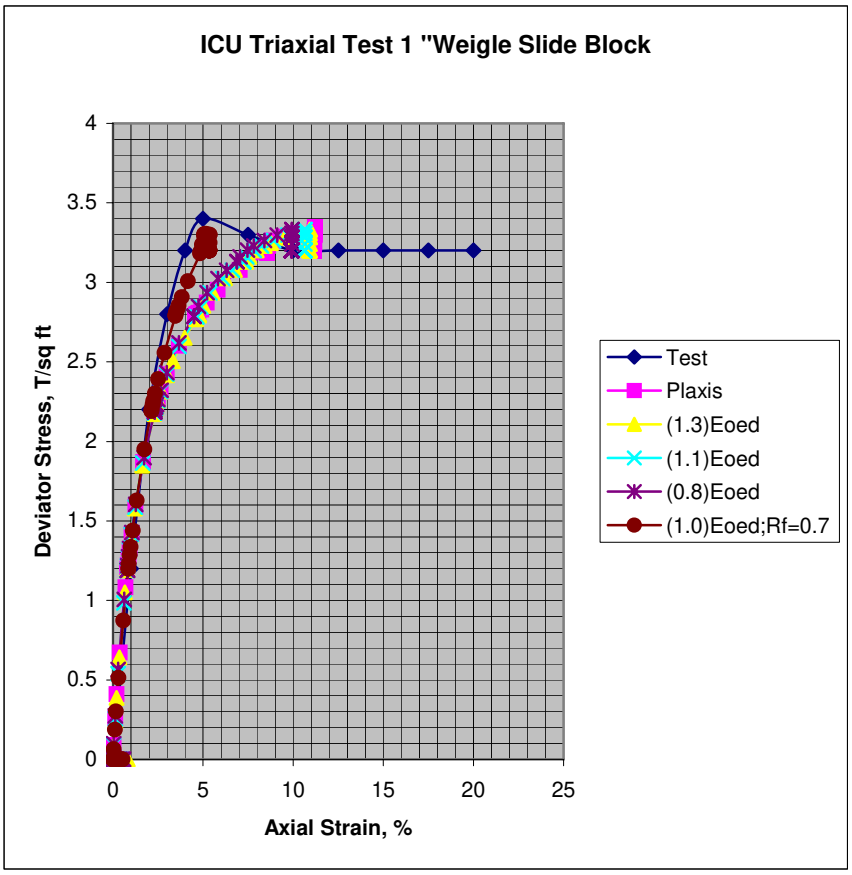

Figure B.2. Deviator stress versus axial strain for test 1 results on weigle slide block

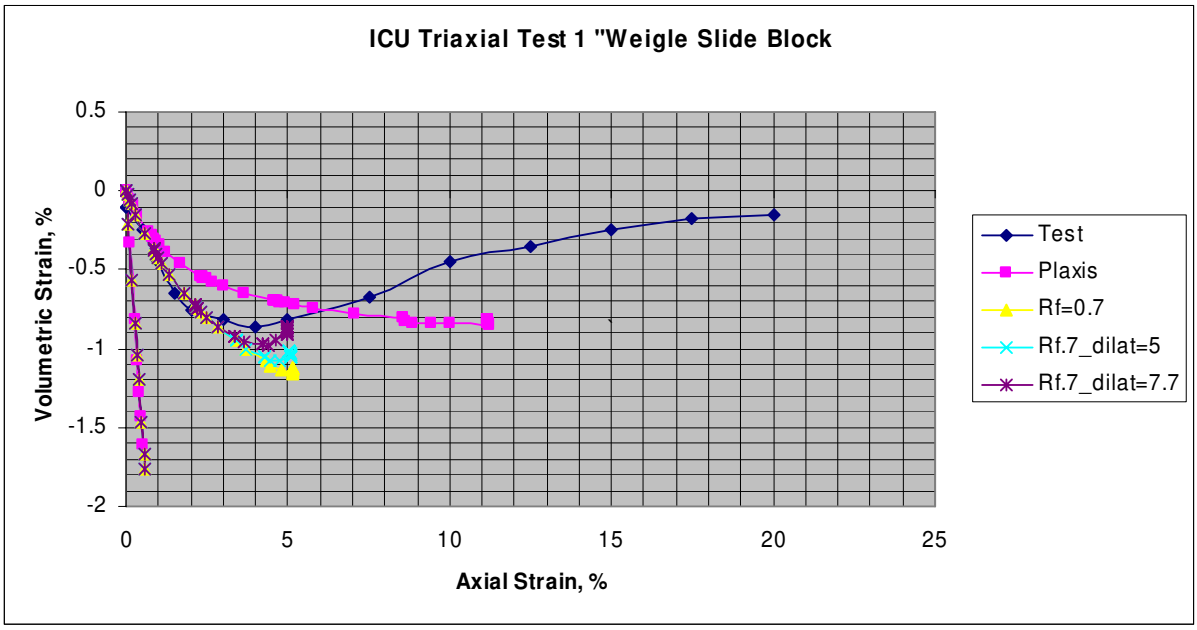

Figure B.3. Volumetric strain versus axial strain for test 1 results on weigle slide block

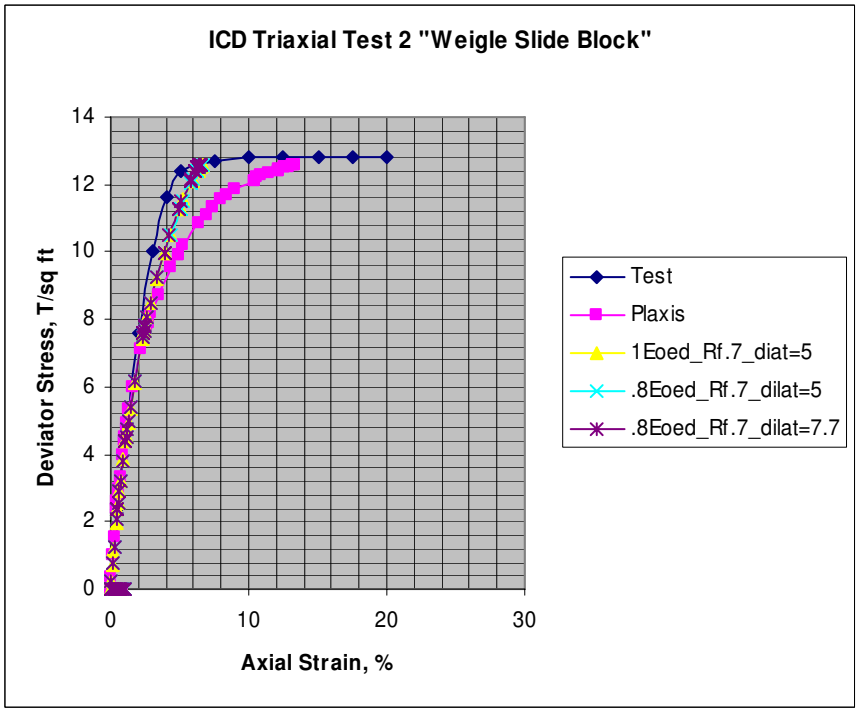

Figure B.4. Deviator stress versus axial strain for test 2 results on weigle slide block

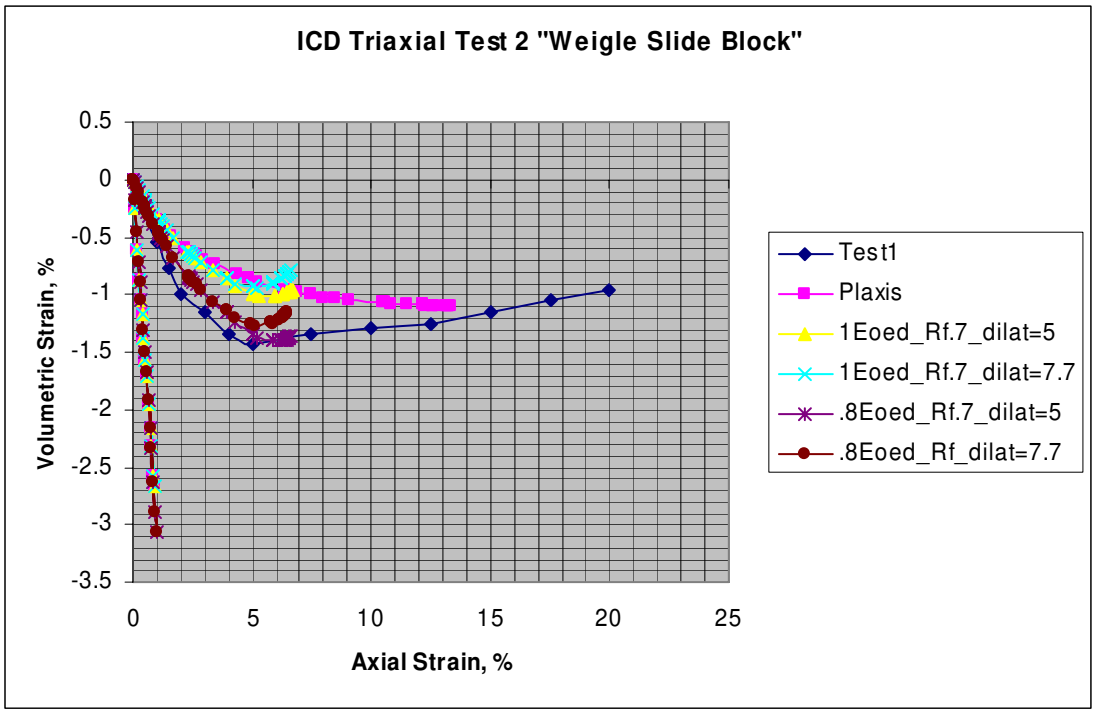

Figure B.5. Volumetric strain versus axial strain for test 2 results on weigle slide block

APPENDIX C

SUMMARY OF THE CURRENT 2-D PROCEDURE FOR CASE STUDY WALL NO. 2

In general practice, the use of soil pressure envelopes (often referred to as apparent pressure diagrams) as loading on a beam on rigid support analysis are used for the final design of flexible tieback wall systems. The Rigid 1 method is commonly used in the design and analysis of flexible tieback wall systems. In this method, a vertical section of the tieback is modeled as a multiple-span beam supported on rigid supports located at the tiebacks in the upper region of the wall. The lowermost rigid support is assumed to occur at finish grade. The wall is loaded on the driving side with an apparent earth pressure loading. A summary of the results of a Rigid 1 analysis/design of the case study wall no. 2 is presented below.

Texas _A&M Rigid_1

I. Compute "earth" pressure factor (EPS) for sand

$\phi := 32 \cdot deg$ $\gamma := 115$ pcf $H := 25$ ft

$EPF := 22.97 psf$

Total earth pressure load (P_{tl}) used in apparent pressure diagram

$P_{tl} := EPF \cdot H^2$

$P_{tl} = 1.436 \cdot 10^4$ lbs

EPF based on "Limiting equilibrium analysis"

$\phi_{mob} := \operatorname{atan}\left(\frac{\tan(\phi)}{1.3}\right)$

$\phi_{mob} = 0.448$

$\phi_{mob} := \phi_{mob} \cdot \frac{180}{\pi}$

$\phi_{mob} = 25.672$ deg

$K_A := 0.395$

$p_{tl} := K_A \cdot \gamma \cdot \frac{H^2}{2}$

$p_{tl} = 1.42 \cdot 10^4$ lb/ft

"Effective" pressure factor,

$EPF2 := \frac{p_{tl}}{H^2}$

$EPF2 = 22.713$ pcf

II. Apparent earth pressure diagram tieback with multiple rows of anchors

$H_1 := 6$ ft $\quad H_3 := 9$ ft

$H_2 := 10$ ft $\quad H := 25$ ft

Using anchor spacing (vertical/direction), the effective earth, Pe, for the FHWA nonsymmetrical apparent pressure diagram can be determined from (Figure 5.4b Strom Ebeling 2001).

$Pe := \frac{p_{tl}}{H - \frac{H_1}{3} - \frac{H_3}{3}}$

$Pe = 709.766$ psf

III. Bending moments on soldier beam

$M_1 := \frac{13}{54} \cdot H_1^2 \, Pe$

$M_1 = 6.151 \cdot 10^3$ lb-ft/ft

$MM_1 := \frac{1}{10} \cdot H_2^2 \cdot Pe$

$MM_1 = 7.098 \cdot 10^3$ lb·ft

$MM_3 := \frac{1}{10} \cdot (9)^2 \cdot Pe$

$MM_3 = 5.749 \cdot 10^3$ lb-ft/ft

IV. Ground anchor load horizontal component

Using information contained Figure 5.4(b) Strom and Ebeling (2001) to compute horizontal componet of each anchor load, on per ft. run of wall.

Top tier:

$$T_1 := \left(\frac{2}{3}\cdot H_1 + \frac{1}{2}\cdot H_2\right) Pe$$

$T_1 = 6.388\cdot 10^3$ lb/ft

$T_{1D} := T_1\cdot(8\cdot\cos(30\cdot deg))$

$T_{1D} = 4.426\cdot 10^4$ lb/ft

$$T_2 := \left(\frac{H_2}{2} + \frac{23}{48}\cdot H_3\right) Pe$$

$T_2 = 6.61\cdot 10^3$ lb/ft

$T_{2D} := T_2\cdot(8\cdot\cos(30\cdot deg))$

$T_{2D} = 4.579\cdot 10^4$ lb/ft

V. Subgrade reaction using tributary area using information in Fig. 5.4 of Strom and Ebeling (2001)

Compute subgrade reaction (R)

$$R_B := \left(\frac{13}{16}\cdot H_3\right) Pe$$

$R_B = 5.19\cdot 10^3$ lb/ft

VI. Sizing Soldier beam

Note: min permissible spacing is 4ft. (Fig 8.5 Strom and Ebeling 2001)
Max Soldier design moment is

$$M_{max} := \frac{M_1}{1000}\cdot 8$$

$M_{max} = 49.21$ kips*ft

$M_{max2} := M_{max}\cdot 12$

$M_{max2} = 590.525$ Kips*in

In accordance Corps Criteria allowable bending for soldier beam and wall is

Bending (combined axial and bending): $f_b := 0.5 \quad f_u := 0.33$

Allowable bending stress Grade 50 steel: $F_b := 0.5 \; F_v := 0.33$

$F_b := f_b \cdot 50 \qquad F_b = 25$

$F_u := F_v \cdot 50 \qquad F_u = 16.5$

Required Soldier beam section modulus Grade 50 steel

$$S := \frac{M_{max2}}{F_b}$$

$S = 23.621 \quad in^3$

APPENDIX D

MODIFIED RIGID 2 PROCEDURE FOR STIFF TIEBACK WALLS

Recall, the 2-D simplified design procedure (RIGID 2) is a simplified excavation sequencing analysis using an equivalent beam on rigid supports. Earth pressures are in accordance with classical earth pressure theory, assuming a wall retaining nonyielding soil backfill (at-rest earth pressure distribution). In the RIGID 2 method, the rigid supports are located at tieback points. The lowest support location is assumed to be below the bottom of the excavation at the point of zero net pressure (Ratay 1996). In the method, two earth pressure diagrams describing the loads behind and in front of the wall are used in each of the incremental excavation, anchor placement, and pre-stressing analyses. Active earth pressure (or at-rest pressure when wall displacements are critical which was used for this tieback wall) is applied to the driving side of the wall and extends from the top of ground to the actual bottom of the wall. Passive earth pressure (based on a factor of safety of 1.0 applied to the shear strength of soil) is applied to the resisting side of the wall and extends from the bottom of the excavation to the actual bottom of the wall.

The 3-D nonlinear FEM results indicated the potential for enhancement to RIGID 2 method. The RIGID 2 procedure uses a factor of safety equal to one applied to the shear strength of the soil below the excavation level (i.e., a passive limit state). The plots of mobilized shear at intermediate construction stages indicated that there is reserve passive resistance available in the soil, (Refer to Figure D1). Therefore, a parametric study was performed utilizing the computed 3-D FEM results of average horizontal earth pressure coefficient $K_{h(ave)}$ and average mobilized interface friction angle $\delta_{mob(ave)}$ as the basis for

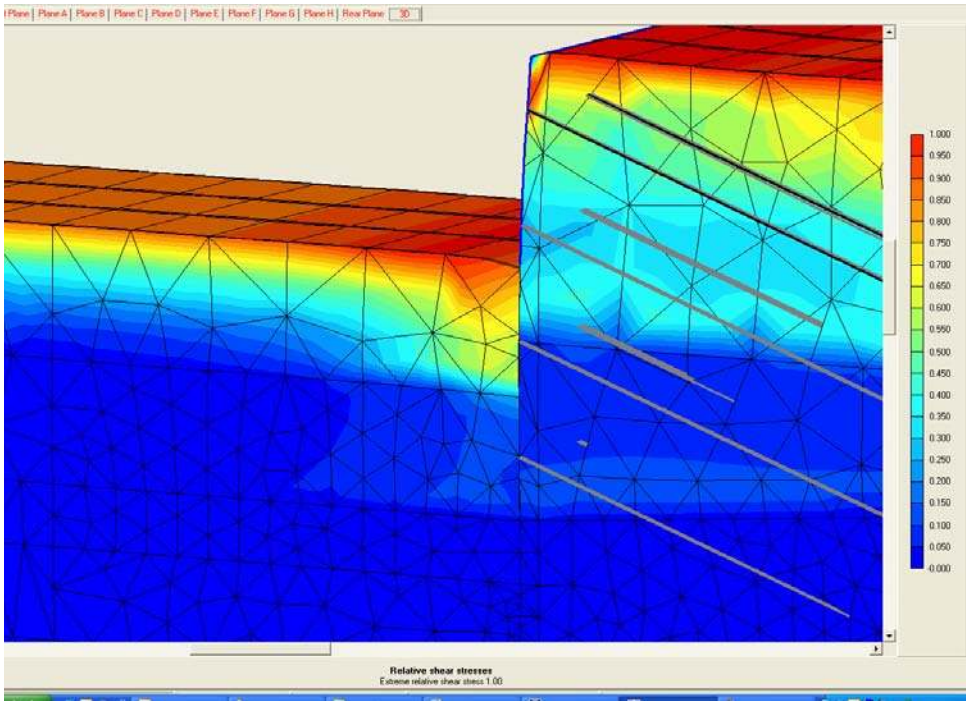

Figure D.1 Fraction of mobilized shear "stiff tieback wall at an intermediate stage of construction

comparison. A corresponding value of factor of safety (FS) was computed for the soil below each of the excavated levels by setting the Plaxis $K_{h(ave)}$ value equal to the horizontal component of the passive earth pressure coefficient (K_p), (K_p)*cos(δ). The mobilized shear strength, defined for this cohesionless soil as $\tan(\phi_{mob}) = \frac{\tan(\phi)}{FS}$ was used in the (K_p) calculation. An iterative procedure was used to determine the value for FS in order to obtain $K_p(\phi_{mob})*\cos(\delta_{mob(ave)})$ equal to Plaxis $K_{h(ave)}$. The resulting $K_p(\phi_{mob})*\cos(\delta)$ value was used in the Rigid 2 computation. This process was repeated for each of the three stage of excavation that were reanalyzed and discussed in this appendix.

Table D.1 shows the horizontal component $K_p^* \cos(\delta_{mob})$ used at intermediate construction stages that used in the initial Rigid 2 procedure for the stiff tieback wall system (an asterisk is used to denote the initial Rigid 2 analysis). Recall, this procedure is based on a FS_p of one

applied to the shear strength of soil on the resisting side of the wall. The value of K_p^* was determined from the Caquot and Kerisel chart of active and passive earth pressure coefficients (after Caquot and Kerisel 1973; See Figure A.2). In the initial Rigid 2 analysis δ_{mob} was estimated as $\frac{\phi}{2}$. The value of K_p^* acts at an angle $\cos(\delta_{mob})$. As shown in Table D.1, the same value of $K_p^* \cos(\delta)$ was used for each stage of construction.

Table D.1. Horizontal Component of Values of K_p*cos(δ)
Used in the Initial Rigid 2 Analysis

Construction Stage	Excavated Side [ft]	m_1^* [ft]	$K_p^* \cos(\delta)$ [-]	K_p^* [-]
Stage 1	78.50	9.80	4.85	6.50
Stage 2	67.50	2.50	4.85	6.50
Stage 3	56.50	3.75	4.85	6.50
* Initial Rigid 2 analysis using $FS_{(p)}$ = 1.0				

The results of the parametric study utilizing the computed 3-D FEM results of the average horizontal earth pressure coefficient $K_{h(ave)}$ and the average mobilized interface friction angle $\delta_{mob(ave)}$ as the basis for obtaining the modified horizontal component of the passive earth pressure coefficient to be used in the Rigid 2 is summarized in Table D.2. Recall, that the passive earth pressure coefficient is a function of mobilized internal friction angle ϕ_{mob} and δ_{mob}. The factor of safety was adjusted in the relationship for ϕ_{mob} until the computed horizontal component of passive earth pressure coefficient K_p*R* cos(δ) was approximately equal the $K_{h(ave)}$ computed by the 3-D nonlinear FEM. The average factor of safety resulting from these three intermediate construction stages is reported in Table D.3. This average factor of safety of 1.4 along with an average interface friction angle $\delta_{mob(ave)}$ equal to 20 degrees computed from 3-D nonlinear FEM was used to obtain the new horizontal component of

Table D.2. Summary of Parametric Study of Horizontal Component of Passive Earth Pressure Coefficient (Kp*R* cos(δ))

Construction Stage	El. on Excavated Side [ft]	Plaxis $(K_h)_{ave}$ [-]	Plaxis $(\delta_{mob})_{ave}$ [deg]	FS [-]	ϕ [deg]	ϕ_{mob} [deg]	K_p [-]	Reduction Factor (R) [-]	K_p*R [-]	K_p* R* cos(δ_{mob}) [-]
Stage 1	78.50	1.77	19.80	2.10	34.00	17.81	2.50	0.75	1.88	1.79
Stage 2	67.50	6.73	19.66	1.00 **	34.00	34.00	9.00	0.77	6.93	5.75 **
Stage 3	56.50	6.41	19.84	1.10	34.00	31.52	8.40	0.88	7.39	6.30
** FS never less than 1.0										

Table D.3 Average Factor of Safety for Intermediate Construction Stage

Construction Stage	El. on Excavated Side [ft]	FS
Stage 1	78.50	2.10
Stage 2	67.50	1.00
Stage 3	56.50	1.10
		1.40 Avg.

the passive earth pressure coefficient (K_p*R* cos(δ)) to be used in the second Rigid 2 analysis. Table D.4 shows a summary of results for the simplified 2-D procedures and both 2-D and 3-D FEM. The Rigid 2 procedure with a $FS_{p(ave)}$ equal to 1.4 generally computes slightly larger maximum bending moments than the Rigid 2 procedure with FS_p equal to one for these intermediate construction stages. However, for stages 2 and 3, Rigid 2 procedure with a $FS_{p(ave)}$ equal to 1.4 computes much smaller bending moments as compared to the simplified Winkler 1 procedure, and 2-D and 3-D FEM results. Recall, that the simplified Rigid 2 procedure is based on the assumption that a point of fixity in the soil below the excavation elevation occurs at a depth of zero net pressure for the second and all subsequent construction stages. These results indicate that the simplified approach used to estimate the depth to fixity might be a key reason for the disparity in results.

Table D.4. Summary of Analysis Results

	RIGID 2 $FS_{(p)}$=1.0	RIGID 2 $FS_{(p)(ave)}$=1.4	WINKLER 1 Cmultianc	2-D Plaxis FEM	3-D Plaxis FEM
Stage 1 Excavation					
Max. Anchor Load (Kips)	NA	NA	NA	NA	NA
Max. Moment (Ft-Kips/ft run of wall)	26.2	31.2	35.2	28	22.3
Max. Computed Displ. (in.)	NA	NA	-0.21	-0.15	-0.12
Stage 2 Excavation					
Max. Anchor Load (Kips)	89.6	94.7	359.4	272	272
Max. Moment (Ft-Kips/ft run of wall)	39.5	44.3	115	122	161
Max. Computed Displ. (in.)	NA	NA	-0.25	0.22	0.31
Stage 3 Excavation					
Max. Anchor Load (Kips)	310.0	334.8	361.2	292	292
Max. Moment (Ft-Kips/ft run of wall)	56.7	65.1	138.1	158	172.5
Max. Computed Displ. (in.)	NA	NA	-0.39	0.37	0.44

VITA

Kevin Abraham was born May 25, 1962, in Shreveport, Louisiana. He grew up and attended high school in Logansport, Louisiana. An interest in bridges and a like of mathematical problem solving initiated his interest in the civil engineering profession. He attended Southern University in Baton Rouge, Louisiana, graduating from there in 1984 with a bachelor's degree in civil engineering. He accepted a position as a civil engineer at the Engineer Research and Development Center, Waterways Experiment Station, in Vicksburg, Mississippi. He has been involved with various projects related to soil-structure interaction analyses using finite element procedures. While working at the Waterways Experiment Station, he received his master's degree in civil engineering (structural/geotechnical focus) from Mississippi State University, graduating in 1995. He entered Louisiana State University in the fall of 1998 to pursue a Doctor of Philosophy Degree in the Department of Civil and Environmental Engineering. Having completed his research on three-dimensional behavior of retaining wall systems, he is now a candidate for that degree.